Rheinische Friedrich-Wilhelms-Universität Bonn

Mathematisch-Naturwissenschaftliche Fakultät

Characterisation of a MAPKK kinase from *Craterostigma plantagineum*

Interaction of VIK kinases and LEA proteins

Dissertation

zur Erlangung des Doktorgrades (Dr. rer. nat.)

vorgelegt von

Verena Anika Braun

aus Bonn, Deutschland

Angefertigt am Institut für Molekulare Physiologie und Biotechnologie der Pflanzen

Bonn, 2017

Angefertigt mit Genehmigung der Mathematisch-Naturwissenschaftlichen Fakultät der

Rheinischen Friedrich-Wilhelms-Universität Bonn

Tag der Promotion: 09.01.2018

Erscheinungsjahr: 2018

1. Gutachterin: Prof. Dr. Dorothea Bartels
2. Gutachter: Priv.-Doz.-Dr. Hans-Hubert Kirch

Table of Contents

List of abbreviations

Units were applied according to the “International System of Units” (SI).

DNA and amino acid sequences are given in the notation formalised by the International Union of Pure and Applied Chemistry (IUPAC).

[v/v]	volume/volume
[w/v]	weight/volume
AA	amino acid
ABA	abscisic acid
Amp	ampicillin
ANK	ankyrin repeat motif(s)
ANKKs	ankyrin repeat-containing kinases
ANKMAPKKKs	ankyrin repeat-containing MAPKKKs
APS	ammonium persulfate
ATP	adenosine triphosphate
ATPase	adenosine 5'-triphosphatase
BiFC	bimolecular fluorescence complementation
BSA	bovine serum albumin
bp	base pairs
BRs	brassinosteroids
CaMV	cauliflower mosaic virus
CD	circular dichroism
CHAPS	3–[3–(cholamidopropyl) dimethylammonio] –1–propanesulfonate
CK2	casein kinase 2
C-lope	carboxyl-terminal lobe
Col–0	Columbia–0
DEPC	diethylpyrocarbonate
DFG motif	D (aspartic acid), F (phenylalanine), G (glycine)
dH_2O	distilled “milli–Q" water
DMF	N,N-Dimethylformamide
DMSO	dimethyl sulfoxide
DNaseI	Deoxyribonuclease I
DOC	sodium deoxycholate
DTT	dithiothreitol
E	einstein (light intensity in energy per mole of photons)
ECL	enhanced chemiluminescence
EDTA	ethylene diamintetraacetatic acid
EGTA	ethylene glycol-bis(β-aminoethyl ether)-N,N,N',N'-tetraacetic acid
EF1α	elongation factor 1 α
e-value	expectation value
GFP	green fluorescent protein
GST	glutathione S-transferase
GTPases	guanosine triphosphate hydrolase enzymes
His–tag	histidine–affinity tag
IEF	isoelectric focusing
IgG	immunoglobulin G
IPG	immobilized pH gradient
IPTG	isopropyl–β–D–thiogalactopyranoside
Kan	kanamycin
LB	Lysogeny broth
LC-MS/MS	liquid chromatography tandem-mass spectrometry
LEA	late embryogenesis

	abundant
MALDI	matrix-assisted-laser-desorption/ionization
MAPK	mitogen-activated protein kinase(s)
MAPKK	mitogen-activated protein kinase kinase(s)
MAPKKK	mitogen-activated protein kinase kinase kinase(s)
MES	2-(N-morpholino)ethane-sulfonic acid
MOAC	metal oxide affinity chromatography
MOPS	3-(N-morpholino)propanesulfonic acid
MS–salt	Murashige–Skoog–salt
NCBI	National Center for Biotechnology Information (Bethesda, USA)
N-lobe	NH2(amino)-terminal lobe
NTA	nitrilotriacetic acid
OD	optical density
PA	phosphatidic acid
PAGE	polyacrylamide gel electrophoresis
PBS	phosphate-buffered salt solution
PEP	percolator posterior error probability
pI	isoelectric point
PLD	phospholipase D
PMF	peptide mass fingerprint
PTM Score	post-translational modification probability
QTL	quantitative trait locus
RNase	ribonuclease
ROS	reactive oxygen species
rpm	rounds per minute
RT	room temperature
RT–PCR	reverse transcription polymerase chain reaction
RubisCO	ribulose-1,5-bisphosphate carboxylase/ oxygenase
RWC	relative water content
SALK	Salk–Institute (La Jolla, USA)
SDS	sodium dodecylsulfate
SNP	single nucleotide polymorphism
SOC	super optimal broth
Taq	*Thermus aquaticus*
TBS	tris– buffered salt solution
TBST	TBS supplemented with TWEEN
T–DNA	transfer DNA
TEMED	tetramethylethylendiamine
TFB	transfer buffer
T_m	melting temperature
TOF	time of flight
Tris	tris(hydroxymethyl)–aminomethane
TWEEN20	polyoxyethylene(20) sorbitan monolaurate
VH1	VASCULAR HIGHWAY1 (provascular/ procambial cell-specific receptor kinase)
VIK	VH1-interacting kinase
WT	wild type
λ	wavelength
Ω	Ohm

List of tables

List of figures

1 Introduction

1.1 Water deficiency causes drought stress

Drought is a key factor of yield loss in agriculture. During drought stress the transpiration rate of plants exceeds the water uptake, leading to severe damage and plant death. At the cellular level, reduced water leads to membrane impairment followed by the fusion of cellular membranes resulting in the loss of electrochemical potentials, concentration gradients and their functionality (Buitink et al. 2002). Proteins lose their hydration shell and three-dimensional structure, resulting in the loss of function (Walters et al. 2002). In order to compensate periods of low precipitation and high temperatures 70 % of the world's fresh water is used for irrigation of agricultural areas (Schlosser et al. 2014). Sufficient irrigation is not always possible, resulting in supply shortages during drought. Some plant species can tolerate extreme drought conditions and are desiccation tolerant. These plants are edowed with various protective machanisms. The mechanisms for droght tolerance are not fully understood and subject of the current research.

1.2 Resurrection plants are models to reveal mechanisms of drought tolerance

Drought tolerance is defined by the duration of survivable drought stress periods and the amount of water plant species can lose prior to plant death. A loss of 30 % of the intrinsic water is lethal for most species (Schopfer et al. 1999). Resurrection plants can however survive a water loss of up to 99 % due to specific protective mechanisms and can rehydrate upon availability of water (Bartels et al. 1990; Fischer 1992a; Moore et al. 2009). The most extensively studied dehydration-tolerant plant species is the resurrection plant *Craterostigma plantagineum* Hochst, which belongs to the family of Linderniacea (Bartels 2005). Even after a severe water loss, it regains its full biological function after 24 hours of rewatering (Gaff 1977). One of the protective mechanisms is the increase in the osmotic potential of the plant cells by enrichment of sugars, and sugar alcojols, such as mannitol, sorbitol, trehalose or sucrose and other compatible solutes such as proline, serine, glutamate or glycine betaine (Bartels 2005). This increase in compatible solutes results in a reduced water efflux from the cell. In addition, the hydroxyl groups of sugars and compatible solutes can form hydrogen bonds with proteins and polar head groups of membrane lipids leading to the

stabilisation of intracellular structures (Buitink et al. 2002). Also, a reversible shrinkage of the leaves, including cell wall folding during dehydration, can be observed (Hartung et al. 1998; Farrant 2000; Giarola et al. 2016). A differential accumulation of various protective proteins (Alamillo et al. 1995; Mariaux et al. 1998; van den Dries et al. 2011; Rodriguez et al. 2010a), detoxifying enzymes (Ingram et al. 1997; Kirch et al. 2001) and secondary metabolites (Bartels 2005, Bartels and Sunkar 2005) is observed during dehydration. In addition to *de novo* accumulation of proteins, post-translational modifications during dehydration, such as phosphorylation are involved in stress response. One family of protective proteins expressed and activated by phosphorylation under drought stress in *C. plantagineum* are the late embryogenesis abundant proteins (LEA proteins) (Röhrig et al. 2006; van den Dries et al. 2011). LEA proteins are predicted to replace the missing hydration shell of ions by their charged residues (Dure 1993; Hoekstra et al. 2001). An up-regulation and activation of kinases that mediate phosphorylation of proteins is essential and was observed in various species during drought stress (Mizoguchi et al. 1996; Munnik et al. 1999; Kiegerl et al. 2000; Ullah et al. 2017).

1.3 Seed development and vegetative desiccation tolerance share similar protective mechanisms

Most of the higher plant species are sensitive to drought stress during the vegetative growth period. However, they survive desiccation in the seed state due to protective mechanisms including the accumulation of protective proteins. LEA proteins are expressed at high levels during the later stages of embryo development in plant seeds (Roberts et al. 1993) and during the dehydration and rehydration phase in the vegetative tissue of desiccation-tolerant species (Ingram and Bartels 1996; Phillips et al. 2008; van den Dries et al. 2011). Therefore, LEA proteins, first discovered in cotton seeds (Dure 1993), have been linked to drought tolerance (Cuming 1999), despite the limited knowledge of their biochemical function. In the desiccation tolerant plant species *Oropetium thomaeum* orthologs to seed-specific LEA proteins from desiccation sensitive species have shown to be highly expressed during desiccation in vegetative tissues (VanBuren et al. 2017). Röhrig et al. (2006) reported a dehydration-dependent accumulation and phosphorylation of the LEA-like protein CDeT11–24 in *C. plantagineum.* In Arabidopsis the closest homologue RD29A/B is expressed in seeds and vegetative tissues under dehydration stress (Yamaguchi-Shinozaki and Shinozaki

1993; Kreps et al. 2002). Five phosphorylation sites were identified in RD29B extracted from seeds (Wolschin and Weckwerth 2005). In RD29A extracted from seedlings 19 phosphorylation sites were identified (Reiland et al. 2009, Li et al. 2009). Several phosphorylation sites of CDeT11–24, RD29A and RD29B are predicted to be phosphorylated by mitogen-activated protein kinases (MAPKs). MAPKs play crucial roles in seed germination processes (Xing et al. 2009; Liu et al. 2013b) and the abiotic stress response to dehydration, salt and osmotic stress (Droillard et al. 2004; Teige et al. 2004; Hua et al. 2006; Kim et al. 2011; Kim et al. 2013; Tsugama et al. 2012) demonstrating the conjunction of signalling networks associated with seed germination and vegetative desiccation tolerance.

1.4 Activation of proteins during stress requires signal transduction controlled by Mitogen-activated protein kinases

Desiccation initiates signalling cascades which lead to differential expression and activation of dehydration related proteins (Bartels et al. 1990; Piatkowski et al. 1990; Bartels and Sunkar 2005; Röhrig et al. 2006). Deciphering the interplay of protein-protein interactions and signalling molecules like reactive oxygen species (ROS) or Ca^{2+} in desiccation tolerant plants, provides insight to understand the protection strategies. Reversible phosphorylation of proteins mediated by kinases is one of the major regulatory mechanisms in the signalling network (Trewavas and Malho 1997). MAPK cascades play an important role in signal transduction (Nakagami et al. 2005; Popescu et al. 2009; Danquah et al. 2014; Ullah et al. 2017).

1.4.1 Protein kinases

Protein kinases catalyse the transfer of the γ-phosphate group of adenosine triphosphate (ATP) to the hydroxyl groups of serine/threonine or tyrosine residues of proteins. These enzymes act as key regulators of signalling pathways and most cellular processes in eukaryotes are regulated by protein phosphorylation mediated by kinases (Cohen 2002; Brognard and Hunter 2011). Protein kinases are involved in diverse processes not only related to stress in plants, but also to growth and development im various ther organisms. More than 518 genes encoding kinases have been identified in humans (Manning et al. 2002) and several disorders are associated with malfunction or deregulation of kinases (Zhang et al. 2009; Johnson 2009; Dar and Shokat 2011). The

protein kinase superfamily in plants has expanded, resulting in a much larger kinome with 600 to 2500 members per species (Arabidopsis Genome Initiative 2000; Lehti-Shiu and Shiu 2012). This reflects their importance in plant signal transduction and metabolism during biotic and abiotic stresses. Protein phosphorylation mediated by kinases leads to an altered activity of target proteins and serves as molecular switch. The transfer of a phosphate group can activate or inhibit proteins through allosteric conformational changes or by impairing substrate recognition (Barford et al. 1991; Groban et al. 2006; Serber and Ferrell 2007; Nishi et al. 2011; Nishi et al. 2013). This affects the formation and reorganization of dynamic protein interaction networks (Olsen et al. 2006; Schwartz and Murray 2011). Moreover, the intracellular localisation of proteins can be determined by the phosphorylation state (Mehlen and Arrigo 1994; Kawakami et al. 1999; Jin et al. 2005; Sjö et al. 2010). The phosphorylation reaction is a reversible process whereby phosphatases catalyse the dephosphorylation reaction.

Structure of the catalytic domain

Eukaryotic protein kinases share a conserved catalytic domain, the so-called ”kinase domain” consisting of about 290 amino acid residues forming two structurally and functionally distinct connected lobes, the small N-lobe and the larger C-lobe (Hanks 1988). The N-lobe is composed of a five stranded β-sheets coupled to a αC-helix subdomain. During the catalytic cycle the internal organisation of the N-lobe determines accessibility of the kinase. The C-lobe, or catalytic lobe, contains majorly α-helices and loops (Hanks 1988). It harbours a tethering surface for substrates, and the so-called DFG motif (Moran et al. 1988; Nagar 2007; Treiber and Shah 2013) (**Figure 1**).

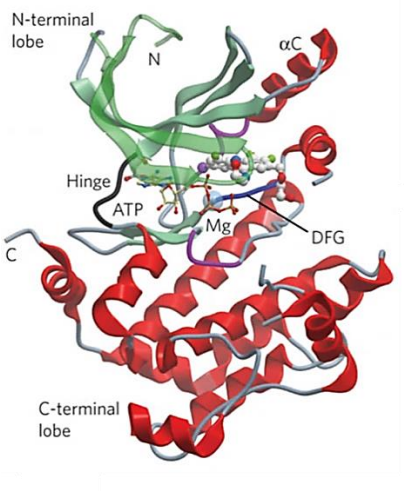

Figure 1: Kinase structure
Structural overview of a catalytic domain visualised in a ribbon diagram. Modified from Fedorov et al. 2010. The main regulatory elements are marked. The figure shows the MEK1 kinase in complex with ATP/Mg2+ and an allosteric inhibitor.

The active site is formed in the cleft between the two lobes where the phosphotransfer reaction occurs (Kornev et al. 2006; Meharena et al. 2013). This hinge region connects the two lobes and consists of two hydrophobic structures called the regulatory spine (R-spine) determining the activity of the kinase (Kornev et al. 2006) and the catalytic spine (C-spine) responsible for the binding of the adenine ring of ATP (Kornev et al. 2008; Taylor and Kornev 2011). The activation loop within the C-lobe recognizes phosphorylatable residues of substrate proteins (Adams et al. 2003; Nolen et al. 2004). For many kinases this loop needs to be modified by phosphorylation of regulatory sites leading to an activation of the kinase prior to substrate recognition or ATP-binding (Lew and Burke 2003; Adams et al. 2003). Phosphorylation of the kinase involves also changes in the orientation of the αC-helix of the N-lobe (Kornev et al. 2006) leaving the ATP-binding site accessible. During the catalytic cycle the conformation of the active kinase alternates between open and closed (Taylor and Kornev 2011).

The DFG motif

The DFG motif as part of the activation loop within the C-lobe is crucial for phosphorylation of substrates and autophosphorylation and consists of three amino acids: D (aspartic acid), F (phenylalanine), G (glycine).

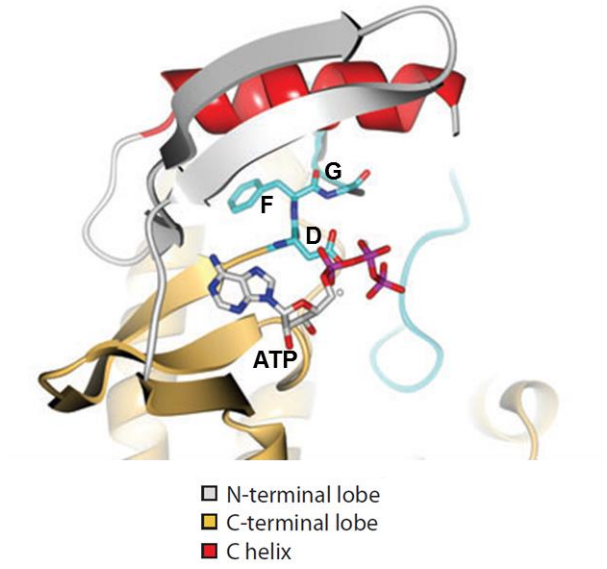

Figure 2: DFG Motif
Details of the C-helix and DFG motif visualised in a ribbon diagram. Modified from Endicott et al. (2012).

In the active conformation, the negatively charged aspartate residue of the DFG motif binds either directly to ATP or chelates the associated magnesium ions to orientate the ATP substrate (Kornev et al. 2006). The phenylalanine residue influences the positioning of the αC-helix and the catalytic loop. The role of the glycine residue of the DFG motif is still unknown but its high conservation among the kinome points to an essential role (Kornev et al. 2006). In inactive kinase conformations, the DFG motif is flipped and the phenylalanine is turned toward the ATP binding site so that it is not accessible for ATP binding (Taylor and Kornev 2011; Endicott et al. 2012). Due to the essential role of the DFG motif it is often the target for loss of function mutation approaches and kinase inhibitors.

1.4.2 Mitogen-activated protein kinases (MAPKs)

Multiple kinases are assigned to the MAPK superfamily due to structural similarities and their phosphorylation-recognition sites. The name „Mitogen-activated kinases“ was determined by ERK1 (MAPK3), the first MAPK that has been identified. This mammalian MAPK is activated by mitogen and involved in growth factor signalling (Lewis et al. 1998; Pearson et al. 2001; Yoon and Seger 2006). However MAPKs transduce a diverse set of stimuli apart from mitogens, such as hormones, osmotic stress, heat shock and proinflammatory cytokines into specific intracellular responses. The importance of MAPks is determined by their functional organisation in cascades which allows the amplification of signals. The signal is transduced by sequential phosphorylation of the cascade members (Lewis et al. 1998; Madhani and Fink 1998;

Schaeffer and Weber 1999; Widmann et al. 1999). Fine adjustment of the downstream responses can be achieved by up-/down-regulation or de-/activation of the involved MAPKs. The activation of a MAPK cascade represents one of the earliest cellular responses and can occur within one minute after stimulation (Betsuyaku et al. 2011). A typical MAPK cascade involves activation of a MAPK kinase kinase (MAPKKK) by extracellular stimuli, which phosphorylates two Ser/Thr residues within the S/TXXXXXS/T motif of a MAPK kinase (MAPKK) which in turn phosphorylates the Thr and Tyr residues within the TXY motif of a MAPK (Popescu et al. 2009). Phosphorylated MAPKs are known to phosphorylate various proteins such as transcription factors, protein kinases, metabolic enzymes, and cytoskeletal proteins. The MAPK cascades, however, are not always linear, demonstrated by the imbalance of the numbers of MAPKKKs, MAPKKs, and MAPKs in organisms as shown exemplary for three plant species in table 1.

Table 1: Identified MAPK, MAPKK and MAPKKK genes in different plant species

Species	***MAPK genes***	***MAPKK genes***	***MAPKKK genes***	***Source***
Arabidopsis thaliana	*20*	*10*	*80*	*(MAPK Group et al. 2002; Colcombet and Hirt 2008)*
Cucumis sativus	*14*	*6*	*59*	*(Wang et al. 2015)*
Oryza sativa	*17*	*8*	*75*	*(Agrawal et al. 2003; Hamel et al. 2006; Rao et al. 2010)*

It has been shown that MAPK-activated pathways overlap (Knight and Knight 2001; Colcombet and Hirt 2008) and different stimuli can activate MAPKs to different levels and with different kinetics (Tena et al. 2001). To ensure signal specificities, various combinations of MAPK cascade components allow specific responses to different stimuli (Whitmarsh 1998; Elion 2001; Tanoue and Nishida 2003). MAPKKs and MAPKKKs can also directly phosphorylate substrate proteins instead of downstream MAPKs (Malinin et al. 1997; Champion et al. 2004; Hoffmann et al. 2005; Wingenter et al. 2011). MAPKs are involved in plant signal transduction during drought, salinity, cold and oxidative stress (Teige et al. 2004; Shen et al. 2012; Xing et al. 2009; Gasulla et al. 2016). Improving plant stress tolerance by engineering MAPK cascades is a promising

approach (Gurr and Rushton 2005; Umezawa et al. 2006; Shitamichi et al. 2013; Wang et al. 2016; Ullah et al. 2017).

1.4.3 The diverse family of MAPKKKs

MAPKKKs belong to a large gene family that compromises more members than the MAPK and MAPKK gene families in plants (**Table 1**). According to their structure signatures MAPKKK genes have been divided into the RAF, MEKK, and ZIK subgroups. Kinases belonging to the RAF subgroup harbour the specific signature GTXX (W/Y) MAPE (Rodriguez et al. 2010b). Plant MEKK-like kinases are determined by the conserved signature G (T/S) PX(F/Y/W) MAPEV and ZIK kinases contain the conserved signature GTPEFMAPE (L/V/M) (Y/F/L).

Table 2: Identified MAPKKK genes in different plant species divided into subgroups; table modified from Wang et al., 2016

Species	***MAPKKK***			***Total number of MAKKKs***
	MEKK	***ZIK***	***RAF***	
Arabidopsis	*21*	*11*	*48*	*80*
tomato	*33*	*16*	*40*	*89*
wheat	*29*	*11*	*115*	*155*
rice	*22*	*10*	*43*	*75*
maize	*22*	*6*	*46*	*74*
soybean	*34*	*24*	*92*	*150*

In Arabidopsis MEKK-like MAPKKK genes have shown to be involved in several signal transduction pathways specific for cell division (Krysan 2002; Lukowitz et al. 2004), stomatal development (Bergmann et al. 2004) cell death and reactive oxygen species homeostasis (Ichimura et al. 2006; Nakagami et al. 2006). Functional data on ZIK-like genes are rare but gene expression of most rice ZIK-like MAPKKK genes is upregulated by at least one abiotic stress (Rao et al. 2010), indicating participation in stress signalling transduction pathways. RAF kinases became a lot attention because

they are involved in hormone signalling transduction, salt stress response, stomatal opening, leaf venation, growth regulation and pathogen resistance in Arabidopsis (Kieber et al. 1993, 1993; Frye 1998; Frye et al. 2001; Gao and Xiang 2008; Ceserani et al. 2009; Wingenter et al. 2011; Sasayama et al. 2011). Participation in the formation of drought resistance could be shown for the rice RAF-like MAPKKK DSM1 (Ning et al. 2010). So far, no MAPKK target of RAF-like MAPKKKs has been identified. This raises the question whether the annotation of this subfamily as MAPKKK needs to be revised (Zulawski and Schulze 2015).

1.5 Kinases in *C. plantagineum*

Several proteins that are phosphorylated in response to drought have been identified in *C. plantagineum* (Mariaux et al. 1998; Röhrig et al. 2006; Röhrig et al. 2008). However, only two kinases have been described in *C. plantagineum*, CPPK1 (Heino 1998) and CpWAK(1/2) (Giarola et al. 2016). Homologs of CPPK1, a serine/threonine kinase, have been found in Arabidopsis (Park et al. 2001) and wheat (Anderberg and Walker-Simmons 1992). Interestingly, a down regulation of cppk1 expression during dehydration has been shown in leaf tissue of *C. plantagineum*. CpWAK is a cell wall-associated serine/threonine kinase that shows a high homology to the WAK proteins in Arabidopsis. Two isoforms (CpWAK1 and CpWAK2) were identified in *C. plantagineum*. CpWAK1 interacts with an apoplastic glycine-rich protein (CpGRP1) and the CpGRP1-CpWAK1 complex contributes in dehydration-induced morphological changes in the cell wall during dehydration. Also for CpWAK1 a down regulation of expression has been observed in response to dehydration (Giarola et al. 2016). Contrastingly, several proteins in *C. plantagineum* showed a drought stress-dependent phosphorylation (Röhrig et al. 2006; Röhrig et al. 2008) indicating the abundance of stress inducible kinases. Bioinformatic analysis revealed the presence of various kinases according to the identified phosphorylation sites in protective proteins. Multiple sites were predicted to be phosphorylated by MAPKKKs. Peterson (2012) showed that during dehydration several kinases are activated in *C. plantagineum* leaf tissue. To identify specifically kinases that phosphorylate protective proteins, the stress-dependently phosphorylated CDeT11-24 LEA-like protein was used as bait substrate in an *in gel* kinase assay. After specific enrichment of interacting kinases two peptides were identified *via* mass spectrometry (MS). The direct assignment to a protein or gene sequence was not possible since the genome of *C. plantagineum* is not sequenced. Due to sequence homology it was nevertheless possible to hypothesise, that a homologue to the Casein Kinase II (CK2) and a homologue to the RAF MAPKKK VH1-

interacting kinase (VIK) from Arabidopsis (At1g14000) have to be present in *C. plantagineum*. An *in vitro* kinase assay demonstrated that the CDeT11-24 LEA-like protein can be phosphorylated by the human CK2 holoenzyme (Petersen 2012) and the VIK from Arabidopsis (unpublished). Since VIK is known to be induced by osmotic stress in Arabidopsis and highly expressed in seeds (Wingenter et al. 2011), the identification and characterisation of this MAPKKK in *C. plantagineum* (CpVIK) will give new insights in the stress-dependent phosphorylation of protective proteins in resurrection plants. Further characterisation of Arabidopsis *Δvik* mutants in terms of seed germination will reveal the pathways shared by desiccation tolerance in seeds and vegetative of resurrection plants.

1.6 Aims of this study

The primary goal of this study was to contribute to the understanding of the complex mechanisms of desiccation tolerance by the characterisation of a MAPKKK in *C. plantagineum* (CpVIK) as well as its homolog in *A. thaliana* (AtVIK).

Petersen (2012) demonstrated in *in-gel*-kinase assays with the stress-related LEA-like protein CDeT11-24 as bait that a homologue to the RAF-like MAPKKK VH1-interacting kinase (VIK) from Arabidopsis (At1g14000) is present in extracts of *C. plantagineum* (CpVIK). Whether CpVIK is involved in the drought stress response in *C. plantagineum* was investigated in this study. In addition the role of AtVIK was examined in *A. thaliana* to demonstrate the functional consistency between desiccation tolerance in seeds of drought sensitive species and in vegetative tissues of drought tolerant species.

A first attempt was to gain a deeper insight into the structure CpVIK by *in silico* analyses. Predictions on the presence of functional domains and putative phosphorylation sites were extrapolated from bioinformatics software tools and databases.

The phylogenetic history of *VIK-like* genes was analysed to learn more about the origin of the *VIK* gene and to examine whether an important functional property of the *VIK* gene is reflected by conservation in other species. In addition, the homology of CpVIK and AtVIK was evaluated to examine their evolutionary relationship.

The results from Petersen (2012) raised the question whether the LEA-like protein CDeT11-24 is indeed a kinase substrate for CpVIK. Therefore, interaction of CpVIK with CDeT11-24 was determined in co-immunoprecipitation analyses and the phosphorylation of CDeT11-24 by CpVIK was analysed in *in vitro* kinase assays.

To elucidate if the CpVIK and CDeT11-24 proteins are localised in the same subcellular compartment and to delimit further potential CpVIK substrates, the intracellular distribution of a chimeric CpVIK-GFP protein was analysed by fluorescence microscopy.

The expression of the *CpVIK* gene and the CpVIK protein were examined under various stress conditions to learn more about the involvement of CpVIK in drought response. Functionally related proteins are often co-expressed. Therefore, it was investigated whether CpVIK and CDeT11-24 are induced by the same stresses on the RNA and protein level. CpVIK phosphorylation during dehydration was monitored, to explore a putative activation or deactivation upon stress treatment.

Since an involvement of CpVIK in abiotic stress response was hypothesised, the question arose whether AtVIK participates in stress response in *A. thaliana*. To explore, if *AtVIK A. thaliana* knock-out mutants (*Δvik*) show divergent phenotypic changes during stress treatments compared to wild type, *Δvik A. thaliana* plants were exposed to dehydration and salt stress at different developmental stages. In addition, germination of *Δvik* seeds was monitored, to compare desiccation tolerance in seeds and vegetative tissues.

In attempting to investigate downstream targets of AtVIK in seeds, comparative seed proteome analyses were performed and aberrant proteins were analysed *via* mass spectrometry.

The focus of this study was to demonstrate correlation of VIK proteins with downstream targets and to decipher common mechanisms of desiccation tolerance involving phosphorylation of LEA proteins.

2 Materials and Methods

2.1 Plant material

2.1.1 Provenance of plant materials

Craterostigma plantagineum

Originally collected in South Africa by Professor Volk from Würzburg (Volk, O. H. and Leippert 1971) *Craterostigma plantagineum* was further cultivated in the Max Planck Institute for Breeding Research in Cologne and in the Botanical Institute of the University of Bonn. Sterile *in vitro* cultured and non-sterile plants have been used for the experiments.

Lindernia brevidens* and *Lindernia subracemosa

Originally collected in Kenia on the Taita Hills by Professor E. Fischer from Koblenz (Fischer 1992b), *Lindernia brevidens* and *Lindernia subracemosa* were further cultivated in the Botanical Institute of the University of Bonn. Non-sterile plants have been used for the experiments.

Arabidopsis thaliana

In this study the ecotype Columbia-0 has been used which was selected by Rédei from the non-irradiated Laibach Landsberg population (Rédei 1992). Wild type plants and two transgenic lines were used:

SALK_133072

(Carrying a T-DNA insertion in the *VIK* Promoter [1000 bp prior to start codon])

SALK_002267

(Carrying a T-DNA insertion in the eleventh *VIK* exon)

Initial seeds of the transgenic lines were kindly provided by Prof. Neuhaus (University of Kaiserslautern) and derive originally from the Salk Institute Genomic Analysis Laboratory (http://signal.salk.edu/cgi-bin/tdnaexpress). Sterile *in vitro* cultured and non-sterile plants have been used both for the experiments.

2.1.2 Plant cultivation

Craterostigma plantagineum

Sterile plants were grown on MS agar in a light intensity of 80 µE/m^2/s at 22°C in a day/night cycle of 16/8 hours and subcultivated every six weeks.

Non-sterile plants were cultivated in LamstedtTon® granulate (Leni, Bergneustadt DE), watered with a 0.1 % solution of Wuxal (Manna, Ammerbuch–Pfäffingen, DE) at 18°C in a day/night cycle of 13/11 hours.

Lindernia brevidens* and *Lindernia subracemosa

Non-sterile plants were grown on soil in a light intensity of 80 µE/m^2/s in a day/night cycle of 8 hours of light at 22°C and 16 hours of darkness at 20°C.

Arabidopsis thaliana

Non-sterile plants were grown on wet, Lizetan® (Bayer, Leverkusen, DE) treated soil in a light intensity of 80 µE/m^2/s in a day/night cycle of 8 hours of light at 22°C and 16 hours of darkness at 20°C after vernalisation for 2 days at 4°C in the dark. At the four-leaf state (after 2 weeks) seedlings were transferred into new separate pots. Genotyping was performed after 4 weeks after sowing.

Six-week-old plants were transferred to a day/night cycle of 16 hours of light at 22°C and 8 hours of darkness at 20°C for seed production.

Sterile propagation of plants was performed as described in **2.1.5**.

2.1.3 Plant stress treatment

Craterostigma plantagineum

a) Stress treatment of whole plants

Dehydration stress treatments were imposed to adult *C. plantagineum* plants growing on LamstedtTon® granulate by withholding watering for different periods. The maximal dehydration was reached after 10 days without watering with a relative water content of 5-2 %.

b) Stress treatment of detached leaves

Leaves were cut off from untreated adult *C. plantagineum* plants and incubated in water for 8 hours in a light intensity of 80 µE/m^2/s at 22°C, followed by 8 hours of darkness at 20°C. For osmotic stress treatment the water was replaced by either 100 mM sodium chloride or 400 mM mannitol. Leaves were placed in open Petri dishes in a light intensity of 80 µE/m^2/s at 22°C in a day/night cycle of 13/11 hours for 48 h for dehydration stress treatments. Cold stress was applied by incubation in water at 4 °C for 8 hours in day light followed by 8 hours of darkness.

Lindernia brevidens and Lindernia subracemosa

a) Stress treatment of whole plants

Dehydration stress treatments were imposed to adult *L. brevidens* and *L. subracemosa* plants growing on soil by withholding watering for different periods.

b) Stress treatment of detached leaves

Leaves were cut off from untreated adult *L. brevidens* and *L. subracemosa* plants and incubated in water for 8 hours in a light intensity of 80 µE/m^2/s at 22°C, followed by 8 hours of darkness at 20°C. The water was replaced by either 100 mM or 300 mM sodium chloride or 400 mM mannitol for osmotic stress treatments. Leaves were placed in open Petri dishes in a light intensity of 80 µE/m^2/s at 22°C in a day/night cycle of 13/11 hours for 48 h for dehydration stress treatments.

Arabidopsis thaliana

c) Stress treatment of large plants on soil

For phenotypic analyses: Non-sterile plants of wild type and the *SALK_002267* line were sown as described in **2.1.2** on soil separately. At the four leaves state single plants of both wild type and *SALK_002267* were transferred together into new pots. The plants were further grown as described for 21 days (approximately 35 days after sowing) prior to stress treatment. The pots were then placed into Petri dishes, which were watered with 50 ml dH_2O per week as a control, or for osmotic stress treatments either with 100 mM or 200 mM sodium chloride solution. Dehydration stress was applied by withholding watering. Plants were transferred to 4°C for cold stress treatments. Phenotypic responses and changes in the relative water content were examined during stress treatments for 21 days or until the plants died.

For leaf proteome analyses: Plants of wild type and the *SALK_002267* line were grown as as described in **2.1.2. c)**. Salt stress was applied by watering with 100 mM NaCl at day four and two prior harvest.

d) Stress treatment of small and medium size plants on soil

Non-sterile plants of wild type and the *SALK_002267* line were sown as described in **2.1.2** on soil. At the four-leaf state single plants were transferred into new pots. The wild type and *SALK_002267* plants were further grown as described for 5 days (approximately 20 days after sowing; small plants) or 14 days (approximately 28 days after sowing; medium size plants) prior to stress treatment. The pots were then placed into big open Petri dishes, which were watered equally with 100 ml dH_2O per week. The water was replaced by 100 mM sodium chloride solution for osmotic stress treatments. For dehydration stress treatments watering was stopped completely. Plants were transferred to 4°C for cold stress treatments. Phenotypic responses and changes in the relative water content were examined during stress treatments for 21 days or until the plants died.

2.1.4 Determination of the relative water content

The relative water content (RWC) of plants was calculated according to the formula:

Formula 1: Calculation of the relative water content

$$RWC = \frac{(\mathrm{FW} - \mathrm{DW})}{(TW - DY)} \times 100$$

RWC: Relative water content (%). Fwt (fresh weight); Twt (turgescent weight): weight after rehydration of leaves for 24 h in H_2O. Dwt (dry weight): weight of leaves after 24 h at 80°C.

2.1.5 Germination assay

Germination assay on MS-media

All seeds of wild type and *SALK_002267* were surface-sterilised twice for 10 min with 100 % EtOH and plated in lots of 25 seeds per Petri dish containing MS agar media supplemented with or without 100 mM sodium chloride. The plates were incubated for 2 days at 4°C in the dark. Afterwards the plates were transferred to a light intensity of 80 µE/m^2/s in a day/night cycle of 8 hours of light at 22°C and 16 hours of darkness at 20°C. The germination rate was determined after 4 days under a stereoscopic microscope by counting the number of seeds with and without an emerged radical. Plates were photographed after 8 days when seedlings developed. The student t-test for two-sample sets assuming unequal variances was applied for significance measurement. Results with a confidence interval (1- [student's t-test]) of 95 % and higher were defined as statistically significant.

Germination assay on soil

Soil was dried at 80°C over night and watered with 1 ml/g of H_20 or 100 mM sodium chloride. Seeds of wild type and *SALK_002267* were sown in lots of 25 individuals per pot. For vernalisation the pots were incubated for 2 days at 4°C in the dark. The pots were then transferred to a light intensity of 80 µE/m^2/s in a day/night cycle of 8 hours of light at 22°C and 16 hours of darkness at 20°C. The germination rate was observed after 8 days by counting the number of seedlings in relation to the number of seeds that have been sown. The student t-test for two-sample sets assuming unequal variances was applied for significance measurement. Results with a confidence interval (1- [student's t-test]) of 95 % and higher were defined as statistically significant.

2.2 Bacterial strains

2.2.1 Genotypes of bacterial strains

***Escherichia coli* DH10B (Lorow, D. and Jessee, J. 1990)**; used for cloning

Genotype: F¯mrcAΔ(mrr-hsdRMS-mcrBC)ϕ80d lacZΔ M15 Δ lacX74 endA1 recA1 deoRΔ (ara, leu) 7697 araDD139 galU galK nup6 rpsLλ¯

***Escherichia coli* BL21(DE3) (Pharmacia, Freiburg, Germany)**; used for over-expression of proteins

Genotype: F⁻. ompT. hsdS(r⁻⁻B. m⁻B). gal. dcm. /λDE3 (lacI. lacUV5–T7 gene 1. ind1. sam7. nin5)

2.2.2 Cultivation of bacterial strains

Escherichia coli

The *E. coli* strains DH10B and BL21(DE3) were grown at 37°C in LB media.

After transformation with plasmids LB media, supplemented with the selective antibiotic, was used for growth.

2.3 Vectors

pET–28a (Novagen)

This plasmid harbours a 6x N/C–terminal histidine–tag (His–tag), the IPTG inducible T7lac promoter and a kanamycin resistance. The vector was used for (over-)expression of His-tagged proteins.

pET-16b (EMD Chemicals)

This plasmid harbours a 10x N/C–terminal histidine–tag (His–tag), the IPTG inducible T7lac promoter and an ampicillin resistance. The vector was used for (over-)expression of His-tagged proteins.

pGEX-2T (GE Healthcare)

This plasmid harbours a glutathione S-transferase (GST) coding region, the IPTG inducible tac promoter and an ampicillin resistance. The vector was used for (over-)expression of GST-tagged proteins.

pGJ280 (Dr. G. Jach; Max-Planck-Institute Cologne)

This plasmid harbours the constitutive CaMV35S promoter, a gene encoding for the green fluorescent protein (GFP) and an ampicillin resistance. The vector was used for localisation studies. The vector was constructed by Dr. G. Jach (Max-Planck-Institute, Cologne, DE).

2.4 Primers

The Primer3 program was used to generate stable primer pairs with compatible melting temperatures and a low self-complementary. Primers were obtained from Sigma–Aldrich (München, DE) and Eurofins Genomics (Ebersberg, DE). All primers were diluted to a concentration of 100 mM and stored at -20°C.

The following table shows all primers that were used in this study:

Table 3: Primer list

Name	***Sequence (5' → 3')***	***Restriction site***
Mutagenesis primers		
NcoI rev	GCTTGTCCATGGAGCTCGA	NcoI
cpVIKdead_f	ACCATTTGAAAGTCGGGAACTTTGGCCTAAGCAAG	
cpVIKdead_r	CTTGCTTAGGCCAAAGTTCCCGACTTTCAAATGGT	
Sequencing primers		
seq_cpVIK	GCTGTCAAACGAATTCTTCC	
GFPrev	TCCGTATGTTGCATCACCTTC	
p35S-pROK2	CACTGACGTAAGGGATGACGC	
Genotyping primers		
vik_ko_1s	GAAGGTGTCGCTGAGATTGAG	
vik_ko_1as	GAATTGATGACTTTTTCCTCCG	
vik_ko_2s	CAAATCCGCTGCTCATAAATC	
vik_ko_2as	ACCATTACCATCTCCTGAGGG	
LB335	ACTCAACCCTACCTCGGGCTATTC	
RT primers		
cpVIKPrimerfwd	AAGCGAGGGAAGTTCAGGC	
cpRT rev	TTGTTTGGCAGAGGAGGTGG	
LEA-like 11-24for	TCGGAAGACGAGCCTAAGAA	
LEA-like 11-24rev	ACAGCGCCTTGTCTTCATCT	
atVIKforcDNA	GACGGTGGCGAACAAGC	
atVIKrevcDNA	CGTCCCAGCATTTCACAATT	
EF1α_for	AGTCAAGTCCGTCGAAATGC	
EF1α_rev	CACTTGGCACCCTTCTTAGC	
Oligo(dT)18 primer	TTTTTTTTTTTTTTTTTT	
ATH–ACTIN2_FWD	ATGGCTGAGGCTGATGATATTCAAC	
ATH–ACTIN2_REV	GAAACATTTTCTGTGAACGATTCCT	
Vector specific primers		
T7-Promoter	TAATACGACTCACTATAGGG	
T7-Terminator	GCTAGTTATTGCTCAGCGG	
pGEX_3_rev	CCTCTGACACATGCAGCTCCCGG	

2.5 Chemicals, enzymes and marker

Chemicals, enzymes and marker were received from the following companies:

Apolloscientific (Ltd Bredsbury, CZ)

Biomol (Hamburg, DE)

Bio-Rad (München, DE)

BioGenes GmbH (Berlin, DE)

BJ Diagnostik Bioscience (Göttingen, DE)

Dushefa Biochemie B. V. (Haarlem, NL)

Fermentas (St. Leon-Rot, DE)

GE Healthcare (Freiburg, DE)

Invitrogen (Karlsruhe, DE)

Labomedic (Bonn, DE)

LMS Consult (Brigachtal, DE)

Merck (Darmstadt, DE)

Roth (Karlsruhe, DE)

Sigma-Aldrich (München, DE)

Stratagene (Heidelberg, DE)

Thermo Fisher Scientific (Waltham, USA)

Lenie (Bergneustadt, DE)

2.6 Kits

NucleoSpin Extract II Kit (Macherey-Nagel, Düren, DE)

NucleoBond Xtra Maxi Plus Kit (Macherey-Nagel, Düren, DE)

RevertAid First Strand cDNA Synthesis Kit. Fermentas (St. Leon–Rot, DE)

2.7 Equipment

Agarose gel electrophoresis chamber	EasyCast (Owl-Scientific, Portsmouth, USA)
Blotting chambers for proteins	XCell IITM Blot Module (Invitrogen, Carlsbad, USA) and Criterion Blotter (Biorad, Munich, DE)
Centrifugal Filter	Amicon Centrifugal Filter Devices 10K (Millipore, Billerica, USA)
Centrifuges	5415D; 5417R, 5810R; Vacuum centrifuge: Concentrator 5301 (Eppendorf, Hamburg, DE)
Confocal Laser Scanning Microscope	Nikon Eclipse TE2000-U/D-Eclipse C1 (Nikon, Düsseldorf, DE)
Consumables	Pipette tips and centrifugal tubes (Sarstedt AG, Nümbrecht, DE)
Desalting columns	PD–10 (GE Healthcare, Freiburg, DE)
Electroporation device	Gene Pulser II with Pulse Controller II and Capacitance Extender II (Bio-Rad, München, DE)
HIS-Tag purification agarose beads	HIS-Select Nickel Affinity Gel (Sigma-Aldrich, St. Louis, USA)
Isoelectric focuser	Ettan IPGphor II IEF Unit & IEF–strip holder (Amersham, Buckinghamshire, GB)
Luminescent Image Analyser	LAS 1000 (Fujifilm Life Science, Stamford, USA)
Lyophilisation machine	LDC–2 (Christ, Osterode am Harz, DE)
Nanodrop	BioSpec-Nano (Shimadzu Biotech, Chiyoda-ku, J)
Nitrocellulose membrane	Amersham™ Protran™ Premium 0.45 µm NC (GE Healthcare, Freiburg, DE)
Particle Gun	Biolistic Particle Delivery System-1000/He Device System (Bio-Rad, München, DE)
PCR cycler	“T3 Thermocycler” (Biometra, Göttingen, DE)

pH-meter	SCHOTT GLAS (Mainz, DE)
Rotator	neoLab–Rotator 2–1175 (neoLab, Heidelberg, DE)
Spectrometer	SmartSpec 3000 (Bio-Rad, München, DE)
Scanner	Typhoon 9200 (Amersham, Piscataway, USA); Image scanner (Amersham, Buckinghamshire, Great Britain)
Sonification water bath	Sonorex Super RK102P (Bandelin electronics, Berlin, DE)
Ultrasonic Processor	UP200S (Hielscher, Teltow, DE)
UV-light table	PeQlab (Vilber, Eberhardzell, DE)
Whatman paper	(Schleicher und Schüll, Dassel, DE)

2.8 Databases and software

Properties and characteristics of genes and proteins have been analysed with a set of bioinformatic tools provided in the “ExPASy Bioinformatics Resource Portal” (http://expasy.org/tools/). In addition other software and databases were used to process images, translate DNA-sequences, align sequences and develop cloning strategies and locate phosphosites.

The following list contains computer programs and databases used in this thesis:

1001 genome SNPs by region tool (http://polymorph.weigelworld.org)

1001 proteomics tool (http://1001proteomes.masc-proteomics.org)

AIDA Image Analyzer 2.11 (Fujifilm Life Science, Stamford, USA)

Arabidopsis 1001 genome project (http://1001genomes.org/)

Arabidopsis *cis*-regulatory element database (http://agris-knowledgebase.org/)

Blastp – protein blast (http://blast.ncbi.nlm.nih.gov/Blast.cgi)

ClustalW2 (www.ebi.ac.uk/clustalw/)

Conserved domains tool (NCBI, https://www.ncbi.nlm.nih.gov/Structure/cdd/wrpsb.cgi)

eFP cell browser tool (http://bar.utoronto.ca/cell_efp/cgi-bin/cell_efp.cgi)

EZ-C1 3.20 (Nikon, Düsseldorf, DE)

GENtle (Magnus Manske, Cologne, DE http://gentle.magnusmanske.de/)

Group-based Prediction System 3.0 software (Hubei, CN http://gps.biocuckoo.org/)

ImageJ1 (Schneider et al. 2012; Wisconsin, USA; http://imagej.net)

Kinase Phos 2.0 (http://kinasephos2.mbc.nctu.edu.tw/)

MEGA7 (Kumar et al. 2016)

Microsoft Office 2010 (Microsoft, Redmond, USA)

MotifFinder (www.genome.jp/tools/motif/)

National Center for Biotechnology Information (http://www.ncbi.nlm.nih.gov/)

NEBcutter2 (http://tools.neb.com/NEBcutter2)

NetPhos 2.0 (http://www.cbs.dtu.dk/services/NetPhos/)

NetPhosK (http://www.cbs.dtu.dk/services/NetPhosK/)

Nottingham Arabidopsis Stock Centre (http://arabidopsis.info)

Paint.NET (http://www.getpaint.net/index.html)

Primer3 (http://frodo.wi.mit.edu/primer3/)

PROSITE web tool (http://prosite.expasy.org/)

P3DB database (http://digbio.missouri.edu/p3db/)

Protscale (http://web.expasy.org/cgi-bin/protscale/protscale.pl?1)

QuikChange Site-Directed Mutagenesis program (http://www.stratagene.com/qcprimerdesign)

Reverse Complement (www.bioinformatics.org)

Salk–Institute (http://www.salk.edu)

ScanWise software (Agfa, Mortsel, B)

SIM – local similarity protein alignment tool (http://web.expasy.org/sim/)

SnapGene (www.snapgene.com)

The Arabidopsis Information Resource TAIR (Stanford, USA) (www.arabidopsis.org)

T–DNA Express (http://signal.salk.edu/cgi–bin/tdnaexpress)

Uniprot (http://www.uniprot.org/)

2.9 Media

LB-media (Bertani 1951):

1 g/l Tryptone, 10 g/l NaCl, 5 g/l yeast extract, pH 7.0

For plates 15 g/l Select-Agar

SOC-media (Hanahan 1983):

2 % (w/v) Tryptone, 0.5 % (w/v) yeast extract, 10 mM NaCl, 10 mM $MgSO_4$, 10 mM $MgCl_2$

MS-media (Murashige and Skoog 1962):

4.6 g/l MS-salt, 20 g/l sucrose, 1 ml/l vitamin solution (see below), pH 5.8

For plates 8 g/l Select-Agar

Media were autoclaved for 20 min at 121°C and 1.2 bar.

2.10 Media supplements

Ampicillin stock solution:	100 mg/ml in dH_2O. Dilution: 1:1000
Kanamycin stock solution:	50 mg/ml in dH_2O. Dilution: 1:1000
Vitamin solution:	2 mg/l glycine, 0.5 mg/l nicotinic acid, 0.5 mg/l pyridoxin-HCl, 0.1 mg/l thiamin-HCl in dH_2O, Dilution 1:1000

2.11 Isolation methods

2.11.1 Isolation of plasmid DNA from *E. coli*

Plasmid DNA was isolated as described by Sambrook et al. (1989) with modifications. A single clone was incubated overnight in 5 ml liquid LB-media supplemented with selective antibiotics at 200 rpm and 37°C. The bacteria were pelleted at 14,000 g and resuspended in 200 µl buffer 1 (50 mM Tris, 10 mM EDTA, pH 8.0, 100 µg/ml RNase A). Afterwards 200 µl buffer 2 (200 mM NaOH, 1 % (w/v) SDS) was added to the mixture. After the addition of 300 µl buffer 3 (3 M potassium acetate, pH 5.5), the sample was inverted and incubated on ice for 5 min. After centrifugation at 14,000 g for

10 min at RT, 800 µl of the supernatant were transferred to an equal volume of phenol-chloroform (1:1 v/v) and mixed by vortexing. The mixture was centrifuged and the upper phase was precipitated with 0.7 volumes Isopropanol (v/v) on ice for 15 min. Plasmid-DNA was pelleted by centrifugation at 16,000 g for 30 min at RT. The pellet was washed twice with 70 % (v/v) EtOH and dried at RT. The remaining RNA was cleaved by resuspending the pellet in Tris-RNase solution (50 µl 10 mM Tris, pH 8.5, 2 µl RNase A) and subsequent incubation at RT for 10 min. Samples were stored at -20°C.

The “Plasmid Maxi Kit” (Fermentas) was used according to the manufacturer’s instructions for the extraction of high amounts of pure plasmid DNA.

2.11.2 Isolation of genomic DNA from plant tissue

For genotyping PCRs leaf tissue of *A. thaliana* plants was transferred into 1.5 ml Eppendorf tubes and homogenised in 250 µl DNA-extraction buffer (100 mM Tris–HCL, pH 8.0, 100 mM NaCl, 10 mM EDTA, 1 % (w/v) SDS) with a pistil. 100 µl chloroform-Isomylalcohol (24:1) were added to the suspension and mixed prior to centrifugation at 16,000 g for 10 min at RT. The supernatant was transferred into new tubes and 100 µl Isopropanol was added to precipitate the DNA. After 5 minutes of incubation at RT the samples were centrifuged at 16,000 g for 10 min at RT. The supernatant was discarded and the pellet washed with 70 % (v/v) ethanol twice. Afterwards the pellet was resuspended in 100 µl dH_2O. Samples were stored at -20°C.

2.11.3 Isolation of RNA from plant tissue

Plant material (200 mg) was ground to fine powder in liquid nitrogen, transferred to Eppendorf tubes and vortexed with 1.5 ml RNA extraction buffer (38 % (v/v) phenol, 0.8 M guanidine thiocyanate, 0.4 M ammonium thiocyanate, 0.1 M sodium acetate, pH 5.0). The suspension was incubated at RT for 10 min. After centrifugation at RT for 10 min at 10,000 g the supernatant was mixed with 300 µl of chloroform–isoamylalcohol (24:1). The samples were centrifuged (10,000 g, 10 min, 4°C) and the upper phase was precipitated with 375 µl of ice-cold isopropanol and 375 µl buffer 2 (0.8 M sodium citrate/1 M sodium chloride) for 10 min at RT. After centrifugation at 12,000 g for 10 min at 4°C the RNA pellet was air-dried and resuspended in 100 µl sterile dH_2O. 167 µl of 4 M LiCl were added and the mixture was incubated on ice for 2 h. The RNA was pelleted by centrifugation at 14,000 g for 20 min at 4°C. The pellet was washed with cold (-20°C) 70% ethanol. After air drying of the pellet it was resuspended in 20-25 µl

sterile DEPC treated water (diethyl pyrocarbonate 0.1 %, deactivated by autoclaving). The RNA content was quantified and the quality was controlled on an agarose gel.

2.11.4 Isolation of proteins from plant tissues

Quick method (Laemmli 1970)

Plant material (50-200 mg) was ground to fine powder in liquid nitrogen. The powder was dissolved in 100-150 µl of 1 x SDS–sample buffer (2 % (w/v) SDS, 10 % (w/v) glycerol, 60 mM Tris-HCl, pH 6.8, 0.01 % (w/v) bromphenol blue, 0.1 M DTT [freshly added]) and gently mixed. Subsequently the samples were boiled at 95°C for 10 min and insoluble debris was pelleted afterwards for 10 min at 4,000 g at RT. The supernatants were transferred into new reaction tubes. The protein content was quantified or the samples were directly used for gel-electrophoresis (SDS-PAGE). For storage the samples were kept at -20°C.

Total protein extraction (Röhrig et al. 2006 with modifications)

The protein extractions were carried out on ice, whenever possible to prevent protein degradation.

Pulverized plant material (3 ml) was transferred to a 15 ml reaction tube, containing 10 ml ice-cold acetone. The suspension was vortexed and centrifuged for 5 min at 4,000 g at 4°C. The pellet was washed with acetone and resuspended in 10 ml 10 % (w/v) TCA and sonicated in an ice-cold water bath for 10 min. After centrifugation for 5 min at 4,000 g at 4°C, the pellet was washed with 10 % (w/v) TCA in acetone 3 times. Afterwards the pellet was washed with 10 % (w/v) TCA and subsequently twice with 80 % (w/v) acetone. The acetone-wet pellet was resuspended in 5 ml freshly prepared Dense SDS (30 % (w/v) sucrose, 2 % (v/v) SDS, 0.1 M Tris–HCl pH 8.0, 5 % (v/v) 2–mercaptoethanol). 5 ml phenol were added and the suspension was mixed by vortexing. After centrifugation for 5 min at 4,000 g at RT the upper phase was transferred into new reaction tubes. Proteins were precipitated by the addition of 5 volumes of 0.1 M ammonium acetate in methanol at 20°C overnight. Proteins were pelleted by centrifugation for 20 min at 8,000 g at 4°C. The pellet was washed twice with ice-cold 0.1 M ammonium acetate and afterwards once with ice-cold 80 % acetone (w/v). Quantification of the protein content was carried out with the Bradford method (**2.18.2**) and the samples were subsequently used for gel-electrophoresis (SDS-PAGE,

2.13.2) or for phosphoprotein enrichment (**2.11.5**). The samples were kept at -20°C for storage.

2.11.5 Enrichment of Phosphoproteins (Röhrig et al. 2006 with modifications)

Pre-treatment of aluminium hydroxide

Aliquots of 120 mg aluminium hydroxide were washed twice with 1 ml IB-200 (30 mM MES-HCl pH 6.1, 0.25 % (w/v) CHAPS, 8 M urea, 0.2 M Na-glutamate, 0.2 M K-aspartate, 20 mM imidazole) in 2 ml tubes (30 sec, 4,000 g, RT).

Pretreatment of total protein pellets

Total protein pellets were resuspended in IB-A (30 mM MES-HCl pH 6.1, 0.25 % (w/v) CHAPS, 7 M urea, 2 M thiourea) to a final concentration of 3 mg/ml. In a water bath the suspensions were sonicated for 5 min at 4°C and mixed with 2 volumes of IB-B (30 mM MES-HCl pH 6.1, 0.25 % (w/v) CHAPS, 7 M urea, 2 M thiourea, 0.23 M sodium glutamate, 0.23 M potassium aspartate, 30 mM imidazole). The protein solutions were centrifuged at 20,000 g for 10 min at 10°C and the clear supernatants were transferred to new Falcon tubes.

Metal oxide/hydroxide affinity chromatography (MOAC)

The supernatants of the protein solutions were transferred to the prepared aluminium hydroxide in portions of 1 ml per aliquot. The samples were incubated for 60 min at 10°C on a rotating wheel and subsequently washed 6 times with 1.5 ml IB-200 (14,000 g, 1 min, 10°C). With 1 ml EB-300 (300 mM K-pyrophosphate, pH 9.0; 8 M urea) aluminium-bound phosphoproteins were eluted on the rotating wheel for 30 min at RT. Afterwards the suspensions were centrifuged at 16,000 g for 5 min at RT and the aluminium-free supernatants were concentrated in an Amicon Ultra–4 Centrifugal Filter (Ultracel–10K, Milipore) until a final volume of 100 µl was achieved by centrifugation at 6,000 g at 10°C. This concentrated phosphoprotein solutions were transferred to new reaction tubes and the volume was adjusted to 600 µl with dH_2O. The samples were incubated overnight with 7 µl DOC (2 % (w/v) sodium deoxycholate in DMSO) and 70 µl 100 % TCA-solution in 4°C for precipitation. Phosphoproteins were pelleted at 14,000 g for 10 min at 4°C and resuspended in 1 ml 25 % (w/v) TCA–solution (4°C). The suspensions were sonicated in a water bath for 5 min at 4°C and subsequently

centrifuged at 14,000 g for 10 min at 4°C. The pellets were washed twice with 1 ml ice-cold 80 % acetone in Tris–HCl (50 mM, pH 7.5) and stored in 100 % acetone at -80°C.

2.11.6 Enrichment of heat-stable proteins from *A. thaliana*

Plant seeds (0.5 ml) were ground to fine powder in liquid nitrogen and dissolved in 10 ml PBS (8 g/l NaCl, 0.2 g/l KCl, 1.44 g/l Na_2HPO^4, 0.24 g/l KH_2PO_4; pH 7.4) at RT. The suspension was incubated at 95°C for 10 min in a heating block and subsequently centrifuged at 16,000 g for 5 min at RT to pellet cell debris and denatured heat sensitive proteins. The supernatant was transferred to a new tube and the remaining heat stable proteins were precipitated with 5 volumes 100 % acetone overnight at -20°C. After centrifugation at 8,000 g for 20 min at 4°C, the pellet was washed with 10 % (w/v) TCA-solution in acetone. Subsequently the pellet was washed in 10 % (w/v) TCA-solution in dH_2O and twice with 80 % (w/v) acetone. The acetone-wet pellet was resuspended in 5 ml freshly prepared Dense SDS (30 % (w/v) sucrose, 2 % (v/v) SDS, 0.1 M Tris–HCl pH 8.0, 5 % (v/v) 2–mercaptoethanol). 5 ml phenol were added and the suspension was mixed by vortexing. After centrifugation for 5 min at 4,000 g at RT the upper phase was transferred into new reaction tubes. Proteins were precipitated by the addition of 5 volumes of 0.1 M ammonium acetate in methanol at -20°C overnight. Proteins were pelleted by centrifugation for 20 min at 8,000 g at 4°C. The pellet was washed twice with ice-cold 0.1 M ammonium acetate and afterwards once with ice-cold 80 % acetone (w/v). For storage the samples were kept at -20°C.

2.12 PCR

The polymerase chain reaction (PCR) was performed according to Mullis et al. (1986) with modifications. Typically the following reaction mixture and PCR programme were used:

	Sample (20 µl)		**Programme**		
14.8 µl	dH_2O	95°C	denaturation	30 s	
2 µl	PCR 10x buffer	95°C	denaturation	30 s	x 25
1 µl	template–DNA (1 µg/µl)	T_m-5°C	primer annealing	1 min	
0,5 µl	primer fwd. (10 mM)	72°C	DNA synthesis	1 min/kb	
0,5 µl	primer rev. (10 mM)	72°C	final DNA synthesis	5 min	
1 µl	dNTPs (10 mM)	4°C	storage	∞	
0.2 µl	*Taq* DNA-Polymerase (2.5 U/µl)				

The following reaction mixture and PCR programme were used for mutagenisis:

	Sample (20 µl)		**Programme**		
11 µl	dH_2O	95°C	denaturation	60 s	
4 µl	PCR 5x buffer	95°C	denaturation	30 s	x 35
2 µl	template–DNA (1 µg/µl)	T_m-5°C	primer annealing	1 min	
1 µl	primer fwd. (10 mM)	72°C	DNA synthesis	2 min/kb	
1 µl	primer rev. (10 mM)	72°C	final DNA synthesis	5 min	
0,5 µl	dNTPs (10 mM)	4°C	storage	∞	
0.5 µl	Phusion Taq				

2.13 Electrophoresis

2.13.1 Electrophoresis of nucleic acids (Adkins & Burmeister 1996)

Agarose gel electrophoresis was performed according to Adkins et al. (1996) with minor modifications to separate DNA fragments. Concentrations of 0.8% to 2% (w/v) agarose were chosen to separate the negatively charged DNA in an electric field.

The agarose was boiled in 1 x TAE buffer (40 mM Tris, 10 mM EDTA, pH 8.0) and cooled afterwards to about 50°C prior to supplementation with 0.001 volumes (v/v) of ethidium bromide stock solution (0.1 µg/µl ethidium bromide in 1 x TAE buffer). Subsequently, the liquid gel was poured into a gel tray and a comb was inserted to form wells. After the gel solidified the tray was inserted into a gel chamber filled with 1 x TAE buffer. The samples were mixed with 10 x loading dye (2.5 mg/ml bromphenol blue, 2.5 mg/ml xylencyanol, 2 % (v/v) 50 x TAE, 30 % glycerol) and loaded into the wells. In addition to the samples, a marker (GeneRuler 1 kb DNA ladder, Fermentas) was used to estimate the size of the DNA fragments. Electrophoresis was performed at a voltage of 90 *V*-130 *V* for 20-100 minutes and the gel was then analysed under UV light.

2.13.2 Electrophoresis of proteins (adapted from Laemmli 1970)

One dimensional SDS gel electrophoresis

SDS-polyacrylamide gel electrophoresis (SDS-PAGE) has been performed to separate proteins depending on their molecular weight. In this study discontinuous gels consisting of a stacking gel (2.16 ml dH_2O, 375 µl1 M Tris–HCl pH 6.8, 405 µl acrylamid 30 %, 30 µl 10 % (v/v) SDS, 30 µl 10 % (w/v) APS, 2.5 µl TEMED) and a separation gel (2.88 ml dH_2O, 2.34 ml 1.5 M Tris–HCl pH 8.8, 3.60 ml acrylamid 30 %, 90 µl 10 % (v/v) SDS, 90 µl 10 % (w/v) APS, 3.6 µl TEMED) were used. The gels were assembled into an electrophoresis chamber filled with Tris-glycine running buffer (25 mM Tris, 192 mM glycin, 0.1 % (w/v) SDS).

Protein pellets were dissolved in 1 x SDS–sample buffer (2 % (w/v) SDS, 10 % (w/v) glycerol, 60 mM Tris-HCl, pH 6.8, 0.01 % (w/v) bromphenol blue, 0.1 M DTT [freshly added]) and protein solutions were mixed with 1 volume of 2 x SDS–sample buffer. The samples were then boiled at 95°C for 10 min in a heating block and centrifuged prior to loading on the collection gel. Electrophoresis in the stacking gel was performed

in a current of 10 mA. Proteins were separated in the separation gel in a current of 20 mA.

Two dimensional SDS gel electrophoresis

Proteins were first separated according to their isoelectric point (first dimension) by isoelectric focussing (IEF) and then and subsequently separated by SDS-PAGE according to their molecular weight (second dimension) for two dimensional SDS gel electrophoresis.

Protein pellets were resolved in 130 µl of freshly prepared rehydration solution (7 M urea, 2 M thiourea, 2 % (w/v) CHAPS, 0.002 % (w/v) bromphenol blue, 0.2 % (w/v) DTT, 0.5 % (v/v) IPG buffer) and incubated at RT for 3 h. To remove any insoluble components the samples were centrifuged at 20,000 g for 5 min at 4°C and 125 µl of the supernatants were applied in the IEF strip holder. The IPG strip (GE Healthcare) was transferred into the holder and covered with mineral oil. The strip holder was then covered with a lid and inserted into the IEF device (Ettan IPGphor II IEF Unit & IEF–strip holder, Amersham, Buckinghamshire, GB). Prior to separation of the proteins in the electric field, the strip was firstly rehydrated for 15 h. Proteins were subsequently separated with a voltage step gradient als follows: 30 min in 500 *V*, 30 min in 1000 *V* and finally 100 min in 5000 *V*. Afterwards the IPG strip was incubated for 15 min at 50 rpm on a shaker in 5 ml equilibration buffer (50 mM Tris HCl pH 6.8, 2 % SDS, 6 M Urea, 30 % Glycerol, 0.002 % bromphenolblue) supplemented with 50 mg DTT. Subsequently, the strip was transferred to 5 ml equilibration buffer with 125 mg iodacetamide. Finally the IPG strip was placed on a SDS-PAGE gel and sealed with IEF agarose prior to separation.

2.14 Staining of polyacrylamide gels

2.14.1 Coomassie staining

Gels were stained with Coomassie blue according to Zehr et al. (1989) to visualise proteins after SDS-PAGE (**2.13.2**). Gels were incubated in fixation solution (50 % (v/v) methanol, 10 % (v/v) acetic acid) for one hour or overnight at RT on a shaker. After 3 washing steps for 10 min with dH_2O gels were incubated in the staining solution (80 g/l ammonium sulphate, 0.8 % (v/v) phosphoric acid, 0.08 % (w/v) Coomassie G250, 20 % methanol) on a shaker overnight at RT. The gels were washed several times with water to reduce background staining.

2.14.2 Pro–Q® Diamond phosphoprotein staining

The Pro-Q® Diamond phosphoprotein gel stain (Molecular Probes) binds specifically to phosphorylated serine, threonine and tyrosine residues of proteins. For staining of phosphorylated proteins gels were incubated 30 min in fixing solution (50 % (v/v) methanol, 10 % (v/v) acetic acid) on a shaker at RT. Afterwards fixation solution was discarded and the gels were incubated in fresh fixation solution without shaking at RT overnight. After 3 washing steps for 10 min in dH_2O gels were incubated in 30 ml Pro-Q® Diamond phosphoprotein in the dark for 90 min under continuous shaking. Gels were washed 3 times with destaining solution (20 % (v/v) acetonitrile, 50 mM sodium acetate pH 4.0) for 30 min in the dark to reduce background signals. Gels were rinsed with water and the signals were detected with the Typhoon scanner (excitation wavelength 532 nm, emission filter 610 nm).

2.15 Western blot

2.15.1 Transfer of proteins

Protein blots were performed according to Towbin et al. (1979) with modifications after separation of the proteins in a SDS-PAGE (**2.13.2**). Proteins were transferred by electrophoresis to a nitrocellulose membrane (Amersham™ Protran™ Premium 0.45 µm NC). The transfer took place in the XCell IITM Blot Module (Invitrogen, Carlsbad, USA) filled with Towbin buffer (25 mM Tris-HCl, 0,192 mM glycine, 20 % (v/v) methanol) at a voltage of 30 *V* for 1 h.

The efficiency of the protein transfer was verified according to Sambrook et al. (1989) by incubation of the blotted membrane for 10 min in 50 ml Ponceau staining solution (0.2 % (w/v) Ponceau S, 3 % (w/v) TCA-solution) and subsequent washing with dH_2O. After documentation of visualised proteins, the staining was removed by successive washes with TBST (20 mM Tris-HCL pH 7.5, 150 mM NaCl, 0.1 % (v/v) Tween-20).

2.15.2 Immunological detection of proteins (Towbin & Gordon, 1984)

The immunological detection of proteins was performed according to (Towbin & Gordon (1984) with modifications. After the Ponceau staining was removed the nitrocellulose membrane was incubated overnight at 4°C in 50 ml blocking solution (4

% [w/v] non-fat milk powder in TBST) to avoid unspecific interaction of the antibody with the membrane. Subsequently the membrane was washed with 50 ml TBST buffer for 10 min prior to incubation in 50 ml of the primary antibody at RT. The concentration of primary antibodies was different for each antibody and ranged from 1:1,000 to 1:5,000 (v/v) in blocking solution. After incubation, the membrane was washed 5 times with TBST (once briefly, once for 15 min and 3 times for 5 min) followed by the incubation for 45 min in 50 ml of secondary antibody raised against rabbit IgG (1:5,000 in blocking solution) at RT. The secondary antibody binds to the rabbit IgG of the primary antibody during the incubation. The membrane was washed as described above and incubated with the two components of the “ECL Western Blotting Detection Reagent” kit (GE Healthcare) according to manufacturer’s instructions to allow the horseradish peroxidase enzyme, coupled to the secondary antibody, to catalyse the oxidation of luminol leading to chemiluminescence with a wavelength of 425 nm. The chemiluminescence signals were detected with the “Intelligent Dark Box II” (Fujifilm Corporation) and are proportional to the amount of protein present on the blots.

Antibodies used in this study:

Anti-CpVIK (raised in this study)
Polyclonal primary antibody
Rabbit antiserum
Final bleeding (11.04.2014)
Dilution 1:2500
BJ Diagnostik Bioscience (Göttingen, DE)

Anti-CDeT11-24
Polyclonal primary antibody
Rabbit antiserum
Final bleeding
Dilution 1:1000

“Anti-Rabbit IgG–Peroxidase antibody”
Polyclonal Secondary antibody
Goat antiserum
Dilution 1:5000
Sigma-Aldrich (München, DE)

2.16 Reverse transcription PCR (Sambrook et al. 2001 with modifications)

The reverse transcription PCR was performed after isolation of RNA (**2.11.3**) to analyse abundance and quantity of transcrips. The “RevertAid H Minus First Strand cDNA Synthesis Kit” (Fermentas) was used according to manufacturer’s instructions.

2.16.1 DNase Treatment

Remaining genomic DNA in RNA samples was removed by digestion with the DNase I enzyme.

Sample (10 µl)		**Incubation**
1 µg	RNA	30 min at 37°C
1 µl	DNase I, RNase-free (Fermentas)	
0.1 x final volume	10 x reaction buffer (Fermentas)	
x µl	dH_2O	

The DNase I was inactivated afterwards by the addition of 1 µl 50 mM EDTA and incubation for 10 min at 65°C.

2.16.2 cDNA-Synthesis

Reverse transcription was performed after DNase treatment.

Sample (12 µl)

5 µl	DNase-treated RNA
2 µl	Oligo(dT)10-Primer (10 mM)
1 µl	dNTPs (10 mM)
4 µl	DEPC H_2O

The samples were incubated at 65°C for 5 min to denature any remaining RNA and to allow primer annealing and immediately cooled on ice. Afterwards the following components were added:

Sample (20 µl)		**Incubation**
4 µl	First-Strand 5 x buffer (Fermentas)	1 h at 42°C
0.5 µl	Transcriptase (Fermentas)	
3.5 µl	DEPC H_2O	

The samples were heated for 10 min at 70°C to deactivate the transcriptase and subsequently used for PCR or stored at -20°C. A reaction mixture without transcriptase enzyme was processed in parallel with the remaining DNase-treated RNA to ensure the absence of genomic DNA.

2.17 Cloning methods

2.17.1 Site-directed mutagenesis

Site-directed mutagenesis was performed according to Zheng et al. (2004) to generate point mutations in the ATP Co-factor binding site of CpVIK. The pET–28a plasmid harbouring the *CpVIK* gene was amplified with mutagenized primers in a PCR. Subsequently the parental matrix plasmid was digested with the DpnI restriction enzyme.

In addition the same procedure was applied to generate an NcoI restriction site in pET–28a harbouring the *CpVIK* gene for subsequent C-terminal GFP fusion.

Primer design

Mutagenesis primers were designed with the "QuikChange Site-Directed Mutagenesis" program (http://www.stratagene.com/qcprimerdesign).

The melting temperature (T_m) should be ≥ 78 ° C and was calculated according to the following formula:

Fomula 2: Calculation of the melting point for the mutagenesis primers according to the "QuikChange Site-Directed Mutagenesis" -manual

$$T_m = \frac{81.5 + 0.41(\%\,\mathrm{GC}) - 675}{primer\ lenght\ (bp) - \%_{Mismatch}}$$

Inserted point mutations should be located in the middle of the primers. Primers were obtained from Eurofins Genomics.

Mutagenesis PCR

The mutagenesis polymerase chain reaction as a modified version of the PCR was performed as follows:

	Sample (25 µl)		**Programme**		
19 µl	dH_2O	95°C	denaturation	30 s	
2,5 µl	PCR 10x buffer	95°C	denaturation	30 s	x 16
1 µl	plasmid DNA (25 ng)	55°C	primer annealing	1 min	
0,5 µl	primer fwd. (62,5 ng)	68°C	DNA synthesis	5 min	
0,5 µl	primer rev. (62,5 ng)	68°C	final DNA synthesis	5 min	
1 µl	dNTPs (5 mM)	4°C	storage		
0,5 µl	*PfuUltra HF* DNA-Polymerase (2,5 U/µl)				

The amplified plasmids harboured a mutation according to the mutation in the primers. The parental matrix plasmids have been isolated form *E. coli* and are consequently methylated, in contrast to the plasmids synthesized in the PCR. Therefore, the matrix

plasmids could be selectively digested with the DpnI restriction enzyme, which exclusively digests methylated DNA.

***DpnI* digestion**

Sample (26 µl)		**Incubation**
25 µl	mutagenesis PCR product	overnight at 37°C
1 µl	*DpnI* (10 U/µl)	

The remaining amplified plasmids were then transformed into *E. coli* and subsequently isolated for further experiments. Successful mutagenesis was confirmed *via* DNA sequencing.

2.17.2 Restriction digestion

To digest DNA with restriction enzymes according to Sambrook et al. (1989) the following reaction mixture was used:

Sample (20 µl)		**Incubation**
100 ng-1 µg	DNA	2 ½ h at 37°C
5 U	1. restriction enzyme	
0.1 x final volume	10 x reaction buffer	
x µl	dH_2O	

The volume of restriction digestion enzyme in the reaction mixture did not exceed 10 % of the total volume in order to avoid nonspecific reactions.

2.17.3 Phenol-chloroform-extraction

A purification of the DNA according to Chomczynski and Sacchi (1987) with few modifications was necessary in some cases for further use of restriction products. The

volume of the restriction mixture was first adjusted to 400 µl with distilled water. Then, 400 µl of phenol/chloroform/isoamyl alcohol (24-25-1) was added and the sample mixed by inverting. The samples were centrifuged for 10 min at 13,000 g at RT and the aqueous phase was transferred to a new reaction tube. This step was repeated with 100% chloroform to remove phenol residues. The aqueous phase was mixed with 1 volume of isopropanol and 1/10 volume of 3 M Na acetate and incubated for 2 minutes at RT. The subsequent centrifugation was carried out for 10 min at 12,000 g and 4°C. The resulting pellet was washed with 70 % ethanol, dried and dissolved in dH_2O.

2.17.4 Ligation

The following reaction mixture was used to ligate DNA fragments according to Sambrook et al. (1989) and the recommendations of Fermentas (http://www.fermentas.de/product_info.php?info=p580):

Sample	**(10 µl)**	**Incubation**
6 µl	dH_2O	16°C overnight
1 µl	10 x ligase buffer	
1 µl	vector DNA (x ng/µl)	
1 µl	insert (y ng/µl)	
1 µl	*T4-DNA-Ligase* (5 U/µl)	

The optimal ratio of vector and insert DNA in ligation reactions was calculated according to the formula:

Formula 3: Calculation of the optimal amount of DNA to be used for the ligation of insert and vector following the recommendations of Fermentas for the *T4 DNA* ligase

$$concentration\ (insert) = \frac{[concentration\ (vector)]\ *\ [length\ (insert)\ in\ kb\ ]*\ 3}{[lenght\ (vector)\ in\ kb]}$$

2.17.5 Transformation of bacteria

Escherichia coli

The preparation of chemically competent *E. coli* cells and their transformation was carried out according to (Hanahan (1983) with modifications by Stiti et al. (2007).

a) Production of chemically competent E. coli cells

A bacterial colony from a fresh LB plate was transferred into 3 ml of LB medium and incubated overnight on a shaker at 250 rpm at 37°C. From this preculture, 1 ml was transferred into 50 ml of fresh LB medium. This main culture was incubated at 200 rpm at 37°C until an OD_{600} of 0.35-0.45 was reached. Subsequently, the bacteria were pelleted by centrifugation for 10 minutes at 4000 g at 4°C. The pellet was resuspended in 15 ml of ice-cold TFBI buffer (30 mM KOAc, 100 mM RbCl, 10 mM $CaCl_2$, 50 mM $MnCl_2$, 15 % glycerol, pH 5.8, sterile filtered) and incubated for 10 min on ice. This was followed by centrifugation for 10 min at 4,000 g at 4°C, resuspension of the pellet in 15 ml ice-cold TFBII buffer (10 mM MOPS, 75 mM $CaCl_2$, 10 mM RbCl, 15% glycerol, pH 6.5, sterile filtered) and the incubation on ice for 5 min. After centrifugation for 10 min at 4,000 g at 4°C, the cells were resuspended in 2 ml of TFBII and frozen in 50 µl aliquots in liquid nitrogen. The competent cells were stored at -80°C.

b) Transformation of chemically competent E. coli cells

A 50 µl aliquot of competent *E. coli* cells was slowly thawed on ice for about 10 minutes and mixed with 1 µl of plasmid DNA (100 ng / µl) or 5 µl of ligation mixture. Mixing was carried out by slow inversion. After 30 minutes of incubation on ice, a heat shock was carried out in a heating block for 52 seconds at 42°C. The cells were quickly placed on ice, incubated for 2 min and then regenerated with 500 µl of 37°C prewarmed SOC medium. The mixture was incubated on a shaker for 1 h at 250 rpm and 37°C. Subsequently, the cells were plated in portions of 50-350 µl on LB plates containing the appropriate antibiotics. The plates were incubated overnight at 37°C.

2.17.6 Colony-PCR

Colony PCRs were performed according to Sambrook et al. (1989) to verify whether colonies of *E. coli* contained the desired construct. For this purpose, 1 µl of distilled water was pipetted next to the colony and cells were resuspended. 1 µl of the mixture was used for the PCR.

	Sample (20 µl)		**Programme**		
14.8 µl	dH_2O	95°C	denaturation	30 s	
2 µl	PCR 10x buffer	95°C	denaturation	30 s	x 25
1 µl	colony in dH_2O	T_m-5°C	primer annealing	1 min	
0,5 µl	primer fwd. (10 mM)	72°C	DNA synthesis	5 min	
0,5 µl	primer rev. (10 mM)	72°C	final DNA synthesis	5 min	
1 µl	dNTPs (10 mM)	4°C	storage	∞	
0.2 µl	*Taq* DNA-Polymerase (2.5 U/µl)				

2.17.7 Glycerol stocks

E. coli clones were grown in selective medium, mixed with sterile 100 % glycerol in a ratio of 1:1, frozen in liquid nitrogen and stored at -80°C.

2.17.8 DNA-sequencing

DNA-sequencing was performed by Eurofins Genomics (Elbersberg, Germany). 15 µl purified plasmid-DNA (100 ng/µl) and 2 µl of a sequencing primer (10 pmol/µl) were dissolved in a total volume of 17 µl.

2.18 Quantification methods

2.18.1 Determination of nucleic acid concentrations

The concentrations of DNA and RNA were measured with the nanodrop spectrophotometer (BioSpec-Nano, Shimadzu Biotech, J). This device measures the absorption of different wavelengths in a sample and thus determines the purity and quantity of the nucleic acids. An OD_{260}/OD_{280} quotient between 1.8 and 2.0 indicates a high purity of nucleic acids.

The concentration (C) of nucleic acids is calculated with the absorption at 260 nm (OD_{260}) in combination with the dilution factor (F) and a DNA/RNA– specific constant according to the following formula:

Formula 4: Calculation of DNA and RNA concentration

$$OD_{260} \times specific\ constant \times F = C\ (\frac{ng}{\mu l})$$

$$specific\ constant\ for\ DNA\ = \frac{50\ ng}{1000}$$

$$specific\ constant\ for\ RNA\ = \frac{40\ ng}{1000}$$

2.18.2 Determination of protein concentrations

Pre-treatment of samples

a) *Proteins in 1 x SDS–sample buffer (Quick method samples)*

   5 µl of proteins dissolved in 1 x SDS–sample buffer were transferred into new tubes and mixed with 100 mM sodium phosphate buffer (pH 6.8). After incubation at RT for 10 min the samples were centrifuged at 12,000 g for 5 min at RT. Supernatants were used for quantification with the Bradford reagent.

b) *Protein pellets (Total protein extraction samples)*

   Protein pellets were centrifuged for 10 min at 8,000 g at 4°C. Acetone was removed and the pellets were dissolved acetone-wet in 7 M urea/2 M thiourea

overnight. Resolved proteins were used for quantification with the Bradford reagent.

Estimation of protein concentration

The "Bio-Rad Protein Assay" according to Bradford (1976) was used for determination of the concentration of proteins. In a 1 ml cuvette, 1 ml of 20 % Bradford reagent was mixed with 10 µl of a protein solution by inverting. After 10 minutes of incubation, the absorbance at 595 nm was measured with a photometer and assigned to a protein concentration with a calibration line, prepared with different concentrations of the standard protein BSA (bovine serum albumin) (Figure 3).

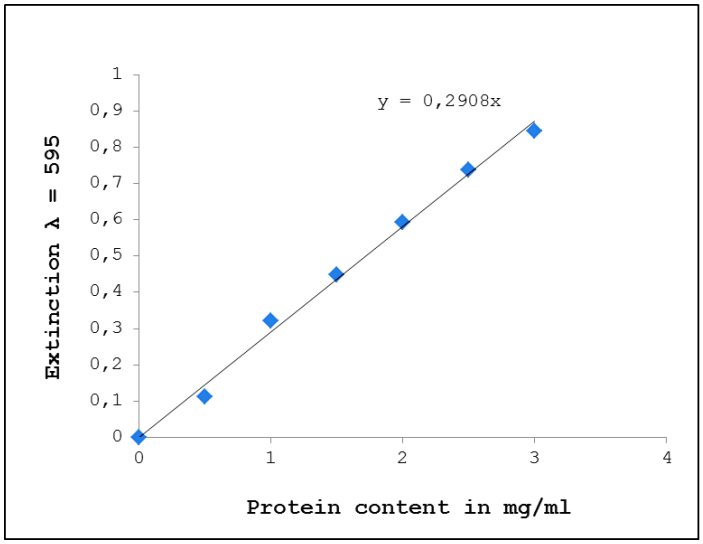

Figure 3: BSA-calibration line

2.18.3 Determination of the bacterial concentration in a suspension

To determine the concentration of bacteria in a suspension, the absorption at 600 nm was measured with a photometer. The corresponding bacteria-free solution was used as a reference. To calculate from the measured absorbance (A) the number of cells per ml, the following formula was used:

Formula 5: Calculation of the number of bacterial cells per ml from the absorbance at 600 nm according to the SmartSpec ™ 3000 Instruction Manual

$$\frac{cells}{ml} = A_{600} \times (5 \times 10^8) \times dilution\ factor$$

2.18.4 Quantification of protein and cDNA bands

Signals of protein and cDNA bands were quantified with the programme ImageJ as described by Dr. Daniel Kraus (http://home.arcor.de/d-kraus/lab/ImageJ_Western_blots.html).

Scans of protein blots or EtBr-DNA gels were opened with ImageJ and the areas of signals were defined with the selection tool. The bands of interest were automatically quantified with the tracing tool. The assigned values are proportional to the signal intensity. The procedure was repeated for a corresponding constitutive gene (elongation factor 1α) or protein (RubisCO), respectively for normalisation. To compare the normalised values for the bands of interest with each other, the value of one band was set to 100 % (for example untreated material) to achieve relative values (%).

The relative values of three independent experiments were used to calculate the median and the associated standard deviations.

2.19 Transient transformation of plants via particle bombardment

The leaf tissue of *C. plantagineum* was transformed biolistically *via* particle bombardment with a *CpVIK*::GFP fusion construct for intracellular localisation. The bombardment was performed according to Sanford et al. (1993) with minor modifications of van den Dries et al. (2011).

2.19.1 Preparation and loading of the microcarrier particles

30 mg of the gold "microcarrier" particles (1.6 µm in diameter, Bio-Rad) were weighed in a 1.5 ml Eppendorf reaction tube and 1 ml of 70 % ethanol was added. The mixture was mixed for 5 min by vortexing and incubated for 15 min at RT. After sterilization, the supernatant was carefully removed and the particles washed 3 times with dH_2O. Afterwards, the gold particles were resuspended in 500 µl of sterile 50 % glycerol to reach a final concentration of the gold particles of 60 mg/ml. This gold suspension was stored at 4°C for not longer than 2 weeks.

The gold particles were resuspended for 5 min by vortexing and 50 µl were transferred to a new 1.5 ml Eppendorf reaction tube. While continuous mixing, the following ingredients were added successively in the following order:

5 µg DNA of the pet28A vector containing the *CpVIK*::GFP construct (1 µg/µl)

50 µl of 2.5 M $CaCl_2$

20 µl of 0.1 M spermidine (dissolved in dH_2O)

The sample was then vortexed for 5 min, incubated for 1 min for sedimentation at RT and the supernatant carefully removed. The gold particles loaded with DNA were washed with 140 µl of 70 % ethanol, mixed by vortex for 5 min and then incubated for 1 min at RT for sedimentation. After removal of the supernatant, this washing step was repeated with 100 % ethanol and the gold particles were finally suspended in 30 µl of 100 % ethanol.

2.19.3 Particle bombardment of leaf tissue

Prior to bombardment leaves of 3-month old *in vitro* grown *C. plantagineum* plants were detached and distributed centrally on the surface of a Petri dish filled with ½ MS solid medium. An area of 5 cm^2 was covered. The Petri dish was placed on the sample holder. The bombardment was carried out according to the manufacturer's instructions with a helium-driven microprojector gun (bio-wheel). The required equipment was sterilized with 70 % ethanol. The macrocarrier was placed in the macrocarrier holder and 15 µl of DNA loaded gold were pipetted into the centre of the macrocarrier. As soon as the ethanol of the gold suspension was evaporated, the microcarrier holder and the sample holder were adjusted in the particle gun in a distance of 6 cm. The DNA loaded gold particles were accelerated with a helium pressure of 9.3 MPa in a vacuum of 3.6 MPa to transform the leaf material.

2.20 Determination of GFP activity in bombarded leaves

24 hours after the bombardment, the leaves were placed between two micro cover glass slides with a thickness of 0.13 to 0.17 mm. The visualization of the GFP fluorescence was performed with an inverted confocal laser scanner microscope. The GFP was excited at a wavelength of 488 nm and detection was conducted at 515 nm. The auto-fluorescence of chloroplasts was excited at 543 nm and detected at 570 nm. Images were stored with the EZ-C1 software version 3.20.

2.21 Overexpression of recombinant proteins

The expression systems pET–28a, pET–16b and pGEX-2T were used in the *E. coli* strain BL21 for overexpression of recombinant proteins.

A bacterial colony carrying the construct of interest was transferred from a fresh LB plate into 20 ml of LB liquid medium supplemented with the appropriate antibiotic and incubated overnight on a shaker at 250 rpm at 37°C. A main-culture of 100 ml was inoculated with 5 ml of the pre-culture in a 2 L Erlenmeyer flask and grown at 37°C and 200 rpm. When an OD_{600} of 0.5 was reached, the culture was incubated at 26°C for 15 min in the dark before isopropyl–β–D–thiogalactopyranoside (IPTG) was added (final concentration 1 mM) to induce the expression of the desired recombinant protein. The culture was incubated for 3 h at 26°C at 200 rpm und subsequently centrifuged at 4,000 g for 20 min at 4°C in 50 ml Falcon tubes. The bacterial pellets were stored at -20°C or directly used for affinity chromatography.

2.22 Purification of recombinant Proteins from *Escherichia coli*

For the purification of proteins with or without affinity tags the *E. coli* cells were firstly grown and induced as described in section **2.21**.

The frozen bacteria pellets were then incubated on ice for 15 min and subsequently dissolved in 5 ml of buffer A (50 mM NaH_2PO^4, 300 mM NaCl, 5 mM imidazole, 10 % (v/v) glycerol, 0,1 (v/v) Triton X-100) freshly supplemented with 1 mg/ml lysozyme. The suspensions were incubated for 30 min on ice. Further lysis of the cells was achieved by sonification with an ultrasonic processor (6 x 20 s). The samples were centrifuged at 14,000 g for 30 min at 4°C to remove cell debris and other insoluble cell components. The supernatants were sterile filtered (0,45 µm) into new tubes and further processed as described below.

2.22.1 Purification of recombinant CDeT11-24 without His-tag

After pretreatment **2.22** the lysate was incubated for 10 min in a water bath at 95°C, then cooled on ice for 10 min and centrifuged (14,000 g, 20 min, 4°C) to remove precipitated proteins. The heat-stable CDeT11-24 protein in the supernatant was then demineralised and rebuffered either into dH_2O or ammonium bicarbonate (100 mM NH_4HCO_3) using a PD-10 column (PD-10 Desalting Column, GE Healthcare, DE).

The purity and quantity of purified proteins was determined by Bradford assay (**2.18.2)** and SDS-PAGE (**2.13.2)**.

2.22.2 Affinity chromatography of His-tagged proteins

CpVIK6His-tag and AtVIK10His-tag

A column was filled with 1 ml Ni-NTA agarose and equilibrated successively with 3 ml dH_2O, 5 ml Ni-loading buffer (50 mM $NiSO_4$) and 3 ml buffer A (50 mM NaH_2PO_4, 300 mM NaCl, 5 mM imidazole, 10 % (v/v) glycerol, 0,1 (v/v) Triton X-100) (flow rate 0,5 ml/min). Then the lysate (**2.22**) was loaded to the pretreated column. To remove unspecifically bound proteins, the column was washed with 10 ml of buffer A followed by 8 ml of buffer B (50 mM NaH_2PO_4, 500 mM NaCl, 10 mM imidazole, 10 % (v/v) glycerol, 0,1 (v/v) Triton X-100). The elution of the proteins bound to the column was performed with 6 times 0.5 ml of buffer C. The purity and quantity of purified proteins was determined by Bradford assay **2.18.2** and SDS-PAGE **2.13.2**.

The fractions with the highest protein content were demineralised and rebuffered into either dH_2O, ammonium bicarbonate (100 mM NH_4HCO_3) or 1 x phosphorylation buffer (37.5 mM Tris pH 7.5, 26.5 mM $MgSO_4$, 750 mM NaCl, 5 mM EGTA, 5 mM DTT) using a PD-10 column (GE Healthcare) following the manufacturer's instructions.

The regeneration of the Ni-NTA agarose was carried out with 3 ml regeneration buffer (20 mM Tris-HCl pH 8, 500 mM NaCl, 100 mM EDTA). For storage, the column was washed with 20 % ethanol.

CDeT11-246His-tag

After pretreatment (**2.21**) the lysate was incubated for 10 min in a water bath at 95°C, then cooled on ice for 10 min and centrifuged (14,000 g, 20 min, 4°C) to remove precipitated proteins. The heat-stable CDeT11-246His-tag protein in the supernatant was then loaded on a Ni-NTA column and purified as described for CpVIK6His-tag and AtVIK6His-tag. A imidazole concentration of 20 mM has been used in buffer B for CDeT11-246His-tag.

The fractions with the highest protein content were demineralised and rebuffered into either dH_2O or ammonium bicarbonate (100 mM NH_4HCO_3) using a PD-10 column (GE Healthcare) following the manufacturer's instructions.

2.22.3 Affinity chromatography of GST-tagged proteins

After pretreatment (**2.22)** the lysate of 6-19GST-tag expressing cells was loaded on a column filled with 1 ml Glutathione Sepharose 4B matrix (GE Healthcare or Sigma) equilibrated with 5 ml PBS pH 7.3 (140 mM NaCl, 2.7 mM KCl, 10 mM Na_2HPO_4, 1.8 mM KH_2PO_4) (flow rate 0,2 ml/min). To remove unspecifically bound proteins, the column was washed with 10 ml PBS pH 7.3. The elution of the proteins bound to the column was performed 6 times with 0.5 ml of elution buffer (50 mM Tris-HCL, 10 mM reduced glutathione pH 8.0). The purity and quantity of purified proteins was determined by Bradford assay (**2.18.2)** and SDS-PAGE (**2.13.2)**. The fractions with the highest protein content were demineralised and rebuffered into either dH_2O or ammonium bicarbonate (100 mM NH_4HCO_3) using a PD-10 column (GE Healthcare) following the manufacturer's instructions.

2.23 Lyophilisation of proteins

In order to freeze-dry proteins, protein solutions were rebuffered in ammonium bicarbonate (100 mM NH_4HCO_3) or PBS buffer (8 g/l NaCl, 0.2 g/l KCl, 1.44 g/l Na_2HPO^4, 0.24 g/l KH_2PO_4; pH 7.4) using a PD-10 column (GE Healthcare), lyophilized for 2-3 days in a lyophiliser (LDC–2, Christ) and stored at -20°C.

2.24 Pull down assay

Pull down assays have been performed in this study to detect protein-protein interactions. A His-tagged bait protein was bound to a Ni-NTA column in order find prey proteins in crude plant extracts or pure protein solutions.

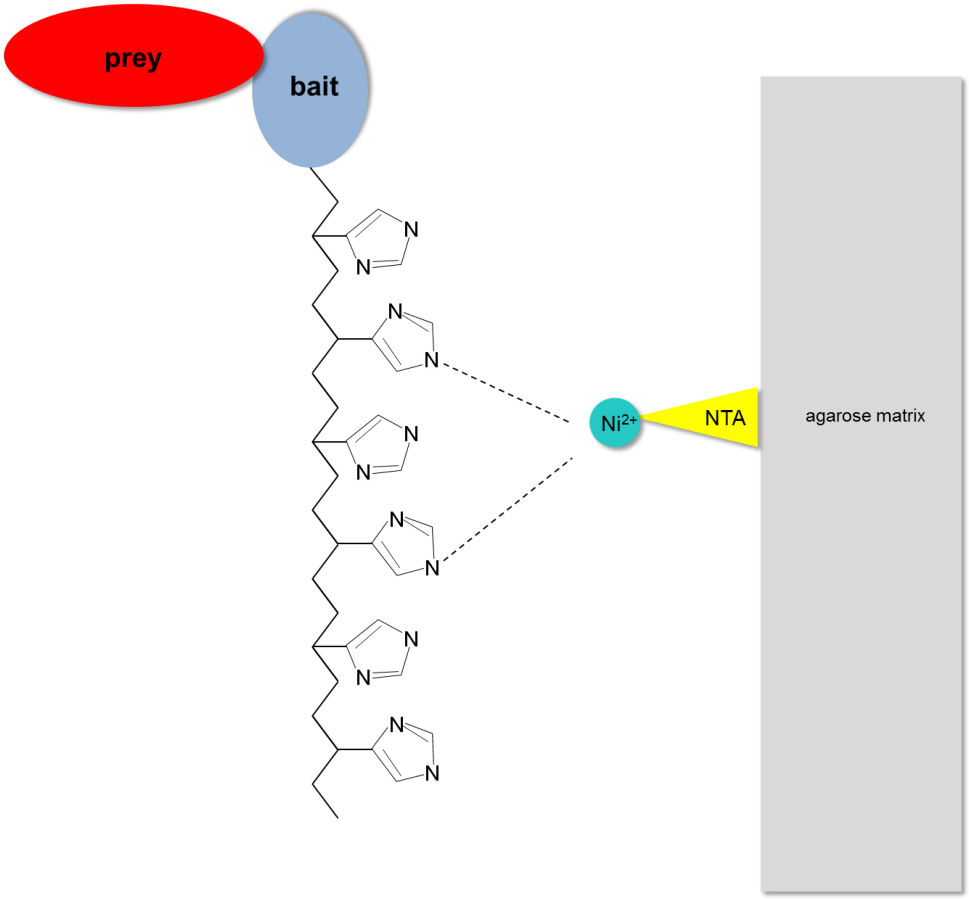

Figure 4: Principle of pull down assay

2.24.1 Pull down assay with pure proteins

After pretreatment **2.20** the lysate of bacteria expressing CpVIK6His or CpVIK$_{dead}$6His was supplemented with 250 mg of CDeT11-24 protein (without His-tag), 8 µl of 500 µM ATP and 90 µl phosphorylation buffer (187.5 mM Tris pH 7.5, 26,5 mM $MgSO_4$, 750 mM NaCl, 5 mM EGTA, 5 mM DTT). The mixture was incubated on ice for 15 min and subsequently loaded on a Ni-NTA column and affinity chromatography was performed as described in **2.22.2**. A higher imidazole concentration of 30 mM has been used in buffer B for pull down assays.

The quantity of the purified bait protein was determined by Bradford assay (**2.16.2)** and the fractions with the highest protein content were precipitated with 1/10 V 100% TCA-solution. Pellets were washed with 80 % acetone and stored at -20°C prior to use for identification of bait-prey interactions via SDS-PAGE (**2.13.2)** and Western blot analyses (**2.15**).

2.24.2 Pull down assay with plant extract

250 mg of lyophilized, recombinant CDeT11-246His-tag protein was incubated with leaf material of desiccated *C. plantagineum* plants, ground in buffer A (50 mM NaH_2PO_4, 300 mM NaCl, 5 mM imidazole, 10 % (v/v) glycerol, 0,1 (v/v) Triton X-100), for 15 min on ice. Subsequently the mixture was loaded on a Ni-NTA column and affinity chromatography was performed as described in **2.22.2** Elution fractions were used for identification of bait-prey interactions via SDS-PAGE (**2.13.2)** and Western blot analyses (**2.15**).

2.25 In vitro kinase assays

To determine kinase activity, *in vitro* kinase assays were performed according to Petersen (2012) with modifications.

Sample (50 µl)		**Incubation**
10 µl	substrate protein solution (0,5 µg/µl) in dH_2O	1-3 h at 30°C
10 µl	5 x phosphorylation buffer	
10 µl	kinase protein solution (0,001 - 0,5 µg/µl) in 1 x phosphorylation buffer	
1 µl	ATP 500 µM in 1 x phosphorylation buffer	
19 µl	dH_2O	

5 x Phosphorylation buffer: 187.5 mM Tris pH 7.5, 26.5 $MgSO_4$, 750 mM NaCl, 5 mM EGTA; 5 mM DTT

The reaction was stopped by the addition of 1 V of 1 x SDS–sample buffer (see section **2.13.2**). Differential kinase concentrations have been tested to investigate the kinase activity of CpVIK6His and $CpVIK_{dead}$6His. For each experiment a sample without substrate protein was included to determine autophosphorylation activity of the tested kinase. A sample with substrate protein but without kinase protein served a negative control of the reaction.

After the reactions have been stopped, the samples were separated by SDS-PAGE (**2.13.2**), stained with phosphostain (**2.14.2**) and subsequently with Coomassie (**2.14.1**) or lyophilised after *in vitro* reaction.

3 Results

Most of the cellular processes in eukaryotes are regulated by protein phosphorylation, mediated by kinases (Cohen 2002; Brognard and Hunter 2011) and MAP kinase cascades play crucial roles in plant signal transduction. Recently, MAPK networks that transduce extracellular stimuli and developmental signals got into the focus of science. Their role in biotic and abiotic stress responses emphasizes the importance of research in this field. So far, no MAPK has been characterised in *C. plantagineum*, but several proteins are predicted to be phosphorylated by MAPKs in response to drought stress (see **1.5**). A dehydration-stress specific *in-gel* kinase assay indicated the presence of a homolog to the MAPKKK VH1-interacting kinase (AtVIK; At1g14000) from Arabidopsis in *C. plantagineum* (Petersen 2012). The *AtVIK* transcript is known to be induced by salt and osmotic stress in Arabidopsis and is highly expressed in seeds (Wingenter et al. 2011). In the current work, a MAPKKK from *C. plantagineum*, CpVIK, has been characterised to gain insights in stress-dependent phosphorylation of desiccation or dehydration induced protective proteins in resurrection plants. To further decipher pathways shared by seed development and vegetative desiccation tolerance, analyses of seed germination in a *Δvik* knock out were carried out in Arabidopsis.

3.1 *In silico* analysis of the proteins CpVIK and AtVIK

In silico analysis is important to investigate the putative function of a protein and to identify specific motifs. This data provides information about various parameters, such as presence of localisation signals, isoelectric point and molecular weight of a protein, similarity of proteins, phylogenetic history, functional domains, putative phosphorylation sites and generally helps to interpret heterologous sets from genome, transcriptome and proteome data. In this study, a subset of bioinformatic tools was applied to analyse CpVIK and AtVIK.

3.1.1 Basic characterisation of CpVIK

The CpVIK protein consists of 443 amino acids (deduced from the nucleic acid sequence) and has a theoretical pI of 6.18. The calculated molecular weight is approximately 49.7 kDa (GENtle, Cologne, DE). The protein sequence comprises an ankyrin repeat region and a protein kinase domain (**Figure 5**) (http://prosite.expasy.org).

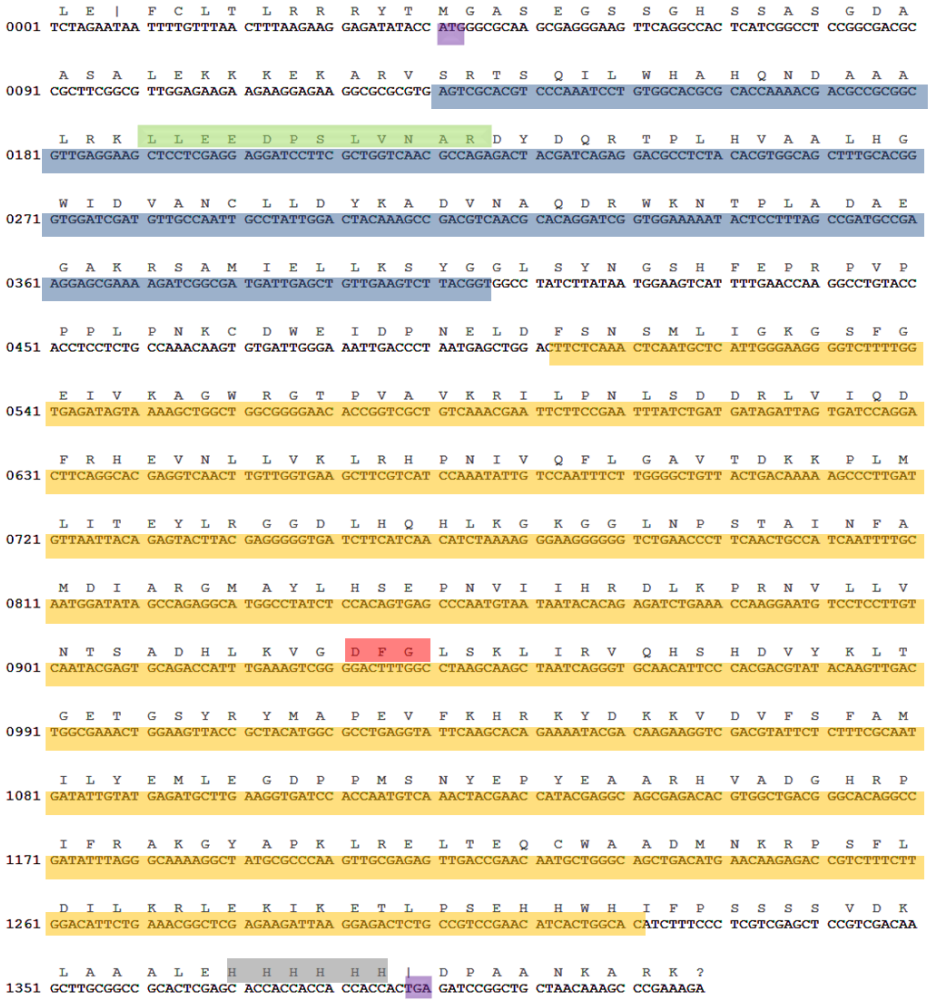

Figure 5: Nucleotide and protein sequence of CpVIK
Purple: Start and stop codon of the CpVIK gene; Green: Peptide identified by MS–analysis (Petersen, 2012); Blue: Ankyrin repeat region; Yellow: Kinase domain; Red: DFG motif; Grey: C-terminal 6x-His tag.

Signature patterns specific for serine/threonine kinases and tyrosine kinases have been identified in CpVIK (**Figure 6**).

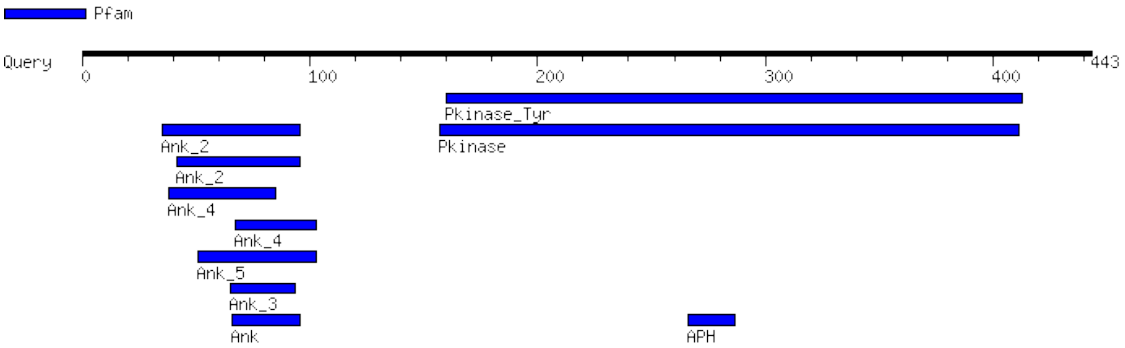

Figure 6: Motifs of the CpVIK protein
Graphical representations of the CpVIK domains generated by the MotifFinder (www.genome.jp/tools/motif/); Black: Query protein sequence; Blue: predicted motifs; Ank: Ankyrin repeat; Pkinase_Thyr: Protein tyrosine kinase; Pkinase: Protein serine/threonine kinase; APH: Phosphotransferase enzyme family.

CpVIK harbours overlapping tandem-repeat ankyrin motifs (ANK) as depicted in **Figure 6**, which are known to function as protein-protein interaction domains. Ankyrin motifs are modules of about 33 amino acids consisting of two alpha helices separated by loops (Sedgwick and Smerdon 1999). In 1987, the repetitive sequence motifs were first described in yeast, *Drosophila melanogaster* and *Caenorhabditis elegans* (Breeden and Nasmyth 1987). The number of ANKs in proteins typically ranges from two to over 20 ankyrin-repeats and they occur in a large number of functionally diverse proteins (Bork 1993). In *A. thaliana* 105 ANK proteins have been identified (Becerra et al. 2004; Huang et al. 2009). To further characterise the kinase domain, the sequence was analysed with the "Conserved Domains" tool (NCBI, https://www.ncbi.nlm.nih.gov/Structure/cdd/wrpsb.cgi). The serine/threonine kinase domain of CpVIK is classified as MAPKKK-like **(Figure 7)**.

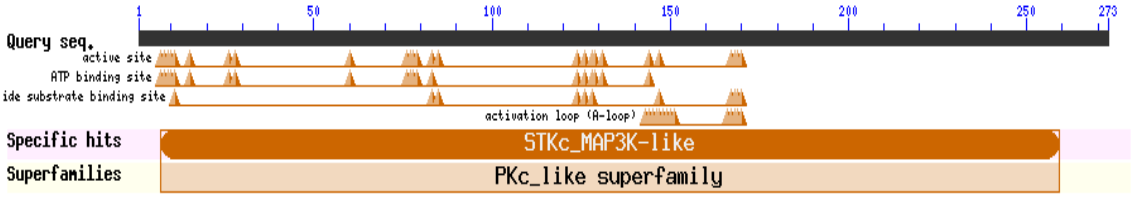

Figure 7: Kinase domain CpVIK
Domain classification generated by the Conserved Domains tool of NCBI (https://www.ncbi.nlm.nih.gov/Structure); Black: Query protein sequence; Orange: Predicted motifs; STKc_MAP3K-like: Catalytic domain of Mitogen-Activated Protein Kinase (MAPK) Kinase Kinase-like Serine/Threonine kinases; PKc_like super-family: Protein Kinases, catalytic domain.

MAPKKKs phosphorylate and activate MAPKK kinases and, respectively other substrate proteins mediating cellular responses to extracellular signals **(see 1.4.2)**.

3.1.2 Homology of CpVIK and AtVIK

The protein sequence of CpVIK is 80,7 % identical to AtVIK of *A. thaliana* (**Figure 8**).

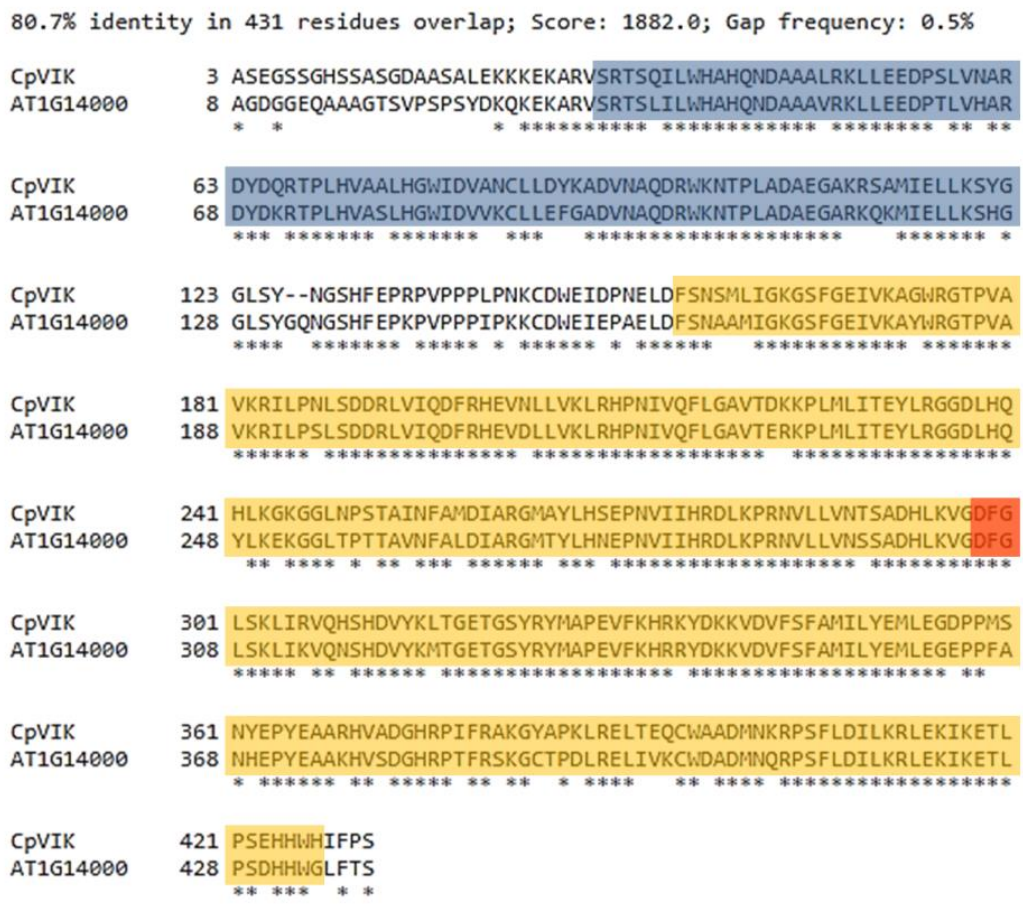

Figure 8: Alignment of the protein sequences of CpVIK and AtVIK
Amino acids marked with an asterisk are identical; Blue: Ankyrin repeat region; Yellow: Kinase domain; Orange: DFG motif; Alignment was generated with the SIM - Alignment Tool for protein sequences from http://web.expasy.org/sim/.

Except for the N-terminal part, which has a low identity of 32.1 %, the overall similarity of both proteins is very high. The ANK regions have an identity of 82.6 % and the kinase domains show an identity of 86 % (**Table 4**). Also the sequence between the ANK region and the kinase domain is highly conserved. It seems that both genes from different species evolved from a common ancestral gene by speciation. CpVIK can consequently be classified as an ortholog of AtVIK.

Table 4: Protein sequence identity of *CpVIK and AtVIK*
Determined with the “SIM - Alignment Tool” for protein sequences; AA = amino acid

Region (AA CpVIK / AA VIK)	***Identity in %***
Full-length (1-443 / 1-438)	*81*
N-terminal part (1-30 / 1-35)	*32.1*
ANK-repeat region (31-122 / 35-127)	*82.6*
Intermediate area (122-155 / 127-162)	*79.4*
Kinase domain (155-427 / 162-434)	*86*

3.1.3 Orthologs of CpVIK

CpVIK orthologs in the NCBI data bank

The CpVIK protein harbours two functional domains that belong to superfamilies, MAPKKK- and ANK superfamily, respectively. Ankyrin repeat-containing kinases (ANKKs) are widely distributed in various taxa. They play essential roles not only in plants (Ceserani et al. 2009; Wingenter et al. 2011; Hayashi et al. 2017), but also in several other organisms, such as humans (Chiswell et al. 2010; Grzywacz et al. 2012; Jabłoński et al. 2013; Garcia-Garcia et al. 2017) or mice (Holland et al. 2002; Hoenicka et al. 2010). The 100 protein sequences with the highest homology to CpVIK determined by pblast analysis (https://blast.ncbi.nlm.nih.gov/Blast.cgi) enclose putative orthologs mainly in angiosperms including both monocots and dicots. They show an identity above 80 % with an expectation value of 0 (full list in the supplementary data files). The functions of most of these highly homologous sequences are unknown. **Table 5** lists the five loci with the highest homology from different species.

Table 5: Orthologs of CpVIK in the NCBI data bank (highest identity)
Loci from different species with the highest homology to CpVIK identified with pblast analysis (https://blast.ncbi.nlm.nih.gov/Blast.cgi)

Locus	***Organism***	***Query cover***	***Identity***	***E-value***
XP_019234052.1	*Nicotiana attenuata*	*93 %*	*87 %*	*0*
XP_006348750.1	*Solanum tuberosum*	*93 %*	*87 %*	*0*
XP_011075534.1	*Sesamum indicum*	*92 %*	*88 %*	*0*
XP_017634171.1	*Gossypium arboreum*	*95 %*	*85 %*	*0*
XP_016580655.1	*Capsicum annuum*	*92 %*	*87 %*	*0*

CpVIK orthologs in Linderniaceae

Lindernia subracemosa, *Lindernia brevidens*, and *C. plantagineum* are closely related species of the *Linderniaceae* family (Rahmanzadeh et al. 2005; Phillips et al. 2008). Most members of this family, like *L. subracemosa*, are desiccation-sensitive. However, *L. brevidens* and *C. plantagineum* are desiccation-tolerant (Bartels et al. 1990; Fischer 1992b; Phillips et al. 2008). Due to the close phylogenetic relationship between *C. plantagineum*, *L. brevidens* and *L. subracemosa* comparative analyses on the abundance and regulation of CpVIK and putative orthologs in *Lindernia subracemosa* and *Lindernia brevidens* could give insights in the involvement of CpVIK in the formation of dehydration tolerance. The cDNA libraries of *C. plantagineum, L. brevidens and L. subracemosa* (Rodriguez et al. 2010a) were screened for paralog and ortholog transcripts of *CpVIK*.

Expression data doesn't reveal any paralogs in *C. plantagineum* (full Blast result in the **supplemental figure 63**). Since the genome sequence is not available, the presence of CpVIK paralogs cannot be excluded. In both, *L. brevidens* and *L. subracemosa*, one contig shows high sequence homology to the *CpVIK* gene (**Table 6**).

Table 6: Orthologs of CpVIK in *L. brevidens and L. subracemosa*
Contigs with the highest homology to CpVIK identified with nblast analysis in the transcriptome data bank of Rodriguez et al. (2010)

Contig	***Organism***	***Query cover***	***Identity***	***E-value***
CL3353	*L. brevidens*	*91 %*	*91 %*	*0*
CL5906	*L. subracemosa*	*91 %*	*92 %*	*0*

These ortholog DNA sequences of *L. subracemosa* and *L. brevidens* are highly identical to the *CpVIK* gene, demonstrating a strong conservation of the sequence in the *Linderniaceae* family (full Blast result in the **supplemental figures 64** and **65**).

The corresponding proteins exhibit only minor changes compared to CpVIK while most changes occur in both *L. subracemosa* and *L. brevidens,* respectively (**Figure 11)**.

Figure 9: Protein sequence alignment of CpVIK (*CP*) and the corresponding orthologs in *L. brevidens* (*LB*) and *L. subracemosa* (*LS)*
Amino acids marked with an asterisk are matching; Alignment was generated with the GENtle software (http://gentle.magnusmanske.de/).

The presence of further CpVIK orthologs in *L. subracemosa* and *L. brevidens* that were not expressed in the analysed tissues cannot be excluded due to missing genome sequence.

3.1.4 Phylogenetic analysis of ANKMAPKKKs

In Arabidopsis AtVIK and five other proteins (At3G59830, At2G43850, At2G31800, At4G18950 and At3G5876) are clustered in the subgroup C1 of the MAPKKK family, which is characterised by ankyrin repeat domains (Ichimura et al., 2002; Rudrabhatla et al., 2006). The VIK gene is not only present in *A. thaliana* and *C. plantagineum* but conserved in various taxa. Already early during evolution tandem-repeat ankyrin motif containing MAPKKKs (ANKMAPKKKs) belonging to the RAF-typ of MAPKKKs developed and can be found in several taxa. Already in bacterial genomes, corresponding genes are present. Protein sequences with the highest identity to CpVIK or one of the members of the MAPKKK subgroup C1 from *A. thaliana* from selected fully sequenced organisms were used to generate a phylogenetic tree based on Neighbour-Joining (**Figure 10**). Only sequences of MAPKKKs harbouring ankyrin-repeat motifs (ANKMAPKKKs) were considered. Additionally the CpVIK orthologs of the not sequenced *L. brevidens* and *L. subracemosa* (**3.1.4**) were included. *Homo sapiens* and the bacteria *Coxiella sp.* were chosen as outgroup.

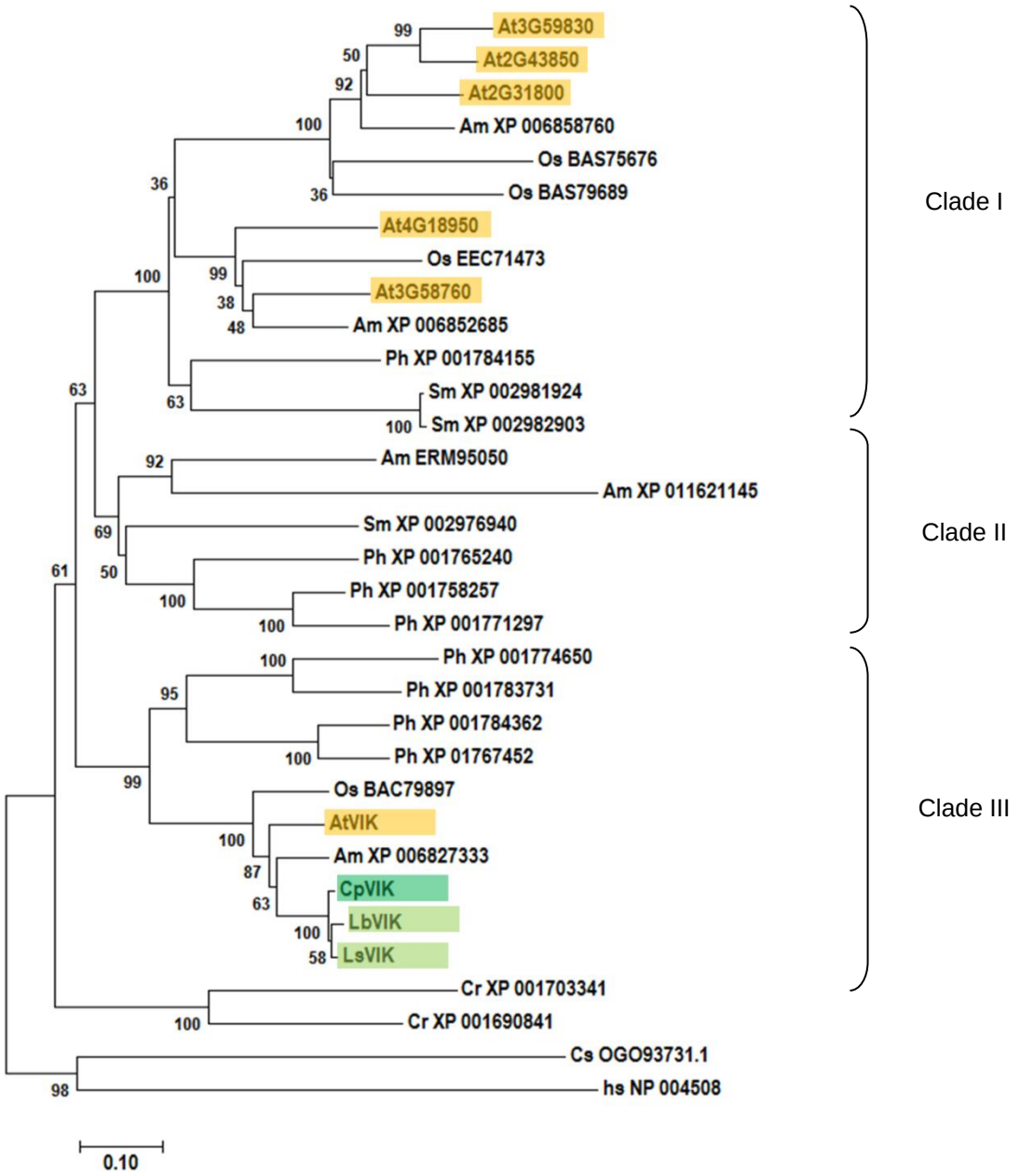

Figure 10: Evolutionary relationships of ANKMAPKKKs in *Arabidopsis thaliana* (At); *Amborella trichopoda* (Am); *Craterostigma plantagineum* (Cp); *Chlamydomonas reinhardtii* (Cr); *Coxiella sp* (Cs); *Homo sarpiens* (hs); *Lindernia brevidens* (Lb); *Lindernia subracemosa* (Ls); *Physcomitrella patens* (Ph) and *Selaginella moellendorffii* (Sm)
The evolutionary history was inferred using the Neighbor-Joining method (Saitou and Nei 1987). The percentage of replicate trees in which the associated taxa clustered together in the bootstrap test (500 replicates) are shown next to the branches. The tree is drawn to scale, with branch lengths in the same units as those of the evolutionary distances used to infer the phylogenetic tree. The evolutionary distances were computed using the Poisson correction method and are in the units of the number of amino acid substitutions per site. The analysis involved 33 amino acid sequences deriving from the NCBI data bank (except for Cp, Lb and Ls). All positions containing gaps and missing data were eliminated. There were a total of 244 positions in the final dataset. Evolutionary analyses were conducted in MEGA7 (Kumar et al. 2016).

During evolution ANKMAPKKKs did undergo fundamental changes and the representatives from plants separated early during evolution from outgroups, represented by human and Chlamydomonas (**Figure 10**). As depicted in **Figure 10** three main clades of ANKMAPKKKs could be identified in land plants. In each of these

clades representatives of the different land plant lineages (moss: *P. patens*, lycophytes: *Selaginella* and angiosperms) can be found. Clade II includes no representatives of the "higher" angiosperms (rice, Arabidopsis or *Lindernieaceae*). This points to a putative evolutionary loss within angiosperms, as an ortholog of the basal most angiosperm *Amborella trichopoda* is present. The other clades contain orthologs from all included species. The AtVIK orthologs of *C. plantagineum*, *L. brevidens*, *L. subracemosa* form a subclade within Clade III with single Amborella and rice orthologs. Contrastingly, in the other clades several paralogs of the other ANKMAPKKKs from Arabidopsis are present. In all clades a subclade division into spermatophyta and non-spermatophyta can be observed. The analogy of the CpVIK homologs in evolutionarily distinct species is also reflected in the domain structure (**supplemental figure 62**) and sequence identity (**supplemental** table 14).

3.1.5 Single nucleotide polymorphisms in *AtVIK*

Various *A. thaliana* ecotypes were sequenced in the 1001 genome project (The 1001 Genomes Consortium 2016). A comparison of single nucleotide polymorphisms (SNPs) within different ecotypes can help to understand the function and importance of a gene for an organism. Genomic sequences of the Arabidopsis ecotypes were analysed with the "SNPs by Region" tool (http://polymorph.weigelworld.org) to detect variable nucleotides in the sequence of *AtVIK* (Chr. 1: 4797358-4800283). In total 43 point mutations were identified in 407 ecotypes (**Figure 11**).

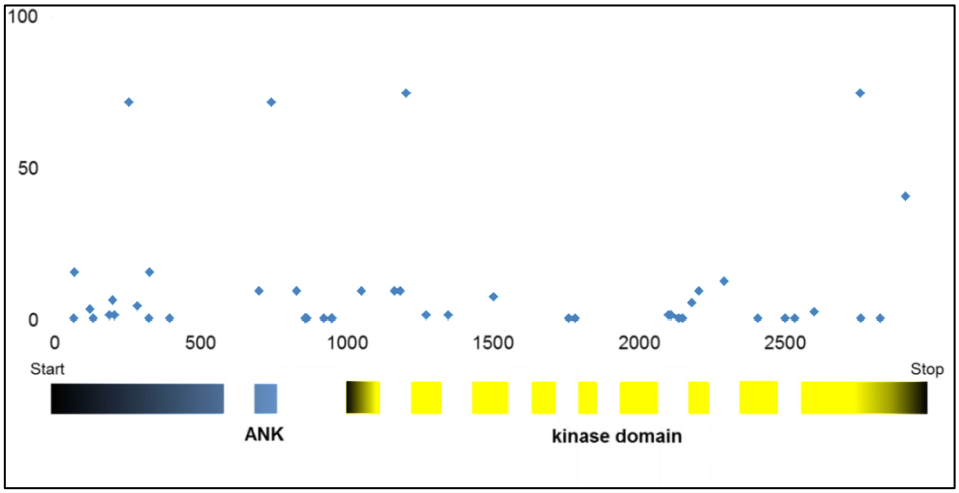

Figure 11: Variable nucleotides in the genomic sequence of *AtVIK* (*At1g14000*)
The position of a variable nucleotide is highlighted. The ordinate lists the number of ecotypes where the nucleotide change occurred. The protein model visualizes the intron-exon structure (NCBI) and represents the compared sections of the sequences; Blue: Ankyrin repeat region; Yellow: Kinase domain.

Of the 43 variable nucleotides 20 are located in introns and 23 in exons. 14 mutations in the coding regions are silent (**Table 8**). Therefore, nine variable amino acids are

located in the protein sequence of AtVIK (2,06 %) (detailed list in the supplementary data files). This result was verified with the "1001 proteomics tool" (http://1001proteomes.masc-proteomics.org). The variable amino acids are evenly distributed and most of them occur in only 1-16 ecotypes. Two amino acids (S-3→F-3 and P-393→R-393) were found to vary in 72 ecotypes.

Table 7: Variations in the DNA and protein sequence of *AtVIK* in *A. thaliana* ecotypes
Genomic sequences of the Arabidopsis ecotypes were analysed with the "SNPs by Region" tool (http://polymorph.weigelworld.org); Exons were identified by alignment with *AtVIK* cDNA (NCBI); Codon changing SNPs were verified with the "1001 proteomics tool" (http://1001proteomes.masc-proteomics.org)

Region	***#SNPs in genomic DNA***	***#SNPs in cDNA***	***# codon changing SNPs***
N-terminal part	*11*	*11*	*3*
ANK-repeat region	*3*	*2*	*2*
Intermediate area	*7*	*2*	*1*
Kinase domain	*22*	*8*	*3*

Thus, the *AtVIK* gene is highly conserved with a low rate of variation on the protein level.

3.1.6 Predicted phosphorylation sites in CpVIK and AtVIK

Most kinases are phosphorylated during activation or deactivation process and substrate phosphorylation mediated by MAPKKKs is known to involve phosphorylation of the MAPKKK by either autophosphorylation or phosphorylation by another kinase (MAPKKKKs) (Qi and Elion 2005; Cargnello and Roux 2011). Therefore, identification of phosphorylation sites is fundamental for our understanding of MAPK-action. Identification of phosphosites of *in vivo* phosphorylated proteins by MS analyses can only reflect a current state of the phosphorylation status of a protein. Therefore, it is challenging or even impossible to identify all phosphorylated sites of a protein *in vivo*. Bioinformatic tools predict putative phosphosites independently from the developmental stage, stress condition or other factors and thus are helpful tools for protein *in silico* analyses. Two phosphosites were previously identified *in vivo* for AtVIK at the positions T-324 and T-327 in a tonoplast enriched membrane fraction of *A. thaliana* (Whiteman et al. 2008).

On the other hand 24 putatively phosphorylated sites of CpVIK and 26 of AtVIK were determined with the Group-based Prediction System 3.0 software (**Table 7**). Only serine and threonine sites were predicted to be phosphorylated.

Table 8: Phosphosite prediction in the protein sequences of CpVIK and AtVIK

Determined with the Group-based Prediction System 3.0 software. Hits with a score higher than 9 and a cut off lower than 50% of the score value were included; Grey highlighted: Sites predicted in both CpVIK and AtVIK; Amino acids marked with an asterisk are predicted to be phosphorylated by MAPKs

CpVIK

#	Position	Code
1	4	S
2	7*	S
3	8*	S
4	11	S
5	12	S
6	14	S
7	19	S
8	34	S
9	68*	T
10	101*	T
11	112	S
12	156	S
13	177*	T
14	310	S
15	317*	T
16	320	T
17	322	S
18	344	S
19	392*	T
20	405	S
21	431	S
22	432	S
23	433	S
24	434	S

AtVIK

#	Position	Code
1	2	S
2	3	S
3	5	S
4	19	T
5	20	S
6	20	S
7	23*	S
8	25	S
9	26	Y
10	62	T
11	73*	T
12	106*	T
13	184*	T
14	256*	T
15	317	S
16	324*	T
17	327	T
18	329	S
19	351	S
20	388	S
21	392*	T
22	412	S
23	426	T
24	429	S
25	437	T
26	438	S

Among the two species eight sites were predicted to be phosphorylated in both, CpVIK and AtVIK, respectively. These conserved phosphorylation sites, mostly located in the kinase domain, include the previously *in vivo* identified sites from AtVIK (T-324 and T-327). MAPK mediated phosphorylation was predicted for seven sites in CpVIK (S-7, T-68, T-101, T-177, T-317, T-392) and six sites in AtVIK (S-23, T-73, T-106, T-184,

T-256, T-324, T-392). For AtVIK an autophosphorylation activity has been observed previously (Wingenter et al. 2011). The autophosphorylation might occur in one or several of the MAPK-predicted sites. Also for CpVIK autophosphorylation activity was shown in this thesis (**Figure 27**) and phosphorylation sites were determined and compared to the prediction (**supplemental table 13**). Since Ser-3 in AtVIK is mutated to Phe-3 in 72 ecotypes of *A. thaliana* (see **3.1.5)** a phosphorylation with functional importance in that site is unlikely.

3.2 Subcellular localization of the CpVIK-GFP protein

Plant cells are subdivided into membrane-bound compartments wherein specific metabolic reactions occur, such as chloroplasts cytoplasm, nucleus, mitochondria, Golgi apparatus, endoplasmic reticulum, peroxisome, vacuoles, cytoskeleton, ribosomes, and extracellular space. After biosynthesis, several proteins are destined to their target site determined by specific signal peptides, mostly located at the N-terminus. Other proteins reside in the cytoplasm. The subcellular localisation can provide information on the function of a protein and can be predicted *in silico* by means of putative signal sequences. For the CpVIK ortholog in Arabidopsis, AtVIK, a cytoplasmic localisation has been predicted by the “eFP cell browser” tool (http://bar.utoronto.ca/cell_efp/cgi-bin/cell_efp.cgi).

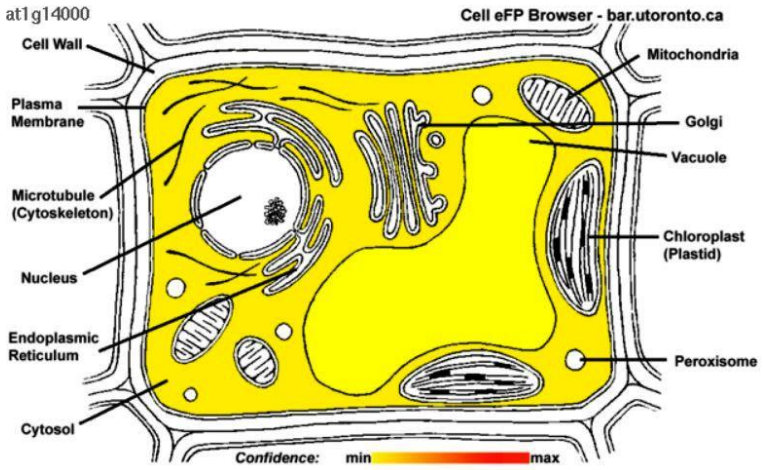

Figure 12: Subcellular prediction of AtVIK (At1g14000) with the Cell eFP Browser (updated Version from 2 July 2014) The electronic fluorescent pictograph is based on the equation described in Winter et al. 2007.

Experimentally AtVIK has been identified by LC-MS/MS in cytosolic preparations (Ito et al. 2011) and in a tonoplast fraction of Arabidopsis leaves (Whiteman et al. 2008). Bimolecular fluorescence complementation analyses (BiFC) in *A. thaliana* protoplasts

with a tonoplast monosaccharide transporter (AtTMT1) demonstrated a functional activity of AtVIK at the tonoplast membrane (Wingenter et al. 2011). *In planta* the subcellular localisation can be visualised by fluorescence microscopy after fusion of the protein coding sequence to the gene sequence of the green fluorescent reporter protein (GFP) in living cells. In this study the coding sequence of the *CpVIK* gene was fused to GFP for subcellular localisation studies, as described in the following paragraphs.

3.2.1 Construction and expression of CpVIK-GFP

Previously the coding sequence of *CpVIK* was cloned into the NcoI and SacI sites of the pET-28a(+) vector (Novagen, Madison, WI) (work by V. Giarola, unpublished). To generate a *CpVIK-gfp* chimeric gene an additional C-terminal NcoI restriction site was introduced into *CpVIK* by amplification of pET-28a(+)-*CpVIK* with phusion taq polymerase as described (**2.12**) with the mutagenesis primer *NcoI rev* and the *T7-Promoter* primer (**Figure 13**).

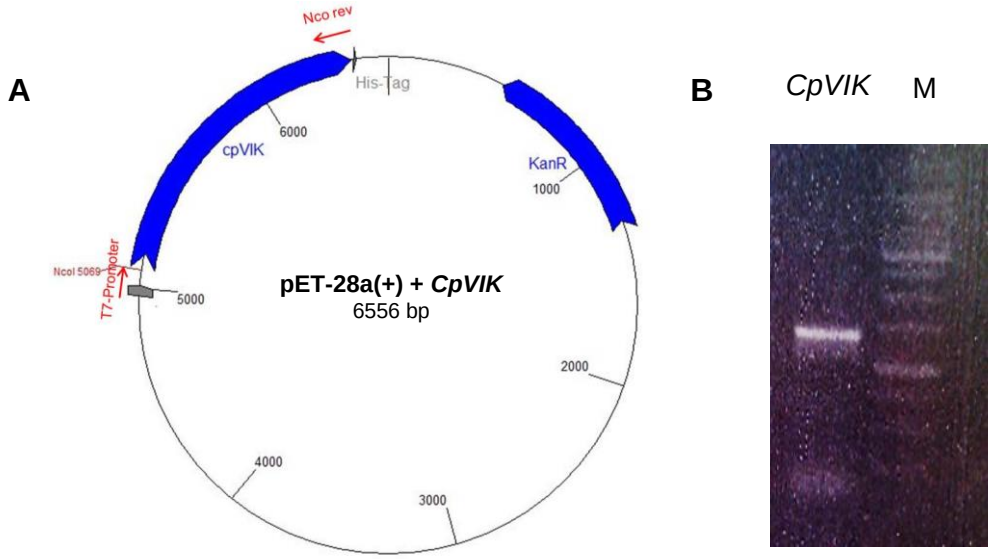

Figure 13: Expression vector pET28-a including the His-tagged *CpVIK*
A: Vector map; *CpVIK* and the kanamycin resistance gene (KanR, Aminoglycoside 3'-phosphotransferase) are represented by blue arrows. Primer binding positions are depicted with red arrows. The IPTG inducible lac-operator is represented by a grey box. The *CpVIK* coding sequence was amplified from a cDNA library of fully dried plants with a RWC of approximately 5% (Rodriguez et al., 2010) and cloned in into the pET-28a(+) vector (Novagen, Madison, WI) into NcoI and SacI restriction sites B: Agarose gel electrophoresis of the amplicon with NcoI rev/T7promoter primers amplicon size: 1396 bp, 1kb marker Fermentas.

The amplicon and the empty pGJ280 vector (Max-Planck-Institute, Cologne, DE; vector map enclosed as supplemental figure) were digested with NcoI. Afterwards *CpVIK* was and ligated into pGJ280. Successful ligation and the C-terminal fusion of GFP to *CpVIK* were confirmed by sequencing with *GFPrev* and *P35S-pROK2* (**Figure 14 A**).

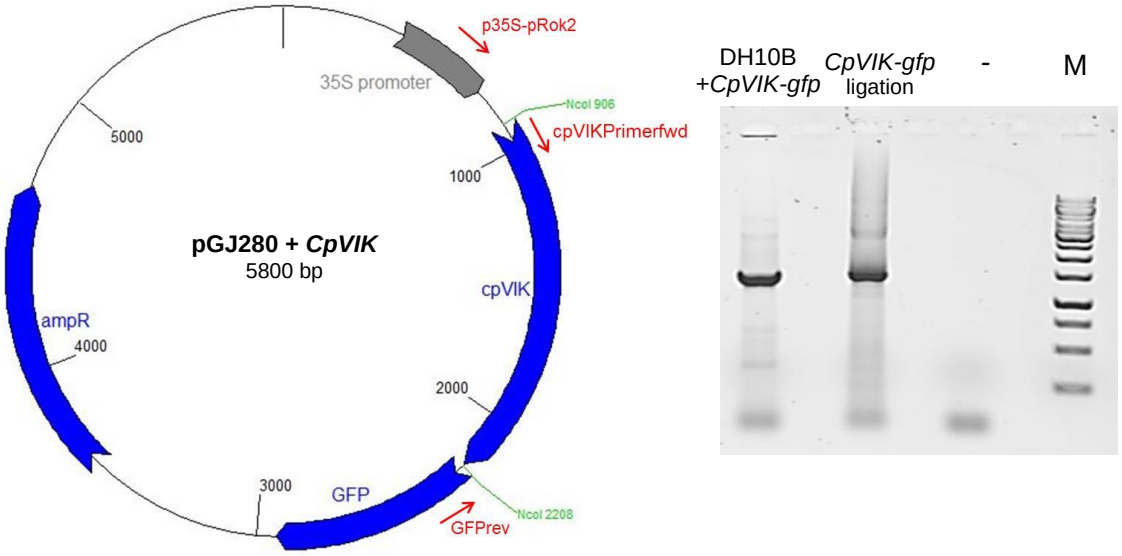

Figure 14: Vector pGJ280 including *CpVIK*
A: Vector map; *CpVIK* the *green fluorescent protein* and the ampicillin resistance gene are represented by blue arrows. The CaMV35S promoter is represented by a grey arrow. Primer binding positions are depicted with red arrows. After digestion of CpVIK and pGJ280 with NcoI and subsequent ligation, C-terminal fusion of GFP to CpVIK was confirmed by sequencing with GFPrev and p35S-pROK2; The resulting fusion protein consists of 1281 amino acids; B: Colony PCR of CpVIK-gfp expressing DH10B *E. coli* cells; Primer combination: CpVIKPrimerfwd/GFPrev; amplicon size: 1413 bp, 1kb marker fermentas.

The pGJ280+*CpVIK-gfp* construct was transformed into DH10B *E. coli* cells as described in **2.17.5**. Successful transformation with *CpVIK-gfp* was confirmed by colony PCR by with *CpVIKPrimerfwd GFPrev* as described in **2.17.6**. As a positive control the ligation mixture was amplified with the same primers (**Figure 14 B**). For transient transformation *via* particle bombardment plasmid DNA was extracted from *E. coli* on a large scale (described in **2.11.1**).

3.6.2 Transient expression of CpVIK-GFP in *C. plantagineum* leaf tissue

Expression and subcellular localisation of the CpVIK-GFP protein under the control of the 35S promoter was monitored in leaves of 3-month old *in vitro* grown *C. plantagineum* plants by fluorescence microscopy (**2.19**) 24 hours after particle bombardment with the pGJ280+CpVIK construct. Visualization of the GFP

fluorescence was performed with an inverted confocal laser scanner microscope and images were stored with the EZ-C1 software. Representative images of CpVIK-GFP fluorescence are shown in **Figure 15**. As shown in **Figure 15**, expression of the CpVIK-GFP protein resulted in an intracellular fluorescence.

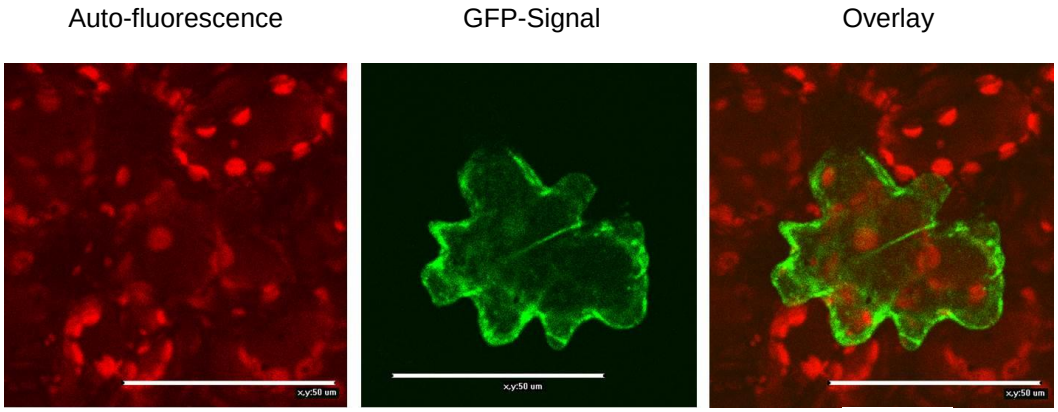

Figure 15: Localisation of CpVIK–GFP fusion protein
35S::CpVIK-gfp expressed in hydrated *C. plantagineum* leaf cells as described in 2.19. Green fluorescence of GFP in the cells was visualised under a laser-scanning confocal microscope (described in 2.20); red signals derive of autofluorescence of chloroplasts and green signals monitor GFP expression. The white scale bar represents 50 µm.

Thus, CpVIK shows the same subcellular localisation as AtVIK (Ito et al. 2011) and CDeT11-24 (Velasco et al. 1998) that has been predicted to interact with CpVIK (see **1.5**).

3.3 CpVIK antibody production

For further expression analysis as well as protein-protein interaction studies an antibody against the full-size CpVIK protein was generated. Recombinant CpVIK6His protein was overexpressed and purified for immunisation of two rabbits.

3.3.1 Expression and isolation of recombinant CpVIK

For overexpression of recombinant CpVIK the coding sequence was amplified by RT-PCR introducing an N-terminal NcoI and a C-terminal SacI restriction site with mutagenesis primers. Subsequently the amplification product was cloned into the respective sites of pET-28a(+) vector to generate a translational fusion in frame with C-terminal poly-His tag (work by V. Giarolla, unpublished).

The sequenced construct pET28a-CpVIK6His was transformed into *E. coli* BL21 cells (**2.17.5**) and cells were grown and induced as described in **2.21**. Recombinant CpVIK6HIS protein was isolated from bacterial pellets by affinity chromatography

(described in **2.22.2)**. As control a sample of the bacterial lysate was taken prior to loading on the Ni-NTA agarose column (F0). This sample included several protein bands, as depicted in **Figure 16 A**. The flow through (Ft) shows the same protein band pattern except for a missing band at about 45 kDa compared to the F0 sample, representing CpVIK6His protein that bound to the column. After washing the column to remove unspecifically bound proteins, CpVIK6His was eluted in six fractions (F1-6) with imidazole. CpVIK6His shows highest abundance in the F3 fraction as depicted in **Figure 16 A** and demonstrated in the elution profile (**Figure 16 B**). The CpVIK6His protein is highly enriched after affinity chromatography.

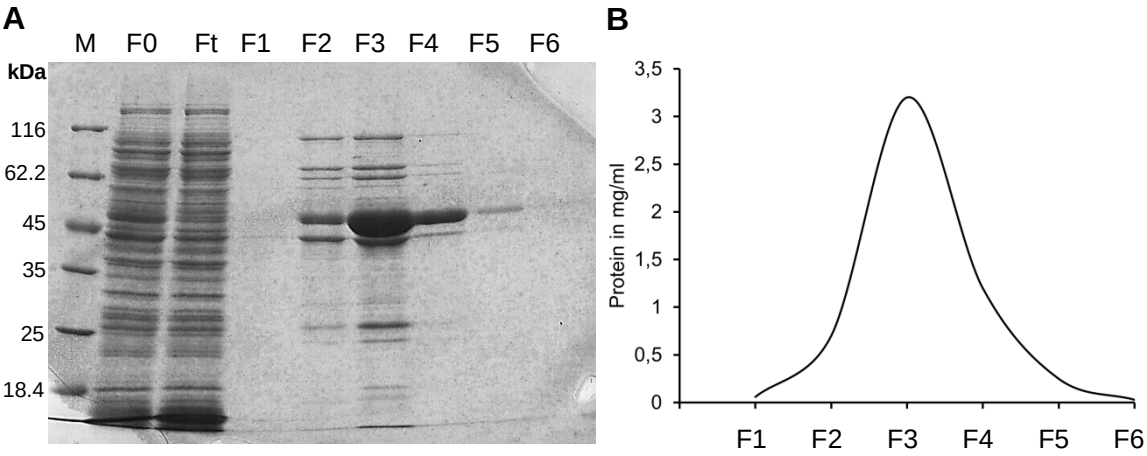

Figure 16: Affinity chromatography of overexpressedCpVIK6His recombinant protein
kDa: Kilodalton; M: Unstained protein marker; F0: bacterial lysate before loading onto the column; Ft: Flow-through; F1–6: Elution fractions; *E. coli* BL21 cells containing the pET-28aCpVIK6His construct were grown and induced (2.21) prior to affinity chroatography (2.22.2) to isolate recombinant CpVIK6His protein. A: Proteins were separated *via* SDS-PAGE (2.13.2) and stained with Coomassie blue (2.14.1); B: Elution profile of fraction F1-6; Protein contents were determined *via* Bradford assay (2.18.2).

After isolation of CpVIK6His, the elution buffer was exchanged to PBS buffer with PD-10 desalting columns (GE Healthcare). The protein content was determined *via* Bradford assay (**2.18.2**) and the quality of rebuffered CpVIK6His was evaluated on a SDS-PAGE gel (**Figure 23**). Known amounts of BSA were co-loaded as an additional control of protein quantity estimation. The CpVIK6His sample for immunisation contained 1.2 mg/ml CpVIK6His protein according to the Bradford measurement and confirmed by comparison of band sizes on a SDS-PAGE gel (**Figure 17**).

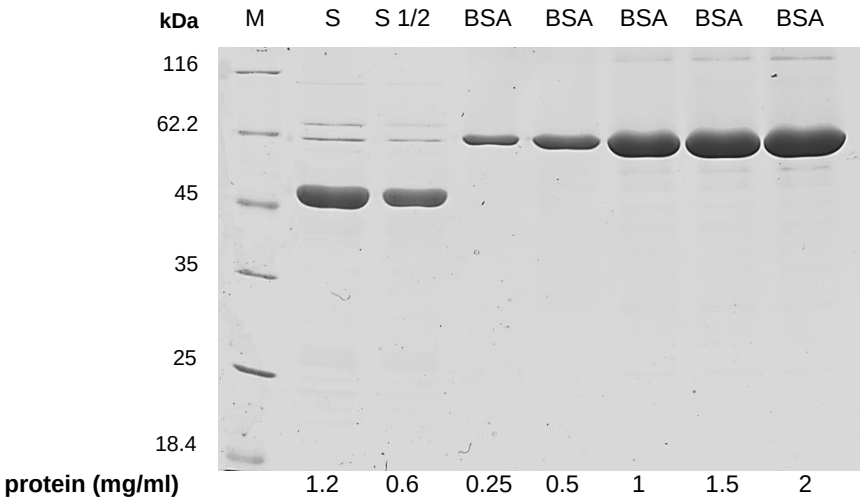

Figure 17: SDS-PAGE of CpVIK6His recombinant protein in PBS
kDa: Kilodalton; M: Unstained protein marker; S: CpVIK6His protein sample; S 1/2: dilution of S 1:2 (or 1 +1); BSA: Bovine serum albumin; Proteins were separated *via* SDS-PAGE (2.13.2) and stained with Coomassie blue (2.14.1); Protein concentrations were determined *via* Bradford assay (2.18.2).

CpVIK was lyophilised as described in **2.23** and 2 mg protein was sent for immunisation to BioGenes GmbH (Berlin, DE). The antisera were received after three months (final bleeding) and tested on pET28a-CpVIK6His expressing *E. coli* BL21 cells before and after induction as well as on purified CpVIK6His protein (**2.22.2**). Additionally preimmune serum taken from the same rabbits was also tested as negative control.

More bands are visible in the preimmune serum of rabbit 1 (**Figure 18 A**) compared to the preimmune serum of rabbit 2 (**Figure 18 B**). In the not induced *E. coli* cells no bands could be detected with the antibody of rabbit 1 in contrast to the antibody of rabbit 2. The pure CpVIK6His protein was clearly detected with both antibodies. However antibody of rabbit 2 showed a more unspecific reaction since several additional proteins aside CpVIK were detected in bacterial protein preparations.

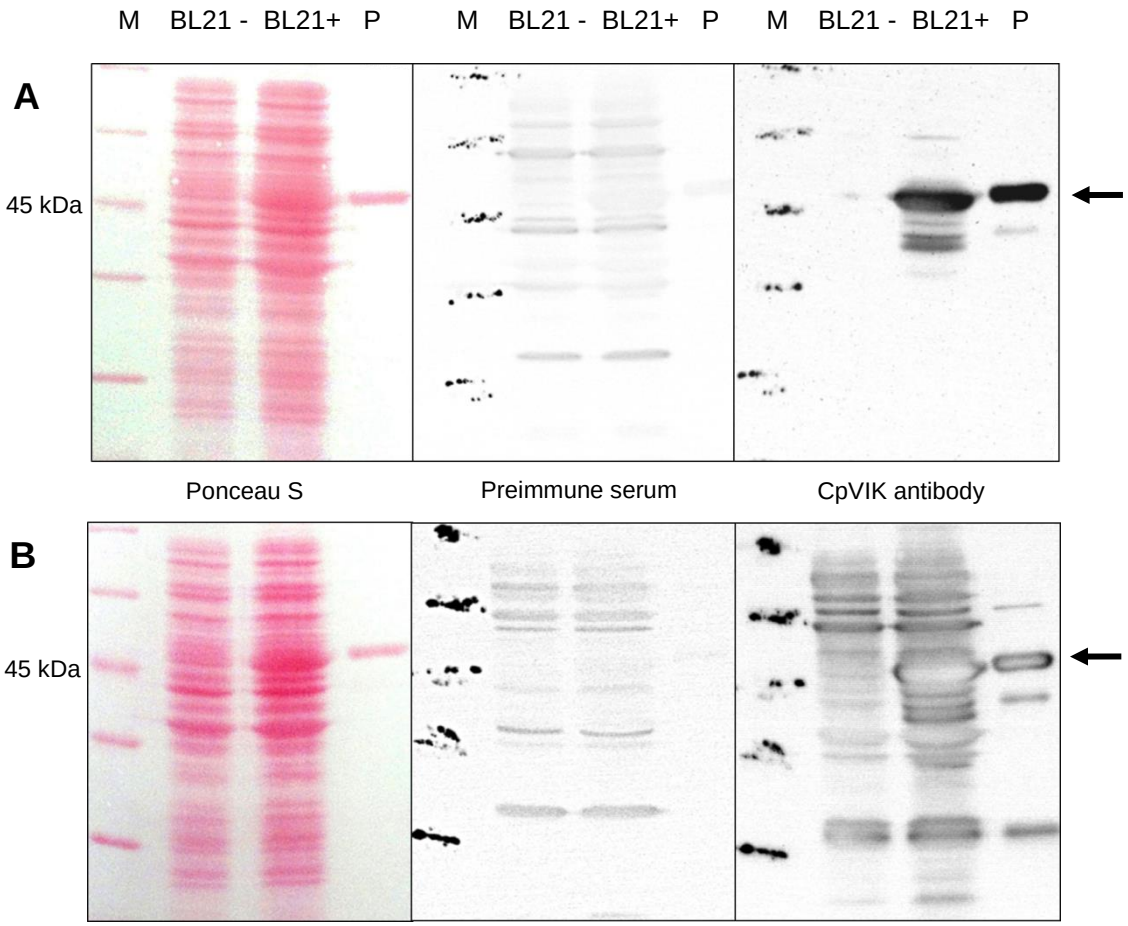

Figure 18: Evaluation of the CpVIK antisera in bacterial extracts
A: Rabbit 1; B: Rabbit 2; BL21-: pET28a-CpVIK6His expressing *E. coli* BL21 cells before (BL21-) and after (BL21+) induction with IPTG; P: 2.5 µg of CpVIK6His protein. Proteins were separated *via* SDS-PAGE (2.13.2) and transferred by electrophoresis to a nitrocellulose membrane for immunological analyses (2.15.1). The efficiency of the protein transfer was verified by staining membrane bound proteins with Ponceau S. Proteins were detected with the corresponding preimmune sera and subsequently with serum antibodies (2.15.2). The black arrow indicates the protein band corresponding to CpVIK.

The antibody of rabbit 2 detected fewer unspecific signals in protein extracts of plants (**Figure 19**). Dehydrated *C. plantagineum* leaf tissue protein samples were used to evaluate the CpVIK antibody efficiency. An *in gel* kinase assay demonstrated the abundance of CpVIK in this tissue (Petersen 2012). In the detection with the preimmune sera of both rabbits no prominent bands can be observed. With the corresponding antibodies a strong band with a size of about 45 kDa can be observed in dehydrated *C. plantagineum* leaf tissue, representing CpVIK. The CpVIK antibody of rabbit 1 shows a second slightly smaller strong band in dehydrated *C. plantagineum* leaf tissue as well as three weak bands in *A. thaliana* flower tissue (about 50 kDa, 45 kDa and 33 kDa) demonstrating that AtVIK cannot be detected in Arabidosis specifically with the CpVIK antibody.

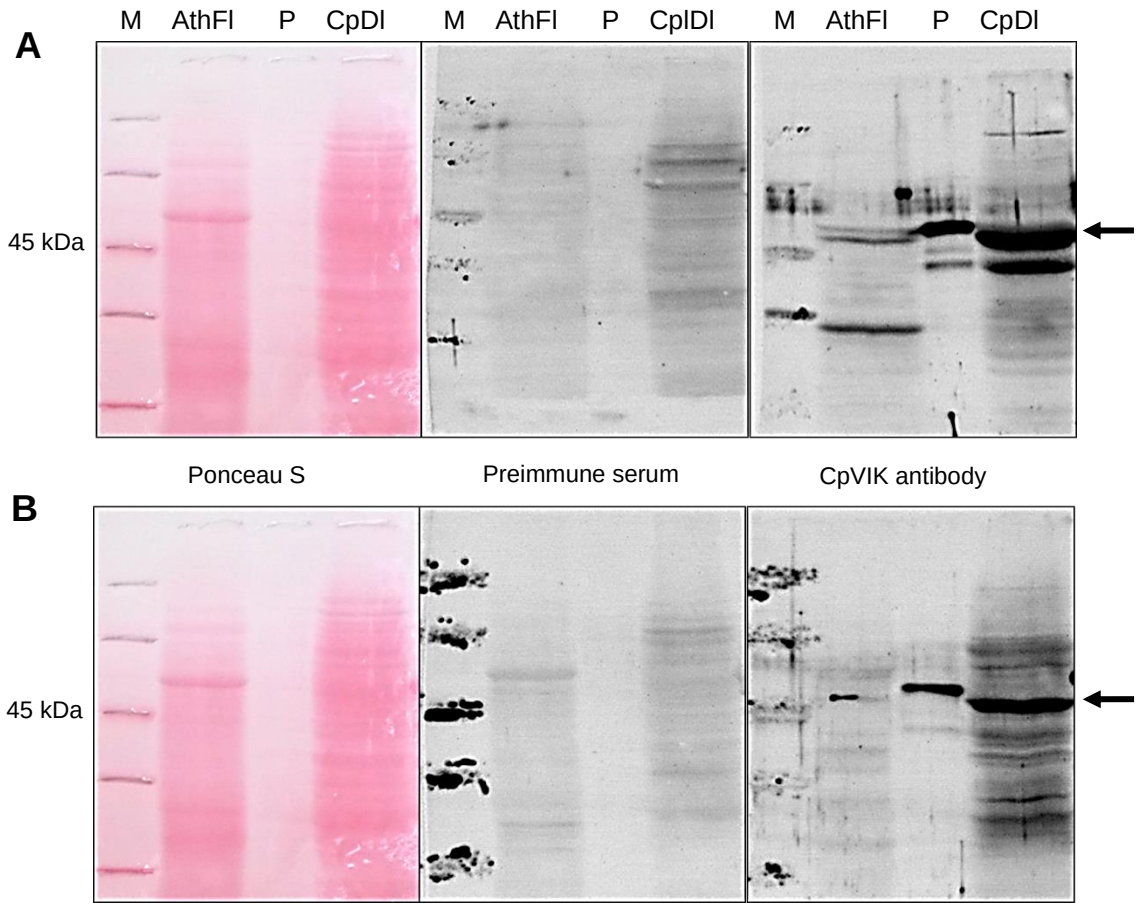

Figure 19: Evaluation of the CpVIK antisera in plant extracts
A: Rabbit 1; B: Rabbit 2; AthFl: *A. thaliana* flower tissue; CpDl: *C. plantagineum* dehydrated leaf tissue; P: 20 ng of CpVIK6His protein; Proteins were separated *via* SDS-PAGE (2.13.2) and transferred by electrophoresis to a nitrocellulose membrane for immunological analyses (2.15.1). The efficiency of the protein transfer was verified by incubation of the blotted membrane in Ponceau S staining solution. After documentation of visualised proteins, the staining was removed and interacting proteins were detected with the corresponding preimmune sera and subsequently with the CpVIK antibodies (2.15.2). The black arrow indicates the protein band corresponding to CpVIK.

3.4 Expression analysis of CpVIK

For expression analyses *CpVIK* transcript levels under different stress treatments have been studied. Previously a transcriptional up-regulation of *AtVIK* transcript by different stresses has been demonstrated (Wingenter et al. 2011). It has also been shown that the *AtVIK* transcript abundance varied in different developmental stages. Additionally the abundance and phosphorylation of the CpVIK protein was evaluated.

3.4.1 Tissue specific expression of CpVIK

Protein expression of CpVIK is detectable in all tested *C. plantagineum* tissues. In most cases protein levels of CpVIK increases during dehydration, especially in leaves (**Figure 20**). In flower tissue CpVIK protein abundance is decreased in desiccated tissue compared to untreated tissue.

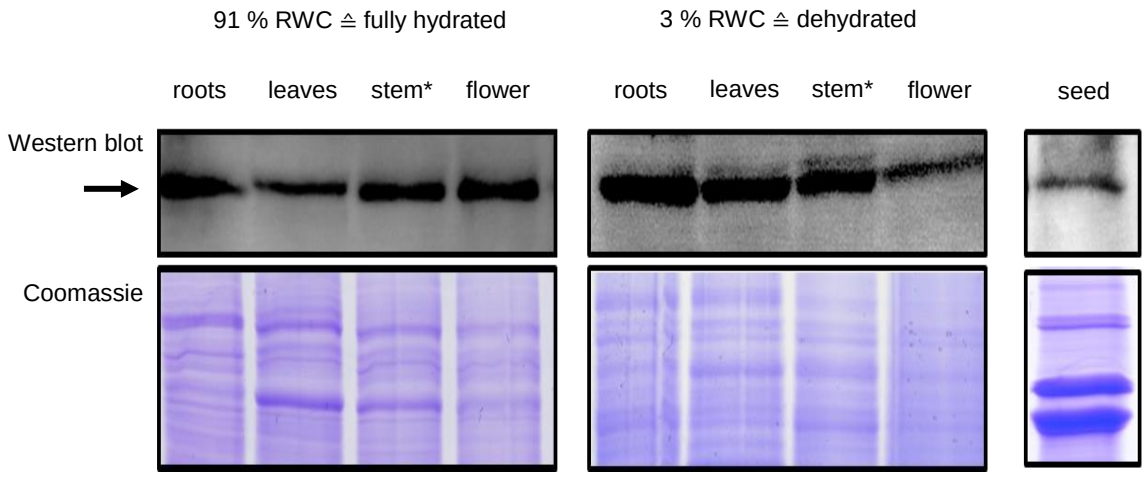

Figure 20: CpVIK protein expression
*stem = flower stem; RWC: Relative water content (determined as described in 2.1.4); Dehydration stress treatments were imposed to adult *C. plantagineum* plants by withholding watering until an RWC of 3 % was reached; Fine ground plant material was dissolved in SDS–sample buffer (2.11.4). Proteins were separated *via* SDS-PAGE (2.13.2) and either stained with Coomassie blue (2.14.1) or transferred by electrophoresis to a nitrocellulose membrane for immunological analyses (2.15.1). CpVIK protein was detected with the antiserum against CpVIK (2.15.2). The black arrow indicates the protein band corresponding to CpVIK.

3.4.2 Stress-dependent expression of CpVIK

The effects of dehydration, osmotic stress, cold and salt stress on transcript and protein-level were analysed by RT-PCR and immunological analyses were performed using detached leaves of adult *C. plantagineum* plants (**Figure 21**). Expression levels are displayed as relative values compared to expression under control conditions.

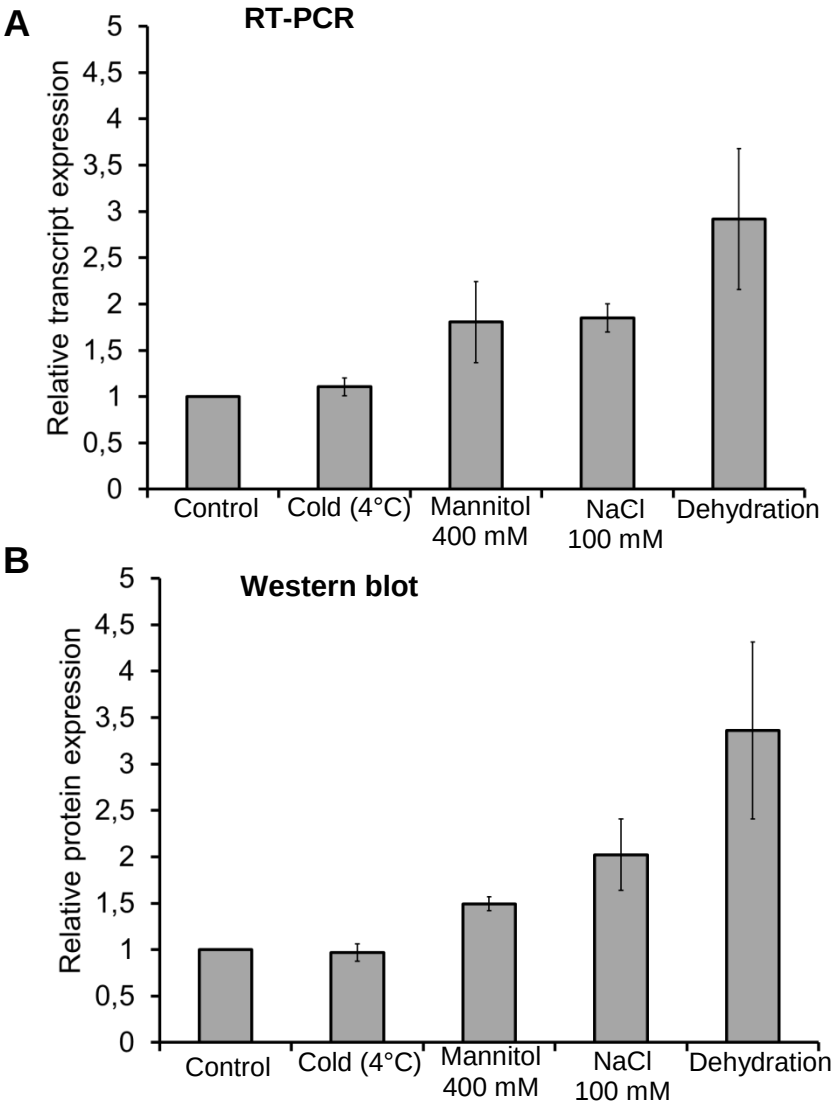

Figure 21: Stress-dependent level of CpVIK transcript and CpVIK protein in detached *C. plantagineum* leaves
RT-PCR: Reverse transcription PCR; A: Transcription of the CpVIK gene was analysed by RT-PCR; B: Protein expression was evaluated by immunological analyses with the CpVIK antibody (2.15.2). Leaves of adult C. plantagineum plants were incubated in water (control), 400 mM mannitol or 100 mM NaCl for 16 hours in standard light and temperature conditions (2.1.3); For dehydration stress treatments detached leaves were placed in open Petri dishes in standard light and temperature conditions for 48 h; Cold stress was applied by incubation in water at 4 °C for 8 hours in day light followed by 8 hours of darkness; Signal strength of protein and cDNA bands were quantified with the programme ImageJ (2.18.4); For normalisation a corresponding constitutive gene (elongation factor 1α) or protein (RubisCO), respectively were co-quantified from the same samples. The normalised expression under control conditions was set to 100 %. Expression levels are given as relative values compared to expression under control conditions. Each value represents the mean of three samples. Samples for RT-PCR and immunological analyses were taken from the same leaves.

While cold stress had no effect, the expression of *CpVIK* transcript and CpVIK protein increases during mannitol, salt and dehydration stress. Dehydration induced transcript and protein expression increased about threefold and more than all other stress

treatments tested. Mannitol and salt induced the expression about two fold in comparison to the expression of untreated control leaf tissue (**Figure 21**).

3.4.3 Developmental stage-specific expression of CpVIK

Immunological analyses were performed in three different developmental stages of *C. plantagineum* (see **Figure 22 A**) to investigate the abundance of the CpVIK protein. In leaves of all analysed developmental stages CpVIK protein expression is detectable and increases during dehydration (**Figure 22 B**). In adult hydrated plants the CpVIK protein level is higher compared to younger plants

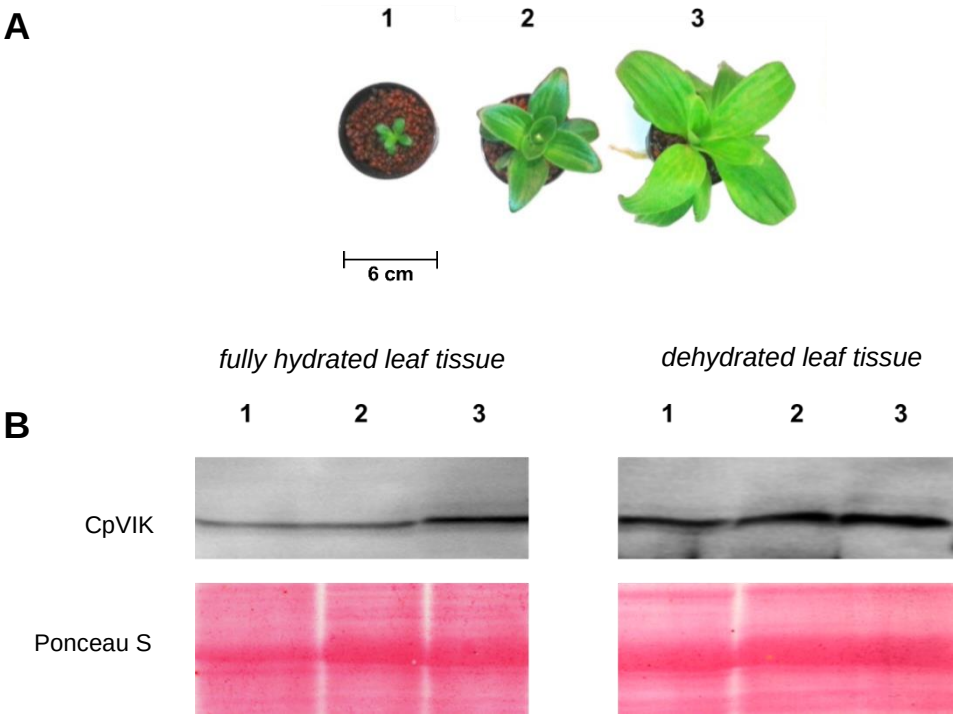

Figure 22: CpVIK protein expression in different developmental stages
A: Pictures of the three developmental stages of *C. plantagineum* plants used for immunological analyses; B: Immunological analyses of CpVIK protein expression in leaf tissue of three developmental stages of *C. plantagineum* plants; Dehydration stress treatments were imposed to *C. plantagineum* plants by withholding watering; Leaves were harvested and ground plant material was dissolved in SDS–sample buffer (2.11.4). Proteins were separated *via* SDS-PAGE (2.13.2) and transferred to a nitrocellulose membrane for immunological analyses by electrophoresis (2.15.1). The efficiency of the protein transfer and equal loading of samples was checked by Ponceau S staining. CpVIK protein was detected with the corresponding antiserum (2.15.2); RWC of hydrated *C. plantagineum* leaves (determined as described in 2.1.4) raged from 90-94 %. RWC of dehydrated *C. plantagineum* leaves ranged from 3-6 %.

3.4.4 Stress affected phosphorylation of CpVIK

To analyse the effects of drought on the phosphorylation of the CpVIK protein, immunological analyses were performed on total proteins and a metal oxide/hydroxide affinity chromatography enriched subfraction of phosphoproteins. Expression levels of CpVIK in both, the total protein fraction and the enriched phosphoproteins are displayed in **Figure 23 A** as relative values compared to expression under control conditions. A representative blot is shown in **Figure 23 B**.

The CpVIK expression increases during dehydration as shown by the differential expression levels in total proteins. In contrast to experiments shown above in **Figure 21**, whole plants were dehydrated for stress tests and leaves were harvested after dehydration. In total proteins the abundance of CpVIK protein was 1.5 fold higher in leaf tissue harvested from dehydrated plants than under control conditions.

This induction of CpVIK is more pronounced in the enriched subfraction of phosphoproteins, where the abundance of CpVIK protein was 3.5 fold higher in leaves of dehydrated plants than in unstressed plants. The same induction pattern was found when the root material of the same plants was tested (**supplemental figure 59**).

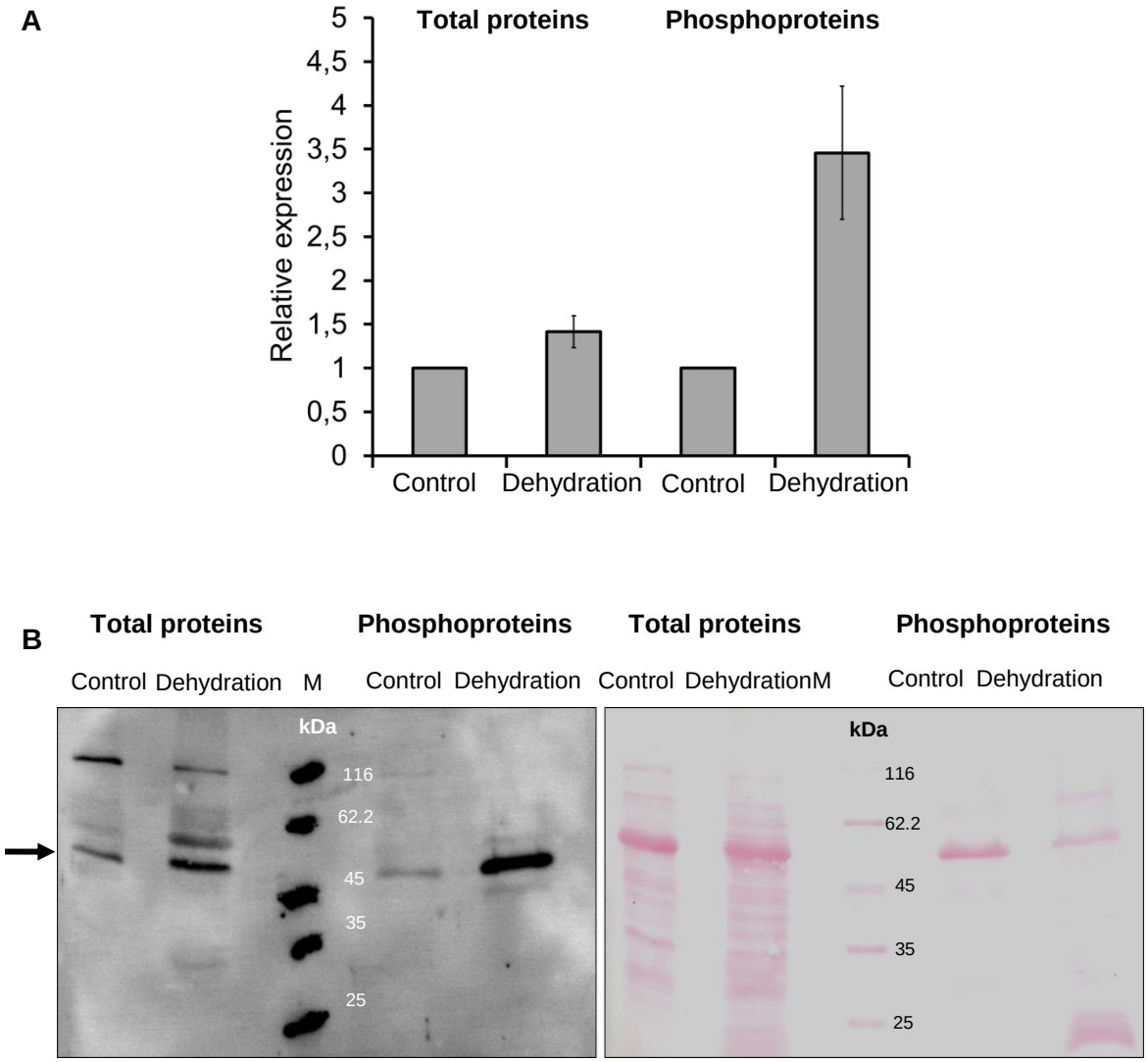

Figure 23: Stress affected phosphorylation of CpVIK protein

kDa: Protein mass in kilo Dalton; Protein expression was evaluated by immunological analyses with the CpVIK antibody (2.15.2). Adult *C. plantagineum* plants were grown as described in 2.1.2 for control condition samples. Dehydration stress treatments were imposed to adult *C. plantagineum* plants by withholding watering; hydrated tissue (control) had a RWC (Relative water content (determined as described in 2.1.4) of 91-93 % and dehydrated tissue a RWC of 3-6 %; The phosphoprotein subtraction was enriched from the displayed total protein extraction *via* metal oxide/hydroxide affinity chromatography as described in 2.11.5. Signals of protein bands were quantified with the programme ImageJ (2.18.4); For normalisation a corresponding constitutive protein (RubisCO) was co-quantified from the same samples. A: Expression levels are given as relative values compared to expression under control conditions. The normalised expression under control conditions was set to 100 %. Each value represents the mean of three samples and the associated standard deviations. C: Exemplary Imunoblot showing CpVIK protein expression in total and phosphoproteins. The black arrow indicates the protein band corresponding to CpVIK to discriminate specific signals from unspecific bands observed in the total protein fraction.

3.4.5 Co-expression of CpVIK and CDeT11-24

An *in gel* kinase assay with CDeT11-24 LEA-like as bait protein identified CpVIK from desiccated *C. plantagineum* leaf tissue as putative interaction partner (see **1.5**). For CDeT11-24 a stress-dependent up-regulation of transcription, translation as well as increased phosphorylation was described previously (Röhrig et al. 2006; van den Dries et al. 2011). As described above a similar regulation is observed for CpVIK (see **3.5.1-4**). To analyse a possible co-induction under stress, the expression profiles of both genes and proteins was investigated using detached leaves of adult *C. plantagineum* plants exposed to various dehydration periods. In addition to dehydration other stress types were also tested.

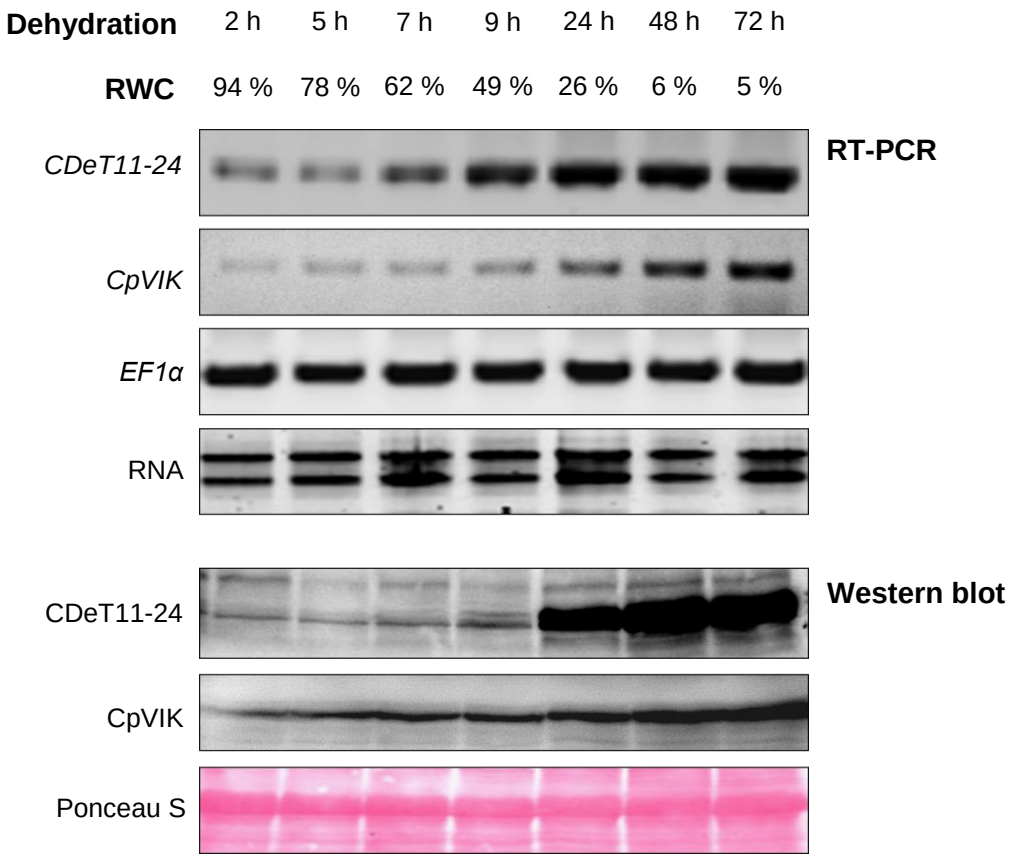

Figure 24: Co-expression of CpVIK and CDeT11-24 on transcript and protein level during dehydration
RWC: Relative water content (determined as described in 2.1.4); RT-PCR: Reverse transcription PCR; Transcription of the EF1α, *CpVIK* and *CDeT11-24* genes was analysed by RT-PCR with 30 cycles (2.16); Protein expression was evaluated by immunological analyses with the CpVIK and CDeT11-24 antibody, respectively (2.15.2). For dehydration stress treatment C. plantagineum leaves were placed in open Petri dishes in standard light and temperature conditions for 72 h; Samples were taken after the various time points as depicted above.

On the transcript level *CDeT11-24* is earlier induced than on protein level during dehydration (**Figure 24**). For *CDeT11-24* an induction of transcription can already be observed, when the RWC reaches 62 %. When the RWC reaches 26 % an induction of transcription can be observed for *CpVIK*. Generally *CDeT11-24* is stronger expressed than *CpVIK*. The protein abundance of both, CDeT11-24 and CpVIK increases strongly

when the RWC reaches 26 % (**Figure 24**). Both proteins show the strongest expression in fully dehydrated tissue. When a RWC of 6 % was reached, a longer desiccation did not lead to changes in protein expression anymore for both proteins.

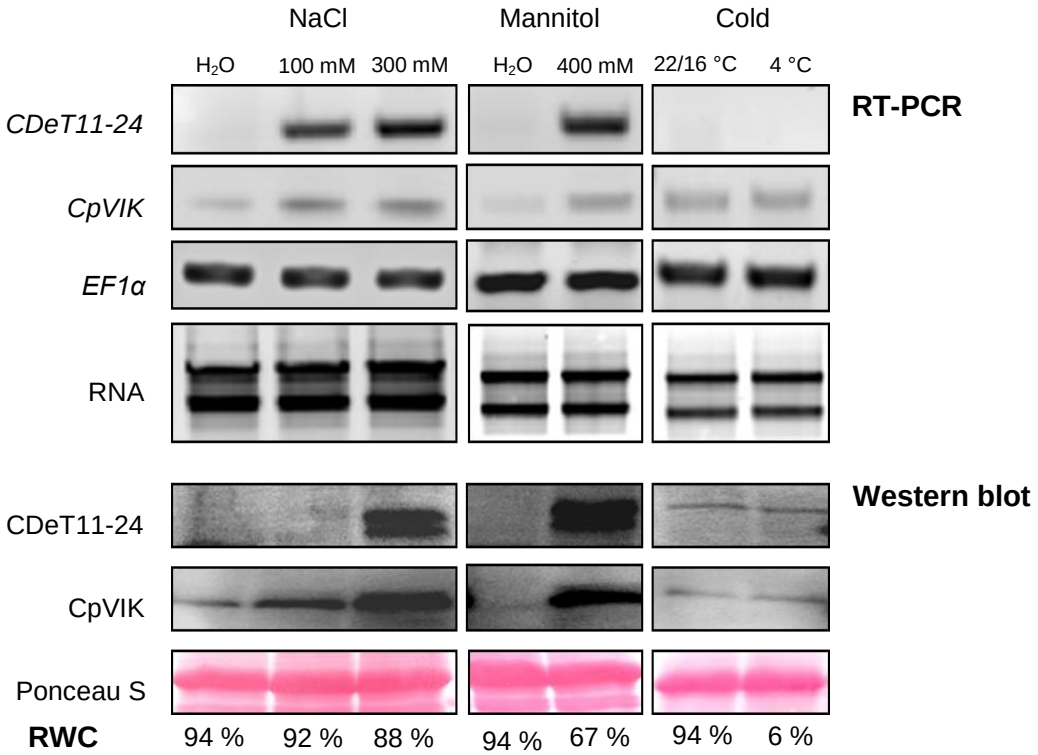

Figure 25: Stress induced co-expression of CpVIK and CDeT11-24
RWC: Relative water content (see 2.1.4); RT-PCR: Reverse transcription PCR; Transcription of the *CpVIK* and *CDeT11-24* genes was analysed by RT-PCR (see 2.16); Protein expression was evaluated by immunological detection with the anti CpVIK and anti CDeT11-24 antiserum, respectively (2.15.2). Leaves of adult *C. plantagineum* plants were incubated in water, 100 mM NaCl, 300 mM NaCl, 400 mM mannitol or plants were kept untreated as control (2.1.3); Cold stress was applied by incubation in water at 4 °C for 8 hours in day light followed by 8 hours of darkness

Also under salt, mannitol and cold stress CDeT11-24 and CpVIK show similar expression profiles (**Figure 25**). Salt treatment with 100 mM NaCl led to an induction of transcription of both genes but on protein level expression kinetics varied between CDeT11-24 and CpVIK. In 300 mM NaCl treatment strong bands can be observed for both, CDeT11-24 and CpVIK. Mannitol treatment induced transcription and translation of both proteins whereas cold had no effect on the expression. Although the mannitol stress treatment with 400 mM mannitol reduces the RWC of the leaf tissue more than the salt treatment with 300 mM NaCl (Figure 25), no significant difference in expression was observed among these two treatments for both proteins. From these experiments it can be summarized that CDeT11-24 is induced earlier on the transcript level upon stress treatments than on protein level as reported (van den Dries et al. 2011). In contrast CpVIK shows no difference between rate of transcription and translation. Both

genes and proteins are induced by dehydration, NaCl and Mannitol treatments whereas cold had no effect on the expression level. This indicates a functional involvement of both proteins in the responses to these stresses.

3.4.5 Expression of LbVIK and LsVIK

In the two species *L. brevidens* and *L. subracemosa* which are closely related to *C. plantagineum*, orthologs of CpVIK were identified in the transcriptome data bank (see **3.1.3**). Using the CpVIK antibody (see **3.5**) immunological analyses were conducted on leaf tissue of *L. brevidens* and *L. subracemosa* to analyse the effects of dehydration stress on the abundance of the putative LbVIK and LsVIK proteins (**Figure 26**). No prominent bands can be observed when preimmune serum was used for western blot analyses. With the CpVIK antiserum a prominent band of about 45 kDa resembling VIK can be detected in leaf tissue of both *L. brevidens* and *L. subracemosa*, respectively. No prominent changes of VIK expression were observed in both species under dehydration stress.

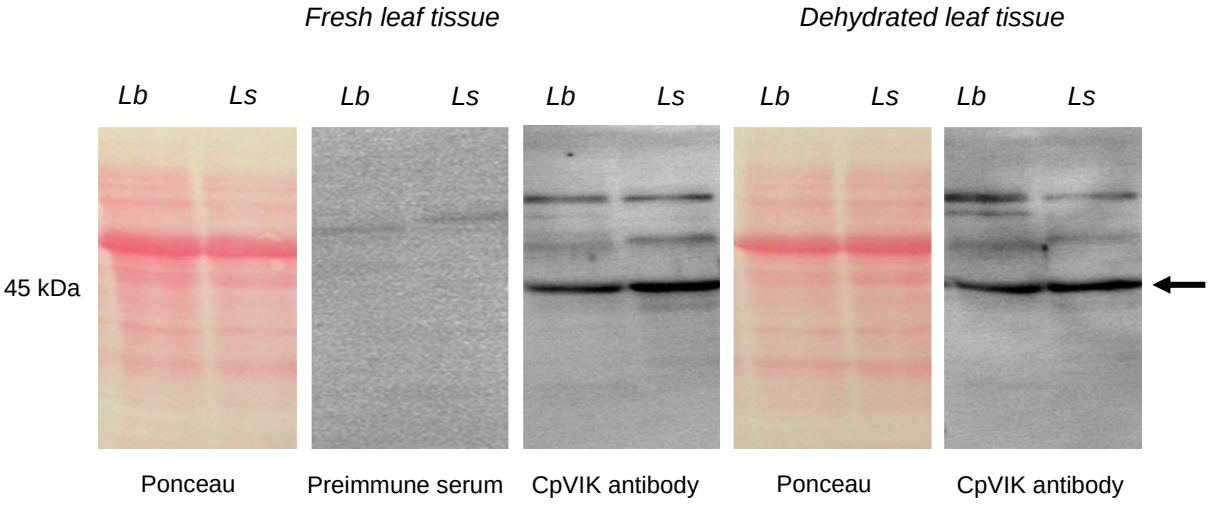

Figure 26: Stress affected expression of LbVIK and LsVIK
kDa: Protein mass in kilodalton ; Protein expression was evaluated by immunological analyses with the CpVIK antisera and preimmune serum (2.15.2 and 3.5). Leaves of adult *L. brevidens* and *L. subracemosa* plants were harvested after dehydration of whole plants. Dehydration stress was applied by withholding water. Fresh leaf tissue had a RWC (Relative water content (determined as described in 2.1.4) of 90 % and dehydrated tissue a RWC of 5 %.The black arrow indicates the protein band corresponding to LbVIK and LsVIK to discriminate specific signals from unspecific bands.

3.5 *In vitro* kinase assays

MAPKKKs are known to catalyse phosphotransfer from ATP to other proteins. The phosphorylation activity of CpVIK was tested first in non-radioactive assays, the so called “cold” *in vitro* kinase assays with the LEA protein CDeT11-24 as substrate as well as CDeT6-19 and Bovine serum albumin (BSA) as negative substrate controls. A mutated CpVIK protein with an amino acid exchange in the DFG motif of the kinase domain ($CpVIK_{dead}$) was constructed and used as negative control for kinase activity. For the analyses of kinase reactions phosphorylation of proteins was determined with the phosphoprotein specific protein gel stain Pro-Q® Diamond (Thermo Fisher Scientific, Waltham, USA). In addition radioactive *in vitro* kinase assays were performed for verification (**supplemental figure 61**). Furthermore, CDeT11-24 phosphorylation by CpVIK was analysed by mass spectrometry.

3.5.1 Phosphorylation of CDeT11-24 by CpVIK *in vitro*

For kinase assays recombinant CpVIK-6His and CDeT11-24-6His were purified by affinity chromatography (**2.22.2**). The *in vitro* kinase assays were performed as described in **2.25**. After reaction, proteins were separated *via* 1D SDS-PAGE and stained with Pro-Q® Diamond phosphoprotein gel stain (Thermo Fisher Scientific, Waltham, USA) to visualise phosphorylated proteins. Subsequently the gels were stained with Coomassie to ensure protein abundance. In a first attempt for the kinase assay CpVIK and substrate CDeT11-24 were used in a ratio of 1:1 (**Figure 27**). When CpVIK and CDeT11-24 were incubated together in kinase assay buffer, both proteins were strongly stained with Coomassie and ProQ® Diamond showing auto-phosphorylation of CpVIK (black arrow, band at 50.5 kDa) and phosphorylation of substrate CDeT11-24 (blue arrow, band at about 62 kDa).

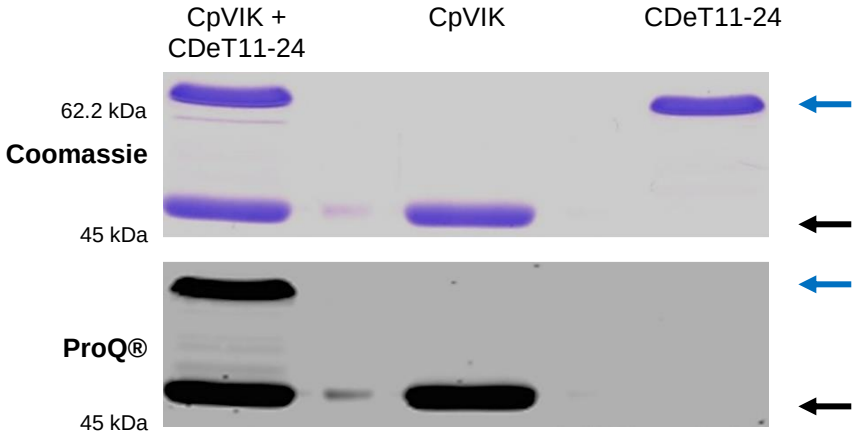

Figure 27: Not-radioactive *in vitro* kinase assay of CpVIK with CDeT11-24 as substrate
kDa: Protein mass in kilo Dalton; Incubation time was 3 hours. Proteins were separated *via* SDS-PAGE (2.13.2), stained with Pro-Q® Diamond phosphoprotein stain (2.14.2) and subsequently with Coomassie (2.14.1). The black arrow indicates the protein band corresponding to CpVIK and the blue arrow indicates the protein band corresponding to CDeT11-24.

3.5.2 Substrate specifity of CpVIK

The LEA protein (CDeT6-19) and bovine serum albumin (BSA) were used as negative substrate control proteins for the *in vitro* kinase assays. As shown in **Figure 28**, only autophosphorylation of CpVIK can be observed (band at 50.5 kDa).

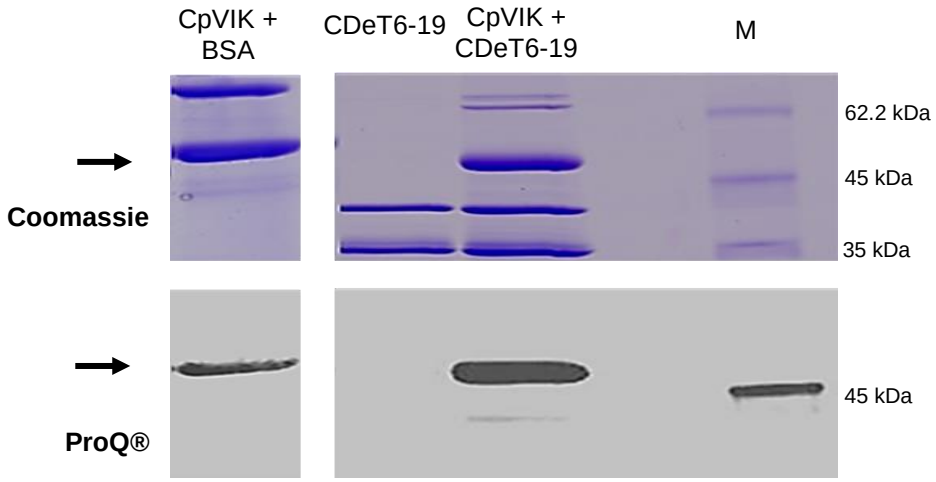

Figure 28: Analytical *in vitro* kinase assay of CpVIK and CDeT6-19
CpVIK-6His and CDeT6-19GST were purified by affinity chromatography (2.22.2 and 2.22.3). BSA was received from Roth (Karlsruhe, DE) as lyophilised powder. *In vitro* kinase assays were performed as described in 2.25. Reactions were stopped after 3 hours. Proteins were separated *via* SDS-PAGE (2.13.2) and stained with ProQ® Diamond phosphoprotein stain (2.14.2) and subsequently with Coomassie (2.14.1). The black arrow indicates the protein band corresponding to CpVIK.

CDeT11-24 was phosphorylated by CpVIK (**Figure 27**) whereas with BSA and CDeT6-19 no kinase reaction could be detected (**Figure 28**) demonstrating the substrate specificity of CpVIK for CDeT11-24.

3.5.3 $CpVIK_{dead}$ mutated kinase

As further negative control a kinase with a specific mutation in the ATP-co-factor binding pocket was generated by QuikChange Site-Directed Mutagenese (Zheng et al.; 2004). This method is based on the amplification of a plasmid by PCR with mutagenised primers and subsequent digestion of the parental plasmid with the restriction enzyme DpnI.

To achieve a D-298 to N-298 exchange in the DFG motif (see **1.4.1**), the pET-28avector harbouring the CpVIK coding sequence was amplified with the mutagenesis primers cpvikdead_f and cpvikdead_r (**Figure 29**). The remaining methylated parental plasmids from *DH10B E. coli* (pET-28avector+CpVIK) were digested with the methylation specific restriction enzyme DpnI. The mutation in the amplified plasmids (pET-28a vector+$CpVIK_{dead}$) was verified by DNA-sequencing.

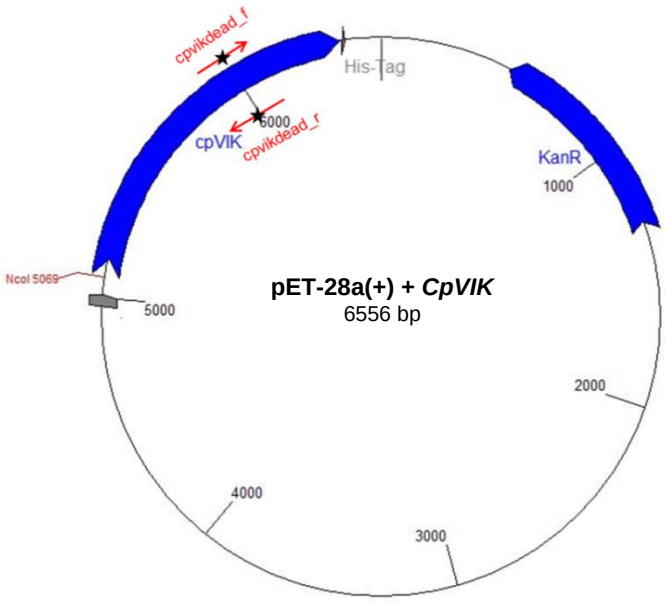

Figure 29: Expression vector pET28-a including the His-tagged *CpVIK* used for mutagenesis
Vector map; *CpVIK* and the kanamycin resistance gene (KanR, Aminoglycoside 3'-phosphotransferase) are represented by blue arrows. Primer binding positions are depicted with red arrows. Mutations in the primers are represented with black asterisk. The IPTG inducible lac-operator is represented by a grey box. The *CpVIK* coding sequence was amplified from a cDNA library of fully dried plants with a RWC of approximately 5 % (Rodriguez et al., 2010) and cloned into NcoI and SacI restriction sites of the the pET-28a(+) vector (Novagen, Madison, WI).

$CpVIK_{dead}$6His was expressed in BL21 *E. coli* as described in **2.21** and purified by affinity chromatography (**2.22.2**). In the *in vitro* kinase assays the mutation in the DFG motif led to a total loss of the kinase activity including the autophosphorylation capability as depicted in **Figure 30**. As a control CpVIK was co-incubated with CDeT11-24 in the same experiment. As shown in **Figure 30**, CpVIK and CDeT11-24 are stained with Coomassie and ProQ® Diamond stain displaying autophosphorylation of CpVIK (band at 50.5 kDa) as well as phosphorylation of CDeT11-24 by CpVIK (band at about 62 kDa). In the case of $CpVIK_{dead}$ no protein band appears in the ProQ® Diamond stain, showing the lack of auto- and substrate phosphorylation activity.

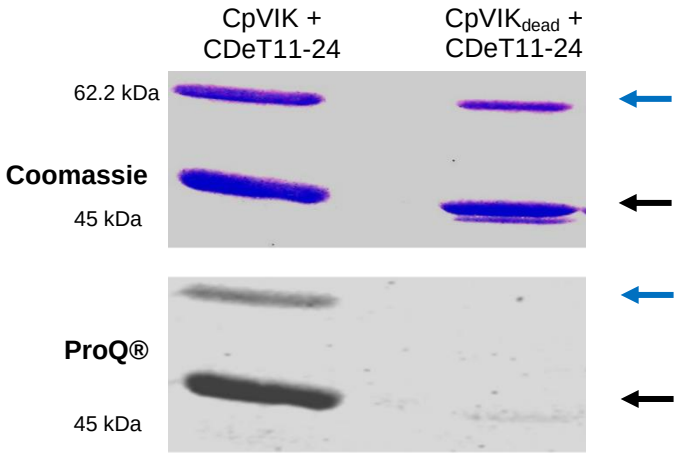

Figure 30: Analytical *in vitro* kinase assay of CpVIK with CDeT11-24 and $CpVIK_{dead}$ with CDeT11-24
CpVIK-6His, $CpVIK_{dead}$-6His and CDeT11-24-6His were purified by affinity chromatography (2.22.2) and *in vitro* kinase assays were performed as described in 2.25. Reactions were stopped after 3 hours. Proteins were separated via SDS-PAGE (2.13.2) and stained with ProQ® Diamond phosphoprotein stain (2.14.2) and subsequently with Coomassie (2.14.1). The black arrow indicates the protein band corresponding to CpVIK or $CpVIK_{dead}$ respectively and the blue arrow indicates the protein band corresponding to CDeT11-24.

3.5.4 CDeT11-24 phosphorylation sites mediated by CpVIK

Seven *in vivo* phosphorylation sites have already been identified in CDeT11-24 from dehydrated *C. plantagineum* leaf tissue (Röhrig et al. 2006). To verify that CDeT11-24 phosphorylation by CpVIK reflects the *in vivo* data, the phosphorylation of CDeT11-24 by action of CpVIK in the above described saturated kinase reaction (amount kinase to substrate was 1:1, 120 µg of each) was determined.

After kinase reaction, the sample was rebuffered in ammonium bicarbonate. A test gel (**Figure 31**) shows successful phosphorylation of CDeT11-24 by CpVIK (lane 2, band at about 60 kDa). Additionally the autophosphorylation activity of CpVIK can be observed at 50 kDa in the same lane. As a negative control CDeT11-24 was incubated without CpVIK in the same conditions and co-loaded on the gel. As depicted in

Figure 31 the protein band of CDeT11-24 of this sample only appears in the Coomassie stain (lane 1) proofing the absence of phosphorylation in the negative control.

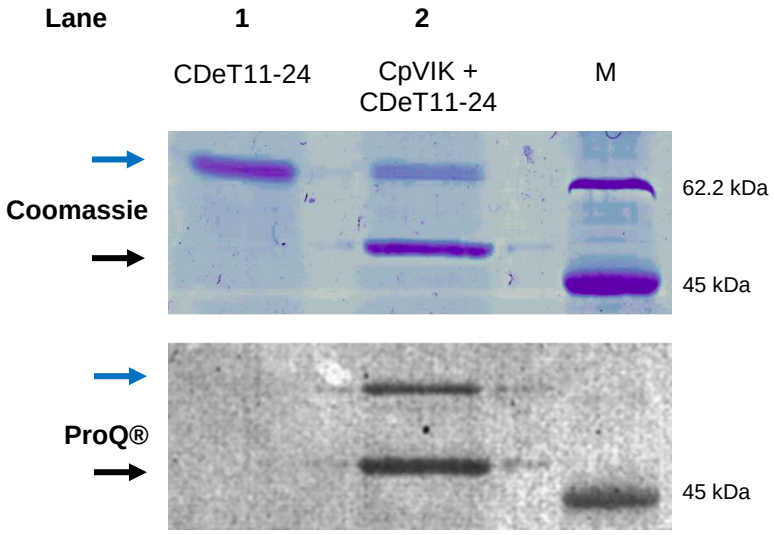

Figure 31: Preparative cold *in vitro* kinase assay for phosphosite analysis of CDeT11-24
CpVIK-6His, $CpVIK_{dead}$-6His and CDeT11-24-6His were purified by affinity chromatography (2.22.2) and *in vitro* kinase assays were performed as described in 2.25. Reactions were stopped after 3 hours. Proteins were separated via SDS-PAGE (2.13.2) and stained with ProQ® Diamond phosphoprotein stain (2.14.2) and subsequently with Coomassie (2.14.1). The black arrow indicates the protein band corresponding to CpVIK and the blue arrow indicates the protein band corresponding to CDeT11-24.

The remaining *in vitro* kinase assay sample was lyophilised and analysed by mass spectrometry after digestion with trypsin, in order to identify post translational modifications (Dr. Marc Sylvester, IBMB University of Bonn, DE). Under these saturated condtions an overall phosphorylation of CDeT11-24 at 50 sites including strong phosphorylation on tyrosine residues was observed (**Figure 32**). In addition the phosphorylation sites in CpVIK were determined (**supplemental figure 58**).

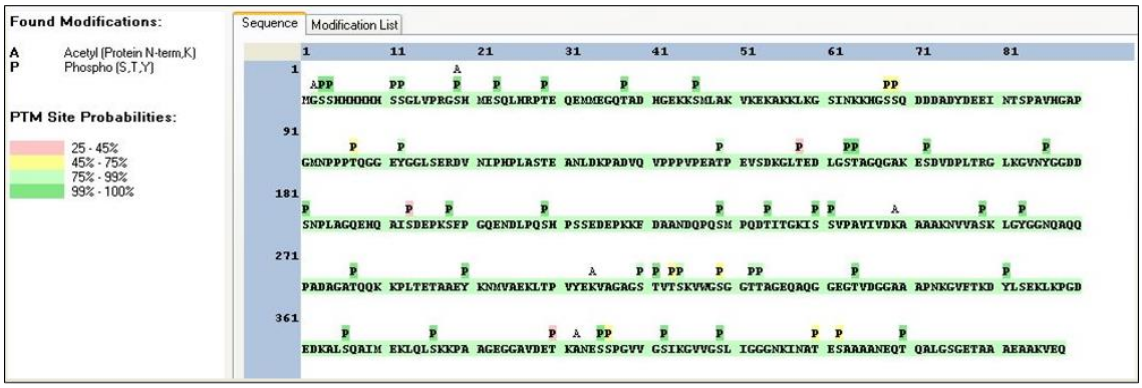

Figure 32: Phosphorylation sites in CDeT11-24 mediated by CpVIK in saturated conditions
Phosphosites were identified by mass spectrometry. Identified peptides are highlighted in green. Phosphorylation sites are highlighted with a colour code reflecting the localisation probability. Mass spectrometric analyses were performed by Dr. Marc Sylvester at the core facility mass spectrometry (Institute of Biochemistry and Molecular Biology, University of Bonn).

To reduce aberrant substrate phosphorylation due to saturated kinase to substrate concentration and to increase phosphosite specificity, different molar ratios of CpVIK and CDeT11-24 were tested in *in vitro* kinase assays (**Figure 33**). In every experiment a positive control with a 1:1 ratio (lane 1 and 5) as well as a negative control, with only CDeT11-24 (lane 2 and 6), have been included. In all assays the amount of substrate CDeT11-24 was kept constant while concentration of CpVIK was reduced. In these experiments autophosphorylation of CpVIK could only be detected until a molar kinase to substrate ratio of 1:50 (band at 50 kDa). In contrast the amount of phosphorylated CDeT11-24 is significantly reduced in comparison to the saturated reaction when a molar ratio of 1:100 (CpVIK : CDeT11-24) was used for the *in vitro* assays. The signal strength for phosphorylated CDeT11-24 remained stable to a large extent until a relation of 1:300 (bands at about 60 kDa).

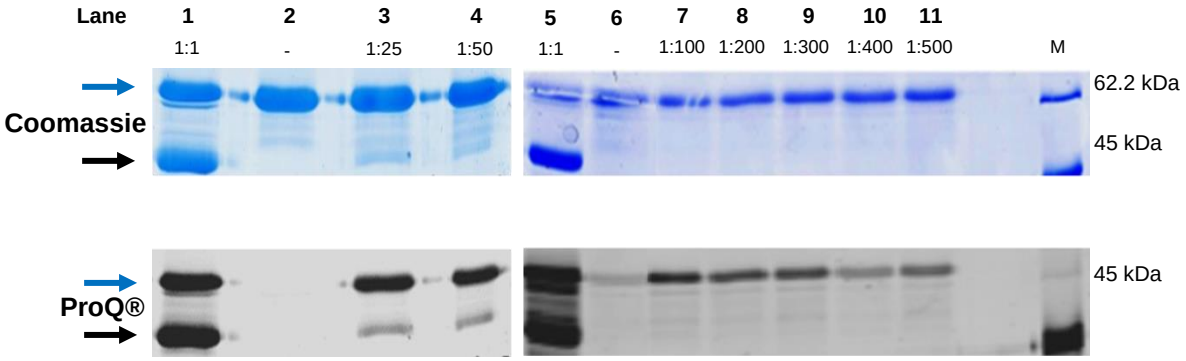

Figure 33: Analytical *in vitro* kinase assay of CpVIK with CDeT11-24 in different ratios
CpVIK-6His and CDeT11-24-6His were purified by affinity chromatography (2.22.2) and *in vitro* kinase assays were performed as described in 2.25. Reactions were stopped after 1 hour. Proteins were separated via SDS-PAGE (2.13.2) and stained with ProQ® Diamond phosphoprotein stain (2.14.2) and subsequently with Coomassie (2.14.1). The black arrow indicates the protein band corresponding to CpVIK and the blue arrow indicates the protein band corresponding to CDeT11-24.

Thus a ratio of 1:250 was used in a new preparative *in vitro* kinase assay for further phosphorylation site determination. The *in vitro* kinase assay sample (46 ng CpVIK + 11.5 µg CDeT11-24) was loaded completely on a SDS-PAGE gel. The gel was stained with Coomassie (**Figure 34**). Afterwards the CDeT11-24 band was cut, digested with trypsin and analysed without further treatment by mass spectrometry (Dr. Marc Sylvester, IBMB Bonn, DE). As shown in the Coomassie stain in **Figure 34** the amount of CDeT11-24 protein is the same in all samples. When CpVIK was used in a 1:250 ratio the CDeT11-24 protein band shows a reduced phospho-specific staining compared to a ratio of 1:1 or 1:50 pointing to a significantly reduced phosphorylation of CDeT11-24 (**Figure 34**).

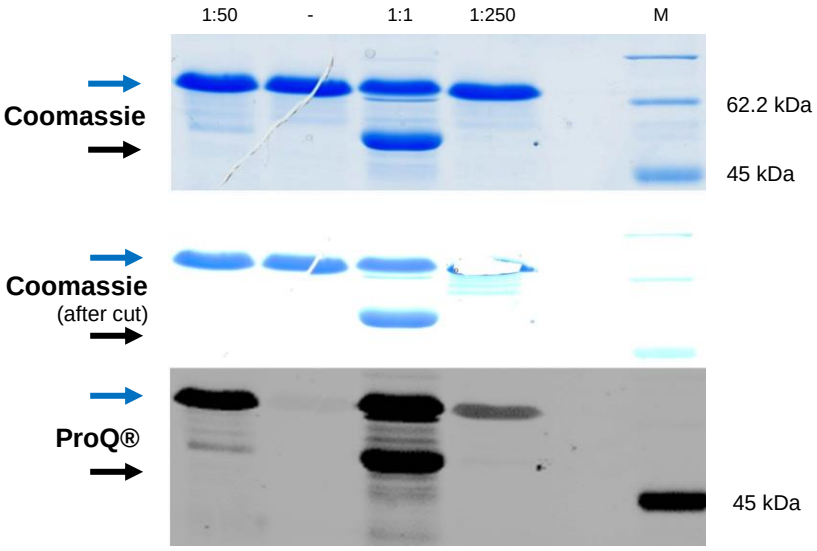

Figure 34: Preparative *in vitro* kinase assay for phosphosite identification CDeT11-24
CpVIK-6His and CDeT11-24-6His were purified by affinity chromatography (2.22.2) and *in vitro* kinase assays were performed as described in 2.25. Reactions were stopped after 1 hour. Proteins were separated *via* SDS-PAGE (2.13.2) and stained with ProQ® Diamond phosphoprotein stain (2.14.2) and subsequently with Coomassie (2.14.1).

Under the above mentioned assay conditions the amount of phosphorylated amino acid residues in CDeT11-24 was reduced to six sites (**Figure 35**; full data in supplemental data files).

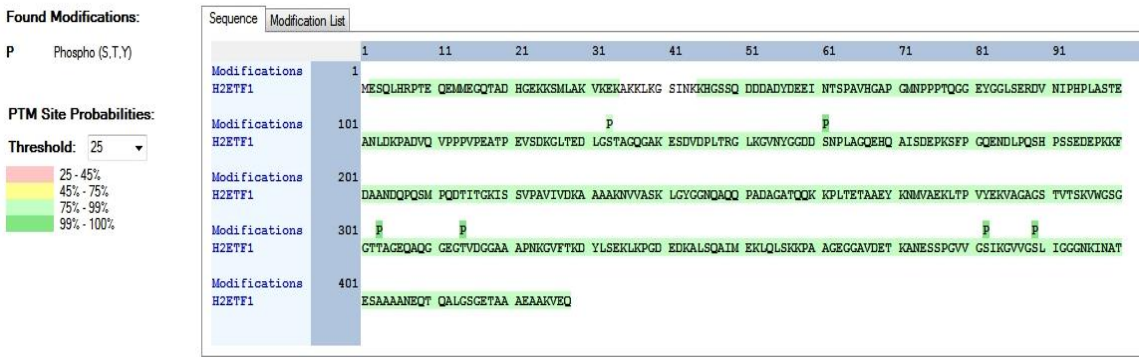

Figure 35: CpVIK mediated phosphorylation of CDeT11-24 under not saturated conditions
(molar ratio kinase to substrate of 1:250). Phosphosites of CDeT11-24 were identified by mass spectrometry. Identified peptides are highlighted in green. Phosphorylation sites are highlighted with a colour code reflecting the localisation probability. Mass spectrometric analyses were performed by Dr. Marc Sylvester at the core facility mass spectrometry (Institute of Biochemistry and Molecular Biology, University of Bonn).

Three of the identified phosphopeptides can be explained by phosphorylated serine residues which were already identified *in vivo* on CDeT11-24 extracted from *C. plantagineum* leaf tissue (Röhrig et al. 2006; **Table 8**). Besides these already known phosphorylation sites three new sites were identified from *in vitro* phosphorylated CDeT11-24 (**Table 8**). Two of these previously not identified sites T303 and S382 have been identified in the Lb11-24 ortholog in leaf tissue of *L. brevidens in vivo*. Three of

the identified phosphopeptides can be explained by phosphorylated serine residues which were already identified *in vivo* on CDeT11-24 extracted from *C. plantagineum* leaf tissue (Röhrig et al. 2006; **Table 8**). Besides theses already known phosphorylation sites, three new sites were identified by the *in vitro* kinase assay (**Table 8**). However, two of these previously not in CDeT11-24 of Craterostigma identified sites, T303 and S382, have been identified in the Lb11-24 ortholog in leaf tissue of *L. brevidens in vivo* (Facchinelli 2009).

Table 9: Identification of CDeT11-24 phosphosites by mass spectrometry
Sites highlighted with red represent most probable sites of phosphorylation after automatic and manual evaluation of tandem mass spectrometry (MS/MS) data. PTM Score: Post translational modification score determined by ptmRS algorithm (Taus, T. et al. Universal and confident phosphorylation site localization using phosphoRS. J Proteome Res 10, 5354-5362, doi:10.1021/pr200611n (2011). Mass spectrometric analyses were performed by Dr. Marc Sylvester at the core facility mass spectrometry (Institute of Biochemistry and Molecular Biology, University of Bonn)
* Data for CDeT11-24 *in vivo* phosphorylation as described byRöhrig et al., 2006;
** Data for Lb11-24 phosphorylation (Facchinelli, 2009)

Phosphorylated peptides	***Position***	***Highest PTM Score***	***CDeT11-24* in vivo***	***Lb11-24** in vivo***
*LTEDLG**S**TAGQGA*	*S133*	*92.87*	•	
*NYGGDD**S**NPLAGQ*	*S161*	*100*	•	
*WGSGGT**T**AGEQAQ*	*T303*	*99.2*		•
*AQGGEG**T**VDGGAA*	*T314*	*100*		
*SPGVVG**S**IKGVVG*	*S382*	*100*		•
*IKGVVG**S**LIGGGN*	*S389*	*100*	•	

Residues Ser133 and Ser389 were already predicted for phosphorylation by MAPKKKs (corresponds to Ser141 and Ser396 in the earlier analysed isoform by Röhrig et al. 2006). CDeT11-24 has been shown to be phosphorylated *in vivo* at four additional sites that were not observed in this *in vitro* kinase reaction (Röhrig et al. 2006).

3.6 Pull down assays

3.6.1 Pull down assay using purified proteins

To identify protein-protein interaction of CpVIK with CDeT11-24 an immobilised metal-affinity chromatography-based (IMAC-based) analysis with CpVIK6His as bait was performed. CpVIK6His was overexpressed and purified as described in **2.21** and **2.22.2** and subsequently incubated with recombinant CDeT11-24 protein without His tag (see

2.24.1) in the presence of ATP. After incubation the sample was loaded on a Ni-NTA column and affinity chromatography was performed as described. After several washing steps CpVIK6His together with interacting proteins was eluted from the column with imidazole in six fractions (F1+ to F6+). As control an assay without bait protein was used to exclude the possibility that the CDeT11-24 protein interacts with the Ni-Sepharose (F1- to F6+). The quantity of the eluted proteins was analysed by by Bradford assay (**2.16.2**). The fraction with the highest protein content (F2+) and the corresponding negative control (F2-) were precipitated with TCA and pellets were prepared for two dimensional SDS-PAGE (**2.13.2**) and Western blot analyses (**2.15**). As shown in **Figure 36** the CDeT11-24 antiserum detected a prominent protein spot with a molecular weight of about 62 kDa and an isoelectric point of about 4 in fraction F2+. Thus the CDeT11-24 protein was co-eluted with CpVIK6His. Minor protein spots with the same molecular weight and a higher isoelectric point can be observed that may represent differential phosphorylation states of CDeT11-24. Since no spots can be detected in the control assay F2- this indicates that CDeT11-24 binding to the resin of the column is mediated by interaction with CpVIK (**Figure 36**).

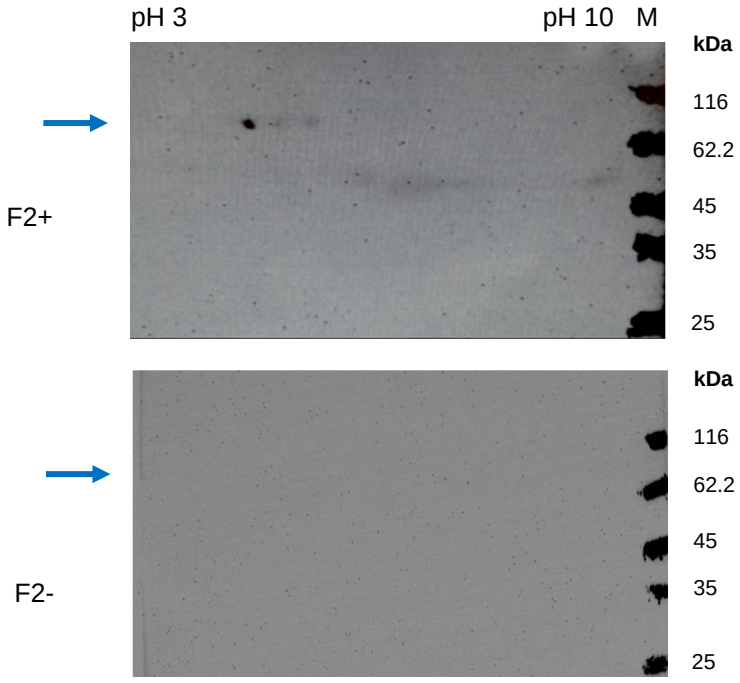

Figure 36: Protein-protein interaction studies with CDeT11-24 as prey and CpVIK6His as bait
Proteins were immobilised by metal-affinity chromatography. Eluted proteins were separated *via* two dimensional SDS-PAGE (2.13.2), transferred to a nitrocellulose membrane and detected with antiserum against CDeT11-24 (2.15.1 and 2.15.2). The blue arrow indicates the protein spot corresponding to CDeT11–24.

As additional control CpVIK6His was incubated and analysed by IMAC in the absence of CDeT11-24 to exclude unspecific binding of the CDeT11-24 antibody ($F2_{only\ kinase}$). As shown in **Figure 37** the CDeT11-24 antibody did not bind any protein spot in fraction $F2_{only\ kinase}$ which demonstrates that the result shown above is not due to unspecific binding of the antiserum against CDeT11-24. Next it was tested whether the interaction of CDeT11-24 and CpVIK requires phosphorylation of CDeT11-24. Therefore CDeT11-24 was incubated with $CpVIK_{dead}$6His and analysed by IMAC ($F2_{dead}$). Although in the fraction $F2_{dead}$ faint protein spots with a molecular weight of about 62 kDa and an isoelectric point of about 4 could be detected the signal strength was significantly reduced in comparison to the result of fraction F2+. Thus phosphorylation of CDeT11-24 seems to be important for binding activity to CpVIK.

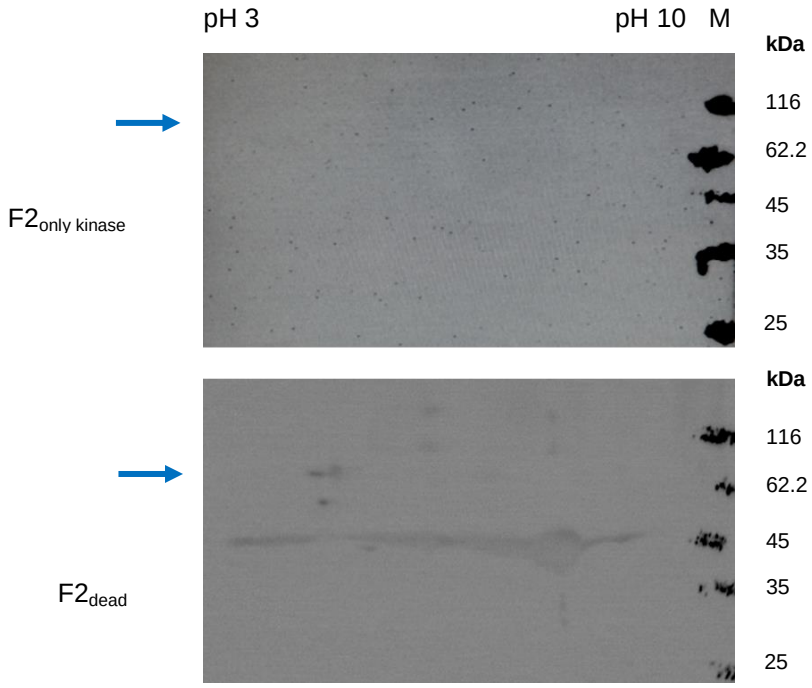

Figure 37: Protein-protein interaction studies without prey and with CDeT11-24 as prey and $CpVIK_{dead}$6His as bait
Proteins were immobilised by metal-affinity chromatography. Eluted proteins were separated via two dimensional SDS-PAGE (2.13.2), transferred to a nitrocellulose membrane and detected with antiserum against CDeT11-24 (2.15.1 and 2.15.2). The blue arrow indicates the protein spot corresponding to CDeT11–24.

To further determine the reduced binding affinity of CDeT11-24 to $CpVIK_{dead}$ and to exclude aberrance between different immunological analyses a one dimensional SDS-PAGE was performed with F2+ and $F2_{dead}$. As shown in **Figure 38** the lower binding affinity of CDeT11-24 to $CpVIK_{dead}$ compared to CpVIK could be validated by the reduced detection of the protein at about 62 kDa in $F2_{dead}$ than in F2+. However, also CpVIK and $CpVIK_{dead}$ seem to be detected on the membrane, due to cross-reactivity of either primary or secondary antisera. Unspecific background binding of antibodies in Western blots has been reported (Johnson et al., 1984; Wu et al., 2002; Baker et al., 2015).

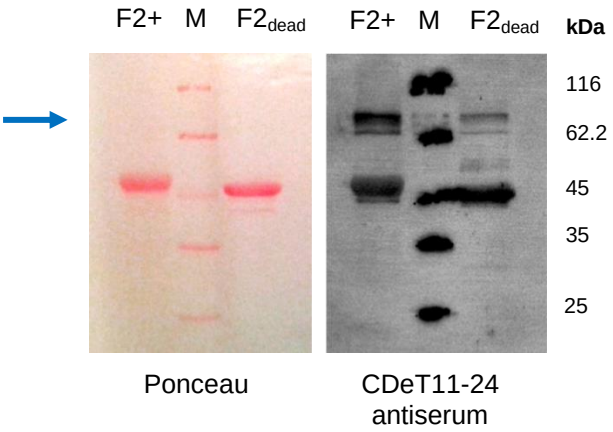

Figure 38: One dimensional protein-protein interaction studies with CDeT11-24 as prey and $CpVIK_{dead}$6His as bait
Proteins were immobilised by metal-affinity chromatography. Eluted proteins were separated *via* one dimensional SDS-PAGE (2.13.2), transferred to a nitrocellulose membrane and detected with antiserum against CDeT11-24 (2.15.1 and 2.15.2). The blue arrow indicates the protein band corresponding to CDeT11–24.

3.6.2 Pull down assays with *C. plantagineum* leaf extract

An immobilised metal-affinity chromatography-based (IMAC-based) analysis with CDeT11-246His as bait was performed to identify protein-protein interactions in *C. plantagineum* extracts. CDeT11-246His was overexpressed and purified as described in **2.21** and **2.22.2** and subsequently incubated in a crude protein extract from dehydrated *C. plantagineum* leaves (see **2.24.2**). After incubation the mixture was loaded on a Ni-NTA column and affinity chromatography was performed as described. Interacting proteins were co-eluted with CDeT11-246His from the column in six fractions (F1+ to F6+). As negative control the same plant extract was analysed by IMAC in the absence of CDeT11-246His (F1- to F6-). SDS-PAGE shows highest CDeT11-246His abundance in the F2+ and F3+ samples as depicted in **Figure 39** by the band at about 62 kDa. Besides CDeT11-246His several other co-eluting proteins can be observed in F2+ and F3+. Without CDeT11-246His only one band at about

20 kDa can be detected which might be explained by unspecific binding of this protein to the Ni-Sepharose matrix (F2- and F3-).

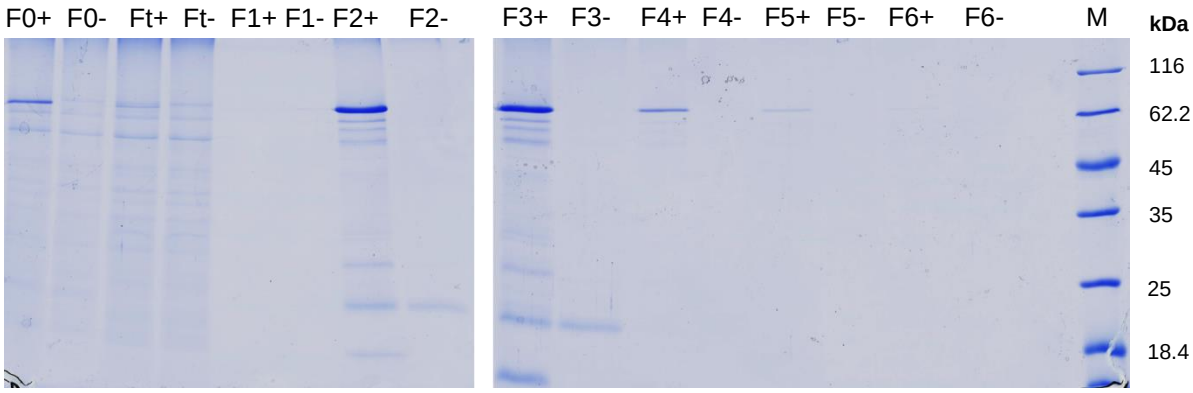

Figure 39: Protein-protein interaction assay using CDeT11-246His as bait and *Craterostigma plantagineum* extract
Immobilised metal-affinity chromatography-based with CDeT11-246His as bait incubated in a crude protein extract from dehydrated *C. plantagineum* leaves (see 2.24.2). Proteins were separated via SDS-PAGE (2.13.2) and stained with Coomassie (2.14.1). RWC of dehydrated *C. plantagineum* leaves was 4 %.

As a control, a sample of the plant extracts with (F0+) and without CDeT11-246His (F0) was taken before loading on the Ni-NTA agarose column. The band pattern is the same for F0+ and F0- except for a stronger band at about 62 kDa in F0+ representing the added CDeT11-246His (**Figure 39**). The flow through (Ft+ and Ft-) shows the same protein band pattern except for a missing band in Ft+ at about 62 kDa compared to the F0+ sample, representing CDeT11-246His protein bound to the column (**Figure 39**).

To further analyse the fractions F2+ and F2- and to determine if native CpVIK from *C. plantagineum* leaf tissue was co-eluted with CDeT11-246His, the protein samples were separated *via* SDS-PAGE and subsequently blotted on a nitrocellulose membrane for immunological analyses with the CpVIK antiserum (**Figure 40**). CpVIK could be detected by immunological analysis in the eluate (F2+) but not in the negative control (F2-) (**Figure 40 C**). This demonstrates that the CDeT11-246His protein is able to interact with the CpVIK protein in crude extracts from desiccated *C. plantagineum* leaf tissue.

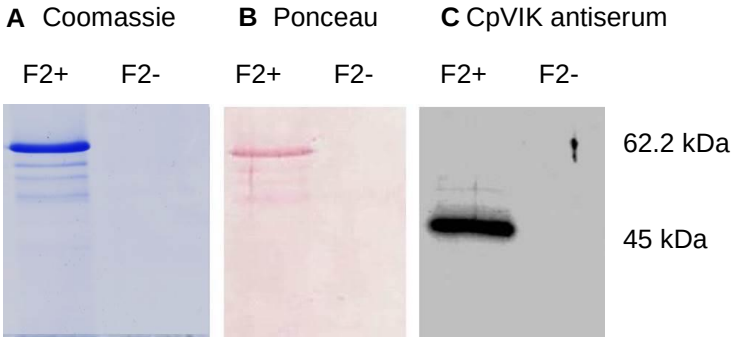

Figure 40: Identification of CpVIK after pull down from crude plant extract with CpCDeT11-24 as bait
Immobilised metal-affinity chromatography-based with CDeT11-246His as bait incubated in a crude protein extract from dehydrated *C. plantagineum* leaves (see 2.24.2). Proteins were separated via SDS-PAGE (2.13.2) and stained with A Coomassie (2.14.1) or transferred by electrophoresis to a nitrocellulose membrane for immunological analyses (2.15.1). B: The efficiency of the protein transfer was verified by incubation of the blotted membrane in Ponceau S staining solution. C: The CpVIK protein was detected in the fraction with the corresponding antiserum (2.15.2); RWC of dehydrated *C. plantagineum* leaves was 4 %

As depicted in **Figure 41** the eluted recombinant CDeT11-246His protein shows phosphoprotein specific staining. This indicates that the CDeT11-246His protein was phosphorylated during the incubation in the crude plant protein extract. However, phosphoprotein signal for CDeT11-24 can also be explained by binding of the phosphorylated endogenous protein from the extract of desiccated *C. plantagineum* leaves to the recombinant CDeT11-246His on the column. In addition to CDeT11-24 several other co-eluted proteins show phosphoprotein specific staining.

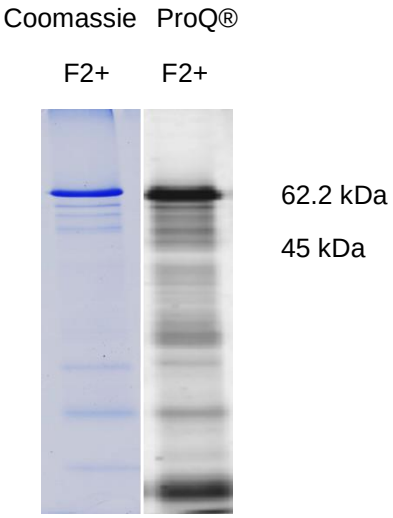

Figure 41: Phosphostain of proteins interacting with CDeT11-24His
Immobilised metal-affinity chromatography-based with CDeT11-246His as bait incubated in a crude protein extract from dehydrated *C. plantagineum* leaves (see 2.24.2). Proteins were separated *via* SDS-PAGE (2.13.2) and stained with ProQ® Diamond phosphoprotein stain (2.14.2) and subsequently with Coomassie (2.14.1)

3.7 Genotyping of Arabidopsis *AtVIK* knock out lines

Reverse genetic approaches provide remarkable progress in deciphering aspects of plant metabolism, especially since the completion of the Arabidopsis genome sequence. Isolation of knockout mutants in a gene of interest in Arabidopsis is a straightforward approach to study the role and function of the encoded protein. Knockout lines were purchased from the Salk Institute Genomic Analysis Laboratory (www.signal.salk.edu) and were generated by *Agrobacterium tumefaciens* mediated insertion of transfer DNA (T-DNA) into the gene of interest into the plant genome. Phenotypic abnormalities can be observed by comparing the knockout *A. thaliana* line to a wild type with the same genetic background. Because of this advantage and since *Arabidopsis thaliana* is a fully sequenced organism we used this plant species for further analyses of VIK kinase function.

3.7.1 Screening for T-DNA insertions

The *A. thaliana* T-DNA insertion lines *SALK_133072* and *SALK_002267* as well as wild type plants have been used in this study (see **2.1.1**). Prior to experiments, genotyping was conducted by PCR with gene and T-DNA-specific primers. Primer sequences are listed in section **2.4**. SALK_133072 carries a T-DNA insertion in the *AtVIK* promoter while SALK_002267 carries a T-DNA insertion in the eleventh *AtVIK* exon (**Figure 42**).

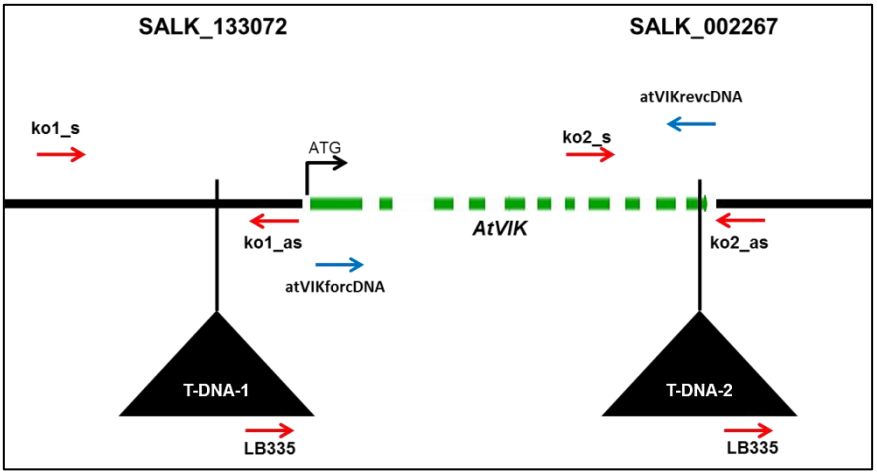

Figure 42: Gene model of *AtVIK* showing T-DNA insertions
The genotyping primer binding positions are indicated by red arrows; The RT PCR primer binding positions are indicated by blue arrows

For SALK_002267 a T-DNA insertion in the *AtVIK* gene and for *SALK_133072* a T-DNA insertion in the *AtVIK* promoter has been confirmed (**Figure 43**). All mutants were homozygous.

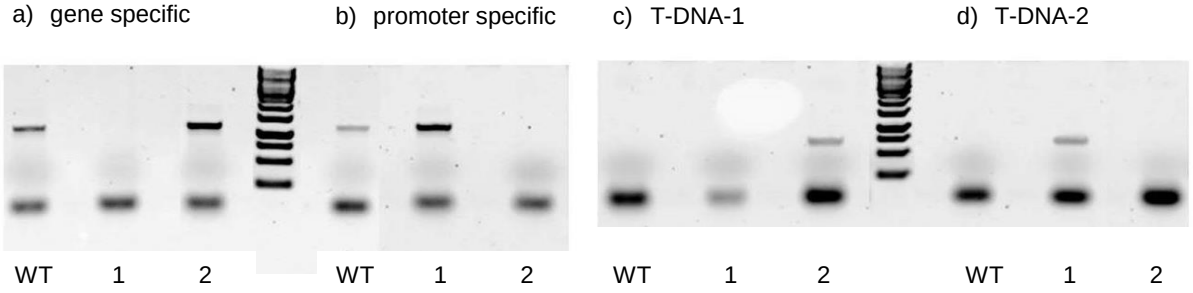

Figure 43: Genotyping of At1g14000 knock-out mutants
WT: wild type; 1: *SALK_002267*; 2: *SALK_133072*; 1-kb marker Fermentas
Primer combinations: a) vik_ko2s/vik_ko2as; b) vik_ko1s/vik_ko1as; c) LB335/vik_ko1as; d) LB335/vik_ko_2as

PCR on genomic DNA of wild type and *SALK_133072* plants resulted in an amplicon of about 1100 bp with gene specific primers (**Figure 43 a**) whereas combination of an insertion-flanking primer and a T-DNA-2 primer resulted in an amplicon of about 750 bp with genomic DNA of *SALK_002267* (**Figure 43 d**).

With promoter specific primers PCR on genomic DNA of wild type and *SALK_002267* plants resulted in an amplicon of about 1100 bp (**Figure 43 b**). When an insertion-flanking primer was used in combination with a T-DNA-1 primer in an amplicon of about 750 bp was obtained by PCR on genomic DNA of *SALK_133072* (**Figure 43 c**).

3.7.1 Screening for abundance of *AtVIK* transcript

Reverse transcription PCR was performed to screen for *AtVIK* transcript abundance in wild type, *SALK_002267* and *SALK_133072* plants. RNA was extracted from leaf tissues of mature plants, since *AtVIK* is known to be expressed highly in mature *A. thaliana* leaves (Wingenter et al., 2011). Actin primers were used as a control for cDNA quality.

Amplification with *AtVIK* specific primers resulted in an amplicon of 1185 bp for wild type and *SALK_133072*. In *SALK_002267* mutants no *AtVIK* transcript could be amplified (**Figure 44 a**) whereas the *actin* specific primer combination amplified a fragment (1130 bp) in all lines (**Figure 44 b**). Since the *AtVIK* transcript is present in wild type plants as well as in *SALK_133072* mutants, the T-DNA insertion in the *AtVIK* promoter (see **3.2.1**) does not prevent *AtVIK* transcription. Contamination with genomic

DNA can be excluded since the amplified fragment would include introns leading to a fragment size of 2308 bp for genomic DNA (primer positions are depicted in **Figure 42**). Further experiments were therefore carried out on *SALK_002267* mutant plants (*Δvik*).

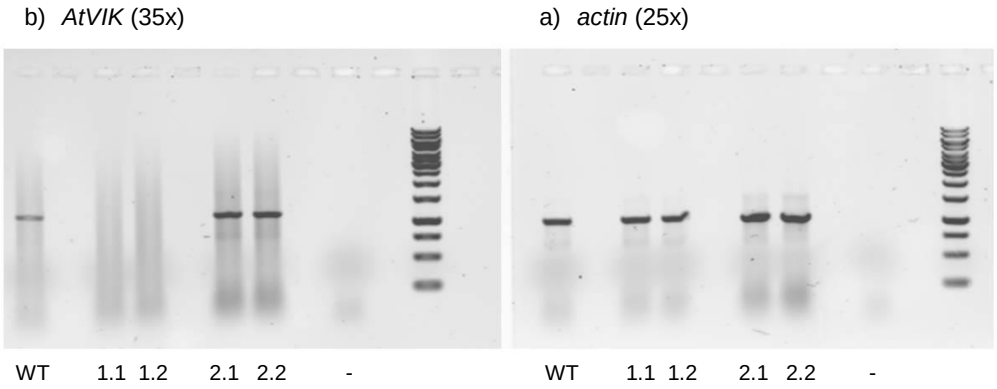

Figure 44: Reverse transcription PCR
WT: wild type; 1.1 and 1.2: two preparations of *SALK_002267*; 2.1 and 2.2: : two preparations of *SALK_133072*; 1-kb marker Fermentas; Primer cobinations: a) AtVIKforcDNA/ AtVIKrevcDNA; b) ATH–ACTIN2_FWD/ ATH–ACTIN2_REV

3.8 Phenotypic analysis of mutant plants

Phenotypic alayses of *SALK_002267* (*Δvik*) and wild type plants were carried out under standard conditions and upon different abiotic stresses (cold, salt, dehydration; see **2.1.2** and **2.1.3**). All plants were cultivated from seeds that were harvested at the same day and subjected to uniform conditions. No prominent phenotypic differences to wild type plants were observed for *Δvik* mutants upon standard cultivation conditions at different developmental stages (14 days, 28 days and 35 days) (**Figure 45**).

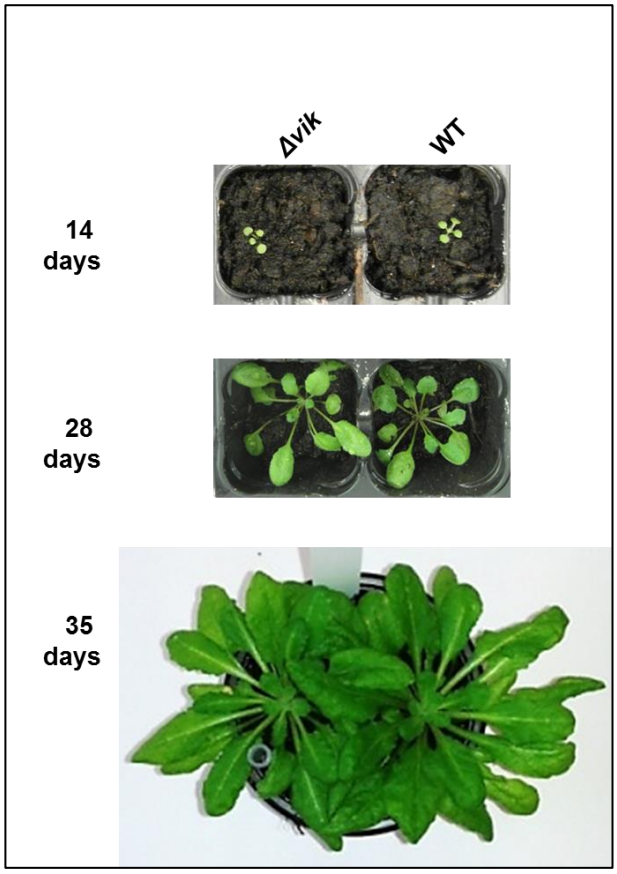

Figure 45: Phenotypic analysis of knock out *A. thaliana* plants (*Δvik*) after different time points upon standard cultivation conditions
WT: wild type; *Δvik*: *SALK_002267*

Adult plants (35 days) were analysed for phenotypic changes over 21 days of stress treatments. For all tested stress treatments no noticeable phenotypic difference could be observed (**Figure 46**). Also for stressed seedlings (14 days) and medium size plants (28 days) no difference in response to stress was observed (**supplemental figure 68**).

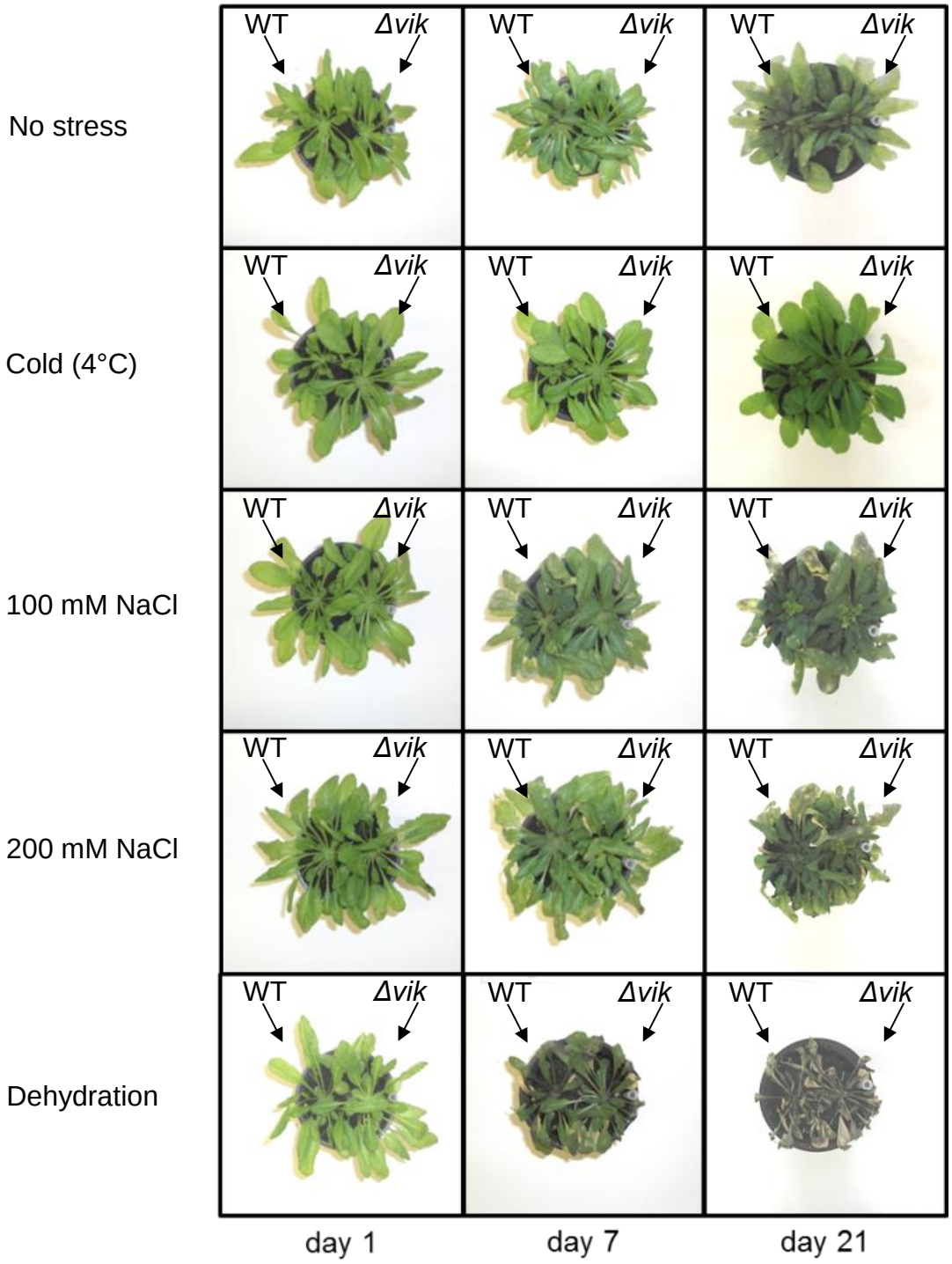

Figure 46: Phenotypic analyses of *Δvik* adult plants during 21 days of stress treatment
WT: wild type; *Δvik*: *SALK_002267*; Wild type plants are shown on the left hand site and *Δvik* plants in the same pot on the right hand side; Non-sterile plants of wild type and the *SALK_002267* line were sown as described in 2.1.2 on soil. At the four leaves state single plants of both wild type and *SALK_002267* were transferred together into new pots. The plants were further grown as described for 21 days (approximately 35 days after sowing) prior to stress treatment. The pots were then placed into Petri dishes, which were watered with 50 ml dH_2O per week as a control, or for osmotic stress treatments either with 100 mM or 200 mM sodium chloride solution. Dehydration stress was applied by withholding watering. Plants were transferred to 4°C for cold stress treatments. Phenotypic responses were examined during stress treatments for 21 days.

The relative water content (RWC) of leaves was monitored from three individual mature plants prior to stress treatments and after for 21 days of stress treatment. No significant difference between wild type and mutant could be observed concerning the reduction of the RWC (**Figure 47**).

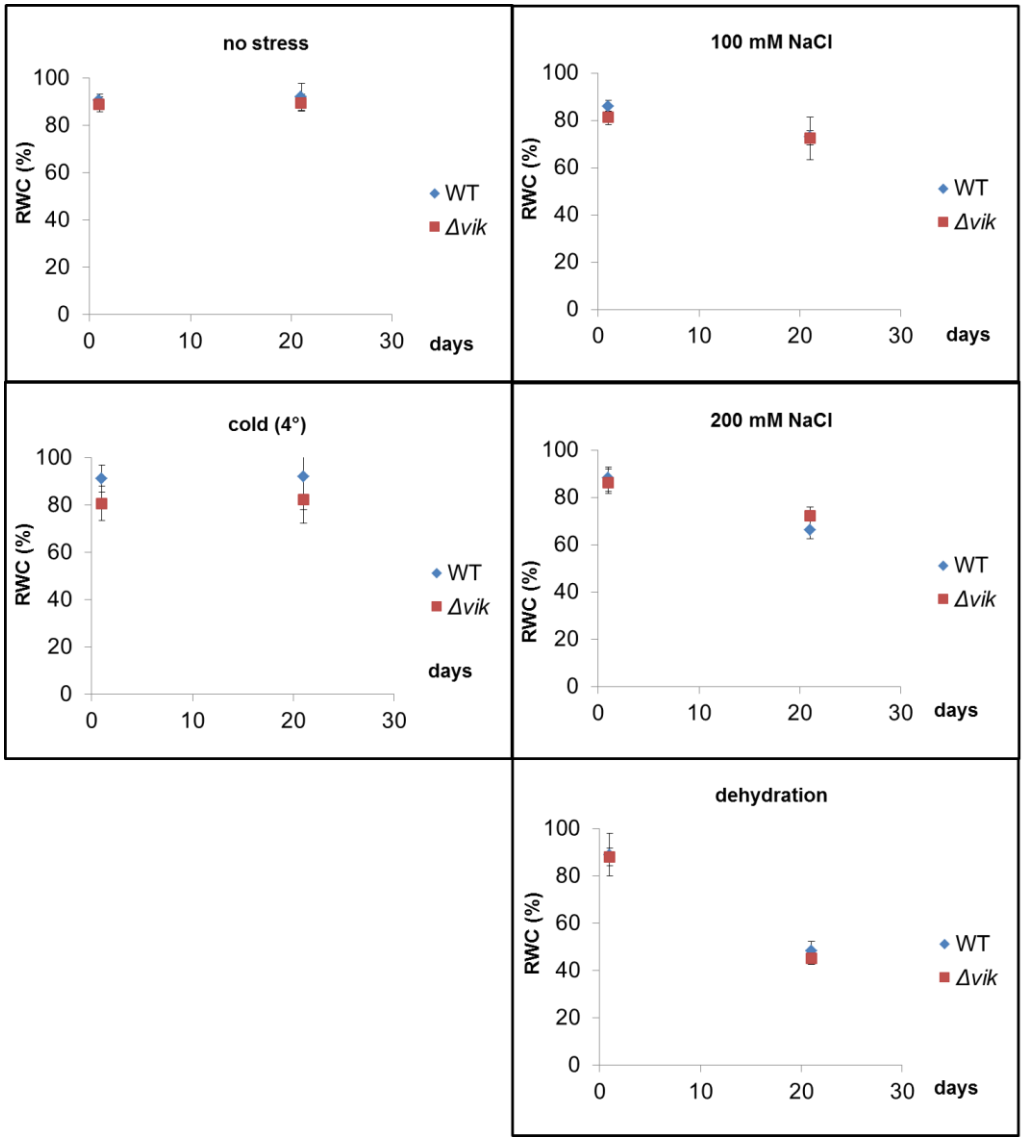

Figure 47: Analyses of the RWC after stress treatment of the knock out mutant *Δvik*
WT: wild type; *Δvik*: *SALK_002267*; Non-sterile plants of wild type and the *SALK_002267* line were sown on soil as described in 2.1.2. At the four leaves state single plants of both wild type and *SALK_002267* were transferred together into new pots. The plants were further grown as described for 21 days (approximately 35 days after sowing) prior to stress treatment. The pots were then placed into Petri dishes, which were watered with 50 ml dH2O per week as a control, or for osmotic stress treatments either with 100 mM or 200 mM sodium chloride solution. Dehydration stress was applied by withholding watering. Plants were transferred to 4°C for cold stress treatments. Changes in the relative water content were examined during stress treatments for 21 days.

3.9 Germination assay

During seed germination, plant seeds shift from a maturation- to a germination-driven developmental program for seedling growth initiation (Nonogaki et al. 2010). The process starts with the uptake of water by the mature dry seed (imbibition) and is terminated by emergence of the radicle through the seed envelopes. To prevent germination under non-optimal conditions, fresh seeds undergo a physiological state of dormancy (Iglesias-Fernández et al. 2011). This so-called after-ripening period can be terminated by a combination of several factors, such as storage time, temperature, light and humidity. Germination relies on the stored and *de novo* synthesized messenger RNAs and proteins involved in the release of seed dormancy, as well as on posttranslational modifications such phosphorylation (Brock et al. 2010; Hubbard et al. 2010). Since protein phosphorylation mediated by MAPKs plays a crucial role in seed germination processes (Xing et al. 2009; Liu et al. 2013b), germination assays on a knock out *A. thaliana* mutant with absent expression of the MAPKKK AtVIK can contribute to the understanding of the function of VIK kinases in plants. Signalling networks associated with both, seed desiccation tolerance and vegetative desiccation tolerance of resurrection plants, have shown to be related (see **1.3**) and a putative involvement of VIK in both pathways was examined in this study.

Seeds of *Δvik* and wild type plants were harvested at the same day from plants that have been subjected to uniform conditions. Germination was examined after stratification on MS-media and soil under standard conditions and osmotic stress conditions (**see 2.1.5**)

Dry seeds of *Δvik* and wild type showed no prominent phenotypic differences (**Figure 48**).

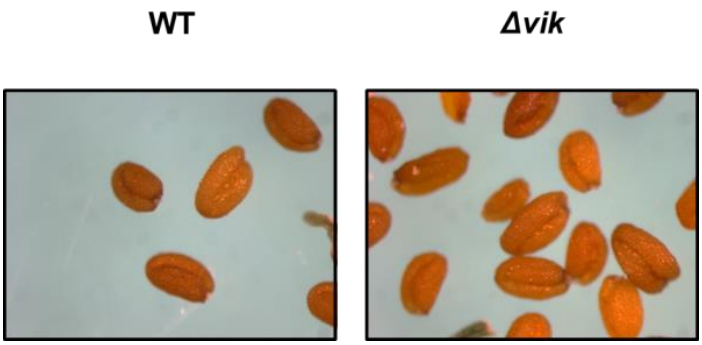

Figure 48: Dry seeds of wild type and *Δvik*
WT: wild type; *Δvik*: *SALK_002267*; pictures were taken with the SMZ 800 Nikon Digital Sight DS-2Mv binocular (Nikon, Düssel-dorf, DE)

3.9.1 Germination on MS media

Germinating seeds of *Δvik* and wild type showed no prominent phenotype under standard and osmotic stress conditions (**supplemental figure 67**). However as shown in **Figure 50** the rate of germinating *Δvik* and wild type seeds differed significantly. The number of seeds with an emerged radical on MS-media was 1.2 fold higher in wild type Arabidopsis plants than in *Δvik* after 4 days. On MS-media supplemented with 100 mM NaCl the germination rate decreased in both wild type and *Δvik*, respectively. The germination rate of wild type seeds under salt stress was reduced to 59 % compared to the germination rate under normal conditions but was twofold higher than for knock out *Δvik* seeds (**Figure 49**). For the *Δvik* seeds the germination rate under stress was reduced to 35 % compared to the *Δvik* germination rate under normal conditions (**Figure 49**).

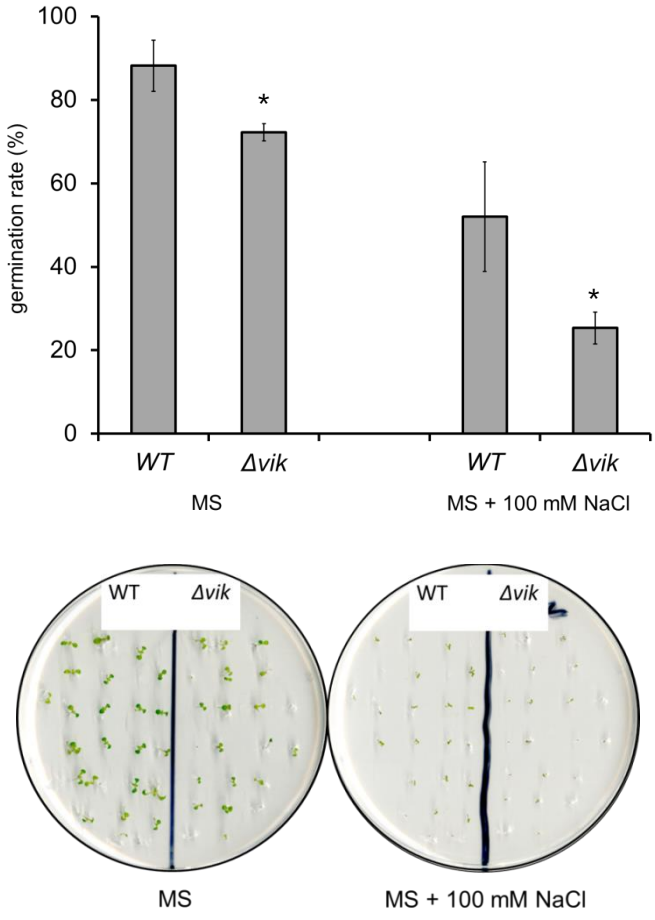

Figure 49: Germination assays with seeds of wild type and *Δvik* on MS media
WT: wild type; *Δvik*: *SALK_002267*; Germination assays were performed as described in 2.1.5. The germination rate was determined for three replicates with 100 seeds each, after 4 days under a stereoscopic microscope by counting the number of seeds with and without an emerged radical. Significant deviations of the *Δvik* germination rate to the wild type germination rate under the same conditions are marked with asterisks. Plates were photographed after 8 days when seedlings developed. A representative experiment is shown here.

3.9.2 Germination on soil

Germination tests were also performed on soil. The number of seedlings on soil watered with water or 100 mM sodium chloride was evaluated after 8 days and related to the number of seeds that were sown.

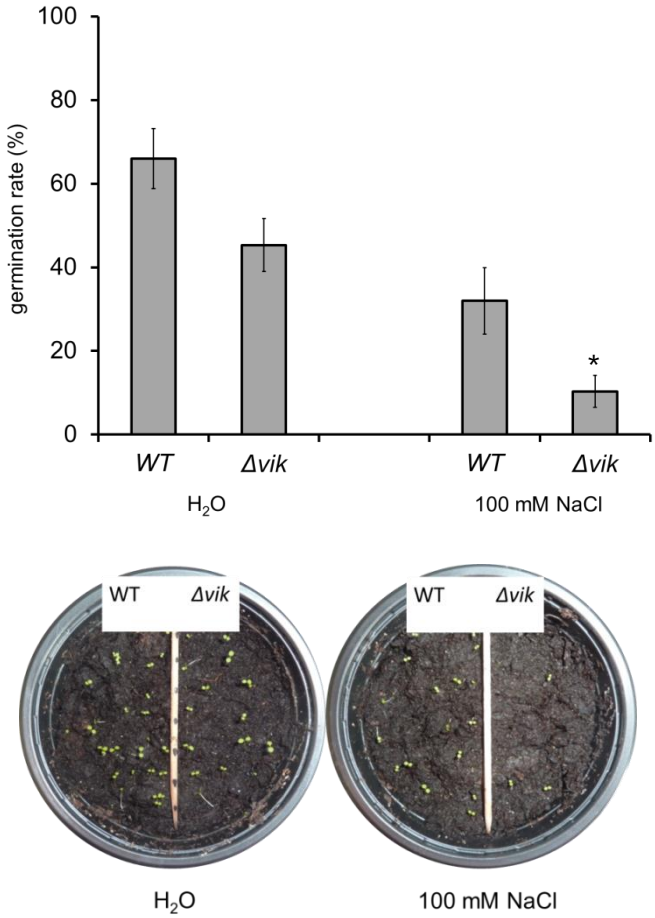

Figure 50: Germination assays with seeds of wild type and *Δvik* on soil
WT: wild type; *Δvik*: *SALK_002267*; Soil was dried at 80°C over night and watered with 1 ml/g of H_20 or 100 mM sodium chloride. Germination assays were performed as described in 2.1.5. The germination rate was determined for three replicates with 100 seeds each after 8 days by counting the number of seedlings in relation to the number of seeds that have been sown. Significant deviations of the *Δvik* germination rate to the wild type germination rate under the same conditions are marked with asterisks. A representative experiment is shown here.

On soil the results shown above (**3.9.1**) could be reproduced but the effect of VIK knock out on the germination rate was more pronounced. Under normal culture conditions the number of wild type seedlings on soil was 1.5 fold higher than the number of *Δvik* seedlings. As shown before the germination rate decreased in both wild type and knock out mutant upon salt stress. However, on soil the germination rate was threefold higher for wt than for *Δvik* (**Figure 50**).

3.10 Comparative seed proteome analyses in *A. thaliana* WT and *Δvik*

The germination rate of *Δvik* mutant seeds is decreased compared to wild type, especially under salt stress conditions (**3.4**). To identify differences in the seed proteome two-dimensional gel analyses were performed. Mass spectrometry analyses were applied to identify proteins putatively controlled by AtVIK.

3.10.1 Total- and phosphoproteins of WT and *Δvik* Arabidopsis seeds

Total- and phosphoproteins of WT and *Δvik* Arabidopsis seeds were extracted and enriched as described in **2.11.4** and **2.11.5**, respectively. To identify putative changes within the *Δvik* proteome two-dimensional gel analyses were performed as described in **2.13.2**. The proteins were stained first for phosphoproteins and subsequently with Coomassie for total proteins. No prominent differences could be observed in the total proteins of WT and *Δvik* (**Figure 51**).

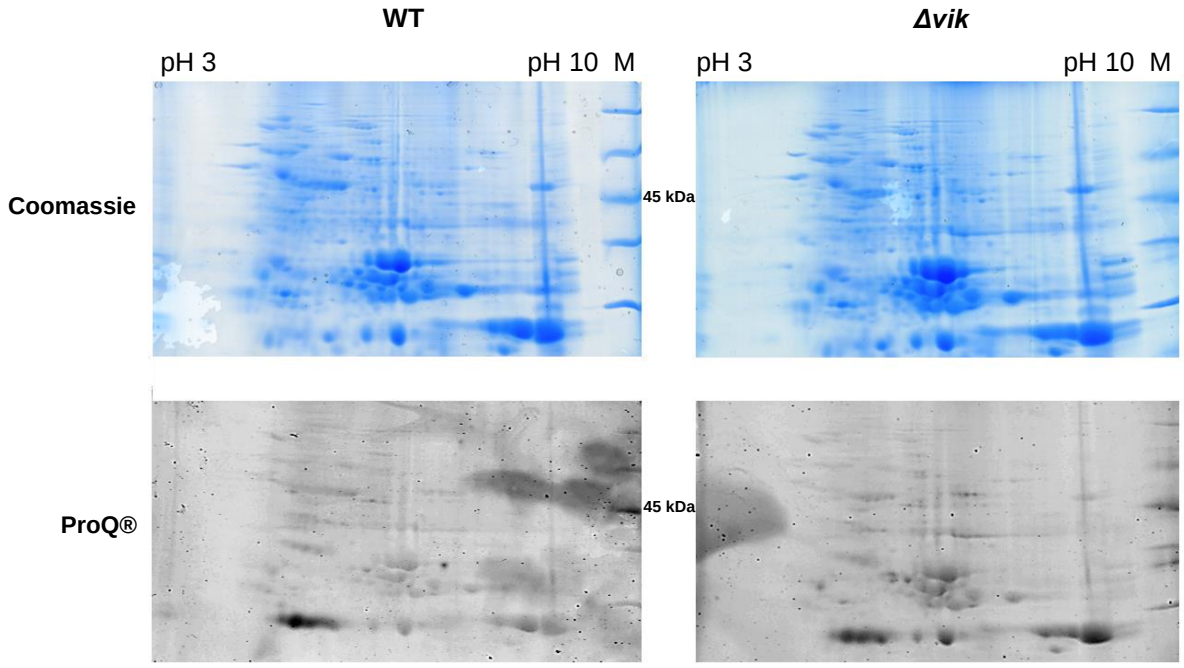

Figure 51: Two dimensional analysis of the total seed proteome in *A. thaliana*
WT: wild type, *Δvik*: *SALK_002267*; Total proteins were extracted from 2 week old seeds as described in 2.11.4. 100 µg total proteins were separated *via* 2D SDS-PAGE (2.13.2). Gels were stained with ProQ® Diamond phospho stain and subsequently with Coomassie blue.

However comparative analysis of the phospho-enriched subfractions of seed proteins showed a clear difference between WT and *Δvik* phosphoproteoms (**Figure 52**). One protein spot with an apparent molecular weight of 110 kDa and an isoelectric point of

about 5 (highlighted in a red box in **Figure 52**) shows clear difference in abundance and shape, whereas the overall protein pattern is highly similar concerning the separation and intensity of the protein spots.

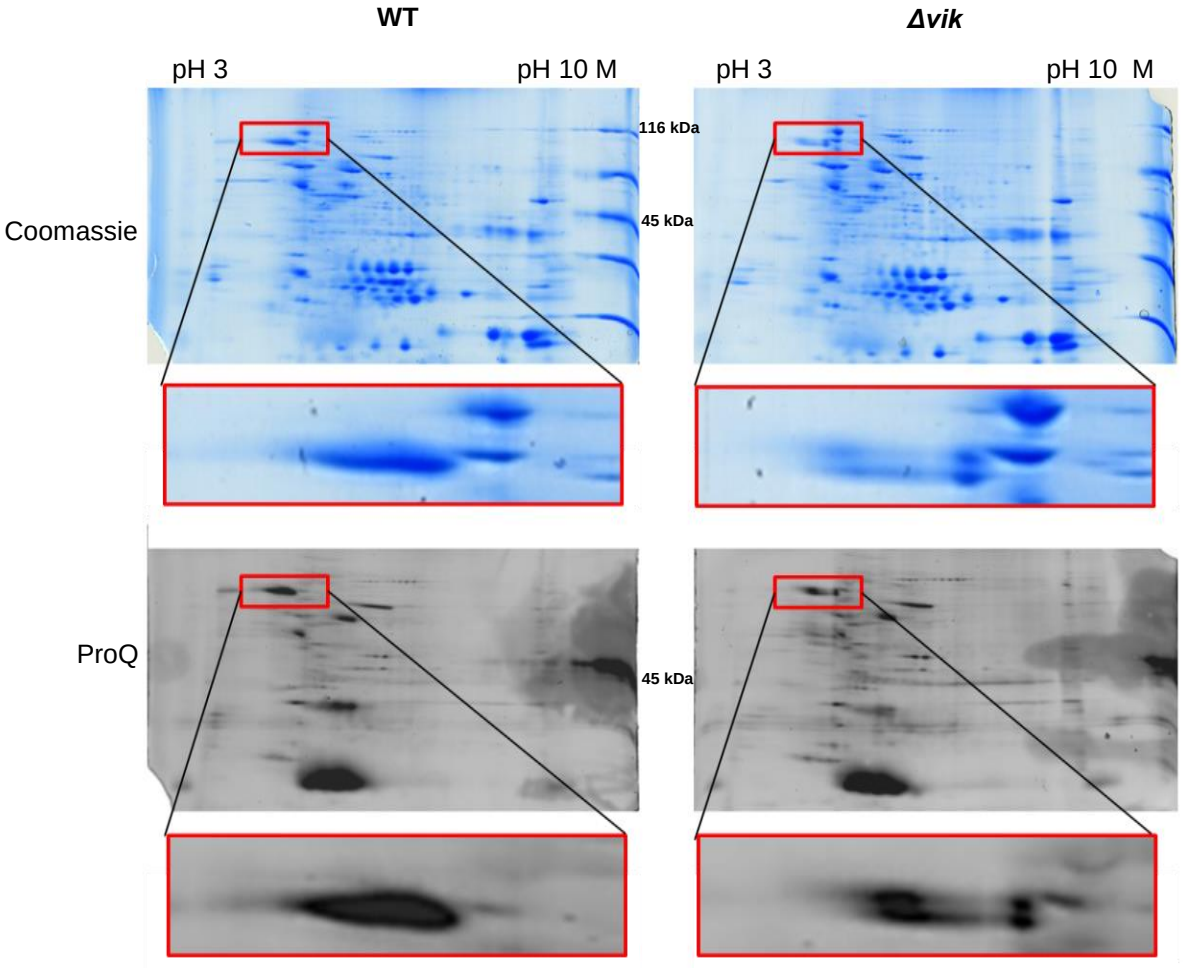

Figure 52: Two dimensional analysis of the phospho seed proteome in *A. thaliana*
WT: wild type, *Δvik*: SALK_002267; Total proteins were extracted from 2 week old seeds as described in 2.11.4 and phosphoproteins were enriched as described in 2.11.5. 100 µg phosphoproteins were separated *via* 2D SDS-PAGE (2.13.2). Gels were stained with ProQ® Diamond phospho stain and subsequently with Coomassie blue.

The above mentioned protein spot which showed a clear difference between wt and knock out plant was identified as RD29B/LTI65 by mass spectrometry analysis (**Table 10**; complete list included in the supplementary data files). Peptides identified by MS analyses (peptide mass fingerprint – PMF) are shown in **Figure 53**.

Table 10: Verification of the aberrant protein spot by LC-MS analysis as RD29B
The same peptide sample used for MALDI-TOF was analysed by LC-MS in order to identify the protein and determine phosphorylation sites. Mass spectrometric analyses were performed by Dr. Marc Sylvester at the core facility mass spectrometry (Institute of Biochemistry and Molecular Biology, University of Bonn).

Group Description	***Protein Group ID***	***# Proteins***	***# Unique Peptides***	***Found in WT***	***Found in Δvik***
[Master Protein] Low-temperature-induced 65 kDa protein / RD29B	*23*	*1*	*176*	*Found*	*Found*

Figure 53: MALDI-TOF Mass spectrometry analysis of the aberrant protein spot RD29B
Tryptic peptides were analysed by MS (peptide mass fingerprint – PMF). Grey highlighted: Coverage of RD29B sequence by assigned peptide mass peaks is shown on top. Selected peptides were fragmented by laser induced dissociation (MSMS, fragment ion spectrum, bottom). Mass spectrometric analyses were performed by Dr. Marc Sylvester at the core facility mass spectrometry (Institute of Biochemistry and Molecular Biology, University of Bonn). In the RD29B amino acid sequence, peptides that were identified in both, wt and *Δvik* are highlighted in grey.

Although RD29B has a calculated molecular weight of 65.53 kDa and a calculated isoelectric point of 5.14 it migrates aberrantly in the two dimensional gel which has been already reported earlier (migration at 82.5 kDa with a pI of 4.9; Irar et al., 2006).

3.10.2 Comparative analyses of RD29B phosphorylation in *A. thaliana* WT and *Δvik*

RD29B (synonyms LTI65; At5g52300) is a LEA protein, that harbours a CAP160 domain, which is present in various plant proteins. RD29B has been reported to be related CDeT11-24 protein from *C. plantagineum* (Velasco et al. 1998; van den Dries et al. 2011; Petersen et al. 2012). Several CAP160-containing proteins are associated with water-stress, such as CAP160 from spinach (Kaye et al. 1998) or the LEA-like CDeT11-24 protein from *C. plantagineum* (Röhrig et al. 2006). Also for RD29A and RD29B from Arabidopsis an induction by dehydration and salt stress has been reported (Yamaguchi-Shinozaki and Shinozaki 1994).

The phosphorylation of RD29B was analysed by mass spectrometry (MS) after tryptic in-gel digestion of proteins. Phosphorylation sites were identified with LC-MS analyses on a high resolution Orbitrap instrument. Altogether ten phosphosites were identified in the RD29B protein spots (**Table 11**). Five sites could only be identified in wild type. Additionally 3 phosphosites were identified with a lower confidence.

Table 11: Phosphosite identification of RD29B
Area: Peak area from the extracted ion chromatograms for the corresponding peptides
* Medians for all RD29B peptides that were identified in *Δvik* were divided by the medians for all RD29B peptides that were identified in WT for normalisation.

Phosphorylated peptides	***Position***	***Area WT***	***Area Δvik ****
*[K].SLSHAGETNVPA**S**EEIVPPGTK.[V]*	*S109*	*1,2E+06*	*/*
*[K].RLEEDPAAPGGG**S**DYLSGVSNYQSK.[V]*	*S240*	*4,4E+05*	*/*
*[R].MKV**T**DE**S**PDQKSR.[Q]*	*S281*	*1,1E+06*	*/*
*[R].DLPTGTHDQF**S**PELSRPK.[E]*	*S354*	*8,0E+05*	*8,0E+05*
*[K].LGYTGENGGGQSE**S**PVKDETPR.[S]*	*S421*	*6,4E+06*	*2,4E+06*
*[K].LPLSGGG**S**GVKETQQGEEK.[G]*	*S471*	*3,4E+05*	*3,5E+05*
*[K].GAVT**S**WLGGKPK**S**PR.[S]*	*S577*	*2,0E+07*	*2,7E+06*
*[R].SVEE**S**PQSLGTTVGTM.[G]*	*S584*	*2,2E+05*	*1,6E+06*
*[R].GGVTGKPKSL**S**HAGE**T**NVPASEEIVPPGTK.[V]*	*T104*	*9,5E+05*	*/*
*[R].EAHQEPLN**T**PVSLLSATEDVTR.[T]*	*T191*	*1,2E+06*	*/*

The extent of phosphorylation can be estimated by comparing chromatographic peak areas of phosphopeptide masses. The difference in abundance of RD29B between WT and *Δvik* samples required a normalisation prior to this comparison. The median peptide abundances of non-modified RD29B peptides were used as a reference for normalisation of peptide abundances from *Δvik* samples. After this normalisation no quantitative difference could be observed for the phosphorylation of S471 and S354

between *Δvik* and WT (**Table 10**). For S421 and S577 a reduced phosphorylation rate could be observed in *Δvik* compared to WT. Phosphorylation of S109, S240, S281, T104 and T191 could only be observed in WT (**Table 10**). Phopho-localisation assessment indicates that T278, and S281 can be phosphorylation sites on the same peptide, both in WT and *Δvik* samples. Similarly, S99 and S581 were found as alternative sites of phosphorylation (full list in the supplemental data files). Exemplary, the ion spectra of the peptide [R].EAHQEPLNTPVSLLSATEDVTR.[T] in WT and *Δvik* is shown in **Figure 54**.

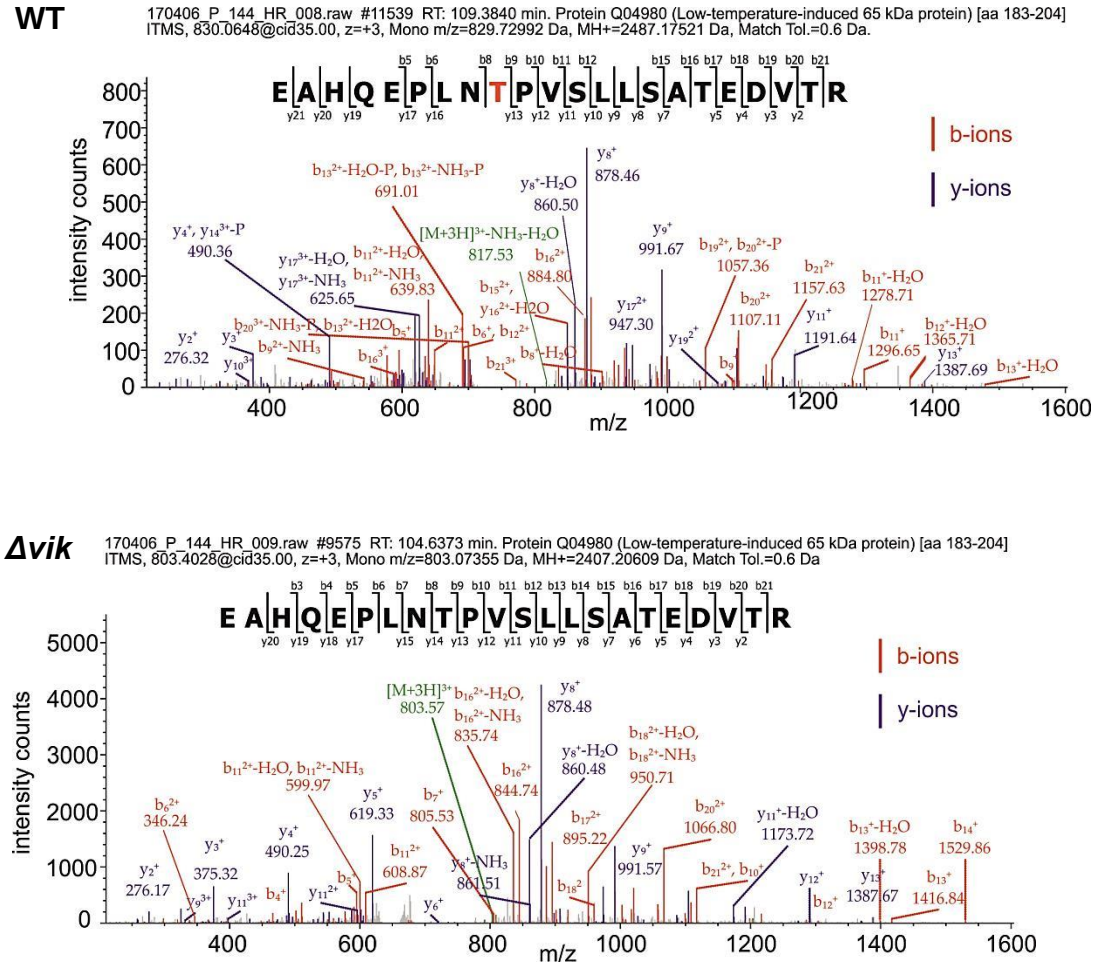

Figure 54: Exemplary ion spectra of identified phosphosites in RD29B

Exemplary ion spectra of distinctly phosphorylated residues of the peptide [R].EAHQEPLNTPVSLLSATEDVTR.[T] in WT and *Δvik*; Figure. Top fragment ion spectrum exemplifying evidence for phosphorylation on Thr191 in wild type sample. Retention time (RTT): 109.38 min, precursor mass to charge ratio (m/z)= 829.730 Da, (z=3, [M+H]+= 2487.175 Da), Mascot ion score=42, Percolator posterior error probability (PEP)=6.3E-05. Bottom Fragment ion spectrum of non-phosphorylated peptide around Thr191 in knock-out sample. RTT: 106.64 min, precursor m/z= 803.074 Da, (z=3, [M+H]+=2407.206 Da). Mascot ion score=42, Percolator posterior error probability (PEP)=6.3E-05. Match tolerance=0.6 Da was applied in both cases. Not all matching fragment ions are annotated due to space restraints. Precursor ions are shown in green. Fragmentation patterns of peptide sequences were generated with GPMAW10 (Lighthouse Data, Odense, Denmark).

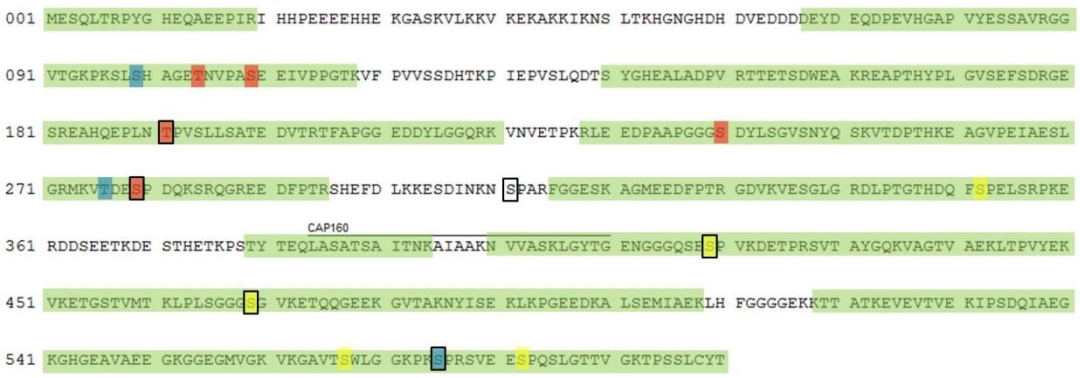

Figure 55: Identified phosphosites in RD29B
Green: Sequence sections that covered by the analysis; Yellow: Phosphosites that were identified in WT and *Δvik*; Blue: Phosphosites in WT and *Δvik* with lower confidence; Red: Phosphosites that were identified only in WT; Outlined sites represent already published sites.

In a previous study (Wolschin and Weckwerth 2005) five of the identified phosphosites were already reported (**Figure 56**). One site identified by Wolschin and Weckwerth (2005) (S313) was not covered. Two of the already known sites was phosphorylated in wild type (S281 and T191) but not in *Δvik*. Eight additional phosphosites, which were not reported so far, were identified in this study (**Figure 55**). For T191 and S577 a phosphorylation by MAPKKKs has been predicted (determined with the Group-based Prediction System 3.0 software).

In summary, a differential phosphorylation of RD29B in *Δvik* was shown.

3.11 Comparative leaf proteome analyses in *A. thaliana* WT and *Δvik*

As reported previously *AtVIK* gene expression is induced by salt stress in *A. thaliana* leaf tissue (Wingenter et al. 2011). To identify differences in the leaf proteome of the *Δvik* mutant, two-dimensional gel analyses were performed.

3.11.1 Phosphoproteins of WT and *Δvik* Arabidopsis leaves

Total- and phosphoproteins of WT and *Δvik* were extracted and enriched (described in **2.11.4** and **2.11.5**) from leaves of salt stressed and unstressed Arabidopsis plants. Two-dimensional gel analyses (described in **2.13.2**) were performed to identify putative changes within the *Δvik* leave proteome. The proteins were stained first for phosphoproteins and subsequently with Coomassie for total proteins. No prominent

differences were observed in the phospho-enriched subfractions of leaf proteins of unstressed WT and *Δvik* (**Figure 56**).

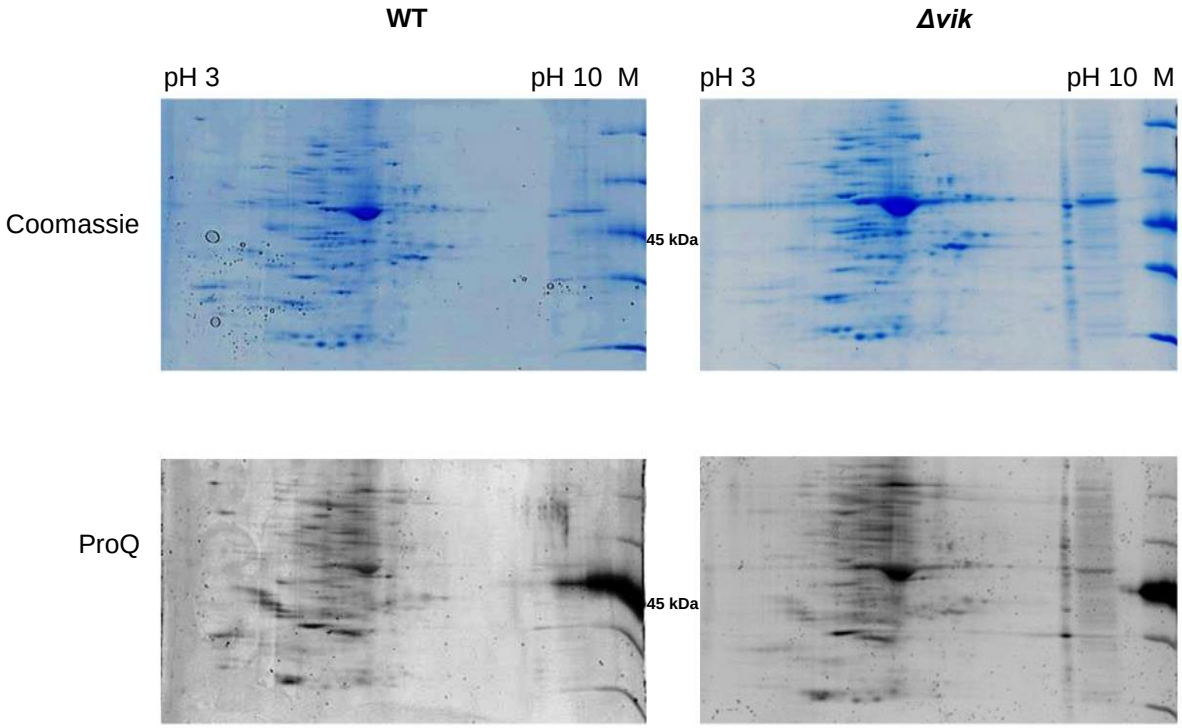

Figure 56: Two dimensional analysis of the phospho leaf proteome in *A. thaliana*
WT: wild type, Δvik: SALK_002267; Total proteins were extracted from 2 week old seeds as described in 2.11.4 and phosphoproteins were enriched as described in 2.11.5. 100 µg phosphoproteins were separated *via* 2D SDS-PAGE (2.13.2). Gels were stained with ProQ® Diamond phospho stain and subsequently with Coomassie blue.

In contrast, in a first attempt a comparative analysis of the leaf phosphoproteins after salt stress treatment showed a clear difference between WT and *Δvik* phosphoproteoms (**Figure 58**). One protein spot with an apparent molecular weight of 40 kDa and an isoelectric point of about 4 (highlighted in a red box in **Figure 57**) was less abundant in wild type than in *Δvik* mutant.

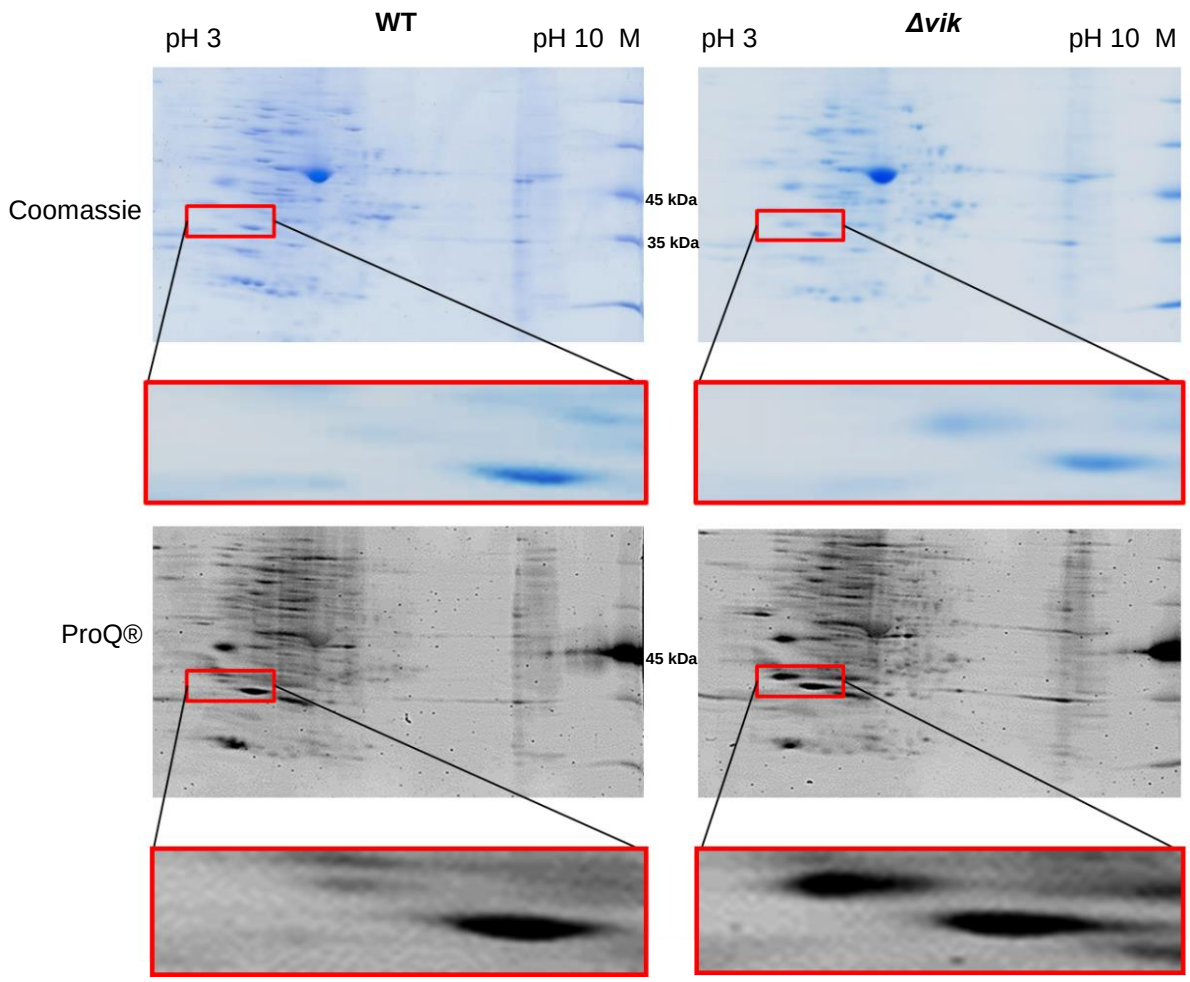

Figure 57:Two dimensional analysis of the phospho leaf proteome in *A. thaliana*
WT: wild type, Δvik: SALK_002267; Total proteins were extracted from adult plants after 2 week old seeds as described in 2.11.4 and phosphoproteins were enriched as described in 2.11.5. 100 µg phosphoproteins were separated *via* 2D SDS-PAGE (2.13.2). Gels were stained with ProQ® Diamond phospho stain and subsequently with Coomassie blue.

The above mentioned protein spot, which showed a reduced abundance in wild type, was more prominent in the phosphoprotein staning. Clear staining in Coomassie blue is essential for identification by mass spectrometry analysis. Further analyses of the *Δvik* leaf phosphoproteom will have to be carried out.

4 Discussion

In this study shared mechanisms between seed germination in a desiccation sensitive plant and vegetative drought tolerance of a resurrection plant were demonstrated by the characterisation of a MAPKKK in *C. plantagineum* (CpVIK) as well as its homolog in *A. thaliana* (AtVIK). MAPKKKs are known to be involved in multiple drought stress related pathways in plants. However their role in the acquisition of drought tolerance in resurrection plants has not been investigated up to now. This work shows that the expression of CpVIK on the RNA level is enhanced by abiotic stresses including dehydration. These data are in accordance with previous studies on AtVIK (Wingenter et al., 2011). A difference between the gene expression of *CpVIK* and *AtVIK* was observed concerning salt and cold stress. Moreover, studies on the protein and phosphoprotein level revealed stress-dependent phosphorylation of the CpVIK protein.

The dehydration-related LEA-like protein CDeT11-24, which was originally used as kinase substrate for the identification of CpVIK by in-gel-kinase assays (Petersen, 2012), is phosphorylated *in vitro* by CpVIK as shown in this study. Furthermore co-expression of CDeT11-24 and CpVIK was demonstrated and both proteins co-localise in the cytosol within plant cells. In addition to the above mentioned indications for a functional coupling of both proteins, interaction of the recombinant CDeT11-24 with the native CpVIK protein was observed in dehydrated leaf tissue.

Evidence is presented for an AtVIK dependent phosphorylation of the CDeT11-24 homolog RD29B in Arabidopsis. Five phosphorylation sites were not phosphorylated in RD29B extracted from seeds of an *AtVIK* knock-out mutant in comparison to wild type plants. Seeds of this *Δvik* mutant showed a lower germination rate particularly under salt stress conditions.

4.1 Gene analysis of CpVIK and AtVIK

The *CpVIK* gene has been identified from *C. plantagineum* by DNA-Blast using the *AtVIK* cDNA sequence against the *C. plantagineum* transcriptome data bank which was generated by Rodriguez et al., 2010. Two overlapping contigs (#08317; 1121 bp and #13110; 364 bp) with high identity to *AtVIK* were identified that represent different sections of the *CpVIK* gene. The total length of the *CpVIK* gene is 1329 bp and the sequence harbours a MAPKKK domain as well as tandem-repeat ankyrin motifs (ANKs) (see **3.1.1**). ANKs are reported to mediate protein-protein interactions between

different proteins. It was already demonstrated for AtVIK, that interaction with the receptor-like kinase VH1 (VASCULAR HIGHWAY1) depends on the ANK domain (Ceserani et al. 2009). However an interaction of an ankyrin-repeat motif protein with LEA or LEA-like proteins, as described in this study, has not yet been reported.

MAPKKKs are mainly involved in signal transduction (**1.4.2**). Comprehensive studies revealed a crucial role for MAPKKK genes in response to biotic and abiotic stresses in plants (Frye et al. 2001; Ichimura et al. 2006; Pitzschke et al. 2009a; Pitzschke et al. 2009b). The MAPKKK family is divided into three clades (A to D; Ichumura et al., 2002) and as reported for several plant species, some members of clade B and C could be subdivided to the Raf-like MAPKKK family (Rao et al. 2010; Kong et al. 2013; Yin et al. 2013). CpVIK also belongs to the C1 group among the Raf-like kinases according to specific conserved signature motifs (**1.4.3; 3.1.1**).

Research on the octaploid plant species *C. plantagineum* is restricted by genomic sequence availability and the unavailability of knock out mutants. However, in the fully sequenced genetic model plant *A. thaliana* a homolog to *CpVIK* with the same functional domains and a protein sequence identity of 80.7 % is present (*AtVIK*). Since a knock out line (*Δvik* ≙ SALK_002267) lacking *AtVIK* gene expression is available (**3.7.1**), an analysis of this closely related gene has been included in this thesis to study the functional role of VIK in *A. thaliana*.

The *AtVIK* chromosomal gene (2925 bp) is located on chromosome 1 and consists of eleven exons. After splicing, the cDNA sequence comprises 1313 bp. In the intergenic region upstream of *AtVIK* (between At1G13990 and At1g14000) several putative *cis*-acting elements related to plant development, biotic and abiotic stresses and seed germination are present on both, sense and antisense strand (**supplemental table 16**). This supports on the sequence level the observed induction of the *AtVIK* gene expression by drought, cold, salt and osmotic stress in mature leaves as well as high expression in developing seeds (Wingenter et al. 2011). However, a functional analysis of these *cis*-acting elements was not carried out in this thesis.

VIK genes are evolutionary conserved (**4.2**) and low variation in the coding regions of the *AtVIK* gene (**3.1.5**) among the 1001 accessions of *A. thaliana* analysed in the “1001 Genomes Project” (http://1001genomes.org/), implies an essential function of *AtVIK*. Only 2.06 % of variable amino acids have been identified in the AtVIK protein sequence. Such a low protein sequence variation was also reported for several other proteins that are involved in plant signalling pathways, such as pathogen and herbivore response (Bakker et al. 2008).

4.2 ANKMAPKKKs in plants

A fundamental role of tandem-repeat ankyrin motif containing MAPKKKs (ANKMAPKKKs) can be assumed, based on their early occurrence during evolution already in bacterial genomes and the conservation in plants as well as metazoa. Within the plant kingdom ANKMAPKKKs show a higher conservation compared to the ANKMAPKKKs from metazoa or fungi as shown in the phylogenetic tree (**Figure 6**). This indicates functional adaption to plant-specific requirements, such as stress-response, seed development and photosynthesis-related pathways as shown for several MAPKKKs in plants (Teige et al. 2004; Xing et al. 2009; Shen et al. 2012; Gasulla et al. 2016). The homology of VIK-like genes increases in the angiosperm taxa. Interestingly VIK orthologs represent unique representatives in a subclade of class III of ANKMAPKKKs implying a unique function, whereas several paralogs of other ANKMAPKKKs are present in the selected species. Several genome wide approaches on MAPKKK identification have demonstrated that the number of ANKMAPKKKs differs in plant species. For tomato it has been reported that only one gene (SIMAPKKK2, Gene ID: 101259335) is present among the MAPKKK family (Wu et al. 2014). In maize two ANKMAPKKKs are present (ZmMAPKKK46 and 47, nomenclature of Kong et al. [2013]) and in *A. thaliana* five ANKMAPKKK were identified (MAPK Group et al. 2002; Rudrabhatla et al. 2006).

Only little is known about the function of ANKMAPKKKs in plants so far. For AT4G18950 it was shown to be essential for stomatal opening in response to blue light together with AtVIK (Hayashi et al. 2017). AtVIK was reported to phosphorylate the tonoplast monosaccharide transporter AtTMT1 and to interact with the receptor-like kinase VH1/BRL2 (Ceserani et al. 2009). An altered sensitivity of *AtVIK* insertion mutants (*Δvik*) to auxin and brassinosteroids has been reported as well as vein pattern defects (Ceserani et al. 2009). Most members of ANKMAPKKKs have only been described on the genetic level *via* genome wide MAPKKK identification approaches including stress and tissue specific gene expression analyses (majorly based on mirco array analyses) or prediction of subcellular protein localisation for some members (Rudrabhatla et al. 2006; Rao et al. 2010; Kong et al. 2013; Wu et al. 2014; Wang et al. 2015; Liu et al. 2015; Wang et al. 2016). Micro array analyses indicate divergent functions of Arabidopsis kinases since a differential tissue and stress specific gene expression was observed for the members of the ANKMAPKKK family (*AtVIK* [*At1g14000*], *At4g18950*, *At3g58760*, *At2g43850*, *At2g31800*) (Rudrabhatla et al. 2006). However, further RT-PCR analyses of *At1g14000* (Wingenter et al. 2011), *At4g18950* (Hayashi et al. 2017) and *At2g31800* (Chinchilla et al. 2008) revealed

divergent expression profiles compared to the results of Rudrabhatla et al. (2006). For *AtVIK* for instance an expression mainly in seedlings and young plants has been reported as well as an up-regulation of expression in senescent leaves, stamen and roots (Rudrabhatla et al. 2006). Contrastingly, RT-PCR analyses revealed highest expression levels in seeds as well as mature leaves (Wingenter et al. 2011). Further analyses of ANKMAPKKKs are therefore essential for elucidating their function.

In summary one can assume, that despite the structural similarity of ANKMAPKKKs the functions of these kinases may be quite diverse and are still poorly understood. The results of previous studies however indicate an involvement in stress response, photosynthesis and development. AtVIK is presumably involved in all three pathways as demonstrated by Ceserani et al. (2009), Wingenter et al. (2011), Hayashi et al. (2017) as well as by this work.

Based on transcriptome data, in the Linderniaceae family only one ANKMAPKKK gene appears to be present in each family member. The identified genes show high identity to *AtVIK* (**3.1.4**). However, due to the lack of saturated sequence information it cannot be excluded that other ANKMAPKKK genes are present in the genome of *C. plantagineum, L. brevidens and L. subracemosa* (Rodriguez et al. 2010a). Nevertheless for some plant species it has been reported, that only one ANKMAPKKK gene is expressed (Wu et al. 2014; Rao et al. 2010). When only one ANKMAPKKK gene is expressed in a plant species, it shows more similarity to *AtVIK* than to one of the other ank-repeat kinases (Wu et al. 2014; Rao et al. 2010; **3.1.4**). This indicates that VIK genes play an essential role in plants.

4.3 Stress and tissue specific CpVIK transcript and protein accumulation

The gene expression of the members of the MAPKKK gene family is highly regulated in different tissues and during stress treatments to direct different physiological processes (Rao et al. 2010; Wingenter et al. 2011; Wu et al. 2014; Liu et al. 2015). In order to gain insight into distinct functions of CpVIK in *C. plantagineum*, the CpVIK protein expression was analysed in different tissues and during various stress treatments. CpVIK was expressed on the protein level in all tested tissues including roots, seeds, flower tissue, flower stem and leaves (**3.4**). Further investigation on *C. plantagineum* leaf tissue revealed induction of protein expression by dehydration, mannitol and salt but not by cold stress. Reverse transcription PCR analyses support these findings for the RNA level. Consequently higher transcription of the *CpVIK* gene contributes to the

higher abundance of the CpVIK protein in stressed tissue, although protein stabilisation and degradation may also be involved. Background expression of CpVIK was detected at all analysed developmental stages, but the expression is minimal in unstressed tissue of younger *C. plantagineum* plants. However, gene and protein expression was induced by dehydration to a similar level than in mature plants. This indicates that higher CpVIK protein levels during dehydration are essential in all developmental stages. The function during non-stressed conditions in mature plants remains to be elucidated.

Since the highest transcript and protein levels are observed after dehydration stress in all cases (**3.4.1**; **3.4.2**; **3.4.3**), it is reasonable to assume that the kinase is involved in drought-stress related pathways. This is supported by the finding that CpVIK is co-expressed with the stress-related LEA-like protein CDeT11-24 from *C. plantagineum* and that both proteins are localised in the cytosol. CDeT11-24 was induced by the same stimuli (**3.4.5**) which agrees with previous studies on CDeT11-24 expression (van den Dries et al. 2011). The function of CDeT11-24 is not fully understood but its contribution in the acquisition of drought tolerance has been postulated based on the observation that expression is tightly linked to dehydration stress in drought tolerant species. Moreover, a protein-stabilising function of CDeT11-24 was demonstrated *in vitro* and it is suspected to play a role in the formation of a steric buffer area that acts as “molecular shield” between neighbouring membranes during dehydration (van den Dries et al. 2011; Petersen et al. 2012).

The gene expression pattern of *CpVIK* shares characteristics with VIK orthologs in other plant species concerning stress and tissue specific induction (**Table 12**). In contrast to the other species, the gene expression of *CpVIK* in *C. plantagineum* in vegetative tissue is higher in than in seeds (**3.4.1**). A lower induction by dehydration than by salt was reported for the orthologs in Arabidopsis and tomato whereas *CpVIK* is induced stronger by dehydration (**3.4.2**). Cold had no effect on *CpVIK* gene expression whereas the orthologs in Arabidopsis and tomato show clear induction after cold treatment. An increase of gene expression in mature leaves compared to young leaves can be observed for most VIK genes (Table 12) indicating a function in later stages of plant development.

Table 12: Comparison of tissue- and stress-dependent gene expression of VIK orthologs
Arabidopsis thaliana (At), *Craterostigma plantagineum* (Cp), *Solanum lycopersicum* (Sl), *Zea mays* (Zm), *Oryza sativa* (Os); Expression in young leaves was taken as reference for tissue specific-expression and up or down regulation is symbolised by arrows and colour intensity; for stress-specific expression, background expression under control conditions was taken as reference; tissue- and stress-specific expression are not compared with each other; grey highlighted boxes indicate absence of expression information.

Plant species	**At**	**Cp**	**Sl**	**Zm**	**Os**
Gene	(*At1g14000*)	(*CpVIK*)	(*SMAPKKK2*)	(*ZmMAPKKK46)*	(*OsMAPKKK74*)
Tissue-specific expression					
Young leaf	→	→	→	→	→
Adult leaf	↑	↑	↑	→	↑
Flowers	→	↑	↑↑↑	→	→
Roots		↑	↓	↑	↓
Seeds	↑	→		↑	↑
Stress-specific expression in vegetative tissue					
Control	→	→	→	→	
Dehydration	↑	↑↑	↑	→	
Cold	↑	→	↑		
NaCl	↑↑	↑	↑↑		
Source	(Wingenter et al. 2011)	This study (**3.4**)	(Wu et al. 2014)	(Liu et al. 2013a; Liu et al. 2015)	(Rao et al. 2010; Hao et al. 2016)

Taken together, a stronger induction of the *VIK* gene expression in leaf tissue during drought stress compared to other stresses was only observed in the resurrection plant *C. plantagineum* to this date, while in desiccation sensitive species a high expression in seeds has been reported (**Table 12**). Thus it is tempting to speculate that VIK participates in the acquisition of drought tolerance in vegetative tissue of desiccation tolerant *C. plantagineum* as well as in seeds of desiccation sensitive plant species.

However, different methods were used to investigate gene expression in the studies mentioned above, such as RNA-sequencing, northern blot, real time PCR or reverse transcription PCR. Thus the results should be compared with caution. Further systematic expression analysis of *VIK* is required to allow the conclusion that the expression pattern of *CpVIK* as representative of a desiccation tolerant plant species differs from *VIK* genes of desiccation sensitive species and correlates with desiccation tolerance. These analyses should be extended to protein expression and phosphorylation analyses of VIK kinases since this has not been done in any other species apart from *C. plantagineum*.

4.4 Dehydration dependent phosphorylation of CpVIK

In leaves and roots of dehydrated plants a much stronger CpVIK phosphorylation was observed compared to unstressed plants (**3.4.4**). Phosphorylation can influence several parameters of target proteins such as activity, conformation, substrate recognition or intracellular localisation. MAPKKKs are known to be activated after perception of extracellular stimuli prior to their enzymatic phosphorylation of MAPKKs or other substrate proteins. The activation of MAPKKKs is frequently regulated by phosphorylation by a MAPKKKK that is linked to the plasma membrane (Qi et al., 2005). MAPKKKs are also often activated by interaction with GTPases, proteolysis and binding to regulatory or scaffold proteins (Qi and Elion 2005; Cargnello and Roux 2011). For human RAF type MAPKKK an activation and deactivation by recruitment to Ras GTPase at membranes together with phosphorylation at regulatory sites has been shown (Wellbrock et al. 2004; McCubrey et al. 2007). The dehydration-induced phosphorylation of the RAF-like CpVIK thus indicates activation during drought stress.

Phosphorylation can also lead to stabilisation of proteins due to decreased ubiquitination which results in decreased proteasomal degradation (Joo et al. 2008; Hong et al. 2011; Moretto-Zita et al. 2010). Recombinant non-phosphorylated CpVIK6His protein was degraded in crude plant extracts of desiccated plants (**supplemental figure 60**), pointing to a low stability of not-phosphorylated CpVIK protein under stress conditions. However, a putative stabilisation effect of CpVIK phosphorylation has not been investigated in this study. Stabilisation of proteins by phosphorylation has been reported to play an important role in abiotic stress response (Lin et al. 2009; Liu and Zhang 2004).

Stress-dependent phosphorylation was observed for several proteins in *C. plantagineum*. These proteins, such as CDeT11-24, were related to drought-

tolerance. Interaction of the CDeT11-24 LEA-like protein with CpVIK has been hypothesised based on an *in gel* kinase assay in previous studies (Petersen 2012) and supported by pull down assays and *in vitro* kinase assays in this study (**3.5** and **3.6**).

For CpVIK autophosphorylation activity was demonstrated *in vitro* (**3.5.1**) and from the sequence 24 sites have been predicted to be phosphorylated in CpVIK of which 8 are conserved in AtVIK (**3.1.6**). Multiple regulatory phosphorylations at several distinct sites were reported for other Raf-type MAPKKKs, such as Raf-1 in humans which is phosphorylated at least in thirteen sites (McCubrey et al. 2007). A complex regulation of CpVIK by phosphorylation in response to drought is therefore assumed.

CDeT11-24 phosphorylation by the action CpVIK *in vitro* involves autophosphorylation of CpVIK (**3.5.1**). Thus, activation by phosphorylation is reasonable to assume. Mutagenesis of phosphorylated sites in CpVIK could reveal whether a non-phosphorylated version CpVIK with an active kinase domain still shows substrate phosphorylation activity.

Dehydration dependent phosphorylation of CpVIK in both, leaves and roots was observed, indicating that regulation of CpVIK by phosphorylation is required to direct physiological processes in both tissues. Since CDeT11-24 is expressed in leaf and root tissue, interaction with CpVIK not only in leaves (**3.6.2**), but also in roots is expected. However, further substrates of CpVIK might be present in leaves and roots.

Further investigation of CpVIK phosphorylation upon other stresses could contribute to the understanding of a putative activation by phosphorylation, since the CpVIK protein expression is increased also under salt and osmotic stress (**3.4.1**; **3.4.5**).

Background gene and protein expression of CpVIK also in untreated tissue points to a putative function apart from stress response. However, since CpVIK is barely phosphorylated in untreated tissues (**3.3.4** and **supplemental figure 59**) one can hypothesise that it is not active under non-stress conditions.

In *A. thaliana* AtVIK interacts only with the phosphorylated receptor-like kinase VH1 (*VASCULAR HIGHWAY1*) *in vitro* (Ceserani et al. 2009) pointing to an upstream activation of AtVIK by the action of VH1 prior to phosphorylation of downstream targets. However, phosphorylation of AtVIK by VH1 was not evaluated by Ceserani et al. (2009).

4.5 Subcellular localisation of CpVIK

Among the eukaryotic plant kinases two major paraphyletic groups can be distinguished; the membrane-located receptor-like kinases and the soluble cytosolic kinases (Champion et al. 2004; Zulawski and Schulze 2015). Besides these two groups atypical kinase families, such as histidine kinases of prokaryotic origin, bc 1 complex kinases in organelles and atypical kinases with nonstandard protein kinase domains were identified in plants.

The subcellular localisation of a kinase can therefore provide information on its function and restricts the number of putative substrates.

In planta analyses of the subcellular localisation of MAPKKKs are rarely available. For twelve selected MAPKKKs in *Brassica napus* the subcellular localisations were determined and the majority showed cytoplasmic and nuclear localisation (Sun et al. 2014). DSM1 from rice shows nuclear localisation (Ning et al. 2010) and the *Physcomitrella patens* Raf-like MAPKKK ARK is localised in the cytoplasm (Saruhashi et al. 2015).

This work provides evidence that CpVIK is localised in the cytoplasm of *Craterostigma plantagineum*. Transient expression of the CpVIK-GFP chimeric protein in non-stressed *C. plantagineum* leaves resulted in a cytoplasmic signal determined by fluorescence microscopy (**3.2**). Similarly, native CDeT11-24 protein shows cytoplasmic localisation in cells of dehydrated leaves of *C. plantagineum*, determined by immunolocalisation (Velasco et al. 1998).

However, it cannot be excluded that CpVIK might be intracellular translocated upon water stress. One can speculate that CpVIK might be translocated to cellular membranes *via* binding to CDeT11-24 during dehydration. CDeT11-24 is able to interact with phosphatidic acid (PA) as demonstrated in lipid-binding assays (Petersen et al. 2012). PAs are major constituents of intracellular membranes and their concentration increases in plants in response to dehydration (Katagiri et al., 2001). Furthermore, it was hypothesised that CDeT11 24 is involved in the formation of a molecular shield between neighbouring membranes during dehydration (Petersen et al. 2012). A translocation from the cytosol to the plasma membrane involving PA has already been reported for a human Raf MAPKKK, Raf-1 (Rizzo et al. 2000). Another example is AtVIK in Arabidosis which was shown to be localised in the cytoplasm (Ito et al. 2011) as well as at the tonoplast membrane (Whiteman et al. 2008; Wingenter et al. 2011). Thus, a translocation of AtVIK from the cytosol to the tonoplast might be possible. Also for the Raf-like MAPKKK BnaRaf30 from *Brassica napus* a subcellular

translocation under osmotic stress was observed. On the other hand, for other MAPKKKs like VIK ortholog BnaRaf17 in *Brassica napus*, no stress-dependent translocation was observed (Sun et al. 2014).

However, further research is required to investigate in which compartment interactions of CpVIK and CDeT11-24 occur and whether an intracellular translocation takes place. For this, a bimolecular fluorescence complementation assay (BiFC) could be used in protoplasts. For dehydration dependent translocation studies GFP microscopy of stressed leaves could be applied.

4.6 Interaction of CpVIK and CDeT11-24

In a previous study interaction of the LEA-like protein CDeT11-24 with the MAPKKK CpVIK has been hypothesised based on an *in gel* kinase assay (Petersen, 2012). In this study interaction of CpVIK with the CDeT11-24 has been demonstrated.

Interaction of both proteins is likely due to the co-expression during various stress treatments (**3.4.5**) and the subcellular co-localisation in the cytoplasm (Velasco et al. 1998; **3.2**). Furthermore, interaction was demonstrated *in vitro* by binding of recombinant CDeT11-24 with native CpVIK from crude plant extracts in a co-immunoprecipitation approach (**3.6.2**). CDeT11-24 showed a lower binding affinity to the truncated $CpVIK_{dead}$ protein compared to CpVIK (**3.6.1**) implying that interaction of both proteins requires a functional kinase domain.

Phosphorylation of CDeT11-24 by CpVIK in *in vitro* kinase assays was shown (**3.5.1**) and mass spectrometric analyses revealed that five of the six phosphorylated sites in CDeT11-24 correspond to *in vivo* identified sites in *C. plantagineum* or *L. brevidens* (**3.5.4**; Röhrig et al. 2006). Four phosphorylation sites of CDeT11-24 found *in vivo* were not phosphorylated by CpVIK *in vitro* under the applied conditions (Röhrig et al. 2006; **3.5.4**). Multiple mechanisms contribute to the site recognition specificity of kinases, including the structure of the catalytic site mediating local and distal interactions between the kinase and substrate as well as the formation of complexes with additional scaffolding and adaptor proteins that regulate the interaction (Ubersax and Ferrell 2007). Scaffold proteins are known to be important coordinators especially in the MAPK mediated signalling response (Meister et al. 2013). Absence of scaffolding and adaptor proteins in *in vitro* kinase assay approaches can consequently lead to impaired site recognition. Thus, phosphorylation of the four mentioned sites in CDeT11-24 may be mediated CpVIK *in planta* but cannot be observed *in vitro*. Even when the substrate to kinase ratio was saturated, only one of the missing sites was phosphorylated by

CpVIK (Röhrig et al. 2006; **3.5.4**). Thus, the absence of co-interacting proteins or other factors could lead to an impaired recognition of the phosphorylation sites in CDeT11-24 by CpVIK *in vitro*.

On the other hand involvement of additional kinases in CDeT11-24 phosphorylation *in vivo* cannot be excluded. There are indications that CDeT11-24 is also phosphorylated by the casein kinase 2 (CK2), since a phosphorylation by CK2 was predicted for at least one site (Röhrig et al. 2006) and an *in gel* kinase assay revealed putative interaction of CDeT11-24 with the CK2α subunit (Petersen 2012). CK2 is a highly conserved Ser/Thr protein kinase involved in a large number of cellular processes and phosphorylation of several LEA proteins by plant CK2 has been reported in plants (reviewed in Vilela et al. 2015). The CK2 holoenzyme is a heterotetrameric complex composed of two catalytic (CK2α) and two regulatory (CK2β) subunits. Generally, phosphorylation activity was reported for CK2α subunit without regulatory subunits in other plant species (Matsushita et al. 2003; Xavier et al. 2012) but recombinant CK2α subunit isolated from *C. plantagineum* did not phosphorylate CDeT11-24 *in vitro* (Tierbach, unpublished; Pierog S. 2011). Availability of a CK2 holoenzyme in *C. plantagineum* is limited, since plant genomes generally contain multiple genes for each subunit leading to differently active holoenzymes (Moreno-Romero et al. 2008). In the octaploid *C. plantagineum* even more than one isoform for each gene is expected to be present. In the transcriptome data bank of *C. plantagineum* (Rodriguez et al. 2010a) eleven contigs are showing high homology to the Arabidopsis CK2 subunit genes (**supplemental data files**). With the commercially available human CK2 holoenzyme CDeT11-24 was successfully phosphorylated *in vitro* (Petersen 2012). The sites in which CDeT11-24 is phosphorylated by CK2 *in vitro* should be determined. More work is required to show, whether action of both kinases, CpVIK and CK2, could influence each other.

Whether phosphorylation CDeT11-24 influences its putative protective function on other proteins or membranes remains unknown. The function of LEA proteins is generally poorly understood but they have been hypothesised to stabilize proteins and membranes in dry seeds of desiccation sensitive plants and vegetative tissue of desiccation tolerant plants (Hand et al. 2011; Petersen et al. 2012; VanBuren et al. 2017). Phosphorylation of LEA proteins is assumed to be important in stress tolerance (Röhrig et al. 2008; Hanin et al. 2011). This is demonstrated by the report that two Tunisian durum wheat cultivars with differential phosphorylation pattern of the LEA protein DHN-5 show divergent tolerance to drought and salt stress (Brini et al. 2007).

One possible effect of phosphorylation on CDeT11-24 might be the functional redirection of the protein by structural changes as reported for other intrinsically disordered proteins, such as the LEA proteins DHN-1 and DHN-2 from *Eutrema salsugineum* (Rahman et al. 2011; Sun et al. 2013). CDeT11-24 was analysed by CD-spectroscopy after phosphorylation with the CK2 holoenzyme to elucidate whether a conformational change occurs (Petersen 2012). No noticeable change in the disordered random coil structure of CDeT11 24 protein was observed after phosphorylation, although for the Arabidopsis LEA protein Cor47 a phosphorylation by human CK2 has shown to lead to structural changes (Mouillon et al. 2008). Whether CDeT11-24 changes its structure after phosphorylation by CpVIK was not investigated yet. However, phosphorylation of CDeT11-24 may have other effects such as subcellular translocation as reported for plant LEA proteins RAB17, WCOR14 and WCOR15 (Goday 1994; Ohno et al. 2006; Jensen et al. 1998; Ohno et al. 2006); or modulation of membrane binding as reported for the *A. thaliana* dehydrin Lti30 (Eriksson et al. 2011). Other LEA proteins show a protective function during drought stress depending on phosphorylation. For TsDHN1, 2 from *Eutrema salsugineum* stabilisation of the cytoskeleton was hypothesised under stress conditions after phosphorylation (Rahman et al. 2011) and in transgenic tobacco phosphorylated ZmLEA5C from maize enhances tolerance to osmotic and low temperature stresses (Liu et al. 2014). Nevertheless, the observation, that CDeT11-24 is phosphorylated in response to drought stress supports the hypothesis that phosphorylation is required for protective activity of the protein.

4.7 Involvement of AtVIK in seed protein phosphorylation

Apart from vegetative desiccation tolerance observed in resurrection plants, like *C. plantagineum*, desiccation tolerance is observed for all orthodox plant seeds. Seeds can sustain severe desiccation and the germination potential is retained over long periods of dry storage (Shen-Miller et al. 2002; Walters et al. 2010; Farrant and Moore 2011). Specific mechanisms are required to maintain the state of metabolic quiescence during the dry state, until reactivation during germination. Protein phosphorylation mediated by kinases plays a fundamental role in seed maturation and germination (Xing et al. 2009; Meyer et al. 2012; Liu et al. 2013b; Yin et al. 2017) and in Arabidopsis 172 phosphorylated proteins were identified in developing seeds ((Meyer et al. 2012). Participation in both, seed development and vegetative dehydration tolerance was reported for kinases (Wohlbach et al. 2008).

In this study a reduced germination rate for *Δvik* seeds was shown (**3.9**), demonstrating the involvement of kinase action by AtVIK in the germination ability of *A. thaliana* seeds. For further analysis, comparative seed phosphoproteom analyses were performed. For the LEA protein RD29B an altered phosphorylation pattern was found in the *Δvik* mutant compared to wild type.

Five phosphorylation sites were identified in RD29B extracted from wild type seeds previously (Wolschin and Weckwerth 2005). Eight additional phosphosites were identified in this study. From these thirteen phosphosites identified in wild type in total, five were shown to be absent in the RD29B protein extracted from *Δvik* (**3.10.2**).

RD29B belongs to the late embryogenesis abundant protein family (LEA proteins), which has been associated with seed desiccation tolerance. They are expressed at high levels during the later stages of embryo development in plant seeds (Roberts et al. 1993). Since LEA proteins have also shown to be expressed during the dehydration in the vegetative tissue of resurrection plants (Bartels et al. 1990; Phillips et al. 2008) they represent an important conjunction of signalling networks associated with seed development and vegetative desiccation tolerance. RD29B is one example of a LEA protein expressed in seeds as well as in vegetative tissues in response to dehydration in *A. thaliana* (Yamaguchi-Shinozaki and Shinozaki 1993). It represents the functional homolog of CDeT11-24 from *C. plantagineum* (Röhrig et al. 2006; Petersen et al. 2012). The results of this study reveal an AtVIK dependent phosphorylation of RD29B for at least five sites. Whether the phosphorylation of RD29B is mediated by AtVIK by direct interaction or indirectly by activation of a downstream kinase or deactivation of phosphatases remains unknown. A direct interaction would be possible, since both proteins have been found to be present in the cytoplasm (Ito et al. 2011; Msanne et al. 2011) and direct interaction of the homologous kinase-substrate proteins in *C. plantagineum* (CpVIK-CDeT11-24) was shown in this study (**3.5**; **3.6**). To answer this question *in vitro* kinase assays and co-immunoprecipitation should be performed with AtVIK and RD29B.

If the reduced germination rate of *Δvik* seeds is caused by the differential phosphorylation of RD29B cannot be said with certainty. *Δrd29b* knock-out mutants show no difference in germination rate but an upregulation of the evolutionary closely related *RD29A* gene. A double knock out *Δrd29A/Δrd29B* is assumed to be lethal according to Msanne et al., 2011. In 2D phosphoprotein analyses on *Δvik* seeds differences were observed only for RD29B in the spot morphology (**3.10.1**). However, further less abundant downstream targets might be involved in the reduced germination rate, which were not identified with the applied technique. Recently, a combination of

shot-gun proteome analysis with phosphopeptide enrichment and high-performance LC-MS/MS has shown to enable the identification of protein kinase substrates by comparative phosphoproteomic analysis between different biological samples (Kettenbach et al. 2011; Koch et al. 2011; Wang et al. 2013; Umezawa et al. 2013). With this technique additional substrate proteins of VIK could be investigated to clarify the contribution of VIK in seed germination.

This study provides the essential information on the suitable conditions under which protein phosphorylation is significantly changed between *Δvik* and wild type. This condition can then be applied for more detailed analyses.

Differential phosphorylation of proteins known to be involved in seed maturation, germination and dormancy would be expected. But also new candidates might be identified with this attempt. *In silico* analyses demonstrated for instance a putative interaction with heat shock proteins (**supplemental table 13** and **supplemental figure 69**).

The germination rate of *Δvik* seeds was even more reduced compaired to wild type under salt stress conditions than under normal conditions (**3.9**). Consequently, it can be assumed that AtVIK is involved in seed salt stress response. Salt stress is an important environmental factor that limits the germination of plant seeds (Hegarty 1978). The molecular response during germination in the presence of salts has been analysed mainly on the basis of natural variation of different *A. thaliana* ecotypes, salt-tolerant mutants or the evolutionary closely related salt-tolerant *Eutrema salsugineum* (Zhu 2000; Quesada et al. 2000; Quesada et al. 2002; Clerkx 2004; Joosen et al. 2010; Vallejo et al. 2010; Yuan et al. 2016). Various QTLs were identified, that are involved in phenotypic variations with respect to the release of seed dormancy by the action of salts. The salt response is triggered by the osmotic stress, as well as by ion-specific toxic effects. Therefore, genes involved in salt stress response are often involved in osmotic stress and drought response as well. The induction of the molecular responses in seeds is often mediated by the plant hormone ABA (Finkelstein et al. 2002). Phosphorylation of proteins invoved in seed germination under both, salt and osmotic stress respectively, has been reported (Wolschin and Weckwerth 2005; Liu et al. 2013b). It is tempting to speculate that AtVIK is involved in the network of drought and salinity response in seeds of Arabidopsis. Examination of the germination rate in response to other salts or osmotic stress could elucidate whether the reduced germination rate of *Δvik* seeds is caused by the osmotic stress during salt treatment or the ion-specific toxic effects of NaCl.

A shotgun proteome analysis on germinating seeds under stressed and non-stressed conditions could reveal further targets of AtVIK involved in stress response in seeds.

Since conserved phosphopeptide clusters among seeds of different plant species have been reported (Meyer et al. 2012) differential phosphorylation in *Δvik* mutants could reveal common VIK substrates in other species.

4.8 Role of AtVIK in seedlings and mature plants

AtVIK has been reported to be involved in blue light-dependent stomatal opening (Hayashi et al. 2017), monosaccharide transport in the tonoplast of adult Arabidopsis plants (Wingenter et al. 2011) and vascular tissue development in seedlings (Ceserani et al. 2009). Additionally an altered sensitivity of AtVIK insertion mutants (*Δvik* ≙ SALK_002267) to auxin and brassinosteroids has been reported (Ceserani et al. 2009).

Hayashi et al. (2017) suggested that signalling for stomatal opening is down-regulated downstream of H+-ATPase activation in the *Δvik* guard cells and assumed that VIK may regulate ion transport in the guard-cell tonoplast leading to increasing guard-cell volume, resulting in stomatal opening. However, involvement of AtVIK in signalling of stomatal movement is not yet fully understood.

Since the uptake of glucose and other carbohydrates into the guard cells of plants was found to inhibit the opening of the stomata (Dittrich and Mayer 1978) and VIK was reported to interact with a glucose transporter in the tonoplast membrane (Wingenter et al. 2011) it is reasonable to assume, that VIK affects the glucose transport into the guard cells leading to an impaired stomatal opening in *Δvik* mutants in response to blue light.

Regulation of stomatal conductance is a key mechanism in response to drought stress (Nilson and Assmann 2007; Cominelli et al. 2010). Thus, the impaired stomatal opening in *Δvik* mutants demonstrates involvement of AtVIK in a drought stress relevant signalling network in mature Arabidopsis plants. This is supported by the transcriptional upregulation of AtVIK during dehydration (Wingenter et al. 2011). However, in this study no phenotypic difference in dehydration response was observed for adult *Δvik* plants (**3.8**). The relative water loss during dehydration of *Δvik* plants did not differ from wild-type plants (**3.8**). Since stomatal closure was not reported to be affected in *Δvik* plants (Hayashi et al. 2017) the stress-dependent closure mechanism during dehydration or salt stress might not be impaired.

During the seedling state VIK appears to be involved in vascular development, since a reduced vernation with fewer cotyledon secondary veins and a more discontinuous vernation with gaps in secondary veins was observed in two week old *Δvik* seedlings (Ceserani et al. 2009). This phenotype was explained by interaction with the brassinosteroid-insensitive leucine-rich reapeat receptor-like kinase VH1/BRL2 and the altered sensitivity to auxin and brassinosteroids. VH1 has been reported to transduce extracellular signals into downstream cell differentiation responses in provascular cells leading to a committed procambial state in vascular development (Clay and Nelson 2002). Crosstalk of signalling pathways related to drought and leaf venation has been reported (Endo et al. 2008; Robles et al. 2010; Scarpeci et al. 2017) but no phenotypic difference in dehydration tolerance could be observed for two week old *Δvik* seedlings or 28 day old plants (**supplemental figure 68**).

Since the germination rate of *Δvik* seeds was more reduced under salt stress conditions than under normal conditions (**3.9**) and salt-response in seeds shares characteristics with salt response in adult plants (Finkelstein et al., 2002; Taji et al., 2004; Munns et al., 2005; Seo et al., 2008) a participation of AtVIK in salt-response in later stages of development would be expected. In addition the AtVIK gene expression is induced by NaCl treatment in adult plants (Wingenert 2011). However, no phenotypic difference was observed under salt stress conditions in seedlings or adult plants (**3.8** and **supplemental figure 68**).

In the light of these new results, VIK mediated phosphorylation appears to be more essential in seeds than in seedlings or mature plants even though interaction with proteins was demonstrated during these later developmental stages (Ceserani et al. 2009; Wingenter et al. 2011) and differences in the *Δvik* leaf proteome after salt stress were observed (**3.11**).

5 Outlook

The work described in this thesis contributes to the understanding of related mechanisms of desiccation tolerance in seeds of *A. thaliana* and vegetative tissue of *C. plantagineum*. Identification and characterisation of kinases that phosphorylate protective proteins in a stress-dependent manner give new insights in the protection of seeds and vegetative tissues from the hazardous effects during desiccation.

New insights are provided in the regulation and function of the MAPKKK CpVIK in *C. plantagineum* and the ortholog AtVIK in *A. thaliana* by protein interaction studies, expression analyses during stress treatments, subcellular localisation and germination assays. The results of this study raise new questions and challenges for future perspectives of reseach in this field.

The *CpVIK* transcript and the CpVIK protein showed increased expression upon osmotic stress, salt and dehydration (**3.4.2**). Phosphorylated CpVIK protein was found in dehydrated tissue and only very low levels in fully hydrated tissue (**3.4.4**). A future task will be to analyse, if salt and osmotic stress can trigger the phosphorylation of CpVIK as well.

The CpVIK::GFP chimeric protein shows cytoplasmic localisation in unstressed *C. plantagineum* leaf tissue (**3.2**) as reported for the putative target CDeT11-24 as well (Velasco et al. 1998). Localisation studies in dehydrated leaves would reveal, whether an intracellular translocation upon stress occurs.

Physical interaction of the MAPKKK CpVIK with the stress-dependently phosphorylated LEA-like protein CDeT11-24 was demonstrated in this study (**3.6**), as well as phosphorylation of CDeT11-24 by CpVIK *in vitro* (**3.5**). To elucidate the functional coupling of both proteins and to investigate in which cellular compartment interactions of both proteins occur *in planta*, a bimolecular fluorescence complementation assay (BiFC) should be performed in protoplasts. Further experimental approaches towards protein-protein interactions should include truncated versions of both proteins. The deletion construct ΔK-CDeT11-24 that lacks a lysine-rich sequence element (K-segment), which is hypothesised to be involved in PA binding and the enzyme-protection function of CDeT11-24 (Petersen et al. 2012), coud be used in co-immunoprecipitation approaches and in BiFC analyses, to determine if this segment is essential for the interaction with CpVIK. Furthermore, phosphorylated recombinant CDeT11-24 could be used for co-immunoprecipitation to investigate, whether both proteins can still interact when all phosphosites are already phosphorylated. In this

thesis, co-immunoprecipitation assays were performed in ATP-containing buffers. The assays could be repeated in an ATP-free environment, to further analyse if the transfer of the γ-phosphate group from ATP to the hydroxyl groups of serine/threonine or tyrosine residues of the substrate proteins is essential for protein binding. BiFC analyses might also include the $CpVIK_{dead}$ recombinant protein that lacks auto- and substrate phosphorylation activity due to a mutation in the DFG-motif (**3.5.3**). Interaction of both proteins is assumed to require a functional kinase domain, since CDeT11-24 showed a lower binding affinity to the truncated $CpVIK_{dead}$ protein compared to CpVIK.

In *in vitro* kinase assays autophosphorylation of CpVIK and substrate phosphorylation by CpVIK occurred in parallel (**3.5.1**). Fifty-three sites were phosphorylated in CpVIK by autophosphorylation (**supplemental data S. 1**). To examine if the phosphorylation of down stream targets by CpVIK requires phosphorylation of CpVIK, the phosphosites should be mutagenized prior to subcequent *in vitro* kinase assays with the identified substrates. Since the number of phosphosites is very high, the conserved and MAPK-predicted sites T177 and T317 (**3.1.6**) should be pre-selected for mutagenisis. Upon dehydration stress CpVIK and CDeT11-24 are phosphorylated. Toghether with the previously decribed results it is tempting to speculate that *in planta* CpVIK is phosphorylated prior to substrate phosphorylation.

The functional effect of CDeT11-24 phosphorylation remains unknown. CD-spectroscopy after phosphorylation with the human CK2 holoenzyme did not lead to noticeable change in the CDeT11-24 protein structure (Petersen 2012). Whether the sites, in which CDeT11-24 is phosphorylated by CK2 *in vitro*, are identical to the sites that are phosphorylated by CpVIK should be investigated. If the phosphorylation pattern is divergent, a CD-spectroscopy of CDeT11-24 after phosphorylation with CpVIK could give new insights in the consequence of phosphorylation on the secundary structure of CDeT11-24 during stress in *C. plantagineum.* It has been reported, that CDeT11-24 protects enzymes against desiccation damage and binds to PA (Petersen et al. 2012). Whether phosphorylation of CDeT11-24 by eighter CpVIK or CK2 affects these functions, should be elucidated. Probably, both kinases phosphorylate CDeT11-24 at different sites *in planta*. An *in gel* kinase assay demonstrated interaction of CDeT11-24 with CK2α (Petersen 2012).

Apart from the interaction of CpVIK and CDeT11-24 in *C. plantagineum*, this study presents evidence for an AtVIK dependent phosphorylation of the CDeT11-24 homolog RD29B in Arabidopsis. An aberrant phosphorylation of RD29B was revealed in *Δvik A. thaliana* dry seeds (**3.10.2**) and a lower germination rate particularly under salt

stress conditions was demonstrated compared to wild type seeds (**3.9**). A future task will be to identify further downstream targets of AtVIK in seeds by comparative analyses on the proteomes of germinating *Δvik* seeds upon different stress treatments. These attemts should include *RD29B* transcript expression analysis. RNAi lines with repression of RD29A and B could help to understand the involvement of these LEA proteins in seed germination. Since no double-knock out was obtained, so far. Co-immunoprecipitation assays with RD29B and AtVIK should be performed to examine, if both proteins interact directly. Alternativly the altered phosphorylation of RD29B in *Δvik* seeds could be a consequence of activation of another kinase or deactivation of phosphatases by AtVIK.

In addition to the functional coupling of VIK kinases with LEA proteins in *C. plantagineum* and *A. thaliana*, *in silico* analyses revealed presence of VIK orthologs in various plant species (**3.1.3**). The phylogeny substantiates the fundamental role of VIK-like tandem-repeat ankyrin motif containing MAPKKKs (**3.1.4**). A promising approach would be the characterisation of VIK orthologs in other species. So far, only a few VIK orthologs have been mentioned in publications. Analyses were mainly restricted to gene expression analyses. However, the results of this study show that differential protein phosphorylation and protein-protein interaction studies harbour a great potential to understand the function of these kinases. Therefore, further research on the protein level in other species should be considered. First steps have already been taken to analyse the protein expression of VIK in *L. brevidens* and *L. subracemosa*. Phosphorylation of the LbVIK and LsVIK proteins, as well as gene expression analysis in these species, are subjects of ongoing research projects.

6 Summary

Drought is a key factor for yield loss in agriculture. However, desiccation tolerant plant species evolved various mechanisms to protect vegetative tissues from the hazardous effects of drought. These mechanisms are not fully understood and the work in this thesis contributes to the understanding of phosphorylation of stress related proteins in the desiccation tolerant plant *Craterostigma plantagineum*.

In desiccation sensitive plant species MAPKKKs are known to be involved in multiple drought stress response pathways. However, their role in the acquisition of desiccation tolerance of resurrection plants has not been investigated up to now.

In the desiccation tolerant plant species *C. plantagineum* several proteins show drought stress-dependent phosphorylation. The phosphorylation of these proteins was predicted to be partially mediated by MAPKKKs (Mariaux et al. 1998; Röhrig et al. 2006; Röhrig et al. 2008). An *in-gel*-kinase assay using the stress-related phosphoprotein CDeT11-24 as substrate demonstrated the presence of a MAPKKK in *C. plantagineum* (Petersen 2012). The identified MAPKKK is a homologue to the RAF-like MAPKKK VH1-interacting kinase (VIK) from *A. thaliana* (At1g14000) and was consequently named CpVIK. Based on this observation it was hypothesised that CpVIK and CDeT11-24 are functionally coupled and interact with each other.

In this study *in silico* analyses demonstrated that CpVIK belongs to the tandem-repeat ankyrin motif containing MAPKKKs (ANKMAPKKKs) that are widely distributed in various taxa. Based on their early occurrence during evolution already in bacterial genomes and the conservation in plants as well as metazoa, it is assumed that the ANKMAPKKKs have essential functions which are not yet fully understood.

Co-immunoprecipitation experiments performed in this work verified a physical interaction of CDeT11-24 and CpVIK. *In vitro* assays confirmed phosphorylation of CDeT11-24 by the enzymatic action of CpVIK.

An increased expression of CpVIK on the RNA and protein level was observed upon abiotic stresses, including dehydration. Phosphorylation of the CpVIK protein revealed to be stress-dependent. CDeT11-24 and CpVIK showed to be co-expressed and the proteins are co-localised in the cytosol. Together with previous findings, showing high expression of *VIK* orthologs in seeds of desiccation sensitive species, it is proposed that VIK participates in the acquisition of drought tolerance in vegetative tissues of

desiccation tolerant *C. plantagineum* as well as in seeds of desiccation sensitive plant species.

In addition to an involvement of CpVIK in drought stress, for most *VIK* orthologous genes, an increase of gene expression in mature leaves compared to young leaves is observed (**4.3**) indicating importance of VIK in later stages of plant development.

In *A. thaliana* plants no phenotypic differences were detected for AtVIK knock-out mutant plants (*Δvik*) in comparison to wild type plants upon dehydration or salt stress at different developmental stages. However, a lower germination rate of *Δvik* seeds was observed especially under salt stress conditions. Comparative seed proteome analyses verified aberrant phosphoproteins in *Δvik* seeds including RD29B, the closest homologue to the CDeT11-24 LEA-like *C. plantagineum* protein. Mass spectrometric analyses demonstrated that five phosphorylation sites were absent in the RD29B protein extracted from *Δvik* seeds in comparison to wild type. This represents an *in vivo* evidence for a functional coupling of VIK and RD29B.

This thesis demonstrated a correlation of VIK proteins with LEA proteins in *C. plantagineum* and *A. thaliana*. Identification of further downstream targets in seeds of Arabidopsis and vegetative tissue of *C. plantagineum* will contribute to the understanding of the mechanisms of desiccation tolerance.

7 References

Adams C, Aldous DJ, Amendola S, Bamborough P, Bright C, Crowe S, Eastwood P, Fenton G, Foster M, Harrison TKP, King S, Lai J, Lawrence C, Letallec J-P, McCarthy C, Moorcroft N, Page K, Rao S, Redford J, Sadiq S, Smith K, Souness JE, Thurairatnam S, Vine M, Wyman B (2003) Mapping the kinase domain of janus kinase 3. Bioorganic & Medicinal Chemistry Letters 13(18):3105–3110.

Adkins S, Burmeister M (1996) Visualization of DNA in agarose gels as migrating colored bands: applications for preparative gels and educational demonstrations. Anal Biochem 240(1):17–23.

Agrawal GK, Iwahashi H, Rakwal R (2003) Rice MAPKs. Biochem Biophys Res Commun 302(2):171–180.

Alamillo J, Almoguera C, Bartels D, Jordano J (1995) Constitutive expression of small heat shock proteins in vegetative tissues of the resurrection plant *Craterostigma plantagineum*. Plant Mol Biol 29(5):1093–1099.

Anderberg RJ, Walker-Simmons MK (1992) Isolation of a wheat cDNA clone for an abscisic acid-inducible transcript with homology to protein kinases. Proc Natl Acad Sci USA 89(21):10183–10187

Arabidopsis Genome Initiative (2000) Analysis of the genome sequence of the flowering plant *Arabidopsis thaliana*. Nature 408(6814):796–815.

Bakker EG, Traw MB, Toomajian C, Kreitman M, Bergelson J (2008) Low levels of polymorphism in genes that control the activation of defense response in *Arabidopsis thaliana*. Genetics 178(4):2031–2043.

Barford D, Hu S-H, Johnson LN (1991) Structural mechanism for glycogen phosphorylase control by phosphorylation and AMP. Journal of Molecular Biology 218(1):233–260.

Bartels D, Schneider K, Terstappen G, Piatkowski D, Salamini F (1990) Molecular cloning of abscisic acid-modulated genes which are induced during desiccation of the resurrection plant *Craterostigma plantagineum*. Planta 181(1):27–34.

Bartels D (2005) Desiccation Tolerance Studied in the Resurrection Plant *Craterostigma plantagineum*. Integr Comp Biol 45(5):696–701.

Bartels D, Sunkar R (2005) Drought and Salt Tolerance in Plants. Critical Reviews in Plant Sciences 24(1):23–58.

Becerra C, Jahrmann T, Puigdomènech P, Vicient CM (2004) Ankyrin repeat-containing proteins in Arabidopsis: Characterization of a novel and abundant group of genes coding ankyrin-transmembrane proteins. Gene 340(1):111–121.

Bergmann DC, Lukowitz W, Somerville CR (2004) Stomatal development and pattern controlled by a MAPKK kinase. Science 304(5676):1494–1497.

Bertani G (1951) Studies on lysogenesis. I. The mode of phage liberation by lysogenic *Escherichia coli*. J Bacteriol 62(3):293–300

Betsuyaku S, Takahashi F, Kinoshita A, Miwa H, Shinozaki K, Fukuda H, Sawa S (2011) Mitogen-activated protein kinase regulated by the CLAVATA receptors contributes to shoot apical meristem homeostasis. Plant Cell Physiol 52(1):14–29.

Bork P (1993) Hundreds of ankyrin-like repeats in functionally diverse proteins: mobile modules that cross phyla horizontally? Proteins 17(4):363–374.

Bradford MM (1976) A rapid and sensitive method for the quantitation of microgram quantities of protein utilizing the principle of protein-dye binding. Anal Biochem 72(1-2):248–254

Breeden L, Nasmyth K (1987) Similarity between cell-cycle genes of budding yeast and fission yeast and the Notch gene of Drosophila. Nature 329(6140):651–654.

Brini F, Hanin M, Lumbreras V, Irar S, Pagès M, Masmoudi K (2007) Functional characterization of DHN-5, a dehydrin showing a differential phosphorylation pattern in two Tunisian durum wheat (*Triticum durum* Desf.) varieties with marked differences in salt and drought tolerance. Plant Science 172(1):20–28.

Brock AK, Willmann R, Kolb D, Grefen L, Lajunen HM, Bethke G, Lee J, Nürnberger T, Gust AA (2010) The Arabidopsis mitogen-activated protein kinase phosphatase PP2C5 affects seed germination, stomatal aperture, and abscisic acid-inducible gene expression. Plant Physiol 153(3):1098–1111.

Brognard J, Hunter T (2011) Protein kinase signaling networks in cancer. Curr Opin Genet Dev 21(1):4–11.

Buitink J, Hoekstra FA, Leprince O (2002) Biochemistry and biophysics of tolerance systems. In: Black M, Pritchard HW (eds) Desiccation and survival in plants: drying without dying. CABI, Wallingford, pp 293–318

Cargnello M, Roux PP (2011) Activation and function of the MAPKs and their substrates, the MAPK-activated protein kinases. Microbiol Mol Biol Rev 75(1):50–83.

Ceserani T, Trofka A, Gandotra N, Nelson T (2009) VH1/BRL2 receptor-like kinase interacts with vascular-specific adaptor proteins VIT and VIK to influence leaf venation. Plant J 57(6):1000–1014.

Champion A, Picaud A, Henry Y (2004) Reassessing the MAP3K and MAP4K relationships. Trends in Plant Science 9(3):123–129.

Chinchilla D, Frugier F, Raices M, Merchan F, Giammaria V, Gargantini P, Gonzalez-Rizzo S, Crespi M, Ulloa R (2008) A mutant ankyrin protein kinase from Medicago sativa affects Arabidopsis adventitious roots. Functional Plant Biol. 35(1):92.

Chiswell BP, Stiegler AL, Razinia Z, Nalibotski E, Boggon TJ, Calderwood DA (2010) Structural basis of competition between PINCH1 and PINCH2 for binding to the ankyrin repeat domain of integrin-linked kinase. J Struct Biol 170(1):157–163.

Chomczynski P, Sacchi N (1987) Single-step method of RNA isolation by acid guanidinium thiocyanate-phenol-chloroform extraction. Anal Biochem 162(1):156–159.

Clay NK, Nelson T (2002) VH1, a Provascular Cell–Specific Receptor Kinase That Influences Leaf Cell Patterns in Arabidopsis. Plant Cell 14(11):2707–2722.

Clerkx EJM (2004) Analysis of Natural Allelic Variation of Arabidopsis Seed Germination and Seed Longevity Traits between the Accessions Landsberg erecta and Shakdara, Using a New Recombinant Inbred Line Population. Plant Physiol. 135(1):432–443.

Cohen P (2002) The origins of protein phosphorylation. Nat Cell Biol 4(5):E127-30. doi: 10.1038/ncb0502-e127

Colcombet J, Hirt H (2008) Arabidopsis MAPKs: A complex signalling network involved in multiple biological processes. Biochem J 413(2):217–226.

Cominelli E, Galbiati M, Tonelli C (2010) Transcription factors controlling stomatal movements and drought tolerance. Transcription 1(1):41–45.

Cuming AC (1999) LEA Proteins. In: Shewry PR, Casey R (eds) Seed Proteins. Springer Netherlands, Dordrecht, pp 753–780

Danquah A, Zelicourt A de, Colcombet J, Hirt H (2014) The role of ABA and MAPK signaling pathways in plant abiotic stress responses. Biotechnol Adv 32(1):40–52.

Dar AC, Shokat KM (2011) The evolution of protein kinase inhibitors from antagonists to agonists of cellular signaling. Annu Rev Biochem 80:769–795.

Dittrich P, Mayer M (1978) Inhibition of stomatal opening during uptake of carbohydrates by guard cells in isolated epidermal tissues. Planta 139(2):167–170.

Droillard M-J, Boudsocq M, Barbier-Brygoo H, Laurière C (2004) Involvement of MPK4 in osmotic stress response pathways in cell suspensions and plantlets of *Arabidopsis thaliana*: Activation by hypoosmolarity and negative role in hyperosmolarity tolerance. FEBS Lett 574(1-3):42–48.

Dure L (1993) A repeating 11-mer amino acid motif and plant desiccation. The Plant Journal 3(3):363–369.

Elion EA (2001) The Ste5p scaffold. J Cell Sci 114(22):3967–3978

Endicott JA, Noble MEM, Johnson LN (2012) The structural basis for control of eukaryotic protein kinases. Annu Rev Biochem 81:587–613.

Endo A, Sawada Y, Takahashi H, Okamoto M, Ikegami K, Koiwai H, Seo M, Toyomasu T, Mitsuhashi W, Shinozaki K, Nakazono M, Kamiya Y, Koshiba T, Nambara E (2008) Drought induction of Arabidopsis 9-cis-epoxycarotenoid dioxygenase occurs in vascular parenchyma cells. Plant Physiol 147(4):1984–1993.

Eriksson SK, Kutzer M, Procek J, Gröbner G, Harryson P (2011) Tunable membrane binding of the intrinsically disordered dehydrin Lti30, a cold-induced plant stress protein. Plant Cell 23(6):2391–2404.

Facchinelli F (2009) Phosphoproteomic Analysis of *Craterostigma plantagineum* upon Abscisic Acid and Desiccation Stress. Dissertation, Rheinische Friedrich-Wilhelms-Universität Bonn

Farrant JM (2000) A comparison of mechanisms of desiccation tolerance among three angiosperm resurrection plant species. Plant Ecology 151(1):29–39.

Farrant JM, Moore JP (2011) Programming desiccation-tolerance: from plants to seeds to resurrection plants. Current Opinion in Plant Biology 14(3):340–345.

Fedorov O, Müller S, Knapp S (2010) The (un)targeted cancer kinome. Nat Chem Biol 6(3):166–169.

Finkelstein RR, Gampala SSL, Rock CD (2002) Abscisic acid signaling in seeds and seedlings. Plant Cell Online 14 (suppl 1):S15-45

Fischer E (1992) Systematik der afrikanischen *Lindernieae* (*Scrophulariaceae*). Tropische und subtropische Pflanzenwelt 81, 1–365. Franz Steiner Verlag Stuttgart

Frye CA (1998) An Arabidopsis Mutant with Enhanced Resistance to Powdery Mildew. Plant Cell Online (6):947–956.

Frye CA, Tang D, Innes RW (2001) Negative regulation of defense responses in plants by a conserved MAPKK kinase. Proceedings of the National Academy of Sciences 98(1):373–378.

Gaff DF (1977) Desiccation tolerant vascular plants of southern Africa. Oecologia 31(1):95–109.

Gao L, Xiang C-B (2008) The genetic locus At1g73660 encodes a putative MAPKKK and negatively regulates salt tolerance in Arabidopsis. Plant Mol Biol 67(1-2):125–134.

Garcia-Garcia M, Via M, Zarnowiec K, SanMiguel I, Escera C, Clemente IC (2017) COMT and DRD2/ANKK-1 gene-gene interaction account for resetting of gamma neural oscillations to auditory stimulus-driven attention. PLoS ONE 12(2):e0172362.

Gasulla F, Barreno E, Parages ML, Cámara J, Jiménez C, Dörmann P, Bartels D (2016) The Role of Phospholipase D and MAPK Signaling Cascades in the Adaption of Lichen Microalgae to Desiccation: Changes in Membrane Lipids and Phosphoproteome. Plant Cell Physiol 57(9):1908–1920.

Giarola V, Krey S, den Driesch B von, Bartels D (2016) The *Craterostigma plantagineum* glycine-rich protein CpGRP1 interacts with a cell wall-associated protein kinase 1 (CpWAK1) and accumulates in leaf cell walls during dehydration. New Phytol 210(2):535–550.

Goday A (1994) The Maize Abscisic Acid-Responsive Protein Rab17 Is Located in the Nucleus and Interacts with Nuclear Localization Signals. THE PLANT CELL ONLINE 6(3):351–360.

Groban ES, Narayanan A, Jacobson MP (2006) Conformational changes in protein loops and helices induced by post-translational phosphorylation. PLoS Comput Biol 2(4):e32.

Grzywacz A, Jasiewicz A, Małecka I, Suchanecka A, Grochans E, Karakiewicz B, Samochowiec A, Bieńkowski P, Samochowiec J (2012) Influence of DRD2 and ANKK1 polymorphisms on the manifestation of withdrawal syndrome symptoms in alcohol addiction. Pharmacological Reports 64(5):1126–1134.

Gurr SJ, Rushton PJ (2005) Engineering plants with increased disease resistance: what are we going to express? Trends Biotechnol 23(6):275–282.

Hamel L-P, Nicole M-C, Sritubtim S, Morency M-J, Ellis M, Ehlting J, Beaudoin N, Barbazuk B, Klessig D, Lee J, Martin G, Mundy J, Ohashi Y, Scheel D, Sheen J, Xing T, Zhang S, Seguin A, Ellis BE (2006) Ancient signals: comparative genomics of plant MAPK and MAPKK gene families. Trends in Plant Science 11(4):192–198.

Hanahan D (1983) Studies on transformation of *Escherichia coli* with plasmids. Journal of Molecular Biology 166(4):557–580.

Hand SC, Menze MA, Toner M, Boswell L, Moore D (2011) LEA proteins during water stress: Not just for plants anymore. Annu Rev Physiol 73:115–134.

Hanin M, Brini F, Ebel C, Toda Y, Takeda S, Masmoudi K (2011) Plant dehydrins and stress tolerance: Versatile proteins for complex mechanisms. Plant Signal Behav 6(10):1503–1509.

Hanks S K, Quinn A, Hunter T (1988) The Protein Kinase Family: Conserved Features and Deduced Phylogeny of the Catalytic Domains. Science 241(4861):42–52.

Hao L, Zhang H, Zhang Z, Hu S, Xue Y (2016) Information Commons for Rice (IC4R). Nucleic Acids Res 44(D1):D1172-1180.

Hartung W, Schiller P, Dietz K-J (1998) Physiology of Poikilohydric Plants. In: Behnke H-D, Esser K, Kadereit JW, Lüttge U, Runge M (eds) Progress in Botany: Genetics Cell Biology and Physiology Ecology and Vegetation Science, vol 59. Springer Berlin Heidelberg, Berlin, Heidelberg, pp 299–327

Hayashi M, Inoue S-I, Ueno Y, Kinoshita T (2017) A Raf-like protein kinase BHP mediates blue light-dependent stomatal opening. Sci Rep 7:45586.

Hegarty TW (1978) The physiology of seed hydration and dehydration, and the relation between water stress and the control of germination: A review. Plant Cell Environ 1(2):101–119.

Heino P (1998) Gene note. Isolation of a cDNA clone corresponding to a protein kinase differentially expressed in the resurrection plant *Craterostigma plantagineum*. Journal of Experimental Botany 49(327):1773–1774.

Hoekstra FA, Golovina EA, Buitink J (2001) Mechanisms of plant desiccation tolerance. Trends in Plant Science 6(9):431–438.

Hoenicka J, Quiñones-Lombraña A, España-Serrano L, Alvira-Botero X, Kremer L, Pérez-González R, Rodríguez-Jiménez R, Jiménez-Arriero MA, Ponce G, Palomo T (2010) The ANKK1 gene associated with addictions is expressed in astroglial cells and upregulated by apomorphine. Biol Psychiatry 67(1):3–11.

Hoffmann A, Preobrazhenska O, Wodarczyk C, Medler Y, Winkel A, Shahab S, Huylebroeck D, Gross G, Verschueren K (2005) Transforming growth factor-beta-activated kinase-1 (TAK1), a MAP3K, interacts with Smad proteins and interferes with osteogenesis in murine mesenchymal progenitors. J Biol Chem 280(29):27271–27283.

Holland PM, Willis CR, Kanaly S, Glaccum MB, Warren AS, Charrier K, Murison JG, Derry JMJ, Virca GD, Bird TA, Peschon JJ (2002) RIP4 Is an Ankyrin Repeat-Containing Kinase Essential for Keratinocyte Differentiation. Current Biology 12(16):1424–1428.

Hong J, Zhou J, Fu J, He T, Qin J, Wang L, Liao L, Xu J (2011) Phosphorylation of serine 68 of Twist1 by MAPKs stabilizes Twist1 protein and promotes breast cancer cell invasiveness. Cancer Res 71(11):3980–3990.

Hua Z-M, Yang X, Fromm ME (2006) Activation of the NaCl- and drought-induced RD29A and RD29B promoters by constitutively active Arabidopsis MAPKK or MAPK proteins. Plant Cell Environ 29(9):1761–1770.

Huang J, Zhao X, Yu H, Ouyang Y, Wang L, Zhang Q (2009) The ankyrin repeat gene family in rice: genome-wide identification, classification and expression profiling. Plant Mol Biol 71(3):207–226.

Hubbard KE, Nishimura N, Hitomi K, Getzoff ED, Schroeder JI (2010) Early abscisic acid signal transduction mechanisms: Newly discovered components and newly emerging questions. Genes Dev 24(16):1695–1708.

Ichimura K, Casais C, Peck SC, Shinozaki K, Shirasu K (2006) MEKK1 is required for MPK4 activation and regulates tissue-specific and temperature-dependent cell death in Arabidopsis. J Biol Chem 281(48):36969–36976.

Iglesias-Fernández R, del Carmen Rodríguez-Gacio M, Matilla AJ (2011) Progress in research on dry afterripening. Seed Sci. Res. 21(02):69–80.

Ingram J, Bartels D (1996) The molecular basis of dehydration tolerance in plants. Annu Rev Plant Physiol Plant Mol Biol 47:377–403.

Ingram J, Chandler JW, Gallagher L, Salamini F, Bartels D (1997) Analysis of cDNA clones encoding sucrose-phosphate synthase in relation to sugar interconversions associated with dehydration in the resurrection plant *Craterostigma plantagineum* Hochst. Plant Physiol 115(1):113–121

Ito J, Batth TS, Petzold CJ, Redding-Johanson AM, Mukhopadhyay A, Verboom R, Meyer EH, Millar AH, Heazlewood JL (2011) Analysis of the Arabidopsis cytosolic proteome highlights subcellular partitioning of central plant metabolism. J Proteome Res 10(4):1571–1582.

Jabłoński M, Jasiewicz A, Kucharska-Mazur J, Samochowiec J, Bienkowski P, Mierzejewski P, Samochowiec A (2013) The effect of selected polymorphisms of the dopamine receptor gene DRD2 and the ANKK-1 on the preference of concentrations of sucrose solutions in men with alcohol dependence. Psychiatr Danub 25(4):371–378

Jensen AB, Goday A, Figueras M, Jessop AC, Pages M (1998) Phosphorylation mediates the nuclear targeting of the maize Rab17 protein. The Plant Journal 13(5):691–697.

Jin S, Zhuo Y, Guo W, Field J (2005) p21-activated Kinase 1 (Pak1)-dependent phosphorylation of Raf-1 regulates its mitochondrial localization, phosphorylation of BAD, and Bcl-2 association. J Biol Chem 280(26):24698–24705.

Johnson LN (2009) Protein kinase inhibitors: contributions from structure to clinical compounds. Q Rev Biophys 42(1):1–40.

Joo S, Liu Y, Lueth A, Zhang S (2008) MAPK phosphorylation-induced stabilization of ACS6 protein is mediated by the non-catalytic C-terminal domain, which also contains the cis-determinant for rapid degradation by the 26S proteasome pathway. Plant J 54(1):129–140.

Joosen RVL, Kodde J, Willems LAJ, Ligterink W, van der Plas LHW, Hilhorst HWM (2010) GERMINATOR: a software package for high-throughput scoring and curve fitting of Arabidopsis seed germination. Plant J 62(1):148–159.

Kawakami S, Padgett HS, Hosokawa D, Okada Y, Beachy RN, Watanabe Y (1999) Phosphorylation and/or presence of serine 37 in the movement protein of tomato mosaic tobamovirus is essential for intracellular localization and stability in vivo. J Virol 73(8):6831–6840

Kaye C, Neven L, Hofig A, Li Q-B, Haskell D, Guy C (1998) Characterization of a Gene for Spinach CAP160 and Expression of Two Spinach Cold-Acclimation Proteins in Tobacco. Plant Physiol. 116(4):1367–1377.

Kettenbach AN, Schweppe DK, Faherty BK, Pechenick D, Pletnev AA, Gerber SA (2011) Quantitative phosphoproteomics identifies substrates and functional modules of Aurora and Polo-like kinase activities in mitotic cells. Sci Signal 4(179):rs5.

Kieber JJ, Rothenberg M, Roman G, Feldmann KA, Ecker JR (1993) CTR1, a negative regulator of the ethylene response pathway in arabidopsis, encodes a member of the Raf family of protein kinases. Cell 72(3):427–441.

Kiegerl S, Cardinale F, Siligan C, Gross A, Baudouin E, Liwosz A, Eklöf S, Till S, Bögre L, Hirt H, Meskiene I (2000) SIMKK, a mitogen-activated protein kinase (MAPK) kinase, is a specific activator of the salt stress-induced MAPK, SIMK. Plant Cell 12(11):2247–2258

Kim S-H, Woo D-H, Kim J-M, Lee S-Y, Chung WS, Moon Y-H (2011) Arabidopsis MKK4 mediates osmotic-stress response via its regulation of MPK3 activity. Biochem Biophys Res Commun 412(1):150–154.

Kim D, Cho Y-H, Ryu H, Kim Y, Kim T-H, Hwang I (2013) BLH1 and KNAT3 modulate ABA responses during germination and early seedling development in Arabidopsis. Plant J 75(5):755–766.

Kirch H-H, Nair A, Bartels D (2001) Novel ABA- and dehydration-inducible aldehyde dehydrogenase genes isolated from the resurrection plant *Craterostigma plantagineum* and *Arabidopsis thaliana*. The Plant Journal 28(5):555–567.

Knight H, Knight MR (2001) Abiotic stress signalling pathways: Specificity and cross-talk. Trends in Plant Science 6(6):262–267.

Koch A, Krug K, Pengelley S, Macek B, Hauf S (2011) Mitotic substrates of the kinase aurora with roles in chromatin regulation identified through quantitative phosphoproteomics of fission yeast. Sci Signal 4(179):rs6.

Kong X, Lv W, Zhang D, Jiang S, Zhang S, Li D (2013) Genome-wide identification and analysis of expression profiles of maize mitogen-activated protein kinase kinase kinase. PLoS ONE 8(2):e57714.

Kornev AP, Haste NM, Taylor SS, Eyck LFT (2006) Surface comparison of active and inactive protein kinases identifies a conserved activation mechanism. Proc Natl Acad Sci USA 103(47):17783–17788.

Kornev AP, Taylor SS, Eyck LFT (2008) A helix scaffold for the assembly of active protein kinases. Proc Natl Acad Sci U S A 105(38):14377–14382.

Kreps JA, Wu Y, Chang H-S, Zhu T, Wang X, Harper JF (2002) Transcriptome changes for Arabidopsis in response to salt, osmotic, and cold stress. Plant Physiol 130(4):2129–2141.

Krysan PJ (2002) An Arabidopsis Mitogen-Activated Protein Kinase Kinase Kinase Gene Family Encodes Essential Positive Regulators of Cytokinesis. THE PLANT CELL ONLINE 14(5):1109–1120.

Kumar S, Stecher G, Tamura K (2016) MEGA7: Molecular Evolutionary Genetics Analysis Version 7.0 for Bigger Datasets. Mol Biol Evol 33(7):1870–1874.

Laemmli UK (1970) Cleavage of structural proteins during the assembly of the head of bacteriophage T4. Nature 227(5259):680–685

Lehti-Shiu MD, Shiu S-H (2012) Diversity, classification and function of the plant protein kinase superfamily. Philos Trans R Soc B, Biol Sci 367(1602):2619–2639.

Lew DJ, Burke DJ (2003) The spindle assembly and spindle position checkpoints. Annu Rev Genet 37:251–282.

Lewis TS, Shapiro PS, Ahn NG (1998) Signal Transduction through MAP Kinase Cascades. In: Vande Woude GF (ed) Advances in Cancer Research, vol 74. Academic Press, London, pp 49–139

Li H, Wong WS, Zhu L, Guo HW, Ecker J, Li N (2009) Phosphoproteomic analysis of ethylene-regulated protein phosphorylation in etiolated seedlings of Arabidopsis mutant ein2 using two-dimensional separations coupled with a hybrid quadrupole time-of-flight mass spectrometer. Proteomics 9(6):1646–1661.

Lin H, Yang Y, Quan R, Mendoza I, Wu Y, Du W, Zhao S, Schumaker KS, Pardo JM, Guo Y (2009) Phosphorylation of SOS3-LIKE CALCIUM BINDING PROTEIN8 by SOS2 protein kinase stabilizes their protein complex and regulates salt tolerance in Arabidopsis. Plant Cell 21(5):1607–1619.

Liu Y, Zhang S (2004) Phosphorylation of 1-aminocyclopropane-1-carboxylic acid synthase by MPK6, a stress-responsive mitogen-activated protein kinase, induces ethylene biosynthesis in Arabidopsis. Plant Cell 16(12):3386–3399.

Liu Y, Zhang D, Wang L, Li D (2013a) Genome-Wide Analysis of Mitogen-Activated Protein Kinase Gene Family in Maize. Plant Mol Biol Rep 31(6):1446–1460.

Liu X-M, Nguyen XC, Kim KE, Han HJ, Yoo J, Lee K, Kim MC, Yun D-J, Chung WS (2013b) Phosphorylation of the zinc finger transcriptional regulator ZAT6 by MPK6 regulates Arabidopsis seed germination under salt and osmotic stress. Biochem Biophys Res Commun 430(3):1054–1059.

Liu Y, Wang L, Jiang S, Pan J, Cai G, Li D (2014) Group 5 LEA protein, ZmLEA5C, enhance tolerance to osmotic and low temperature stresses in transgenic tobacco and yeast. Plant Physiol Biochem 84:22–31.

Liu Y, Zhou M, Gao Z, Ren W, Yang F, He H, Zhao J (2015) RNA-Seq Analysis Reveals MAPKKK Family Members Related to Drought Tolerance in Maize. PLoS ONE 10(11):e0143128.

Lorow, D., & Jessee, J. (1990) Max efficiency DH10B™: a host for cloning methylated DNA. Focus 12(1):19

Lukowitz W, Roeder A, Parmenter D, Somerville C (2004) A MAPKK Kinase Gene Regulates Extra-Embryonic Cell Fate in Arabidopsis. Cell 116(1):109–119.

Madhani HD, Fink GR (1998) The riddle of MAP kinase signaling specificity. Trends in Genetics 14(4):151–155.

Malinin NL, Boldin MP, Kovalenko AV, Wallach D (1997) MAP3K-related kinase involved in NF-kappaB induction by TNF, CD95 and IL-1. Nature 385(6616):540–544.

Manning G, Whyte DB, Martinez R, Hunter T, Sudarsanam S (2002) The protein kinase complement of the human genome. Science 298(5600):1912–1934.

MAPK Group, Ichimura K, Shinozaki K, Tena G, Sheen J, Henry Y, Champion A, Kreis M, Zhang S, Hirt H, Wilson C, Heberle-Bors E, Ellis BE, Morris PC, Innes RW, Ecker JR, Scheel D, Klessig DF, Machida Y, Mundy J, Ohashi Y, Walker JC (2002) Mitogen-activated protein kinase cascades in plants: A new nomenclature. Trends in Plant Science 7(7):301–308.

Mariaux J-B, Bockel C, Salamini F, Bartels D (1998) Desiccation- and abscisic acid-responsive genes encoding major intrinsic proteins (MIPs) from the resurrection plant Craterostigma plantagineum. Plant Mol Biol 38(6):1089–1099.

Matsushita Y, Ohshima M, Yoshioka K, Nishiguchi M, Nyunoya H (2003) The catalytic subunit of protein kinase CK2 phosphorylates in vitro the movement protein of Tomato mosaic virus. J Gen Virol 84(2):497–505.

McCubrey JA, Steelman LS, Chappell WH, Abrams SL, Wong EWT, Chang F, Lehmann B, Terrian DM, Milella M, Tafuri A, Stivala F, Libra M, Basecke J, Evangelisti C, Martelli AM, Franklin RA (2007) Roles of the Raf/MEK/ERK pathway in cell growth, malignant transformation and drug resistance. Biochim Biophys Acta 1773(8):1263–1284.

Meharena HS, Chang P, Keshwani MM, Oruganty K, Nene AK, Kannan N, Taylor SS, Kornev AP (2013) Deciphering the structural basis of eukaryotic protein kinase regulation. PLoS Biol 11(10):e1001680.

Mehlen P, Arrigo A-P (1994) The serum-induced phosphorylation of mammalian hsp27 correlates with changes in its intracellular localization and levels of oligomerization. Eur J Biochem 221(1):327–334.

Meister M, Tomasovic A, Banning A, Tikkanen R (2013) Mitogen-Activated Protein (MAP) Kinase Scaffolding Proteins: A Recount. Int J Mol Sci 14(3):4854–4884.

Meyer LJ, Gao J, Xu D, Thelen JJ (2012) Phosphoproteomic analysis of seed maturation in Arabidopsis, rapeseed, and soybean. Plant Physiol 159(1):517–528.

Mizoguchi T, Irie K, Hirayama T, Hayashida N, Yamaguchi-Shinozaki K, Matsumoto K, Shinozaki K (1996) A gene encoding a mitogen-activated protein kinase kinase kinase is induced simultaneously with genes for a mitogen-activated protein kinase and an S6 ribosomal protein kinase by touch, cold, and water stress in *Arabidopsis thaliana*. Proc Natl Acad Sci USA 93(2):765–769

Moore JP, Le NT, Brandt WF, Driouich A, Farrant JM (2009) Towards a systems-based understanding of plant desiccation tolerance. Trends in Plant Science 14(2):110–117.

Moran MF, Koch CA, Sadowski I, Pawson T (1988) Mutational analysis of a phosphotransfer motif essential for v-fps tyrosine kinase activity. Oncogene 3(6):665–672

Moreno-Romero J, Espunya MC, Platara M, Ariño J, Martínez MC (2008) A role for protein kinase CK2 in plant development: Evidence obtained using a dominant-negative mutant. Plant J 55(1):118–130.

Moretto-Zita M, Jin H, Shen Z, Zhao T, Briggs SP, Xu Y (2010) Phosphorylation stabilizes Nanog by promoting its interaction with Pin1. Proc Natl Acad Sci USA 107(30):13312–13317.

Mouillon J-M, Eriksson SK, Harryson P (2008) Mimicking the plant cell interior under water stress by macromolecular crowding: disordered dehydrin proteins are highly resistant to structural collapse. Plant Physiol. 148(4):1925–1937.

Msanne J, Lin J, Stone JM, Awada T (2011) Characterization of abiotic stress-responsive *Arabidopsis thaliana* RD29A and RD29B genes and evaluation of transgenes. Planta 234(1):97–107.

Mullis K, Faloona F, Scharf S, Saiki R, Horn G, Erlich H (1986) Specific Enzymatic Amplification of DNA *In Vitro*: The Polymerase Chain Reaction. Cold Spring Harbor Symposia on Quantitative Biology 51(0):263–273.

Munnik, Ligterink, Meskiene, Calderini, Beyerly, Musgrave, Hirt (1999) Distinct osmo-sensing protein kinase pathways are involved in signalling moderate and severe hyper-osmotic stress. Plant J 20(4):381–388

Murashige T, Skoog F (1962) A Revised Medium for Rapid Growth and Bio Assays with Tobacco Tissue Cultures. Physiol Plant 15(3):473–497.

Nagar B (2007) c-Abl tyrosine kinase and inhibition by the cancer drug imatinib (Gleevec/STI-571). J Nutr 137(6 Suppl 1):1518S-1523S; discussion 1548S

Nakagami H, Pitzschke A, Hirt H (2005) Emerging MAP kinase pathways in plant stress signalling. Trends in Plant Science 10(7):339–346.

Nakagami H, Soukupová H, Schikora A, Zárský V, Hirt H (2006) A Mitogen-activated protein kinase kinase kinase mediates reactive oxygen species homeostasis in Arabidopsis. J Biol Chem 281(50):38697–38704.

Nilson SE, Assmann SM (2007) The control of transpiration. Insights from Arabidopsis. Plant Physiol. 143(1):19–27.

Ning J, Li X, Hicks LM, Xiong L (2010) A Raf-like MAPKKK gene DSM1 mediates drought resistance through reactive oxygen species scavenging in rice. Plant Physiol 152(2):876–890.

Nishi H, Hashimoto K, Panchenko AR (2011) Phosphorylation in protein-protein binding: Effect on stability and function. Structure 19(12):1807–1815.

Nishi H, Fong JH, Chang C, Teichmann SA, Panchenko AR (2013) Regulation of protein-protein binding by coupling between phosphorylation and intrinsic disorder: Analysis of human protein complexes. Mol Biosyst 9(7):1620–1626.

Nolen B, Taylor S, Ghosh G (2004) Regulation of protein kinases; controlling activity through activation segment conformation. Mol Cell 15(5):661–675.

Nonogaki H, Bassel GW, Bewley JD (2010) Germination—Still a mystery. Plant Science 179(6):574–581.

Ohno R, Takumi S, Nakamura C (2006) Phosphorylation of wheat chloroplast-targeting COR/LEA proteins via 50-kDa protein kinase. Wheat Inf. Serv. 101:1-3, Japan, Kobe University

Olsen JV, Blagoev B, Gnad F, Macek B, Kumar C, Mortensen P, Mann M (2006) Global, *in vivo*, and site-specific phosphorylation dynamics in signaling networks. Cell 127(3):635–648.

Park AR, Cho SK, Yun UJ, Jin MY, Lee SH, Sachetto-Martins G, Park OK (2001) Interaction of the Arabidopsis receptor protein kinase Wak1 with a glycine-rich protein, AtGRP-3. J Biol Chem 276(28):26688–26693.

Pearson G, Robinson F, Beers Gibson T, Xu BE, Karandikar M, Berman K, Cobb MH (2001) Mitogen-activated protein (MAP) kinase pathways: regulation and physiological functions. Endocr Rev 22(2):153–183.

Petersen J (2012) Biochemische Untersuchungen zur Funktion, Struktur und Phosphorylierung des Stressproteins CDeT11-24 aus der trockentoleranten Pflanze *Craterostigma plantagineum*: Dissertation, Rheinische Friedrich-Wilhelms-Universität Bonn

Petersen J, Eriksson SK, Harryson P, Pierog S, Colby T, Bartels D, Röhrig H (2012) The lysine-rich motif of intrinsically disordered stress protein CDeT11-24 from Craterostigma plantagineum is responsible for phosphatidic acid binding and protection of enzymes from damaging effects caused by desiccation. Journal of Experimental Botany 63(13):4919–4929.

Phillips JR, Fischer E, Baron M, van den Dries N, Facchinelli F, Kutzer M, Rahmanzadeh R, Remus D, Bartels D (2008) *Lindernia brevidens*: a novel desiccation-tolerant vascular plant, endemic to ancient tropical rainforests. Plant J 54(5):938–948.

Piatkowski D, Schneider K, Salamini F, Bartels D (1990) Characterization of Five Abscisic Acid-Responsive cDNA Clones Isolated from the Desiccation-Tolerant Plant *Craterostigma plantagineum* and Their Relationship to Other Water-Stress Genes. Plant Physiol 94(4):1682–1688

Pierog S. (2011) Biochemische Bindungsstudien des Stressproteins CDeT11-24 aus *Craterostigma plantagineum*. Bachelor Thesis. Rheinische Friedrich-Wilhelms-Universität Bonn

Pitzschke A, Djamei A, Bitton F, Hirt H (2009a) A major role of the MEKK1-MKK1/2-MPK4 pathway in ROS signalling. Mol Plant 2(1):120–137.

Pitzschke A, Schikora A, Hirt H (2009b) MAPK cascade signalling networks in plant defence. Current Opinion in Plant Biology 12(4):421–426.

Popescu SC, Popescu GV, Bachan S, Zhang Z, Gerstein M, Snyder M, Dinesh-Kumar SP (2009) MAPK target networks in *Arabidopsis thaliana* revealed using functional protein microarrays. Genes Dev 23(1):80–92.

Qi M, Elion EA (2005) MAP kinase pathways. J Cell Sci 118(Pt 16):3569–3572.

Quesada V, Ponce MR, Micol JL (2000) Genetic analysis of salt-tolerant mutants in *Arabidopsis thaliana*. Genetics 154(1):421–436

Quesada V, García-Martínez S, Piqueras P, Ponce MR, Micol JL (2002) Genetic architecture of NaCl tolerance in Arabidopsis. Plant Physiol. 130(2):951–963.

Rahman LN, Smith GST, Bamm VV, Voyer-Grant JAM, Moffatt BA, Dutcher JR, Harauz G (2011) Phosphorylation of *Thellungiella salsuginea* dehydrins TsDHN-1 and TsDHN-2 facilitates cation-induced conformational changes and actin assembly. Biochemistry 50(44):9587–9604.

Rahmanzadeh R, Müller K, Fischer E, Bartels D, Borsch T (2005) The *Linderniaceae* and *Gratiolaceae* are further lineages distinct from the *Scrophulariaceae* (Lamiales). Plant Biol (Stuttg) 7(1):67–78.

Rao KP, Richa T, Kumar K, Raghuram B, Sinha AK (2010) In silico analysis reveals 75 members of mitogen-activated protein kinase kinase kinase gene family in rice. DNA Res 17(3):139–153.

Rédei GP (ed) (1992) A heuristic glance at the past of Arabidopsis genetics: Methods in Arabidopsis Research. World Scientific, Singapore

Reiland S, Messerli G, Baerenfaller K, Gerrits B, Endler A, Grossmann J, Gruissem W, Baginsky S (2009) Large-scale Arabidopsis phosphoproteome profiling reveals novel chloroplast kinase substrates and phosphorylation networks. Plant Physiol 150(2):889–903.

Rizzo MA, Shome K, Watkins SC, Romero G (2000) The recruitment of Raf-1 to membranes is mediated by direct interaction with phosphatidic acid and is independent of association with Ras. J Biol Chem 275(31):23911–23918.

Roberts JK, DeSimone NA, Lingle WL, Dure L (1993) Cellular Concentrations and Uniformity of Cell-Type Accumulation of Two Lea Proteins in Cotton Embryos. Plant Cell 5(7):769–780.

Robles P, Fleury D, Candela H, Cnops G, Alonso-Peral MM, Anami S, Falcone A, Caldana C, Willmitzer L, Ponce MR, van Lijsebettens M, Micol JL (2010) The RON1/FRY1/SAL1 gene is required for leaf morphogenesis and venation patterning in Arabidopsis. Plant Physiol 152(3):1357–1372.

Rodriguez MCS, Edsgärd D, Hussain SS, Alquezar D, Rasmussen M, Gilbert T, Nielsen BH, Bartels D, Mundy J (2010a) Transcriptomes of the desiccation-tolerant resurrection plant *Craterostigma plantagineum*. Plant J 63(2):212–228.

Rodriguez MCS, Petersen M, Mundy J (2010b) Mitogen-activated protein kinase signaling in plants. Annu Rev Plant Biol 61:621–649.

Röhrig H, Schmidt J, Colby T, Bräutigam A, Hufnagel P, Bartels D (2006) Desiccation of the resurrection plant *Craterostigma plantagineum* induces dynamic changes in protein phosphorylation. Plant Cell Environ 29(8):1606–1617

Röhrig H, Colby T, Schmidt J, Harzen A, Facchinelli F, Bartels D (2008) Analysis of desiccation-induced candidate phosphoproteins from *Craterostigma plantagineum* isolated with a modified metal oxide affinity chromatography procedure. Proteomics 8(17):3548–3560.

Rudrabhatla P, Reddy MM, Rajasekharan R (2006) Genome-wide analysis and experimentation of plant serine/ threonine/tyrosine-specific protein kinases. Plant Mol Biol 60(2):293–319.

Saitou N, Nei M (1987) The neighbor-joining method: a new method for reconstructing phylogenetic trees. Mol Biol Evol 4(4):406–425

Sambrook J., Fritsch E. F., Maniatis T. (1989) Molecular Cloning: A Laboratory Manual, 2. ed. Cold Spring Harbor laboratory Press, USA

Sanford JC, Smith FD, Russell JA (1993) Optimizing the biolistic process for different biological applications. Meth Enzymol 217:483–509

Saruhashi M, Kumar Ghosh T, Arai K, Ishizaki Y, Hagiwara K, Komatsu K, Shiwa Y, Izumikawa K, Yoshikawa H, Umezawa T, Sakata Y, Takezawa D (2015) Plant Raf-like kinase

integrates abscisic acid and hyperosmotic stress signaling upstream of SNF1-related protein kinase2. Proc Natl Acad Sci USA 112(46):E6388-96.

Sasayama D, Matsuoka D, Oka M, Shitamichi N, Furuya T, Azuma T, Itoh K, Nanmori T (2011) MAP3Kδ4, an Arabidopsis Raf-like MAP3K, regulates plant growth and shoot branching. Plant Biotechnology 28(5):463–470.

Scarpeci TE, Frea VS, Zanor MI, Valle EM (2017) Overexpression of AtERF019 delays plant growth and senescence, and improves drought tolerance in Arabidopsis. Journal of Experimental Botany 68(3):673–685.

Schaeffer HJ, Weber MJ (1999) Mitogen-Activated Protein Kinases: Specific Messages from Ubiquitous Messengers. Mol. Cell. Biol. 19(4):2435–2444.

Schlosser CA, Strzepek K, Gao X, Fant C, Blanc É, Paltsev S, Jacoby H, Reilly J, Gueneau A (2014) The future of global water stress: An integrated assessment. Earth's Future 2(8):341–361.

Schneider CA, Rasband WS, Eliceiri KW (2012) NIH Image to ImageJ: 25 years of image analysis. Nat Meth 9(7):671–675. doi: 10.1038/nmeth.2089

Schopfer P, Brennicke A, Mohr h (1999) Pflanzenphysiologie, 5., grundlegend überarb. und aktualisierte Aufl. Springer-Lehrbuch. Springer, Berlin

Schwartz PA, Murray BW (2011) Protein kinase biochemistry and drug discovery. Bioorg Chem 39(5-6):192–210.

Sedgwick SG, Smerdon SJ (1999) The ankyrin repeat: A diversity of interactions on a common structural framework. Trends Biochem Sci 24(8):311–316.

Serber Z, Ferrell JE (2007) Tuning bulk electrostatics to regulate protein function. Cell 128(3):441–444.

Shen H, Liu C, Zhang Y, Meng X, Zhou X, Chu C, Wang X (2012) OsWRKY30 is activated by MAP kinases to confer drought tolerance in rice. Plant Mol Biol 80(3):241–253.

Shen-Miller J, Schopf JW, Harbottle G, Cao R-J, Ouyang S, Zhou K-S, Southon JR, Liu G-H (2002) Long-living lotus: germination and soil {gamma}-irradiation of centuries-old fruits, and cultivation, growth, and phenotypic abnormalities of offspring. Am J Bot 89(2):236–247.

Shitamichi N, Matsuoka D, Sasayama D, Furuya T, Nanmori T (2013) Over-expression of MAP3Kδ4, an ABA-inducible Raf-like MAP3K that confers salt tolerance in Arabidopsis. Plant Biotechnology 30(2):111–118.

Sjö A, Magnusson K-E, Peterson KH (2010) Protein kinase C activation has distinct effects on the localization, phosphorylation and detergent solubility of the claudin protein family in tight and leaky epithelial cells. J Membr Biol 236(2):181–189.

Stiti N, Triki S, Hartmann M-A (2007) Formation of triterpenoids throughout Olea europaea fruit ontogeny. Lipids 42(1):55–67.

Sun X, Rikkerink EHA, Jones WT, Uversky VN (2013) Multifarious roles of intrinsic disorder in proteins illustrate its broad impact on plant biology. Plant Cell 25(1):38–55.

Sun Y, Wang C, Yang B, Wu F, Hao X, Liang W, Niu F, Yan J, Zhang H, Wang B, Deyholos MK, Jiang Y-Q (2014) Identification and functional analysis of mitogen-activated protein

kinase kinase kinase (MAPKKK) genes in canola (*Brassica napus L.*). Journal of Experimental Botany 65(8):2171–2188.

Tanoue T, Nishida E (2003) Molecular recognitions in the MAP kinase cascades. Cell Signal 15(5):455–462.

Taylor SS, Kornev AP (2011) Protein kinases: Evolution of dynamic regulatory proteins. Trends Biochem Sci 36(2):65–77.

Teige M, Scheikl E, Eulgem T, Dóczi R, Ichimura K, Shinozaki K, Dangl JL, Hirt H (2004) The MKK2 pathway mediates cold and salt stress signaling in Arabidopsis. Mol Cell 15(1):141–152.

Tena G, Asai T, Chiu W-L, Sheen J (2001) Plant mitogen-activated protein kinase signaling cascades. Current Opinion in Plant Biology 4(5):392–400.

The 1001 Genomes Consortium (2016) Genomes Reveal the Global Pattern of Polymorphism in Arabidopsis thaliana. Cell 166(2):481–491.

Towbin H, Gordon J (1984) Immunoblotting and dot immunobinding — Current status and outlook. Journal of Immunological Methods 72(2):313–340.

Towbin H, Staehelin T, Gordon J (1979) Electrophoretic transfer of proteins from polyacrylamide gels to nitrocellulose sheets: procedure and some applications. Proc Natl Acad Sci USA 76(9):4350–4354

Treiber DK, Shah NP (2013) Ins and outs of kinase DFG motifs. Chem Biol 20(6):745–746.

Trewavas AJ, Malho R (1997) Signal Perception and Transduction: The Origin of the Phenotype. Plant Cell 9(7):1181–1195.

Tsugama D, Liu S, Takano T (2012) Drought-induced activation and rehydration-induced inactivation of MPK6 in Arabidopsis. Biochem Biophys Res Commun 426(4):626–629.

Ubersax JA, Ferrell JE (2007) Mechanisms of specificity in protein phosphorylation. Nat Rev Mol Cell Biol 8(7):530–541.

Ullah A, Sun H, Yang X, Zhang X (2017) Drought coping strategies in cotton: Increased crop per drop. Plant Biotechnol J 15(3):271–284.

Umezawa T, Fujita M, Fujita Y, Yamaguchi-Shinozaki K, Shinozaki K (2006) Engineering drought tolerance in plants: discovering and tailoring genes to unlock the future. Curr Opin Biotechnol 17(2):113–122.

Umezawa T, Sugiyama N, Takahashi F, Anderson JC, Ishihama Y, Peck SC, Shinozaki K (2013) Genetics and phosphoproteomics reveal a protein phosphorylation network in the abscisic acid signaling pathway in *Arabidopsis thaliana*. Sci Signal 6(270):rs8.

Vallejo AJ, Yanovsky MJ, Botto JF (2010) Germination variation in *Arabidopsis thaliana* accessions under moderate osmotic and salt stresses. Ann Bot 106(5):833–842.

van den Dries N, Facchinelli F, Giarola V, Phillips JR, Bartels D (2011) Comparative analysis of LEA-like 11-24 gene expression and regulation in related plant species within the *Linderniaceae* that differ in desiccation tolerance. New Phytol 190(1):75–88.

VanBuren R, Wai J, Zhang Q, Song X, Edger PP, Bryant D, Michael TP, Mockler TC, Bartels D (2017) Seed desiccation mechanisms co-opted for vegetative desiccation in the resurrection grass *Oropetium thomeaum*. Plant Cell Environ 40(10):2292-2306.

Velasco R, Salamini F, Bartels D (1998) Gene structure and expression analysis of the drought- and abscisic acid-responsive CDeT11-24 gene family from the resurrection plant *Craterostigma plantagineum Hochst*. Planta 204(4):459–471.

Vilela B, Pagès M, Riera M (2015) Emerging roles of protein kinase CK2 in abscisic acid signaling. Front Plant Sci 6:966.

Volk, O. H. and Leippert (1971) Vegetationsverhältnisse im Windhoeker Bergland, Südwestafrika. Journal der Südwestafrikanischen wissenschaftlichen Gesellschaft 25:4–44

Walters C, Farrant JM, Pammenter NW, Berjak P (2002) Desiccation stress and damage. In: Black M, Pritchard HW (eds) Desiccation and survival in plants: drying without dying. CABI, Wallingford, pp 263–291

Walters C, Ballesteros D, Vertucci VA (2010) Structural mechanics of seed deterioration: Standing the test of time. Plant Science 179(6):565–573.

Wang P, Xue L, Batelli G, Lee S, Hou Y-J, van Oosten MJ, Zhang H, Tao WA, Zhu J-K (2013) Quantitative phosphoproteomics identifies SnRK2 protein kinase substrates and reveals the effectors of abscisic acid action. Proc Natl Acad Sci U S A 110(27):11205–11210.

Wang J, Pan C, Wang Y, Ye L, Wu J, Chen L, Zou T, Lu G (2015) Genome-wide identification of MAPK, MAPKK, and MAPKKK gene families and transcriptional profiling analysis during development and stress response in cucumber. BMC Genomics 16:386.

Wang M, Yue H, Feng K, Deng P, Song W, Nie X (2016) Genome-wide identification, phylogeny and expressional profiles of mitogen activated protein kinase kinase kinase (MAPKKK) gene family in bread wheat (*Triticum aestivum L.*). BMC Genomics 17:668.

Wellbrock C, Karasarides M, Marais R (2004) The RAF proteins take centre stage. Nat Rev Mol Cell Biol 5(11):875–885.

Whiteman S-A, Serazetdinova L, Jones AME, Sanders D, Rathjen J, Peck SC, Maathuis FJM (2008) Identification of novel proteins and phosphorylation sites in a tonoplast enriched membrane fraction of *Arabidopsis thaliana*. Proteomics 8(17):3536–3547.

Whitmarsh AJ (1998) A Mammalian Scaffold Complex That Selectively Mediates MAP Kinase Activation. Science 281(5383):1671–1674.

Widmann C, Gibson S, Jarpe MB, Johnson GL (1999) Mitogen-activated protein kinase: conservation of a three-kinase module from yeast to human. Physiol Rev 79(1):143–180

Wingenter K, Trentmann O, Winschuh I, Hörmiller II, Heyer AG, Reinders J, Schulz A, Geiger D, Hedrich R, Neuhaus HE (2011) A member of the mitogen-activated protein 3-kinase family is involved in the regulation of plant vacuolar glucose uptake. Plant J 68(5):890–900.

Winter D, Vinegar B, Nahal H, Ammar R, Wilson GV, Provart NJ (2007) An "Electronic Fluorescent Pictograph" browser for exploring and analyzing large-scale biological data sets. PLoS ONE 2(8):e718.

Wohlbach DJ, Quirino BF, Sussman MR (2008) Analysis of the Arabidopsis histidine kinase ATHK1 reveals a connection between vegetative osmotic stress sensing and seed maturation. Plant Cell 20(4):1101–1117.

Wolschin F, Weckwerth W (2005) Combining metal oxide affinity chromatography (MOAC) and selective mass spectrometry for robust identification of *in vivo* protein phosphorylation sites. Plant Methods 1(1):9.

Wu J, Wang J, Pan C, Guan X, Wang Y, Liu S, He Y, Chen J, Chen L, Lu G (2014) Genome-wide identification of MAPKK and MAPKKK gene families in tomato and transcriptional profiling analysis during development and stress response. PLoS ONE 9(7):e103032.

Xavier C-P, Rastetter RH, Blömacher M, Stumpf M, Himmel M, Morgan RO, Fernandez M-P, Wang C, Osman A, Miyata Y, Gjerset RA, Eichinger L, Hofmann A, Linder S, Noegel AA, Clemen CS (2012) Phosphorylation of CRN2 by CK2 regulates F-actin and Arp2/3 interaction and inhibits cell migration. Sci Rep 2:241.

Xing Y, Jia W, Zhang J (2009) AtMKK1 and AtMPK6 are involved in abscisic acid and sugar signaling in Arabidopsis seed germination. Plant Mol Biol 70(6):725–736.

Yamaguchi-Shinozaki K, Shinozaki K (1993) Characterization of the expression of a desiccation-responsive rd29 gene of *Arabidopsis thaliana* and analysis of its promoter in transgenic plants. Molec. Gen. Genet. 236-236(2-3):331–340. Yamaguchi-Shinozaki K, Shinozaki K (1994) A novel cis-acting element in an Arabidopsis gene is involved in responsiveness to drought, low-temperature, or high-salt stress. Plant Cell 6(2):251–264.

Yin Z, Wang J, Wang D, Fan W, Wang S, Ye W (2013) The MAPKKK gene family in *Gossypium raimondii*: genome-wide identification, classification and expression analysis. Int J Mol Sci 14(9):18740–18757.

Yin X, Wang X, Komatsu S (2017) Phosphoproteomics: protein phosphorylation in regulation of seed germination and plant growth. Curr Protein Pept Sci. Epub ahead of print, doi: 10.2174/1389203718666170209151048

Yoon S, Seger R (2006) The extracellular signal-regulated kinase: multiple substrates regulate diverse cellular functions. Growth Factors 24(1):21–44.

Yuan W, Flowers JM, Sahraie DJ, Purugganan MD (2016) Cryptic Genetic Variation for *Arabidopsis thaliana* Seed Germination Speed in a Novel Salt Stress Environment. G3 (Bethesda) 6(10):3129–3138.

Zehr BD, Savin TJ, Hall RE (1989) A one-step, low background Coomassie staining procedure for polyacrylamide gels. Anal Biochem 182(1):157–159.

Zhang J, Yang PL, Gray NS (2009) Targeting cancer with small molecule kinase inhibitors. Nat Rev Cancer 9(1):28–39.

Zheng L, Baumann U, Reymond J-L (2004) An efficient one-step site-directed and site-saturation mutagenesis protocol. Nucleic Acids Res 32(14):e115.

Zhu J-K (2000) Genetic Analysis of Plant Salt Tolerance Using Arabidopsis: Fig. 1. Plant Physiol. 124(3):941–948.

Zulawski M, Schulze WX (2015) The plant kinome. Methods Mol Biol 1306:1–23.

Supplemental data

S.1 CpVIK phosphorylation by autophosphorylation *in vitro*

S.1.1 Determination of phosphorylation sites in CpVIK after autophosphorylation *in vitro*

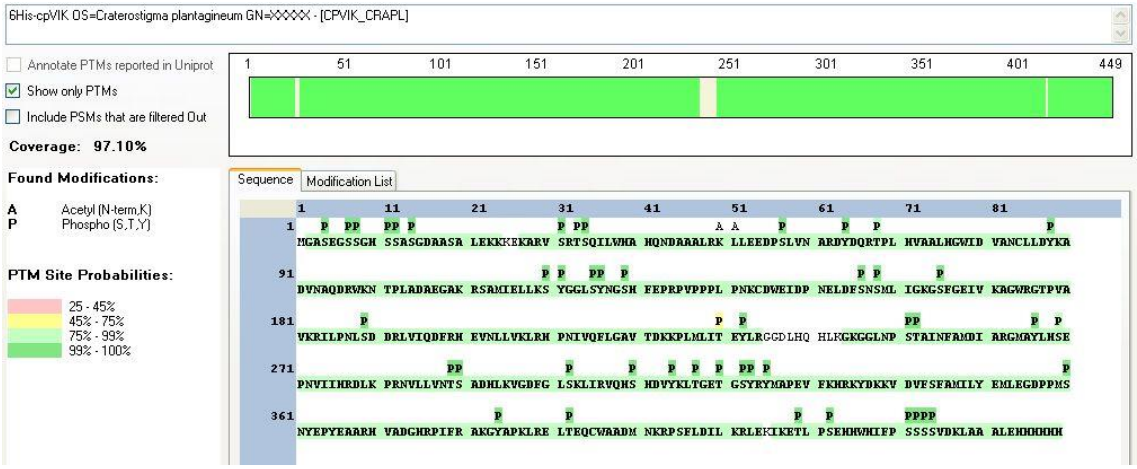

Supplemental figure 58: Phosphorylation sites in CpVIK *in vitro*
Phosphosites were identified by mass spectrometry. Identified peptides are highlighted in green. Phosphorylation sites are highlighted with a colour code reflecting the localisation probability. Mass spectrometric analyses were performed by Dr. Marc Sylvester at the core facility mass spectrometry (Institute of Biochemistry and Molecular Biology, University of Bonn).

The *in vitro* kinase assay was performed as described in **2.25** and the sample was pre-treated prior mass spectrometry analyses as described in **3.5.4**. Phosphorylation of CDeT11-24 by CpVIK and autophosphorylation of CpVIK was shown in a test gel (**Figure 31**). Detailed Mass spectrometry data can be obtained from the supplementary data files.

S.1.2 Comparison of *in vitro* and *in silico* phosphorylation sites

Supplemental table 13: Comparison of phosphosite prediction and *in vitro* phosphorylation of the CpVIK protein

Prediction determined with the Group-based Prediction System 3.0 software. (Hits with a score > 9 and a cut off < 50% included. The *in vitro* data derive from the kinase assay described in S.4.1; Grey highlighted: Amino acids included in both, *in vitro* and *in silico* data; Yellow highlighted: Amino acids only included in the *in vitro* data; Orange highlighted: Amino acids only included in the *in silico* data.

4	S	251	S
7	S	252	T
8	S	266	Y
11	S	269	S
12	S	289	T
14	S	290	S
19	S	302	S
31	S	310	S
33	T	314	Y
34	S	317	T
57	S	320	T
64	Y	322	S
68	T	323	Y
88	Y	325	Y
101	T	344	S
112	S	350	Y
120	S	360	S
121	Y	362	Y
125	S	365	Y
126	Y	384	Y
129	S	392	T
156	S	405	S
158	S	419	T
165	S	422	S
177	T	431	S
189	S	432	S
230	T	433	S
232	Y	434	S

S. 2 CpVIK protein expression and phosphorylation in roots

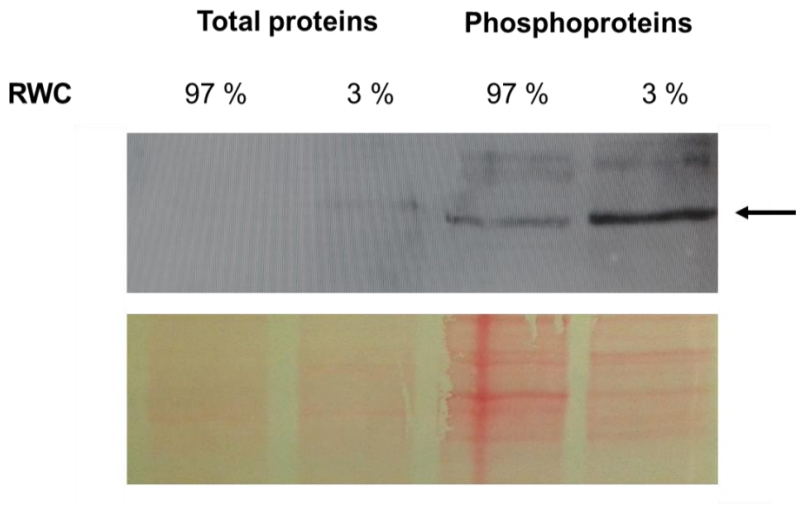

Supplemental figure 59: Stress affected phosphorylation of CpVIK protein in *C. plantagineum* roots
RWC (Relative water content (determined as described in 2.1.4); Protein expression was evaluated by immunological analyses with the CpVIK antibody (2.15.2). Adult *C. plantagineum* plants were grown as described in 2.1.2 for control condition samples (97 % RWC). Dehydration stress treatments were imposed to adult *C. plantagineum* plants by withholding watering; The phosphoprotein subtraction was enriched from the displayed total protein extraction *via* metal oxide/hydroxide affinity chromatography as described in 2.11.5.

S. 3 CpVIK protein degradation in crude plant extracts

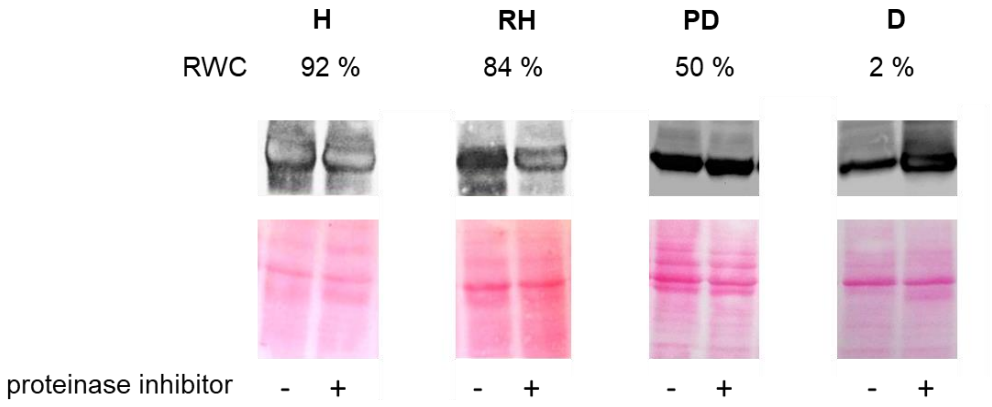

Supplemental figure 60: Degradation of recombinant CpVIK protein in crude plant extracts
30 µg lyophilized, recombinant CpVIK6His-tag protein was incubated with ground leaf material *C. plantagineum* plants in 5 ml buffer A (50 mM NaH2PO4, 300 mM NaCl, 5 mM imidazole, 10 % (v/v) glycerol, 0,1 (v/v) Triton X-100) which were fully hydrated (H), partially dehydrated (PD), dehydrated (D) or rehydrated (RH) for 30 min at room temperature. Buffer A was supplemented with 100 µl proteinase inhibitor cocktail (Sigma-Aldrich; München, DE) in (+)-samples. CpVIK degradation was monitored after SDS-PAGE (2.13.2) and Western blot analyses with the CpVIK antiserum (2.15).

S. 4 *In vitro* kinase assays with radiolabeled ATP

The incorporation of radiolabeled phosphate from [gamma-32P]ATP into CDeT11-24 after incubation with CpVIK was analysed by Jan Petersen (Institute of Molecular Cell and Systems Biology, University of Glasgow, UK) for verification of the results obtained in this thesis (**3.5**).

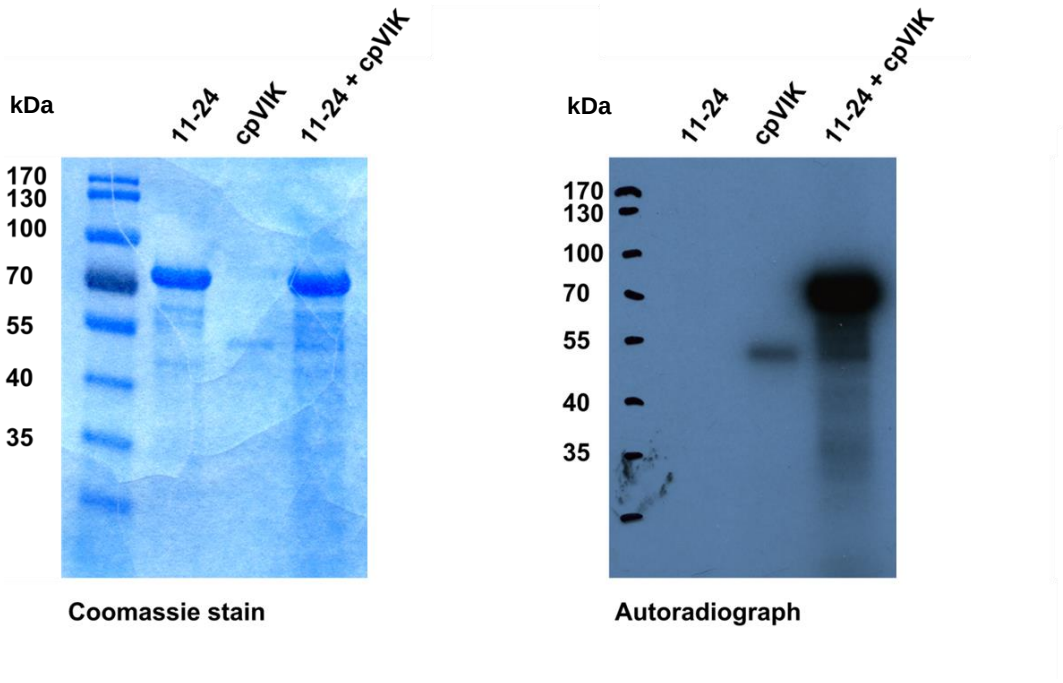

Supplemental figure 61: Radioactive *in vitro* kinase assay of CpVIK with CDeT11-24 as substrate
kDa: Protein mass in kilo Dalton

S. 5 Analogy of the closest CpVIK homologs in evolutionarily distinct species

Supplemental table 14: Closest CpVIK homologs in different kingdoms
Loci from different kingdoms with the highest homology to CpVIK identified with pblast analysis (https://blast.ncbi.nlm.nih.gov/Blast.cgi)

Locus	***Organism***	***Query cover***	***Identity***	***E-value***
OGO93731.1	*Coxiella sp.*	*85 %*	*32 %*	*4e-41*
XP_001703341.1	*Chlamydomonas reinhardtii*	*82 %*	*42 %*	*7e-90*
XP_001784362.1	*Physcomitrella patens*	*95%*	*55%*	*1e-160*
XP_002991787.1	*Selanginella moellendorfii*	*92%*	*62%*	*5e-173*

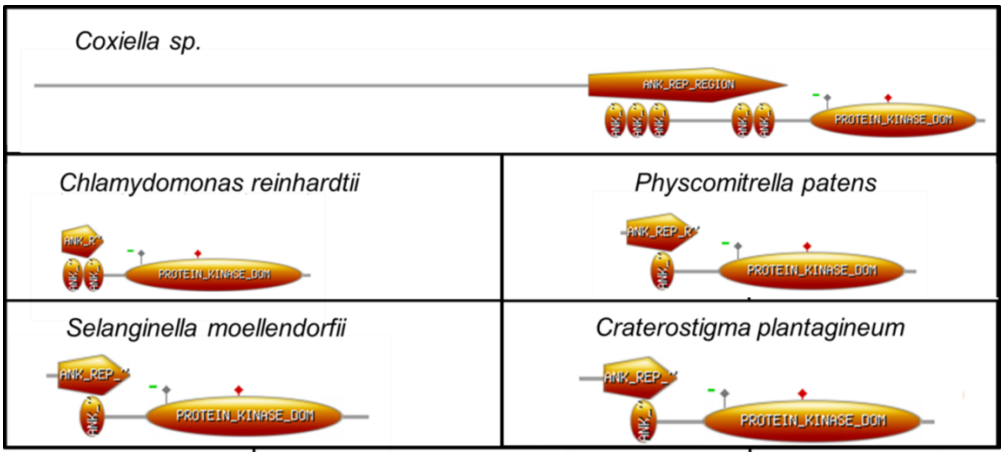

Supplemental figure 62: Domain structure of the closest CpVIK homologs in evolutionarily distinct species
Models created with the PROSITE web tool (http://prosite.expasy.org/)

S. 6 Closest CpVIK homologs in *Linderniaceae*

S.6.1 *C. plantagineum*

Supplemental figure 63: The 10 closest CpVIK homologs in *C. plantagineum*
Database: Craterodb29-09exp
29,430 sequences; 12,841,551 total letters

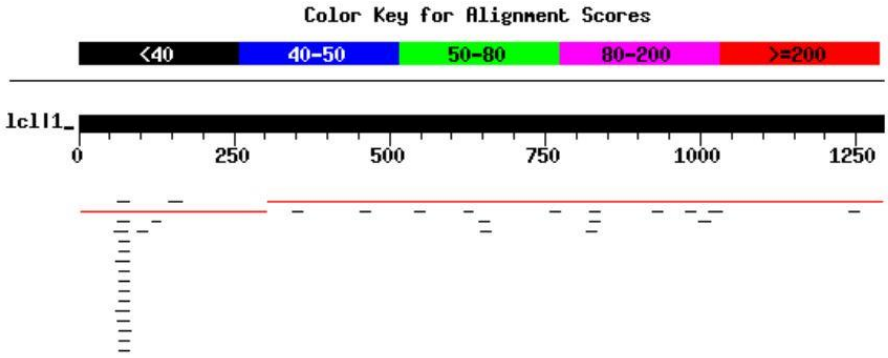

Sequences producing significant alignments:	Score (bits)	E Value
contig08317#length=1121#c_ex=6#ed_ex=8,09#dh_ex=19,68#rh_ex=8,62...	1552	0.0
contig13110#length=364#c_ex=12,32#ed_ex=4,55#dh_ex=4,46#rh_ex=4,...	563	e-160
contig09972#length=1078#c_ex=14,17#ed_ex=4,55#dh_ex=5,87#rh_ex=1...	38	0.051
contig07022#length=462#c_ex=6#ed_ex=24,96#dh_ex=6,7#rh_ex=4,5#Co...	38	0.051
contig26676#length=1230#c_ex=18,78#ed_ex=20,93#dh_ex=42,32#rh_ex...	36	0.20
contig19490#length=465#c_ex=7,28#ed_ex=3,81#dh_ex=3,79#rh_ex=5,7...	36	0.20
contig18702#length=583#c_ex=11,14#ed_ex=5,31#dh_ex=13,17#rh_ex=1...	36	0.20
contig16647#length=1125#c_ex=4,73#ed_ex=6,21#dh_ex=8,35#rh_ex=5,...	36	0.20
contig17581#length=748#c_ex=4,22#ed_ex=17,29#dh_ex=5,87#rh_ex=4,...	34	0.80
contig14746#length=410#c_ex=3,7#ed_ex=3,81#dh_ex=7,53#rh_ex=3,62...	34	0.80

S.6.2 *L. brevidens*

Supplemental figure 64: The 10 closest CpVIK homologs in *L. brevidens*
Database: LB-Unigene_exp.fna
59,700 sequences; 51,669,749 total letters

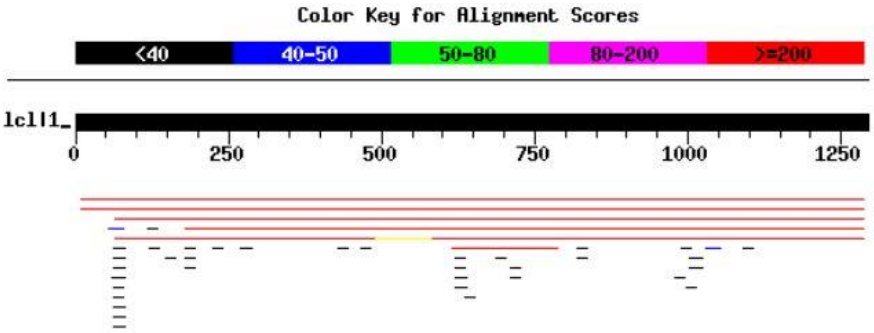

Sequences producing significant alignments:	Score (bits)	E Value
CL3353.Contig4_LB|LENGTH=1691|F=17.78|PD=6.53|D=3.63|R=16.84	1643	0.0
CL3353.Contig3_LB|LENGTH=1436|F=0.67|PD=0.19|D=0.21|R=0.31	1518	0.0
CL3353.Contig5_LB|LENGTH=1468|F=0.25|PD=0.23|D=0.10|R=0.04	1516	0.0
CL3353.Contig2_LB|LENGTH=1305|F=0.16|PD=0.60|D=0.94|R=0.30	1219	0.0
CL3353.Contig1_LB|LENGTH=1373|F=0.27|PD=0.24|D=0.30|R=0.04	841	0.0
Unigene26337_LB|LENGTH=282|F=0.76|PD=0.79|D=0.73|R=0.00	264	2e-69
Unigene30526_LB|LENGTH=246|F=0.22|PD=2.27|D=1.87|R=1.14	46	9e-04
CL4878.Contig2_LB|LENGTH=759|F=3.72|PD=1.10|D=0.07|R=6.48	40	0.053
Unigene15259_LB|LENGTH=590|F=0.00|PD=1.32|D=1.91|R=0.09	38	0.21
Unigene14367_LB|LENGTH=917|F=25.11|PD=18.79|D=6.36|R=33.07	38	0.21

Supplemental figure 65: Alignment of the 5 closest CpVIK homologs in *L. brevidens*

S.6.3 *L. subracemosa*

Supplemental figure 66: The 10 closest CpVIK homologs in *L. subracemosa*
Database: LS-Unigene_exp.fna
63,775 sequences; 60,604,675 total letters

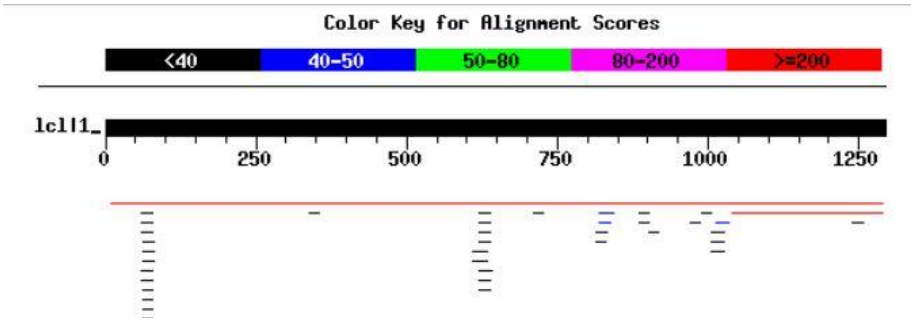

Sequences producing significant alignments:	Score (bits)	E Value
CL5906.Contig1_LS|LENGTH=1693|F=36.09|ED=39.22|LD=36.96	1790	0.0
CL5906.Contig2_LS|LENGTH=253|F=27.38|ED=22.70|LD=26.08	303	3e-81
CL4595.Contig1_LS|LENGTH=2191|F=4.57|ED=11.36|LD=8.98	44	0.004
CL4595.Contig2_LS|LENGTH=1941|F=9.09|ED=7.95|LD=10.53	40	0.063
CL3608.Contig4_LS|LENGTH=4057|F=14.53|ED=15.98|LD=13.71	40	0.063
Unigene21592_LS|LENGTH=1004|F=2.26|ED=4.88|LD=15.11	38	0.25
CL7625.Contig3_LS|LENGTH=598|F=26.70|ED=8.48|LD=5.52	38	0.25
CL7625.Contig1_LS|LENGTH=627|F=6.22|ED=3.50|LD=1.57	38	0.25
CL6170.Contig1_LS|LENGTH=1075|F=46.82|ED=44.00|LD=30.21	38	0.25
CL3882.Contig4_LS|LENGTH=2011|F=2.50|ED=4.28|LD=6.39	38	0.25

S. 7 Germination of *Δvik* and wild type *A. thaliana* seeds

Supplemental figure 67: Germinating seeds of *Δvik* and wild type
WT: wild type; *Δvik*: SALK_002267; germination was observed with the SMZ 800 Nikon Digital Sight DS-2Mv binocular (Nikon, Düssel-dorf, DE) for 6 days. Representative pictures were chosen.

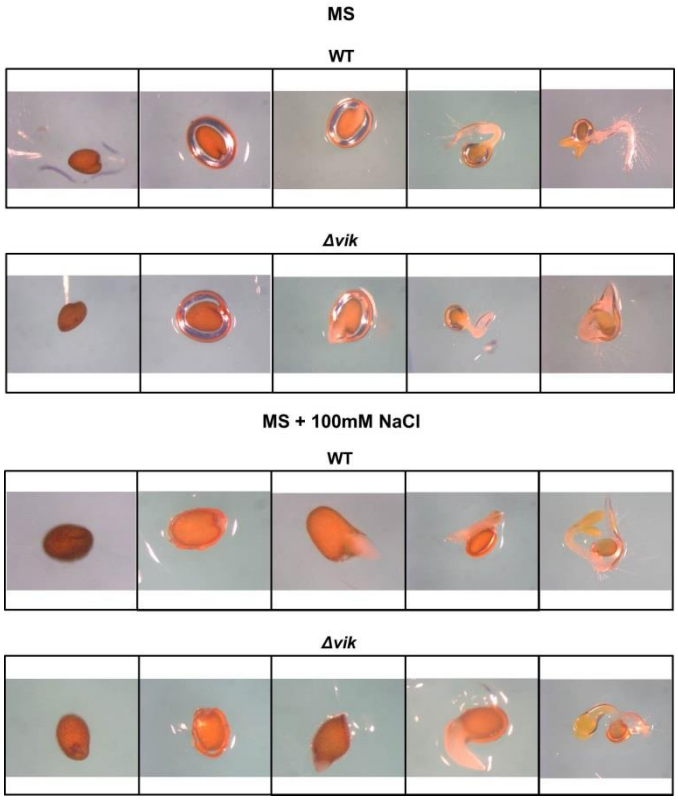

S. 8 Phenotypic analysis of *Δvik* and wild type

Supplemental figure 68: Phenotypic changes over 21 days of stress treatments
Seedlings (14 days old); medium size plants (28 days days old)

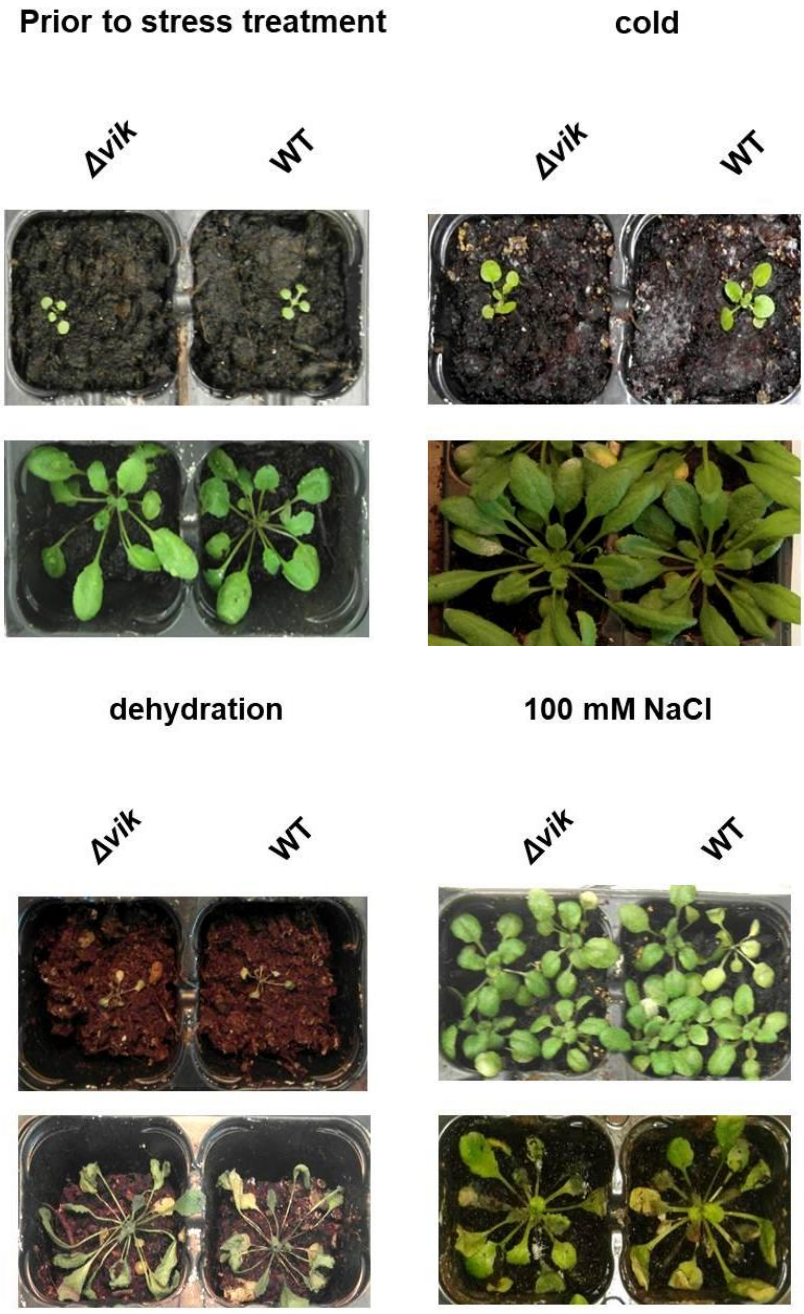

S. 9 Predicted gene interaction networks of AtVIK

The network-building web tool GeneMANIA (http://genemania.org/) was utilised to investigate putative interaction partners of AtVIK.

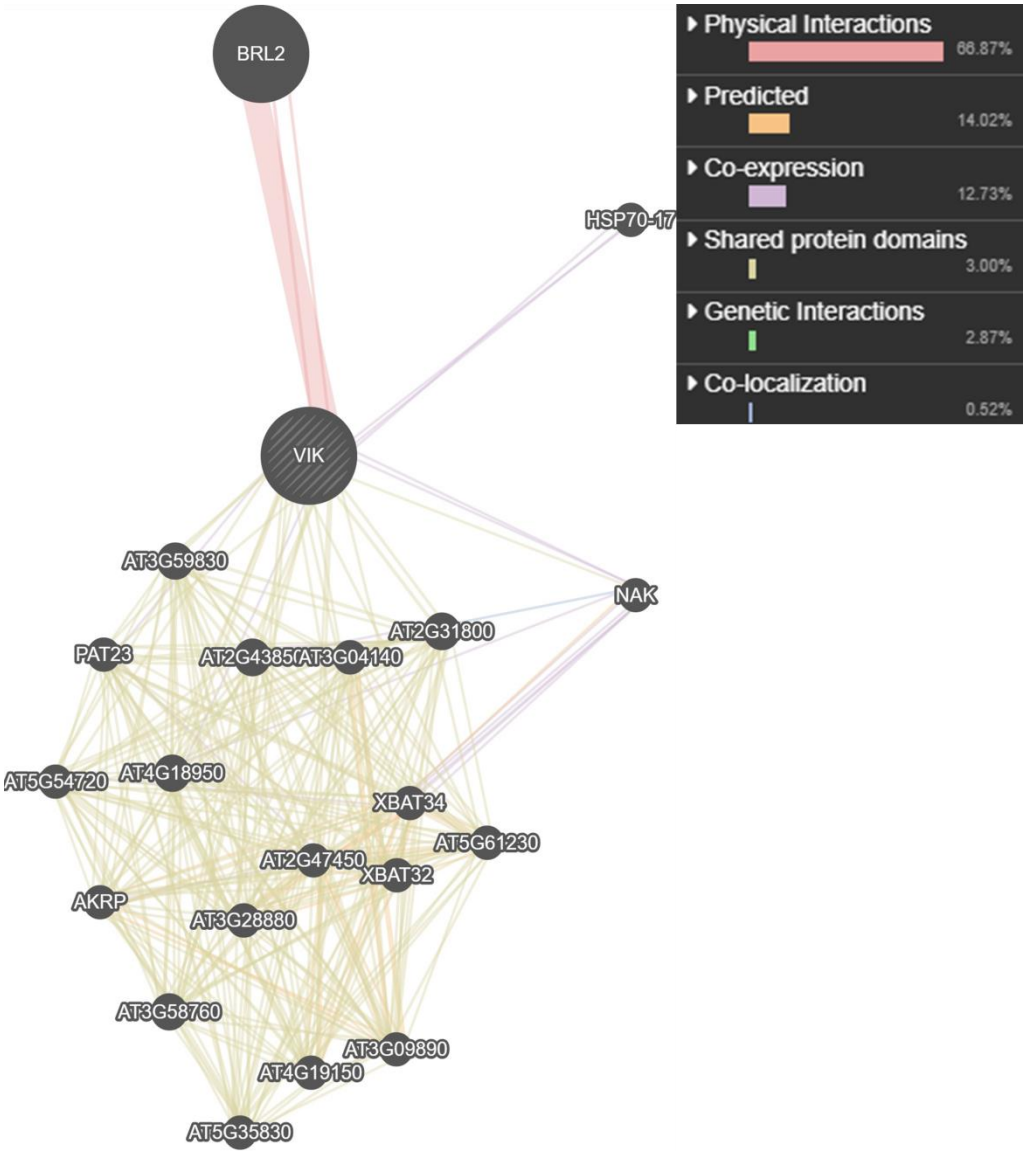

Supplemental figure 69: Predicted gene interaction networks of AtVIK

Genes included in the GeneMANIA report are listed below.

Supplemental table 15: Genes included in the GeneMANIA report

Gene	Description	Rank
VIK	VH1-interacting kinase [Source:TAIR;Acc:AT1G14000]	N/A
BRL2	Serine/threonine-protein kinase BRI1-like 2 [Source:UniProtKB/Swiss-Prot;Acc:Q9ZPS9]	1
AT2G43850	Integrin-linked protein kinase family [Source:TAIR;Acc:AT2G43850]	2
AT2G31800	Integrin-linked protein kinase family [Source:TAIR;Acc:AT2G31800]	3
AT4G18950	Integrin-linked protein kinase family [Source:TAIR;Acc:AT4G18950]	4
AT3G59830	Integrin-linked protein kinase family [Source:TAIR;Acc:AT3G59830]	5
AT3G58760	Integrin-linked protein kinase family [Source:TAIR;Acc:AT3G58760]	6
AT3G04140	Ankyrin repeat family protein [Source:TAIR;Acc:AT3G04140]	7
AT3G28880	Ankyrin repeat family protein [Source:TAIR;Acc:AT3G28880]	8
XBAT32	E3 ubiquitin-protein ligase XBAT32 [Source:UniProtKB/Swiss-Prot;Acc:Q6NLQ8]	9
AT5G61230	Ankyrin repeat family protein [Source:TAIR;Acc:AT5G61230]	10
HSP70-17	Heat shock 70 kDa protein 17 [Source:UniProtKB/Swiss-Prot;Acc:F4JMJ1]	11
AT4G19150	Ankyrin repeat family protein [Source:TAIR;Acc:AT4G19150]	12
PAT23	Probable protein S-acyltransferase 23 [Source:UniProtKB/Swiss-Prot;Acc:Q3EC11]	13
XBAT34	Putative E3 ubiquitin-protein ligase XBAT34 [Source:UniProtKB/Swiss-Prot;Acc:Q9FPH0]	14
AT5G35830	Ankyrin repeat family protein [Source:TAIR;Acc:AT5G35830]	15
AT5G54720	Ankyrin repeat family protein [Source:TAIR;Acc:AT5G54720]	16
AKRP	Ankyrin repeat domain-containing protein, chloroplastic [Source:UniProtKB/Swiss-Prot;Acc:Q05753]	17
AT3G09890	Ankyrin repeat family protein [Source:TAIR;Acc:AT3G09890]	18
NAK	Probable serine/threonine-protein kinase NAK [Source:UniProtKB/Swiss-Prot;Acc:P43293]	19
AT2G47450	Signal recognition particle 43 kDa protein, chloroplastic [Source:UniProtKB/Swiss-Prot;Acc:O22265]	20

S. 10 Promoter binding sites in the upstream region of At1g14000

Supplemental table 16: Promoter binding sites in the upstream region of At1g14000
The Arabidopsis *cis*-regulatory element database (AtcisDB) was utilised to screen for transcription factor binding sites upstream of At1g14000. (http://agris-knowledgebase.org/) table was updated on 15.09.2017.

BS Name	BS Genome Start	BS Genome End	Binding Site Sequence	Binding Site Family/TF
ATHB1 binding site motif	4796502	4796510	caattattg	HB
ATHB5 binding site motif	4796502	4796510	caattattg	HB
ATHB1 binding site motif	4796503	4796511	caataattg	HB
ATHB5 binding site motif	4796503	4796511	caataattg	HB
T-box promoter motif	4796517	4796522	actttg	...
BoxII promoter motif	4796539	4796544	ggttaa	...
SORLREP3	4796559	4796567	tgtatatat	...
DPBF1&2 binding site motif	4796660	4796666	acactag	bZIP
W-box promoter motif	4796683	4796688	ttgacc	WRKY
RAV1-A binding site motif	4796691	4796695	caaca	ABI3VP1
AtMYC2 BS in RD22	4796693	4796698	cacatg	BHLH
LFY consensus binding site motif	4796737	4796742	ccattg	LFY
GATA promoter motif [LRE]	4796788	4796793	agataa	...
DPBF1&2 binding site motif	4796817	4796823	acactag	bZIP
AtMYC2 BS in RD22	4796839	4796844	cacatg	BHLH
GATA promoter motif [LRE]	4796844	4796849	tgatag	...
W-box promoter motif	4796875	4796880	ttgact	WRKY
GATA promoter motif [LRE]	4796955	4796960	tgatag	...
SORLIP1	4796986	4796991	agccac	
T-box promoter motif	4796990	4796995	actttg	...
RAV1-A binding site motif	4797185	4797189	caaca	ABI3VP1
DRE-like promoter motif	4797228	4797236	gaccgacta	...
GATA promoter motif [LRE]	4797279	4797284	agataa	...

S. 11 Vector maps

S.11.1 pET-28a (Novagen)

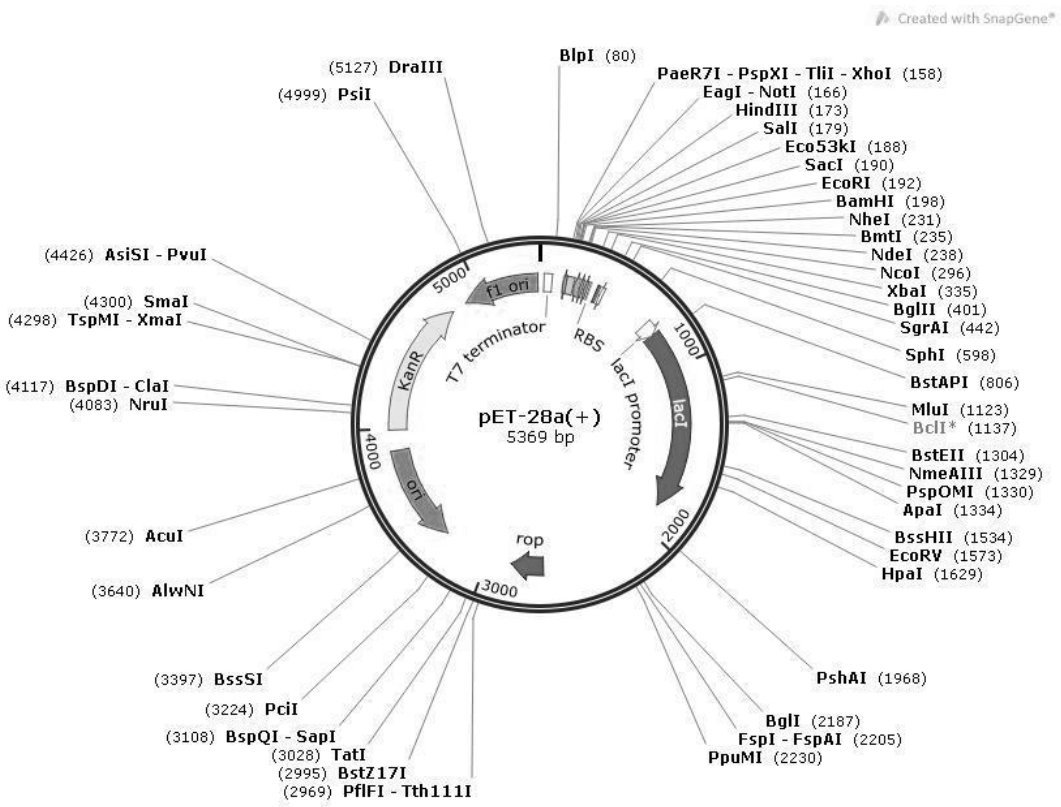

Supplemental figure 70: Vector map of pET-28a
This plasmid harbours a 6x N/C–terminal histidine–tag (His–tag), the IPTG inducible T7lac promoter and a kanamycin resistance. The vector was used for (over-)expression of His-tagged proteins. Map created with SnapGene®.

S.11.2 pET-16b (EMD Chemicals)

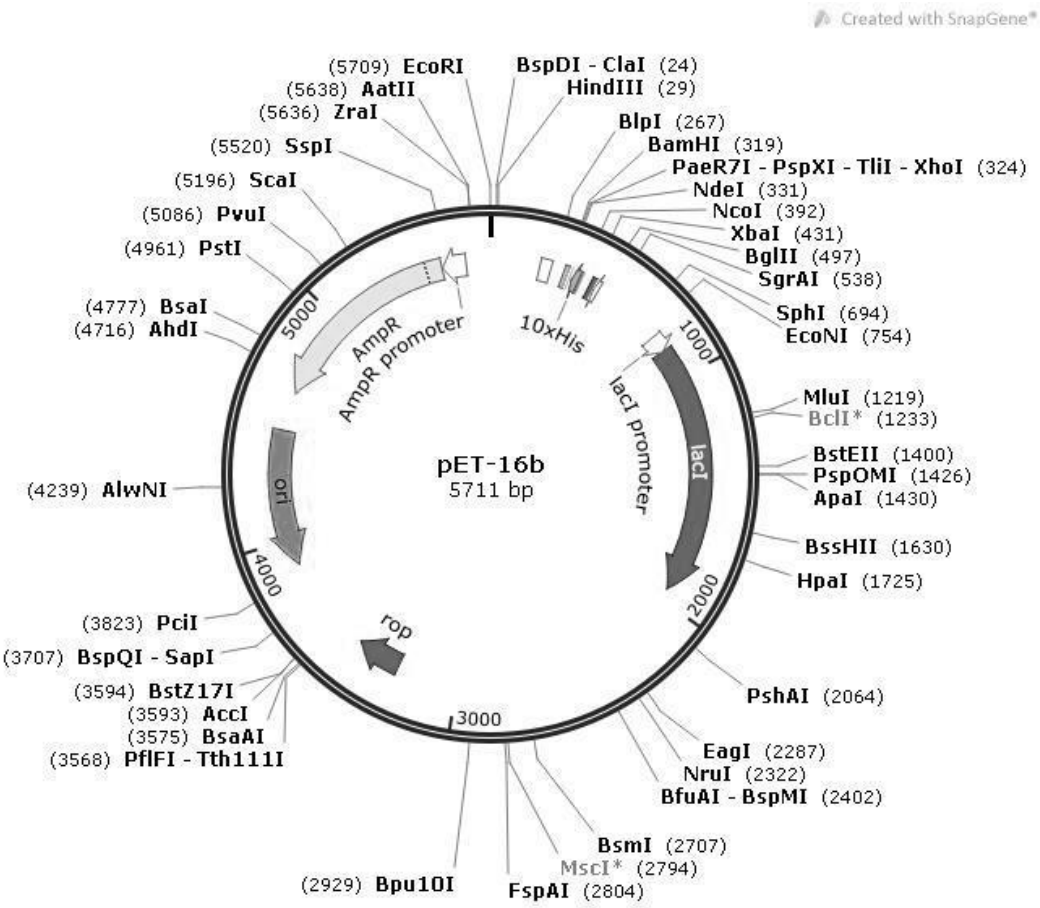

Supplemental figure 71: Vector map of pET-16b
This plasmid harbours a 10x N/C–terminal histidine–tag (His–tag), the IPTG inducible T7lac promoter and an ampicillin resistance. The vector was used for (over-)expression of His-tagged proteins. Map created with SnapGene®.

S.11.3pGEX-2T (GE Healthcare)

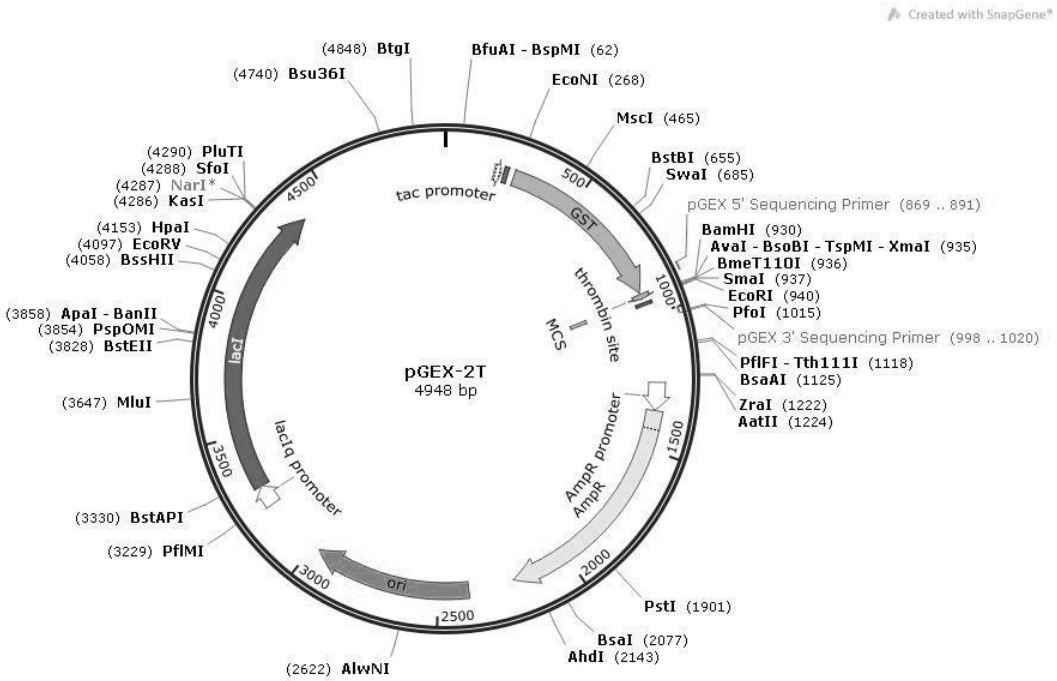

Supplemental figure 72: Vector map of pGEX-2T
This plasmid harbours a glutathione S-transferase (GST) coding region, the IPTG inducible tac promoter and an ampicillin resistance. The vector was used for (over)expression of GST-tagged proteins. Map created with SnapGene®.

S.11.4pGJ280

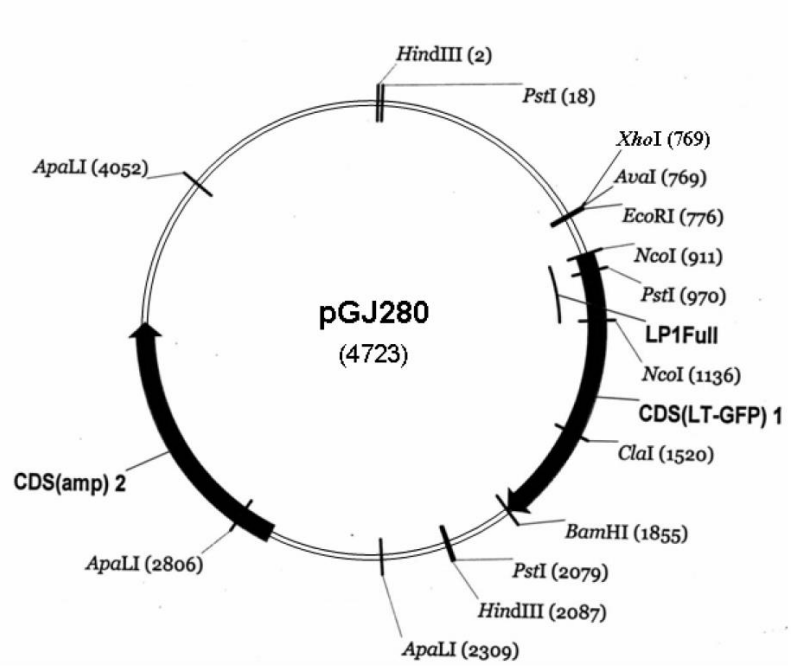

Supplemental figure 73: Vector map of pGJ280
This plasmid harbours the constitutive CaMV35S promoter, a gene encoding for the green fluorescent protein (GFP) and an ampicillin resistance. The vector was used for localisation studies. The vector was constructed by Dr. G. Jach (Max-Planck-Institute, Cologne, DE).

S. 12 Protein sequences

S.12.1 CpVIK

MGASEGSSGHSSASGDAASALEKKKEKARVSRTSQILWHAHQNDAAALRKLLEEDP
SLVNARDYDQRTPLHVAALHGWIDVANCLLDYKADVNAQDRWKNTPLADAEGAKRS
AMIELLKSYGGLSYNGSHFEPRPVPPPLPNKCDWEIDPNELDFSNSMLIGKGSFGEIV
KAGWRGTPVAVKRILPNLSDDRLVIQDFRHEVNLLVKLRHPNIVQFLGAVTDKKPLMLI
TEYLRGGDLHQHLKGKGGLNPSTAINFAMDIARGMAYLHSEPNVIIHRDLKPRNVLLV
NTSADHLKVGDFGLSKLIRVQHSHDVYKLTGETGSYRYMAPEVFKHRKYDKKVDVFS
FAMILYEMLEGDPPMSNYEPYEAARHVADGHRPIFRAKGYAPKLRELTEQCWAADM
NKRPSFLDILKRLEKIKETLPSEHHWHIFPSSS

S.12.2 CpVIK-GFP

MGASEGSSGHSSASGDAASALEKKKEKARVSRTSQILWHAHQNDAAALRKLLEEDP
SLVNARDYDQRTPLHVAALHGWIDVANCLLDYKADVNAQDRWKNTPLADAEGAKRS
AMIELLKSYGGLSYNGSHFEPRPVPPPLPNKCDWEIDPNELDFSNSMLIGKGSFGEIV
KAGWRGTPVAVKRILPNLSDDRLVIQDFRHEVNLLVKLRHPNIVQFLGAVTDKKPLMLI
TEYLRGGDLHQHLKGKGGLNPSTAINFAMDIARGMAYLHSEPNVIIHRDLKPRNVLLV
NTSADHLKVGDFGLSKLIRVQHSHDVYKLTGETGSYRYMAPEVFKHRKYDKKVDVFS
FAMILYEMLEGDPPMSNYEPYEAARHVADGHRPIFRAKGYAPKLRELTEQCWAADM
NKRPSFLDILKRLEKIKETLPSEHHWHIFPSSSS^{GFP}MGKGEELFTGVVPILVELDGDVNGH
KFSVSGEGEGDATYGKLTLKFICTTGKLPVPWPTLVTTFCYGVQCFSRYPDHMKQHD
FFKSAMPEGYVQERTIFFKDDGNYKTRAEVKFEGDTLVNRIELKGIDFKEDGNILGHKL
EYNYNSHNVYITADKQKNGIKANFKIRHNIEDGSVQLADHYQQNTPIGDGPVLLPDNH
YLSTQSALSKDPNEKRDHMVLLEFVTAAGITHGMDELYK

S.12.3 CpVIK$_{dead}$

MGASEGSSGHSSASGDAASALEKKKEKARVSRTSQILWHAHQNDAAALRKLLEEDP
SLVNARDYDQRTPLHVAALHGWIDVANCLLDYKADVNAQDRWKNTPLADAEGAKRS
AMIELLKSYGGLSYNGSHFEPRPVPPPLPNKCDWEIDPNELDFSNSMLIGKGSFGEIV
KAGWRGTPVAVKRILPNLSDDRLVIQDFRHEVNLLVKLRHPNIVQFLGAVTDKKPLMLI
TEYLRGGDLHQHLKGKGGLNPSTAINFAMDIARGMAYLHSEPNVIIHRDLKPRNVLLV
NTSADHLKVGNFGLSKLIRVQHSHDVYKLTGETGSYRYMAPEVFKHRKYDKKVDVFS

FAMILYEMLEGDPPMSNYEPYEAARHVADGHRPIFRAKGYAPKLRELTEQCWAADM
NKRPSFLDILKRLEKIKETLPSEHHWHIFPSS

S.12.4AtVIK

MSSDSPAAGDGGEQAAAGTSVPSPSYDKQKEKARVSRTSLILWHAHQNDAAAVRKL
LEEDPTLVHARDYDKRTPLHVASLHGWIDVVKCLLEFGADVNAQDRWKNTPLADAEG
ARKQKMIELLKSHGGLSYGQNGSHFEPKPVPPPIPKKCDWEIEPAELDFSNAAMIGKG
SFGEIVKAYWRGTPVAVKRILPSLSDDRLVIQDFRHEVDLLVKLRHPNIVQFLGAVTER
KPLMLITEYLRGGDLHQYLKEKGGLTPTTAVNFALDIARGMTYLHNEPNVIIHRDLKPR
NVLLVNSSADHLKVGDFGLSKLIKVQNSHDVYKMTGETGSYRYMAPEVFKHRRYDKK
VDVFSFAMILYEMLEGEPPFANHEPYEAAKHVSDGHRPTFRSKGCTPDLRELIVKCW
DADMNQRPSFLDILKRLEKIKETLPSDHHWGLFTS

S.12.5LbVIK

MSGSEGSSGHSVASGDAASAVGTDKKKEKARVSRTSQILWHAHQNDAAALRKLLEE
DPSLVNARDYDQRTPLHVAALHGWIDVANCLLDYKADVNAQDRWKNTPLADAEGAK
KSTMIELLKSYGGLSYGQNGSHFEPRAVPPPLPNKCDWEIDPNELDFSNSVLIGKGSF
GEIVKAGWRGTPVAVKRILPNLSDDRLVIQDFRHEVNLLVKLRHPNIVQFLGAVTDKKP
LMLITEYLRGGDLHQHLKGKGALNPSTAVNFAMDIARGMAYLHSEPNVVIHRDLKPRN
VLLVNTSADHLKVGDFGLSKLIRVQQHSHDVYKLTGETGSYRYMAPEVFKHRKYDKK
VDVFSFAMILYEMLEGDPPMSNYEPYEAAKYVAEGHRPIFRAKGYAPELRDLTEQCW
AADMSKRPSFLDILKRLERIKEALPSDHHWHIFA

S.12.6LsVIK

MSGSEGSSGHSAASGEAASAMEKDKKKEKARVSRTSQILWHAHQNDAAALRKLLEE
DPSLVNARDYDQRTPLHVAALHGWIDVANCLLDYKADVNAQDRWKNTPLADAEGAK
KSAMIELLKSYGGLSYGQNGSHFEPRPVPPPLPNKCDWEIDPNELDFSNSVLIGKGSF
GEIVKAGWRGTPVAVKRILPNLSDDRLVIQDFRHEVNLLVKLRHPNIVQFLGAVTDKKP
LMLITEYLRGGDLHQHLKGKGALNPSTAVNFAMDIARGIAYLHSEPNVVIHRDLKPRNV
LLVNTSADHLKVGDFGLSKLIRVQHSHDVYKLTGETGSYRYMAPEVFKHRKYDKKVD
VFSFAMILYEMLEGDPPMSNYEPYEAAKHVADGHRPIFRAKGYVPELRELTEQCWAA
DMNNRPSFLDILKRLEKIKETLPSEHHWHIFPSS

S.12.7CDeT11-24

MESQLHRPTEQEMMEGQTADHGEKKSMLAKVKEKAKKLKGSINKKHGSSQDDDADY
DEEINTSPAVHGAPGMNPPPTQGGEYGGLSERDVNIPHPLASTEANLDKPADVQVPP
PVPEATPEVSDKGLTEDLGSTAGQGAKESDVDPLTRGLKGVNYGGDDSNPLAGQEH
QAISDEPKSFPGQENDLPQSHPSSEDEPKKFDAANDQPQSMPQDTITGKISSVPAVIV
DKAAAAKNVVASKLGYGGNQAQQPADAGATQQKKPLTETAAEYKNMVAEKLTPVYE
KVAGAGSTVTSKVWGSGGTTAGEQAQGGEGTVDGGAAAPNKGVFTKDYLSEKLKP
GDEDKALSQAIMEKLQLSKKPAAGEGGAVDETKANESSPGVVGSIKGVVGSLIGGGN
KINATESAAAANEQTQALGSGETAAAEAAKVEQ

S.12.8RD29B

MESQLTRPYGHEQAEEPIRIHHPEEEEHHEKGASKVLKKVKEKAKKIKNSLTKHGNGH
DHDVEDDDDEYDEQDPEVHGAPVYESSAVRGGVTGKPKSLSHAGETNVPASEEIVP
PGTKVFPVVSSDHTKPIEPVSLQDTSYGHEALADPVRTTETSDWEAKREAPTHYPLG
VSEFSDRGESREAHQEPLNTPVSLLSATEDVTRTFAPGGEDDYLGGQRKVNVETPKR
LEEDPAAPGGGSDYLSGVSNYQSKVTDPTHKEAGVPEIAESLGRMKVTDESPDQKS
RQGREEDFPTRSHEFDLKKESDINKNSPARFGGESKAGMEEDFPTRGDVKVESGLG
RDLPTGTHDQFSPELSRPKERDDSEETKDESTHETKPSTYTEQLASATSAITNKAIAAK
NVVASKLGYTGENGGGQSESPVKDETPRSVTAYGQKVAGTVAEKLTPVYEKVKETG
STVMTKLPLSGGGSGVKETQQGEEKGVTAKNYISEKLKPGEEDKALSEMIAEKLHFG
GGGEKKTTATKEVEVTVEKIPSDQIAEGKGHGEAVAEEGKGGEGMVGKVKGAVTSW
LGGKPKSPRSVEESPQSLGTTVGKTPSSLCYT

Acknowledgments

I wish to acknowledge my advisor Professor Dr. Bartels for giving me the freedom to grow as a person in her international working group while guiding me through the process of becoming a scientist. Prof. Dr. Bartels honesty and the fact, that she kept the overview, always brought me back to the bottom of facts, when I was lost.

Furthermore, I wish to thank my mentor Dr. Röhrig for his professional competence, creativity, and optimism. His support promoted my self-belief and his humour let me enjoy my time during this project. The productive ideas of Dr. Röhrig throughout my project were instrumental for the completion of this work.

I thank Dr. Jan Petersen very much for the helpful discussions and support and for processing the *in vitro* kinase assays with radiolabeled ATP as verification to my results.

Further, I would like to thank Monique Krüger, Sara Breitkreutz, Melanie D´Mellow and Jennifer Schneider that carried out side projects with me in practical internships.

I also wish to thank my dissertation committee members, PD Dr. Kirch, Prof. Witke and PD Dr. Lanzerath. Especially, I would like to thank PD Dr. Kirch for the discussions and valuable advices during this research work.

In addition, I wish to thank the other group members, past and present. Helpful discussions and a collaborative atmosphere contributed to my enjoyable and educational experiences in the lab. Especially I would like to thank Dr. Guido Ufer, Dr. Barbara Kampmann, Anna Sergeeva, Jennifer Dell and Cathrin Lanzrath for their support and friendship.

I would like to thank Christiane Buchholz, Tobias Dieckmann, Katrin Hesse and Christa Müller for the technical help and support.

Finally, would like to express my deep gratitude for the continual support of my partner, friends and family throughout my study.

Statement of originality

I declare herewith, that this thesis is my own original work and that all the assistance received in preparing this thesis and sources have been acknowledged. This thesis has not been submitted for any degree or other purposes before.

Bonn,